

2001

Molecular Characterisation of Fluidised Catalytic Cracker Feedstocks using Ruthenium Tetroxide Oxidation: a Study of Model Hydrocarbons

Sturt, Helen Frances

<http://hdl.handle.net/10026.1/1869>

<http://dx.doi.org/10.24382/4042>

University of Plymouth

All content in PEARL is protected by copyright law. Author manuscripts are made available in accordance with publisher policies. Please cite only the published version using the details provided on the item record or document. In the absence of an open licence (e.g. Creative Commons), permissions for further reuse of content should be sought from the publisher or author.

**Molecular Characterisation of Fluidised Catalytic Cracker Feedstocks using
Ruthenium Tetroxide Oxidation: a Study of Model Hydrocarbons.**

by

Helen Frances Sturt

A thesis submitted to the University of Plymouth
in partial fulfilment for the degree of

Doctor of Philosophy

Petroleum and Environmental Geochemistry Group
Department of Environmental Sciences
Faculty of Science

January 2001

90 0453781 3



| UNIVERSITY OF PLYMOUTH | |
|------------------------|----------------|
| Item No. | 9004537813 |
| Date | -7 FEB 2001 S |
| Class No. | 754+.83046 STU |
| Contl. No. | X704203331 |
| LIBRARY SERVICES | |

REFERENCE ONLY

LIBRARY STORE

The Molecular Characterisation of Fluidised Catalytic Cracker Feedstocks by ruthenium tetroxide oxidation.

by
Helen Frances Sturt

Abstract

The world's proven reserves of crude oil will be depleted in 42 years at the current rate of consumption. Oil refiners are under considerable economic and environmental pressure to improve the efficiency of refining and the quality and definition of products. Statistical and fundamental models are extensively used to more accurately model the important refinery processes such as Fluidised Catalytic Cracking (FCC). A major problem with the fundamental approach is that FCC feedstocks are by definition heavy petroleum fractions, and as such constitute highly complex mixtures of aromatic and aliphatic hydrocarbons.

Gas chromatography (GC) analysis of heavy petroleum fractions reveals a broad 'hump' of unresolved compounds termed an Unresolved Complex Mixture (UCM) of hydrocarbons. Conventional instrumental techniques alone are unable to elucidate the composition of UCMs, they are simply too complex. Oxidative degradation of UCMs has already been used with some success to selectively oxidise aliphatic and aromatic UCMs to reveal some of the structures incorporated in UCMs from various natural and anthropogenic sources.

Ruthenium tetroxide (RuO_4) attacks aromatic rings at the *ipso*-carbon of aromatic moieties. Unsubstituted aromatic carbon is oxidised to CO_2 whereas substituents are preserved as carboxylic acids. "Retro-structural analysis" involves reconstruction of the products of oxidation to reveal the original molecule or 'average' molecule. However, previous studies have highlighted problems with the recovery of products from the oxidation of hydroaromatic compounds. Hydroaromatic compounds contain an alicyclic ring attached to an aromatic ring e.g. tetralin.

This study presents evidence that (theoretically) data from RuO_4 oxidation FCC feedstocks can make a significant improvement to the accuracy of FCC modelling at BP Amoco.

RuO_4 oxidation and work-up procedures were developed further in an attempt to overcome problems with 'losses' of oxidation products from hydroaromatic compounds, including an improved carbon dioxide trap. Several novel hydroaromatic compounds and a diaromatic compound proposed in a previous study as being 'average' UCM components were synthesised and fully characterised by GC, GCMS, FTIR and NMR spectroscopy. The compounds synthesised were 6-cyclohexyltetralin, 1-(3'-methylbutyl)-7-cyclohexyltetralin, 1-*n*-nonyl-7-cyclohexyltetralin and 1-*n*-nonyl-7-cyclohexylnaphthalene.

RuO_4 oxidation of the synthetic compounds and commercial tetralin revealed that while losses of between 70 and 50% of the expected water soluble dicarboxylic acids are observed, these losses can be at least partially accounted for by the 'over oxidation' of carboxylic acids to produce smaller carboxylic acids. For example, the RuO_4 oxidation of tetralin produces 1,6-hexanedioic acid as a major product but significant amounts of 1,5-pentanedioic acid is observed along with trace amounts of 1,4-butanedioic acid. Smaller acids are likely to be undetected or lost as butyl esters during the work-up. Where 2-*n*-nonyl-1,6-hexanedioic acid was produced, decanoic and nonanoic acid as well as 1,5-pentanedioic acid and 1,4-butanedioic acid were observed corresponding to oxidation of the 2- position on the dicarboxylic acid.

The three major products from RuO_4 oxidation of 1-*n*-nonyl-7-cyclohexylnaphthalene were partially oxidised compounds including 2-(1-oxo-*n*-decane)-4-cyclohexylbenzoic acid, showing that the oxidation of diaromatic compounds in UCMs gives more complex oxidation products. This is consistent with previous studies where diaromatic UCMs were oxidised to give a more complex 'oxidised UCM' rather than simple carboxylic acids.

The observation of monocarboxylic acids in oxidation products from the alicyclic portion of a hydroaromatic compound has not previously been reported. This represents a new source of monocarboxylic acids in the RuO_4 oxidation products of UCMs and should be taken into account when oxidising UCMs likely to contain a significant proportion of hydroaromatic structures, such as hydro-treated FCC feedstocks.

The synthesis and oxidation of di-substituted tetralins has increased the understanding of RuO_4 oxidation products from UCMs and consequently furthered the use of RuO_4 as a potentially useful tool in the elucidation of FCC feedstock compositions and other aromatic UCMs.

Declaration

At no time during the registration for the degree of Doctor of Philosophy has the author been registered for any other university award.

This study was financed with the aid of a studentship from the EPSRC and a CASE award in collaboration with BP Amoco Research and Engineering (Sunbury-on-Thames).

A programme of advanced study was carried out, with relevant scientific seminars and conferences attended at which work was presented. A period of time was spent studying at the CASE collaborator BP, Sunbury-on-Thames.

Oral Presentations:

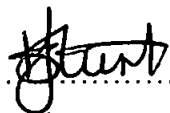
Sturt, H.F.; Wraige, E.J. The synthesis of model UCM components. British Organic Geochemistry Society meeting 1996 (Liverpool, U.K.)

Sturt, H.F. The molecular characterisation of fluidised catalytic cracker feedstocks. Departmental seminar, University of Plymouth, U.K.

External Contacts:

Dr M. Hodges, BP Amoco Research and Engineering, Sunbury-on-Thames.

Dr G. Ketley, BP Amoco Research and Engineering, Sunbury-on-Thames.

Signed..........
Date.....2-2-01.....

Acknowledgements

Firstly I must thank my supervisors Steve Rowland and Anthony Lewis at Plymouth University for invaluable help and advice during my Ph.D.

Thankyou to the EPSRC for providing funding for this Ph.D. and to BP for contributing a CASE award for the study. Mike Hodges (Industrial supervisor, BP) and Graham Ketley (BP) are to be thanked for initiating me into the ways of the oil industry and providing data from the modelling of FCC processes.

Thank you to Emma Wraige for her enthusiastic approach to organic synthesis (they *had* to replace the fume cupboards when we'd finished!)

Thanks also to the technicians Roger Srodzynski and Roger Evens for help with analysis and to Ian Doidge and Andy Tonkin and Andy Arnold for having endless supplies of glassware, chemicals and helpful hints.

A really big thank you goes to my friends and colleagues of the PEGG pub-lunch club *i.e.* Emma Wraige, Lesley Johns, Paul Sutton, Stewart Niven, Ed Stutt, Emma Smith, Guy Allard, Paul McCormack and Raoul Naumann, chips and egg will never be as good.

Thanks too to some past and present researchers from the department who almost succeeded in keeping me sane; Neil, Fiona, Andy, Anita, Emily and especially wee Jamesie.

Lastly, thank you to my family for their unswerving faith in my abilities, and to Mark.

Contents

| | Page No. |
|--|-----------|
| Abstract | ii |
| Declaration | iii |
| Acknowledgements | iv |
| | |
| Contents | 1 |
| Figures in the text..... | 5 |
| Tables in the text..... | 13 |
| Abbreviations used in the text..... | 15 |
| | |
| 1 Introduction | 16 |
| 1.1 The oil problem..... | 17 |
| 1.1.1 Modelling FCC operation..... | 21 |
| 1.2 The analytical problem..... | 21 |
| 1.2.1 The UCM problem..... | 23 |
| 1.2.2 Analysis of UCMs | 24 |
| 1.2.3 Chemical degradation techniques..... | 25 |
| 1.3 Aims of the present study..... | 28 |
| 2 Experimental..... | 30 |
| 2.1 Reagents and consumables..... | 31 |
| 2.2 Analyses | 32 |
| 2.2.1 Gas Chromatography (GC)..... | 32 |
| 2.2.2 Gas Chromatography Mass Spectrometry (GCMS)..... | 32 |
| 2.2.3 Infrared Spectroscopy (IR)..... | 33 |
| 2.2.4 Nuclear Magnetic Resonance Spectroscopy (NMR)..... | 33 |
| 2.3 Ruthenium tetroxide oxidation..... | 33 |
| 2.3.1 Original apparatus..... | 33 |
| 2.3.1.1 CO ₂ determination..... | 34 |
| 2.3.2 Work-up of oxidation products..... | 35 |
| 2.3.2.1 Water-soluble fraction..... | 36 |
| 2.3.2.2 DCM fraction..... | 36 |
| 2.3.3 Modified apparatus for ruthenium tetroxide oxidations..... | 38 |

| | | |
|----------|---|-----------|
| 2.3.3.1 | CO ₂ determination..... | 40 |
| 2.3.3.2 | Work-up of oxidation products..... | 41 |
| 2.3.3.3 | Water-soluble fraction..... | 41 |
| 2.3.3.4 | DCM fraction..... | 42 |
| 2.4 | Organic Synthesis of model UCM compounds..... | 42 |
| 2.4.1 | Preparation of 4-phenyl-(4'-cyclohexyl)-4-oxobutanoic acid (V)..... | 43 |
| 2.4.2 | Preparation of 4-phenyl(4'-cyclohexyl)butanoic acid (VI)..... | 45 |
| 2.4.3 | Preparation of 7-cyclohexyl-1-tetralone (VII)..... | 46 |
| 2.4.4 | Preparation of 6-cyclohexyltetralin (VIII)..... | 47 |
| 2.4.5 | Preparation of 1- <u>n</u> -nonyl-7-cyclohexyltetralin (IX)..... | 48 |
| 2.4.6 | Preparation of 1-(3'-methylbutyl)-7-cyclohexyltetralin (X)..... | 50 |
| 3 | <i>Computer Modelling of FCC Operation</i> | 53 |
| 3.1 | Introduction..... | 54 |
| 3.1.1 | FCC Modelling at BP..... | 56 |
| 3.1.2 | The Oil Characterisation Model (OCM)..... | 57 |
| 3.1.3 | The 'pseudoiser'..... | 59 |
| 3.1.4 | Sunbury Riser Model (SRM)..... | 60 |
| 3.2 | Using data from RuO ₄ oxidations..... | 60 |
| 3.3 | Using pseudo- RuO ₄ oxidation data to generate new ringcore files..... | 63 |
| 3.3.1 | The new ringcore files..... | 64 |
| 3.4 | Results and Discussion..... | 67 |
| 3.4.1 | The OCM..... | 69 |
| 3.4.1.1 | Discussion..... | 72 |
| 3.4.2 | The 'pseudoiser'..... | 73 |
| 3.4.2.1 | Discussion..... | 78 |
| 3.4.3 | The SRM..... | 79 |
| 3.5 | Conclusion..... | 86 |
| 4 | <i>Method Development</i> | 87 |
| 4.1 | Introduction..... | 88 |
| 4.2 | Method evaluation..... | 90 |
| 4.3 | Method developments..... | 94 |
| 4.3.1 | Carbon dioxide determination..... | 94 |
| 4.3.1.1 | Organic solvents for CO ₂ absorption..... | 96 |
| 4.3.1.2 | Silicone tubing..... | 97 |

| | | |
|----------|--|------------|
| 4.3.1.3 | Results..... | 98 |
| 4.3.2 | Liquid/liquid extraction of water-soluble acids..... | 100 |
| 4.3.2.1 | Experiments and results..... | 100 |
| 4.3.3 | Fuller's Earth filtration of colloidal ruthenium salts..... | 103 |
| 4.3.3.1 | Results..... | 104 |
| 4.3.3.2 | Removal of colloidal ruthenium salts..... | 105 |
| 4.3.4 | Base extraction..... | 106 |
| 4.3.5 | Micro-scale derivatisation procedures..... | 106 |
| 4.4 | Summary and Conclusions..... | 107 |
| 5 | <i>Synthesis of UCM model hydrocarbons.</i> | 109 |
| 5.1 | Synthesis of substituted cyclohexyltetralins..... | 110 |
| 5.2 | Substituted cyclohexyltetralins..... | 111 |
| 5.3 | Synthetic strategy..... | 112 |
| 5.4 | Preparation of 4-(4'cyclohexylphenyl)-4-oxobutanoic acid (V)..... | 113 |
| 5.4.1 | Characterisation of 4-(4'cyclohexylphenyl)-4-oxobutanoic acid (V)..... | 115 |
| 5.4.1.1 | GCMS..... | 115 |
| 5.4.1.2 | IR..... | 117 |
| 5.4.1.3 | NMR..... | 118 |
| 5.5 | Preparation of 4-(4'cyclohexylphenyl)butanoic acid (VI)..... | 120 |
| 5.5.1 | Characterisation of 4-(4'cyclohexylphenyl)butanoic acid (VI)..... | 121 |
| 5.5.1.1 | GCMS..... | 121 |
| 5.5.1.2 | IR..... | 123 |
| 5.5.1.3 | NMR..... | 124 |
| 5.6 | Preparation of 7-cyclohexyl-1-tetralone (VII)..... | 127 |
| 5.6.1 | Characterisation of 7-cyclohexyl-1-tetralone (VII)..... | 127 |
| 5.6.1.1 | GCMS..... | 127 |
| 5.6.1.2 | IR..... | 129 |
| 5.6.1.3 | NMR..... | 130 |
| 5.7 | Preparation of 6-cyclohexyltetralin (V)..... | 132 |
| 5.7.1 | Characterisation of 6-cyclohexyltetralin (V)..... | 132 |
| 5.7.1.1 | GCMS..... | 132 |
| 5.7.1.2 | IR..... | 135 |
| 5.7.1.3 | NMR..... | 136 |
| 5.8 | Preparation of 1-alkyl-7-cyclohexyltetralins (VIII, IX and X)..... | 138 |

| | | |
|-----------|---|------------|
| 5.9 | Preparation of 7-cyclohexyl-1- <u>n</u> -nonyltetralin (IX)..... | 138 |
| 5.9.1 | Characterisation of 7-cyclohexyl-1-nonyltetralin (IX)..... | 143 |
| 5.9.1.1 | GCMS | 143 |
| 5.9.1.2 | IR..... | 146 |
| 5.9.1.3 | NMR..... | 147 |
| 5.9.2 | Characterisation of 1- <u>n</u> -nonyl-7-cyclohexylnaphthalene (XI)..... | 149 |
| 5.9.2.1 | GCMS | 149 |
| 5.9.2.2 | IR..... | 153 |
| 5.9.2.3 | NMR..... | 153 |
| 5.9.3 | Preparation of 1-(3'-methylbutyl)-7-cyclohexyltetralin (X)..... | 155 |
| 5.9.3.1 | Characterisation of 1-(3'-methylbutyl)-7-cyclohexyltetralin (X)..... | 156 |
| 5.9.3.1.1 | GCMS | 156 |
| 5.9.3.1.2 | IR..... | 159 |
| 5.9.3.1.3 | NMR..... | 160 |
| 5.10 | Summary | 163 |
| 6 | <i>Ruthenium Tetroxide Oxidation of Synthetic Model UCM components.</i> | 165 |
| 6.1 | Introduction..... | 166 |
| 6.2 | Results and Discussion..... | 168 |
| 6.2.1 | RuO ₄ oxidation of tetralin..... | 169 |
| 6.2.2 | RuO ₄ oxidation of 6-cyclohexyltetralin..... | 172 |
| 6.2.3 | RuO ₄ oxidation of a mixture containing 1- <u>n</u> -nonyl-7-cyclohexyltetralin..... | 176 |
| 6.2.4 | RuO ₄ oxidation of 1-(3'-methylbutyl)-7-cyclohexyltetralin. | 183 |
| 6.2.5 | RuO ₄ oxidation of 1- <u>n</u> -nonyl-7-cyclohexylnaphthalene..... | 188 |
| 6.3 | Conclusions..... | 198 |
| 7 | <i>Overall conclusions and future work.</i> | 203 |
| 7.1 | Overall conclusion. | 204 |
| 7.2 | Suggested further work. | 206 |
| 8 | <i>References</i> | 208 |

Figures in the text.

| | Page No. |
|--|----------|
| <i>Figure 1. Fractionation of a crude oil by distillation. (Adapted from Altgelt and Boduszynski, 1994).....</i> | 19 |
| <i>Figure 2. Schematic of typical refinery processes (BP, in-house literature).....</i> | 20 |
| <i>Figure 3. Number of possible structures of acyclic alkanes by carbon number (Adapted from Altgelt and Boduszynski, 1994).....</i> | 22 |
| <i>Figure 4. Z-number and structure of various hydrocarbons.....</i> | 25 |
| <i>Figure 5. Chromium trioxide oxidation of a T-branched alkane (adapted from Thomas, 1995).</i> | 26 |
| <i>Figure 6. Ruthenium tetroxide oxidation of an alkylbenzene.....</i> | 27 |
| <i>Figure 7. Structures suggested as typical UCM components. (Thomas, 1995).....</i> | 27 |
| <i>Figure 8. Original apparatus for ruthenium tetroxide oxidation.....</i> | 34 |
| <i>Figure 9. Steps of the post-oxidation work-up.....</i> | 35 |
| <i>Figure 10. Modified apparatus for ruthenium tetroxide oxidations.....</i> | 39 |
| <i>Figure 11. Work-up of oxidation products - schematic.....</i> | 41 |
| <i>Figure 12. Scheme for the preparation of alkyl substituted cyclohexyltetralins.....</i> | 43 |
| <i>Figure 13. Apparatus for the Friedel-Crafts acylation of phenylcyclohexane.....</i> | 44 |
| <i>Figure 14. Analytical inputs to the Sunbury Riser Model.....</i> | 57 |
| <i>Figure 15. Carboxylic acids produced on RuO₄ oxidation of selected ringcores from the ringcore file.....</i> | 62 |
| <i>Figure 16. Examples of potential sources of di-, tri- and tetracarboxylic acids from two or more ringcores joined by alkyl bridges.....</i> | 62 |
| <i>Figure 17. Integrating data from RuO₄ oxidations into the Oil Characterisation Model.....</i> | 64 |
| <i>Figure 18. The effect of different ringcore files on predicted aromatic and benzylic hydrogen (sa-n = 'simple acid' ringcore file n, ca-n = 'complex acid' ringcore file).....</i> | 69 |
| <i>Figure 19. The effect on predicted bulk density of different ringcore files (sa-n = 'simple acid' ringcore file n, ca-n = 'complex acid' ringcore file), the degree of substitution is a constant 0.5, one ringcore per molecule.....</i> | 70 |
| <i>Figure 20. The effect of increasing the degree of substitution on predicted benzylic hydrogen.....</i> | 71 |
| <i>Figure 21. The effect on predicted aromatic hydrogen of allowing more than one ringcore per molecule in the OCM. Degree of substitution 0.5 constant.....</i> | 72 |
| <i>Figure 22. Pseudocomponent nomenclature.....</i> | 73 |

| | |
|---|----|
| <i>Figure 23. The effect on selected hydroaromatic pseudocomponent concentrations of different ringcore files and changing degree of substitution. Values are averages of five experiments with varying degrees of substitution from 0 to 1. Error bars show \pm one standard deviation (nil for MH2 and MH3).</i> | 74 |
| <i>Figure 24. The effect on selected aromatic pseudocomponent concentrations of different ringcore files and changing degree of substitution. Values are averages of five experiments with varying degrees of substitution from 0 to 1. Error bars show \pm one standard deviation (nil for MH2 and MH3).</i> | 75 |
| <i>Figure 25. The effect on selected hydroaromatic pseudocomponent concentrations of different ringcore files. Values are averages of results using four ringcore files, with a degree of substitution of 0.5 and allowing one ringcore per molecule. Error bars show values \pm one standard deviation between the four ringcore files.....</i> | 76 |
| <i>Figure 26. The effect on selected aromatic pseudocomponent concentrations of different ringcore files. Values are averages of results using four ringcore files, with a degree of substitution of 0.5 and allowing one ringcore per molecule. Error bars show values \pm one standard deviation across the four ringcore files.</i> | 77 |
| <i>Figure 27. The effect of ringcore files ca1 to ca4 on the aromatic pseudocomponent concentrations with 0.5 degrees of substitution and allowing one ringcore per molecule.</i> | 78 |
| <i>Figure 28. The percentage yields of products predicted by the SRM. The values are average of all experiments on the SRM. Error bars show maximum and minimum of the predicted range.....</i> | 81 |
| <i>Figure 29. Value of products produced daily by a 30,000 BPD FCC unit, expressed in terms of their current market price, (see Table 7), average of all SRM experiments.....</i> | 82 |
| <i>Figure 30. The difference between selected SRM experiments expressed as a percent of the average product yield.....</i> | 85 |
| <i>Figure 31. The influence of selected SRM experiments on the value of products produced daily by a 30,000 BPD FCC unit, expressed as their market value (see Table 7).</i> | 86 |
| <i>Figure 32. Ruthenium tetroxide oxidation of 5-ethyl-2-heptyltetralin.....</i> | 90 |
| <i>Figure 33. Recovery of products from the ruthenium tetroxide oxidation of tetralin.</i> | 91 |
| <i>Figure 34. Work-up procedure for ruthenium tetroxide oxidation products (after Thomas, 1995).....</i> | 93 |
| <i>Figure 35. Diagram showing the original apparatus for the determination of CO₂ trap efficiency (after Thomas, 1995).</i> | 94 |
| <i>Figure 36. Apparatus for testing the efficiency of the benzylamine CO₂ trap.</i> | 97 |

| | |
|--|-----|
| Figure 37. Modified apparatus for the RuO ₄ oxidations of hydrocarbons. | 99 |
| Figure 38. Liquid/liquid extraction apparatus. | 102 |
| Figure 39. The octanol/water partition coefficients (log P) for monocarboxylic and α - ω -dicarboxylic acids (Klopman et al., 1994)..... | 103 |
| Figure 40. Recovery of mono- and dicarboxylic acids filtered through Fuller's Earth. Values are averages (n = 3), error bars show \pm one standard deviation. | 105 |
| Figure 41. T-branched alkylbenzene structure proposed by Gough (1989) as typical aromatic UCM component..... | 110 |
| Figure 42. Substituted alkyltetralin proposed by Thomas (1995) as 'average' monoaromatic UCM component..... | 110 |
| Figure 43. 1-n-propyl-7-cyclohexyltetralin, synthesised by Wraige (1997) to study the environmental impact of UCM hydrocarbons. | 111 |
| Figure 44. General structure of 1-alkyl-7-cyclohexyltetralins - proposed model UCM monoaromatic hydrocarbons..... | 112 |
| Figure 45. Scheme for the synthesis of substituted cyclohexyltetralins. (PPA = polyphosphoric acid)..... | 113 |
| Figure 46. Friedel-Crafts reactions; A = acylation, B = alkylation. | 114 |
| Figure 47. TIC chromatogram of 4-phenyl(4'-cyclohexyl)-4-oxobutanoic acid (V) TMS ester. GC = 12m HP1, 40 – 300°C @ 5°C min ⁻¹ , held 10 min. | 116 |
| Figure 48. Mass spectrum of 4-phenyl(4'-cyclohexyl)-4-oxobutanoic acid (V) TMS ester. | 116 |
| Figure 49. Infrared spectrum of 4-phenyl(4'-cyclohexyl)-4-oxobutanoic acid (V); KBr disk. | 117 |
| Figure 50. ¹³ C NMR spectrum of 4-phenyl(4'-cyclohexyl)-4-oxobutanoic acid (V). | 119 |
| Figure 51. DEPT NMR spectrum of 4-phenyl(4'-cyclohexyl)-4-oxobutanoic acid (V). | 119 |
| Figure 52. ¹ H NMR spectrum of 4-phenyl(4'-cyclohexyl)-4-oxobutanoic acid (V). | 120 |
| Figure 53. TIC chromatogram of 4-phenyl(4'-cyclohexyl)butanoic acid (VI) TMS ester. GC = 12m HP1, 40 – 300°C @ 5°C min ⁻¹ , held 10 min. | 121 |
| Figure 54. Mass spectrum of 4-phenyl(4'-cyclohexyl)butanoic acid (VI) TMS ester. | 122 |
| Figure 55. Mass spectrum of impurity in 4-phenyl(4'-cyclohexyl)butanoic acid (VI)..... | 123 |
| Figure 56. Infrared spectrum of 4-phenyl(4'-cyclohexyl)butanoic acid (VI); KBr disk. | 124 |
| Figure 57. ¹³ C NMR spectrum of 4-phenyl(4'-cyclohexyl)butanoic acid (VI). | 125 |
| Figure 58. DEPT NMR spectrum of 4-phenyl(4'-cyclohexyl)butanoic acid (VI). | 126 |

| | |
|--|-----|
| Figure 59. ¹ H NMR spectrum of 4-phenyl(4'-cyclohexyl)butanoic acid (VI)..... | 126 |
| Figure 60. TIC chromatogram of 7-cyclohexyl-1-tetralone (VII). GC = 12m HP1, 40 – 300°C @ 5°C min ⁻¹ , held 10 min. | 127 |
| Figure 61. Mass spectrum of 7-cyclohexyl-1-tetralone (VII)..... | 128 |
| Figure 62. Infrared spectrum of 7-cyclohexyl-1-tetralone (VII)..... | 129 |
| Figure 63. ¹³ C NMR spectrum of 7-cyclohexyl-1-tetralone (VII). | 130 |
| Figure 64. DEPT NMR spectrum of 7-cyclohexyl-1-tetralone (VII)..... | 130 |
| Figure 65. ¹ H NMR spectrum of 7-cyclohexyl-1-tetralone. | 131 |
| Figure 66. TIC chromatogram of 6-cyclohexyltetralin (V). GC = 12m HP1, 40 – 300°C @ 5°C min ⁻¹ , held 10 min. | 133 |
| Figure 67. Mass spectrum of 6-cyclohexyltetralin (V). | 133 |
| Figure 68. Mass spectrum of (tentatively) 6-(4'-cyclohexylcyclohexyl)tetralin)..... | 134 |
| Figure 69. Infrared spectrum of 6-cyclohexyltetralin (V)..... | 135 |
| Figure 70. ¹³ C NMR spectrum of 6-cyclohexyltetralin (V). | 136 |
| Figure 71. DEPT NMR spectrum of 6-cyclohexyltetralin (V)..... | 136 |
| Figure 72. ¹ H NMR spectrum of 6-cyclohexyltetralin (V). | 137 |
| Figure 73. The Grignard addition of alkyl groups to 7-cyclohexyl-1-tetralones and subsequent dehydration and hydrogenation to 1-alkyl-7-cyclohexyltetralins. | 138 |
| Figure 74. Infrared spectrum of the crude product obtained on the Grignard addition of C ₉ H ₁₉ MgBr to 7-cyclohexyl-1-tetralone (VII), thin film, NaCl windows. | 139 |
| Figure 75. TIC chromatogram of the mixture obtained from the Grignard addition of a nonyl- chain to 7-cyclohexyl-1-tetralone (VII). GC = 12m HP1, 40 – 300°C @ 5°C min ⁻¹ , held 10 min..... | 140 |
| Figure 76. TIC of the mixture obtained from the Grignard addition of a nonyl- chain to 7-cyclohexyl-1-tetralone (VII) after attempted vacuum distillation. GC = 12m HP1, 40 – 300°C @ 5°C min ⁻¹ , held 10 min. | 140 |
| Figure 77. TIC chromatogram of alkane fraction (R _f 0.82-1.00) from the Ag ⁺ TLC separation of the products from the Grignard addition of n-C ₉ H ₁₉ to 7-cyclohexyl-1-tetralone (VII). GC = 12m HP1, 40 – 300°C @ 5°C min ⁻¹ , held 10 min. | 142 |

| | |
|--|-----|
| Figure 78. TIC chromatogram of the monoaromatic fraction (Rf 0.65-0.82) from the Ag ⁺ TLC separation of the products from the Grignard addition of n-C ₉ H ₁₉ to 7-cyclohexyl-1-tetralone (VII). GC = 12m HP1, 40 – 300°C @ 5°C min ⁻¹ , held 10 min. | 142 |
| Figure 79. TIC chromatogram of the di-aromatic fraction (Rf 0.1-0.65) from the Ag ⁺ TLC separation of the products from the Grignard addition of n-C ₉ H ₁₉ to 7-cyclohexyl-1-tetralone (VII). GC = 12m HP1, 40 – 300°C @ 5°C min ⁻¹ , held 10 min. | 143 |
| Figure 80. TIC chromatogram of the monoaromatic fraction obtained from open column chromatography of the crude product of the Grignard reaction to produce 1-n-nonyl-7-cyclohexyltetralin (IX). GC = 12m HP1, 40 – 300°C @ 5°C min ⁻¹ , held 10 min. | 144 |
| Figure 81. Mass spectrum of 1-n-nonyl-7-cyclohexyltetralin (IX). | 145 |
| Figure 82. IR spectrum of the monoaromatic fraction containing 1-n-nonyl-7-cyclohexyltetralin (IX). ... | 146 |
| Figure 83. ¹³ C NMR spectrum of a mixture containing 53% 1-n-nonyl-7-cyclohexyltetralin (VI), 22% 6-cyclohexyltetralin (V) and 11% 1-methyl-7-cyclohexyltetralin. | 147 |
| Figure 84. DEPT NMR spectrum of a mixture containing 53% 1-n-nonyl-7-cyclohexyltetralin (VI), 22% 6-cyclohexyltetralin (V) and 11% 1-methyl-7-cyclohexyltetralin. | 148 |
| Figure 85. ¹ H NMR spectrum of a mixture containing 53% 1-n-nonyl-7-cyclohexyltetralin (VI), 22% 6-cyclohexyltetralin (V) and 11% 1-methyl-7-cyclohexyltetralin. | 149 |
| Figure 86. TIC chromatogram of the diaromatic fraction obtained from open column chromatography on the crude product obtained from the Grignard reaction to produce 1-n-nonyl-7-cyclohexyltetralin (IX). GC = 12m HP1, 40 – 300°C @ 5°C min ⁻¹ , held 10 min. | 150 |
| Figure 87. Mass spectrum of 1-n-nonyl-7-cyclohexylnaphthalene (XI). | 151 |
| Figure 88. Mass spectrum of 2-cyclohexylnaphthalene..... | 151 |
| Figure 89. Mass spectrum of (tentatively) 1-n-nonyl-7-(4'-cyclohexylcyclohexyl)naphthalene..... | 152 |
| Figure 90. Infrared spectrum of 1-n-nonyl-7-cyclohexylnaphthalene(XI); thin film, NaCl windows. | 153 |
| Figure 91. ¹³ C NMR spectrum of 1-n-nonyl-7-cyclohexyltetralin..... | 154 |
| Figure 92. DEPT NMR spectrum of 1-n-nonyl-7-cyclohexyltetralin..... | 154 |
| Figure 93. ¹ H DEPT NMR spectrum of 1-n-nonyl-7-cyclohexyltetralin..... | 155 |
| Figure 94. Compounds used in the attempted formation of Grignard reagents. | 156 |
| Figure 95. TIC chromatogram of 1-(3'-methylbutyl)-7-cyclohexyltetralin (X). GC = 12m HP1, 40 – 300°C @ 5°C min ⁻¹ , held 10 min. | 157 |

| | |
|---|-----|
| Figure 96. Mass spectrum of 1-(3'-methylbutyl)-7-cyclohexyltetralin (X)..... | 158 |
| Figure 97. Mass spectrum of (tentatively) 1-(3'-methylbutyl)-7-(4'-cyclohexylcyclohexyl)tetralin..... | 159 |
| Figure 98. Infrared spectrum of 1-(3'-methylbutyl)-7-cyclohexyltetralin (X)..... | 159 |
| Figure 99. ¹³ C NMR spectrum of 1-(3'-methylbutyl)-7-cyclohexyltetralin (X)..... | 160 |
| Figure 100. DEPT NMR spectrum of 1-(3'-methylbutyl)-7-cyclohexyltetralin (X)..... | 161 |
| Figure 101. DEPT NMR spectrum of alkene precursors to 1-(3'-methylbutyl)-7-cyclohexyltetralin (X)... | 161 |
| Figure 102. ¹ H NMR spectrum of 1-(3'-methylbutyl)-7-cyclohexyltetralin (X)..... | 162 |
| Figure 103. Possible inference from Thomas' (1995) results of the oxidation of 2-ethyltetralin..... | 167 |
| Figure 104. Expected products from the RuO ₄ catalysed oxidation of tetralin..... | 169 |
| Figure 105. Calculation of 'expected' values for the oxidation products of tetralin..... | 170 |
| Figure 106. Recovery of products from the RuO ₄ oxidation of tetralin..... | 171 |
| Figure 107. Partial TIC chromatogram of the water-soluble products from the RuO ₄ oxidation of tetralin (as n-butyl esters, Oxidation No. 10). GC = 25m DB5, 40-300°C @ 5°C min ⁻¹ , held 10 min..... | 171 |
| Figure 108. Theoretical products from the RuO ₄ oxidation of 6-cyclohexyltetralin..... | 172 |
| Figure 109. Recovery of identified products from the ruthenium tetroxide oxidation of 6-cyclohexyltetralin. | 174 |
| Figure 110. TIC chromatogram of the DCM-soluble products from the oxidation of 6-cyclohexyltetralin (as methyl esters, Oxidation No. 12). GC = 25m DB5, 40-300°C @ 5°C min ⁻¹ , held 10 min..... | 175 |
| Figure 111. Postulated product from the further oxidation of cyclohexane carboxylic acid..... | 176 |
| Figure 112. Theoretical products from the ruthenium tetroxide oxidation of a mixture containing 1- <u>n</u> - nonyl-7-cyclohexyltetralin, 6-cyclohexyltetralin and 1-methyl-7-cyclohexyltetralin..... | 176 |
| Figure 113. Recovery of products from the ruthenium tetroxide oxidation of a mixture containing 1- <u>n</u> - nonyl-7-cyclohexyltetralin, 6-cyclohexyltetralin and 1-methyl-7-cyclohexyltetralin..... | 178 |
| Figure 114. Partial TIC chromatogram of DCM-soluble products from the RuO ₄ oxidation of a mixture containing 1- <u>n</u> -nonyl-7-cyclohexyltetralin, 6-cyclohexyltetralin and 1-methyl-7-cyclohexyltetralin (as methyl esters, oxidation No. 22). GC = 25m DB5, 40-300°C @ 10°C min ⁻¹ , held 10 min..... | 179 |
| Figure 115. Mass spectrum of 2- <u>n</u> -nonyl-1,6-hexanedioic acid methyl ester..... | 180 |
| Figure 116. Products observed from the further oxidation of 2- <u>n</u> -nonyl-1,6-hexanedioic acid ('chain shortening')..... | 181 |

| | |
|---|-----|
| <i>Figure 117. Partial TIC chromatogram of the water-soluble products from the RuO₄ oxidation of a mixture containing 1-n-nonyl-7-cyclohexyltetralin, 6-cyclohexyltetralin and 1-methyl-7-cyclohexyltetralin (as n-butyl esters, oxidation No. 23). GC = 25m DB5, 40-300°C @ 10°C min⁻¹, held 10 min.....</i> | 181 |
| <i>Figure 118. Mass spectrum of 2-methyl-1,6-hexanedioic acid n-butyl ester.....</i> | 182 |
| <i>Figure 119. Mass spectrum of 2-methyl-1,5-pentanedioic acid n-butyl ester.....</i> | 183 |
| <i>Figure 120. Theoretical products from the oxidation of 1-(3'-methylbutyl)-7-cyclohexyltetralin.....</i> | 183 |
| <i>Figure 121. Recovery of products from the RuO₄ oxidation of 1-(3'-methylbutyl)-7-cyclohexyltetralin....</i> | 185 |
| <i>Figure 122. Partial TIC chromatogram of DCM-soluble products from the RuO₄ oxidation of 1-(3'-methyl)butyl-7-cyclohexyltetralin (as methyl esters, oxidation no. 27). GC = 25m DB5, 40 – 300°C @ 10°C min⁻¹, held 10 min.</i> | 186 |
| <i>Figure 123. Mass spectrum of 2-(3'-methylbutyl)-1,6-hexanedioic acid methyl ester.....</i> | 187 |
| <i>Figure 124. Mass spectrum of 2-(3'-methylbutyl)-1,5-pentanedioic acid methyl ester.....</i> | 187 |
| <i>Figure 125. Phthalic acids expected from the oxidation of 1-n-nonyl-7-cyclohexylnaphthalene.....</i> | 189 |
| <i>Figure 126. Formation of keto-acid from the RuO₄ oxidation of 1-ethylnaphthalene (Thomas, 1995) and possible keto acid formed from the RuO₄ oxidation of 1-n-nonyl-7-cyclohexylnaphthalene.....</i> | 189 |
| <i>Figure 127. Theoretical products from the ruthenium tetroxide oxidation of 1-n-nonyl-7-cyclohexylnaphthalene, 2-cyclohexylnaphthalene and 1-n-nonyl-7-(4'cyclohexyl)cyclohexylnaphthalene assuming complete oxidation of aromatic carbon.....</i> | 190 |
| <i>Figure 128. recovery of identified products from the ruthenium tetroxide oxidation of 1-n-nonyl-7-cyclohexylnaphthalene.....</i> | 192 |
| <i>Figure 129. Partial TIC chromatogram of the DCM-soluble products from the oxidation of 1-n-nonyl-7-cyclohexylnaphthalene (as methyl esters, oxidation No. 25). GC = 25m DB5, 40 – 300°C @ 10°C min⁻¹, held 10 min.</i> | 193 |
| <i>Figure 130. Mass spectrum of unknown product (1) from the DCM-soluble fraction of products from the RuO₄ oxidation of 1-n-nonyl-7-cyclohexyltetralin.....</i> | 193 |
| <i>Figure 131. Mass spectrum of product (2) from the DCM-soluble fraction of products from the RuO₄ oxidation of 1-n-nonyl-7-cyclohexyltetralin.....</i> | 194 |
| <i>Figure 132. Postulated structure of fragment ions m/z 163 and 245 from o-methylphthalates (Thomas, 1995; McLafferty and Turecek, 1993) and the methyl esters of keto acids (Figure 133).....</i> | 195 |

Figure 133. Fragment ions produced by dimethylphthalate and 2-(1-oxypropyl)benzoic acid methyl ester (Thomas, 1995) and extrapolation to possible RuO₄ oxidation products of 1-n-nonyl-7-cyclohexylnaphthalene..... 196

Figure 134. Mass spectrum of unidentified product (3) from the DCM-soluble fraction of products from the RuO₄ oxidation of 1-n-nonyl-7-cyclohexyltetralin..... 197

Figure 135. Summary of the recoveries of identified oxidation products from the RuO₄ oxidation of compounds synthesised by the author. Values for commercial tetralin are also included. 199

Tables in the text.

| | Page No. |
|--|----------|
| <i>Table 1. Reactions in catalytic cracking (from Gray, 1994).</i> | 18 |
| <i>Table 2. Values used to generate the 'complex acid' ringcore files (% of total).</i> | 65 |
| <i>Table 3. Values used to generate the 'simple acid' ringcore files (% of total).</i> | 66 |
| <i>Table 4. Summary of important parameters input to the OCM.</i> | 66 |
| <i>Table 5. Summary of experiments on the OCM and 'pseudoiser'.</i> | 68 |
| <i>Table 6. Distribution of pseudocomponents in the distillation fractions predicted by the SRM.</i> | 79 |
| <i>Table 7. Summary of uses and value of products obtained from an FCC unit.</i> | 80 |
| <i>Table 8. Summary of experiments on the SRM.</i> | 80 |
| <i>Table 9. The effect of increasing the number of 'ringcores per molecule' allowed on product yields predicted by the SRM.</i> | 82 |
| <i>Table 10. The effect of the ringcore files MH1 and MH2 on product yields predicted by the SRM.</i> | 83 |
| <i>Table 11. The effect of the 'simple acid' ringcore files on product yields predicted by the SRM.</i> | 83 |
| <i>Table 12. The effect of the 'complex acid' ringcore files on product yields predicted by the SRM.</i> | 84 |
| <i>Table 13. The difference between the 'simple acid' and 'complex acid' ringcore files in terms of product yields predicted by the SRM.</i> | 84 |
| <i>Table 14. Products of RuO₄ oxidation of 1-phenyldecane, tetralin, 2-ethyltetralin and 5-ethyltetralin. Thomas (1995).</i> | 89 |
| <i>Table 15. Products recovered from four repeat oxidations of tetralin (this study).</i> | 91 |
| <i>Table 16. Results of two experiments to test the efficiency of the benzylamine CO₂ trap. Observed CO₂ is expressed as percent of expected.</i> | 98 |
| <i>Table 17. Percentage recovery of acids by liquid/liquid extraction into diethylether.</i> | 101 |
| <i>Table 18. Response factors of dicarboxylic acids with respect to ethyloctanoate.</i> | 102 |
| <i>Table 19. Recovery of carbon dioxide from the RuO₄ oxidation of tetralin before and after method development.</i> | 107 |
| <i>Table 20. Composition of monoaromatic fraction from open column chromatography of crude product obtained from the Grignard reaction of 7-cyclohexyltetralone + C₉H₁₉MgBr.</i> | 144 |
| <i>Table 21. Summary of model UCM hydrocarbons synthesised.</i> | 163 |
| <i>Table 22. Ruthenium tetroxide oxidation of ethyltetralins (Thomas, 1995).</i> | 167 |

| | |
|---|------------|
| <i>Table 23. Recovery of products from the ruthenium tetroxide oxidation of tetralin.....</i> | <i>170</i> |
| <i>Table 24. Recovery of identified products from the RuO₄ oxidation of 6-cyclohexyltetralin.....</i> | <i>173</i> |
| <i>Table 25. Recovery (%) of products from the ruthenium tetroxide oxidation of a mixture containing 1-<u>n</u>-nonyl-7-cyclohexyltetralin, 6-cyclohexyltetralin and 1-methyl-7-cyclohexyltetralin.....</i> | <i>177</i> |
| <i>Table 26. Recovery of identified products from the RuO₄ oxidation of 1-(3'-methylbutyl)-7-cyclohexyltetralin.....</i> | <i>184</i> |
| <i>Table 27. Previous RuO₄ oxidations of polycyclic aromatic hydrocarbons.....</i> | <i>188</i> |
| <i>Table 28. Recovery of identified products from the oxidation of 1-<u>n</u>-nonyl-7-cyclohexylnaphthalene.....</i> | <i>191</i> |
| <i>Table 29. Quantification of compounds (1, 2 and 3) in the DCM-soluble fraction of products from the RuO₄ oxidation 1-<u>n</u>-nonyl-7-cyclohexylnaphthalene.....</i> | <i>198</i> |
| <i>Table 30. Summary - recovery of identified oxidation products from the RuO₄ oxidation of compounds synthesised (except tetralin which was obtained from a commercial source) by the author.....</i> | <i>201</i> |

Abbreviations in the text

| | |
|---------------------|--|
| Ag ⁺ TLC | – Argentation Thin Layer Chromatography |
| BPD | – Barrels per Day |
| Bp. | – boiling point |
| ca1, ca2, ca3, ca4 | – ringcore files based on ‘complex acid’ information |
| CCS | – Cat. Cracked Spirit |
| DCM | – dichloromethane |
| DEPT | – Distortionless enhancement by polarisation transfer |
| FIMS | – Field ionisation mass spectrometry |
| FCC | – Fluidised catalytic cracking |
| FTIR | – Fourier transform infrared spectroscopy |
| GC | – Gas chromatography |
| GCMS | – Gas chromatography mass spectrometry |
| HCO | – Heavy cycle oil |
| HPLC | – High performance liquid chromatography |
| IR | – Infrared (spectroscopy) |
| LCO | – Light cycle oil |
| LPG | – Liquid petroleum gas |
| MH1, MH2, MH3 | – ringcore files generated using BP data and experience |
| MS | – Mass spectrometry |
| NMR | – Nuclear magnetic resonance (spectroscopy) |
| OCM | – Oil characterisation model |
| PAH | – Polycyclic aromatic hydrocarbon |
| PPA | – polyphosphoric acid |
| rbf | – round bottomed flask |
| RC | – ringcore |
| RMM | – relative molecular mass |
| sa1, sa2, sa3, sa4 | – ringcore files generated using ‘simple acid’ information |
| SOL | – Structure oriented lumping |
| SPE | – Solid Phase Extraction |
| SRM | – Sunbury Riser Model (FCC model) |
| TIC | – Total ion current (chromatogram) |
| TLC | – Thin layer chromatography |
| TMS | – Trimethylsilyl |
| UCM | – Unresolved complex mixture |
| WCOT | – Wall-coated open tubular (capillary GC column) |
| Z | – Hydrogen deficiency, <i>i.e.</i> C _n H _{n-2} |

1 Introduction

This chapter reviews some of the problems experienced by the oil industry with the characterisation of complex mixtures of hydrocarbons. The concept of Unresolved Complex Mixtures (UCMs) is introduced along with reasons why the detailed molecular composition of UCMs still eludes us.

1.1 The oil problem

'Crude oil' is a general term used to describe a natural resource which in fact varies widely in physical and chemical compositions. The most desirable crude oils by refinery standards are termed 'light' – which means they are composed of mainly low molecular weight alkyl hydrocarbons, and 'sweet' – which refers to an absence of hetero-elements such as sulphur, nitrogen and metals. Figure 1 shows a typical fractionation of a crude oil by distillation.

Such a crude oil is an ideal; it would take little effort to bring to the surface and a high proportion would generate high value light distillate product on refining. Unfortunately reserves of 'light', 'sweet' crude oils are rapidly diminishing. At the same time, demand for light distillate products is increasing and demand for heavy products like fuel oils is falling. Along with this, environmental legislation is increasing the demand for better quality products with less disposable residues (Altgelt and Boduszynski, 1994).

These facts require refiners to increase production of light products from heavy feedstocks whilst at the same time meeting strict quality demands.

After 'straight run' or atmospheric distillation of crude oil, various refinery processes are used to convert heavy feedstocks into lighter products. The processes are under continual development to cope with the increasing amounts of poor quality feedstocks. Figure 2 shows a typical refinery process scheme.

A few of the more common processes are described below:

- Thermal cracking is the oldest refining process in which feedstock is heated to temperatures exceeding 410°C. At this point the hydrocarbons "crack" into smaller hydrocarbons (a free-radical process). This produces large amounts of coke.
- Hydrotreating (HT) is a versatile process used for a variety of purposes. This has the effect of aiding removal of heteroatoms (e.g. sulphur and nitrogen) and to

hydrogenate aromatic rings. HT may be used on heavy feedstocks before a cracking process to remove sulphur or decrease aromatics, or more commonly to improve products from cracking processes for final distillation.

- Fluidised Catalytic Cracking (FCC) is one of the most common refinery processes. Catalysts provide some control of the cracking process and consequently the process gives rise to more valuable products. Table 1 below shows the common reactions in a catalytic cracking process.

| Hydrocarbon | Reactions | Major Products |
|---|---|--|
| Paraffins (<i>n</i> -alkanes) | Cracking, isomerisation. | C ₃ + isoparaffins and olefins. |
| Naphthenes (cycloalkanes) | Cleavage of rings and side chains, Dehydrogenation. | Paraffins, olefins and aromatics. |
| Hydroaromatics (partially hydrogenated aromatics) | Opening of naphthenic ring, cleavage of side chains, dehydrogenation. | Paraffins, olefins and aromatics. |
| Aromatic rings | Negligible cracking. | Coke on catalyst. |
| Aromatic side-chains | Cleavage from ring. | Olefins and aromatics. |
| Olefins (alkenes) | Cracking, hydrogen transfer. | Branched olefins, diolefins and paraffins. |
| Diolefins | Oligomerisation, cycloaddition. | Polyaromatics, coke. |

Table 1. Reactions in catalytic cracking (from Gray, 1994).

There are several problems to be overcome when using heavy feedstocks in FCC units. An increase in heterocompounds (especially metals, N and S) reduces the efficiency and selectivity of the catalyst and also increases emissions of NO_x and SO_x from the catalyst regenerator. The feedstock has a higher proportion of carbon (being more aromatic) and a higher boiling point than a regular feedstock, which means that more coke is generated.

Figure 1. Fractionation of a crude oil by distillation. (Adapted from Allgeil and Boduszynski, 1994)

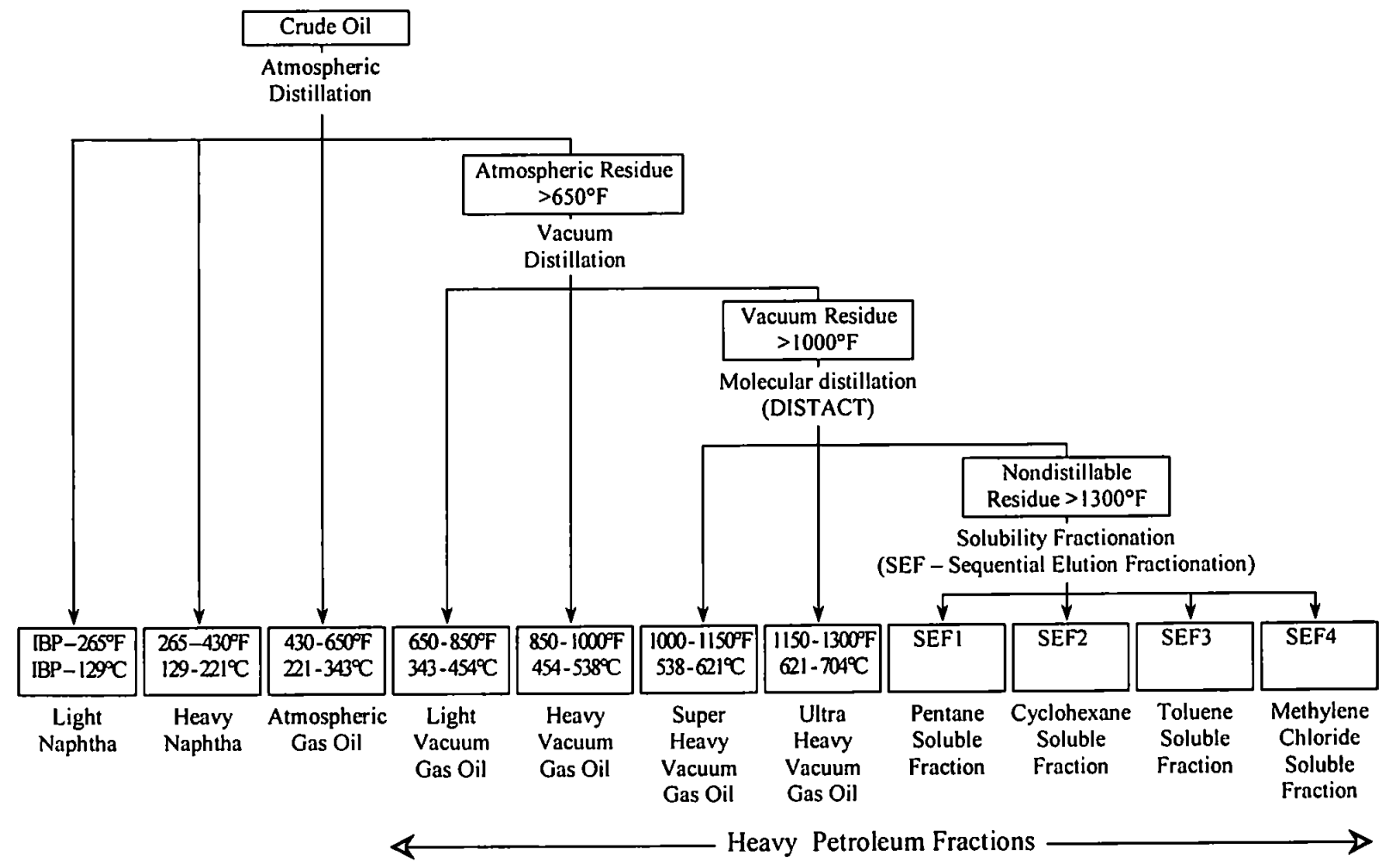
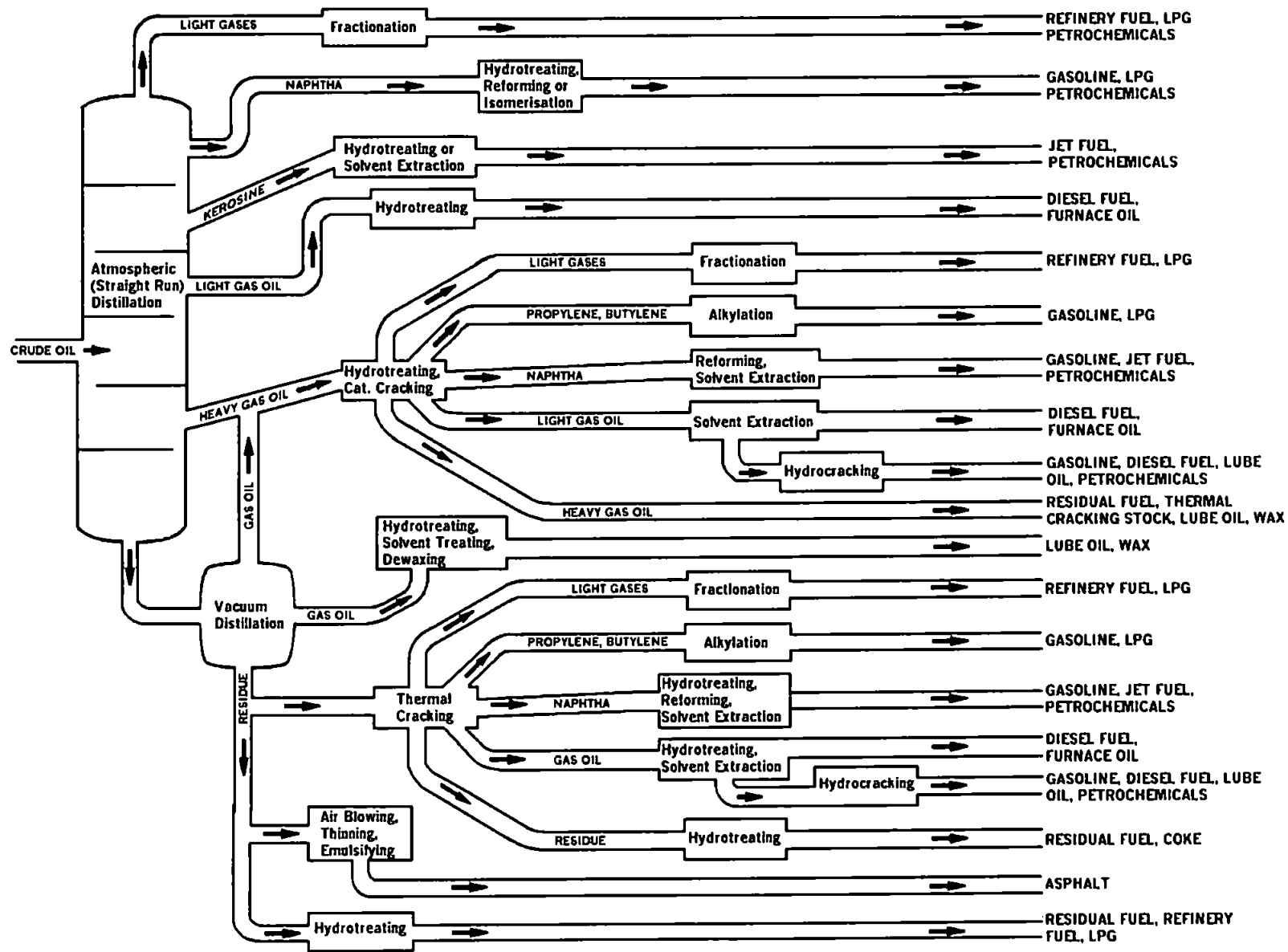


Figure 2. Schematic of typical refinery processes (BP, in-house literature)



1.1.1 Modelling FCC operation

A modern approach to optimisation of the operation of a refinery process like FCC often includes construction of a computer model of FCC operation and use of the model to predict the relative proportions of products under various conditions.

An example of a modern FCC model is that designed by the oil giant BP the so-called 'Sunbury Riser Model'. This 'fundamental' model of FCC operation has been developed in order to optimise production of valuable products from the available feedstocks. The model is fundamental in that it utilises data describing FCC operating conditions and also incorporates much chemical data describing the feedstock composition.

Whilst such models use data from conventional high performance liquid chromatography (HPLC), nuclear magnetic resonance spectroscopy (NMR) and mass spectrometry (MS) analyses to describe a *pseudo*-composition of the feedstock, a major limitation of the model is that no detailed analysis *at the molecular level* is possible for most of the complex mixtures which are not identifiable by the above techniques.

Ideally, a full compositional analysis of a potential feedstock would be used in the model, and additional data that could improve the accuracy of the preliminary 'oil composition' model would be of great benefit. The present study aimed to improve such knowledge of complex feedstock mixtures at the molecular level.

1.2 The analytical problem

Crude oils and heavy refinery fractions are highly complex mixtures of mainly hydrocarbons. Whilst analysis of the lighter end of crude oils such as light naphtha is more-or-less achieved by a single technique such as gas chromatography (GC), analysis of heavy naphtha is considerably more difficult, but achievable using gas chromatography mass spectrometry (GCMS). For heavier fractions of a crude oil, compositional analysis is a much more formidable task.

The number of compounds in such mixtures is very large. For example, for the acyclic alkanes, the number of structures increases exponentially with carbon number, for C₃₀ compounds there are 4.11×10^9 structures possible (Altgelt and Boduszynski, 1994).

Figure 3 shows the number of possible structures for acyclic alkanes at any given carbon number. If the many different compound classes, including cycloalkanes, hydroaromatics and aromatics are added to this, and bearing in mind that all of these may be combined in some form, the numbers increase by further orders of magnitude. This is increased if any heteroatomic compounds are also considered.

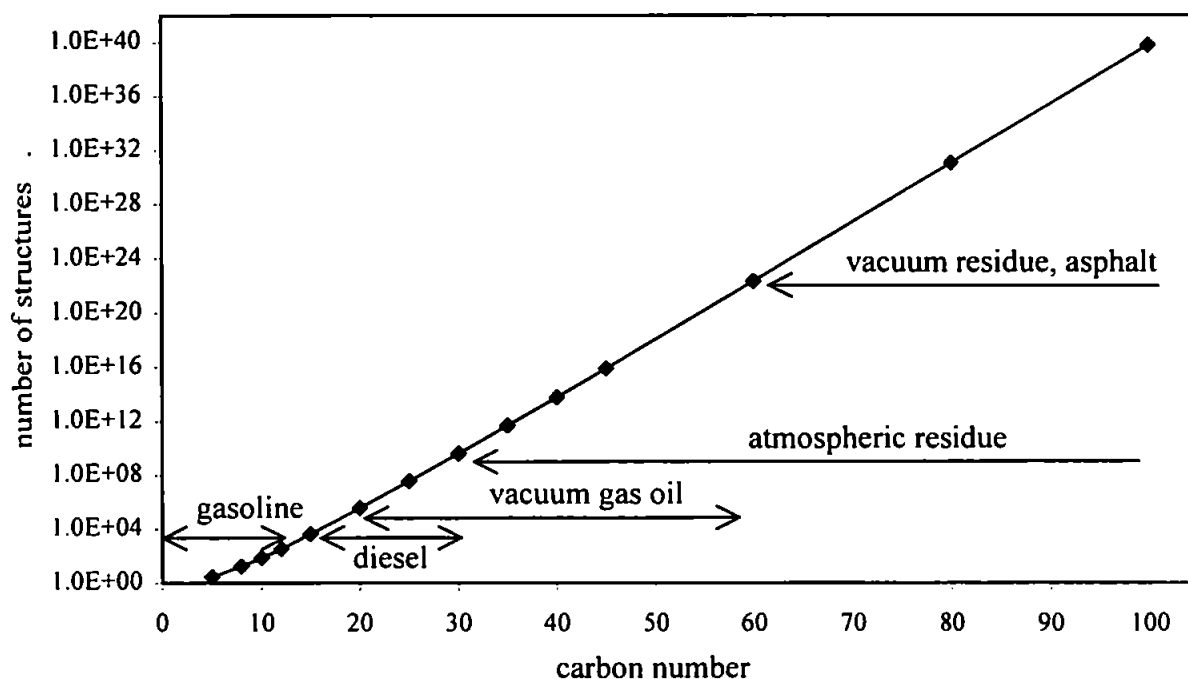


Figure 3. Number of possible structures of acyclic alkanes by carbon number (Adapted from Altgelt and Boduszynski, 1994)

Indeed, the authors of “Composition and Analysis of Heavy Petroleum Fractions” (Altgelt and Boduszynski, 1994) state, “... compositional analysis of heavy petroleum fractions (is) utterly impossible.” Their excellent book then goes on to describe in detail all of the analytical techniques currently being used to try to determine the “impossible”. Clearly knowledge of the *speciation* or actual molecular form of hydrocarbons in an oil

feedstock is essential for improved FCC modelling. For example, there is a significant difference in the FCC reactions of hydroaromatics and aromatics (Table 1), yet instrumental techniques so far cannot distinguish between the two when complex mixtures are analysed.

1.2.1 The UCM problem

In a complex mixture like a heavy petroleum fraction, current chromatographic techniques alone are unable to resolve all of the components. This gives rise to a characteristic 'hump' on a gas chromatogram. The term *unresolved complex mixture* or UCM has been used to describe such a phenomenon (Blumer *et al.*, 1973).

Hydrocarbon UCMs in crude oils are thought to be derived from catagenesis of kerogen; ancient geological organic matter that forms from petrified biological compounds such as proteins and lipids. Revill (1992) reviews theories on the origins of UCMs and kerogen formation.

Removal of resolved compounds (e.g. *n*-alkanes) by biodegradation, *in-situ* or refining, emphasises the contribution of the UCM of a crude oil or heavy petroleum fraction. This is neatly illustrated by Peters and Moldowan (1993). Also, natural processes such as weathering and biodegradation tend to enrich UCMs in the environment, and as a result UCMs are a common feature of organic extracts of environmental samples where they are considered indicative of hydrocarbon pollution. Indeed, a pollution source can sometimes be traced by 'fingerprinting' UCMs to reveal the original hydrocarbon source (e.g. Revill *et al.*, 1992). The potential toxicity of UCMs to organisms has been largely overlooked, but studies by Wraige (1997) and Thomas (1995) have shown UCMs may have significant effects.

The key to molecular analysis of UCMs is simplification. Complex mixtures can be somewhat simplified by separation according to molecular weight or structure. Open

column chromatography is used to fractionate UCMs into compound classes such as so-called 'aliphatics', 'aromatics', and 'polars'. Further separations by HPLC into '1 aromatic ring', '2 ring' fractions and so on are also possible and widely used. While these compound class fractions do provide greater detail, the problem of identifying individual species is still not often addressed.

The analyst also needs to be aware that large hydrocarbons often will bear features of several different compound classes (such as aromatic rings with aliphatic side chains) and there is often significant overlap in the composition of subsequent fractions, where the 'aliphatic', 'aromatic' class distinctions become blurred (Killops and Al-Juboori, 1990).

1.2.2 Analysis of UCMs

Instrumental techniques such as NMR and MS especially when coupled to, or following chromatographic separations, provide further information on the composition of complex mixtures. For example, mass spectrometry provides molecular mass and formula data. Electron impact MS (EIMS) is a high energy technique; examination of fragmentation patterns can give structural information for resolved compounds, useful for distinguishing between isomers.

Some of the most useful MS tools for complex mixtures are non-fragmenting mass spectrometry techniques; one of most common being Field Ionisation MS (FIMS). Since fragmentation of molecules is minimised in FIMS, such techniques produce relatively simple spectra comprising mainly molecular ions. FIMS analysis is thus used widely to determine molecular mass ranges and so called Z series profiles. The Z number of a molecule is defined in the formula C_nH_{2n+z} . Thus for a saturated alkane $Z = 2$, for a monocycloalkane $Z = 0$, for a dicycloalkane $Z = -2$ and so on, the Z number decreasing by two for each additional cycloalkyl ring. Benzene has a Z number of -6, naphthalene $Z = -12$ and so on. As a rule, Z can be calculated from the formula:

$Z = -2(R + DB - 1)$ where **R** = no. of rings and **DB** = no. of double bonds.

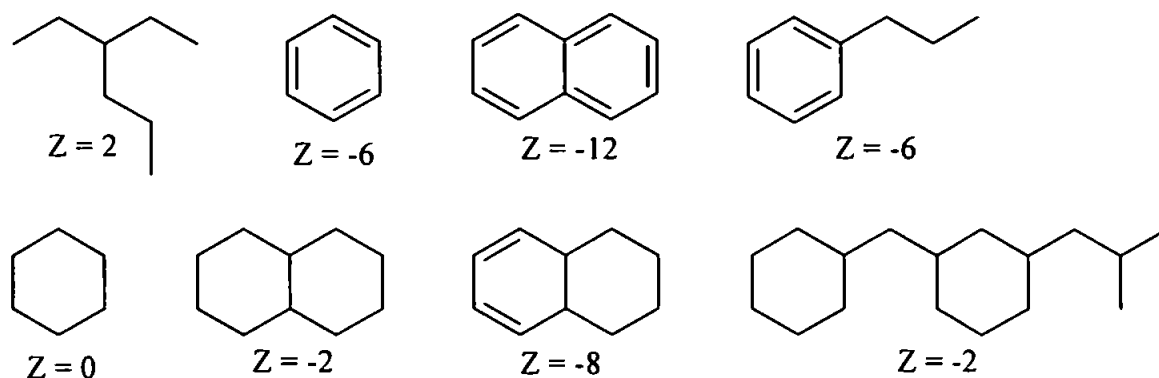


Figure 4. Z-number and structure of various hydrocarbons.

So, a FIMS analysis of an alkane fraction showing a dominant series of peaks with masses including 324, 338, 352, 366, (increasing by 14) shows that the fraction comprises mainly saturated acyclic alkanes (C_nH_{2n+2}). A FIMS analysis of a monoaromatic fraction would be dominated by a $Z = -6$ series. Using Z numbers to identify compound classes in this way is dependent on obtention of pure fractions. An aliphatic fraction must be free from alkenes and aromatics, since for example, an alkylbenzene would have the same Z number as a tetracycloalkane (-6).

Such data from instrumental techniques are vital for the operation of good refinery models, but even these fall short of providing the compositional detail of feedstocks necessary for full optimisation of operations like FCC.

1.2.3 Chemical degradation techniques

Chemical degradation of UCMs before instrumental analysis has already allowed partial structural elucidation of some complex mixtures of hydrocarbons. Use of such techniques has been pioneered in several studies at the University of Plymouth (*e.g.* Gough, 1989; Thomas, 1995) and elsewhere (*e.g.* Killops & Al-Juboori, 1990; Warton, 2000) where the

aliphatic, and more recently the aromatic fractions, of complex hydrocarbon mixtures have been degraded using oxidising agents. The principle behind this approach is use of selective oxidising agents to oxidise specific structural features in a molecule, giving rise to products whose structures can be related back to the parent molecule. The idea of relating UCM degradation products to an original molecule has been called *retro-structural analysis* (Thomas, 1995).

Aliphatic UCMs have been extensively studied (for reviews see Gough, 1989; Revill, 1992). For example, chromium trioxide oxidation of an aliphatic UCM from a lubricating oil produced quantities of resolved *n*-carboxylic acids from the oxidation of T-branched alkanes (Figure 5).

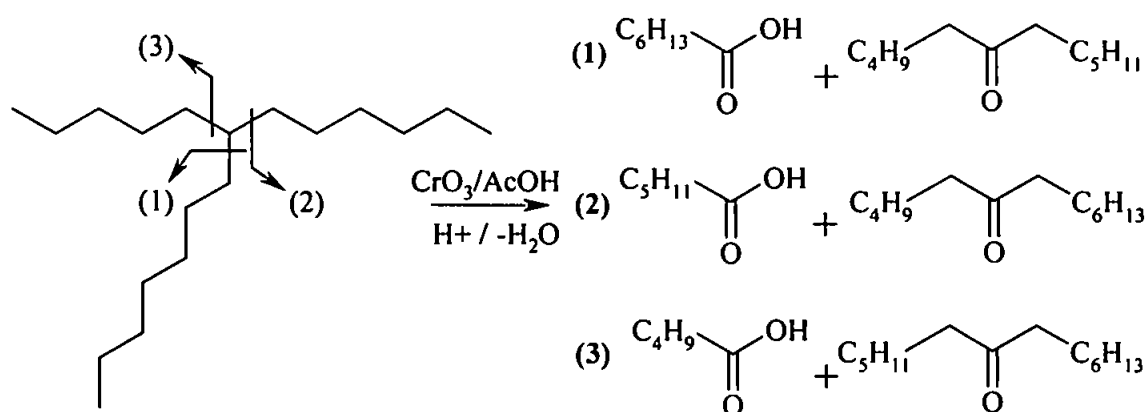


Figure 5. Chromium trioxide oxidation of a T-branched alkane (adapted from Thomas, 1995).

RuO_4 is a useful reagent for the oxidation of a wide range of organic compound classes, including alkenes and aromatic compounds and several reviews on the synthetic and analytical applications are available (*e.g.* Courtney, 1986; Standen, 1992).

Aromatic compounds can be selectively degraded using ruthenium tetroxide (Lee and van den Engh, 1973). RuO_4 is a regio-selective oxidant, in theory attacking only at *ipso*-carbons on an aromatic ring (Figure 6). Alkyl substituents are preserved as a carboxylic acid, whereas aromatic carbons are oxidised further to carbon dioxide.

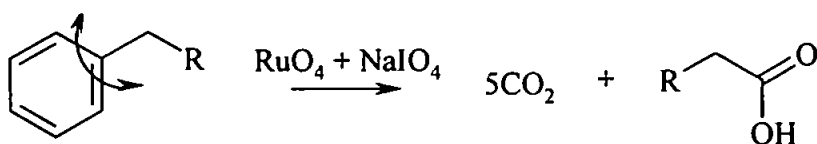


Figure 6. Ruthenium tetroxide oxidation of an alkylbenzene.

A mechanism of the oxidation of naphthalene was proposed by Spitzer and Lee (1975), involving formation of a ruthenium-naphthalene complex, but little is known in detail.

RuO_4 oxidation can be prone to side reactions, the formation of ketones, lactones and other products are reported (Spitzer and Lee, 1974; Stock and Tse, 1983; Thomas, 1995; this study) though in varying proportions depending on the reaction conditions.

Thomas (1995) oxidised aromatic fractions from a biodegraded crude oil using ruthenium tetroxide. With a *retro*-structural analytical approach, Thomas was able to propose several structures as typical components of these fractions (Figure 7).

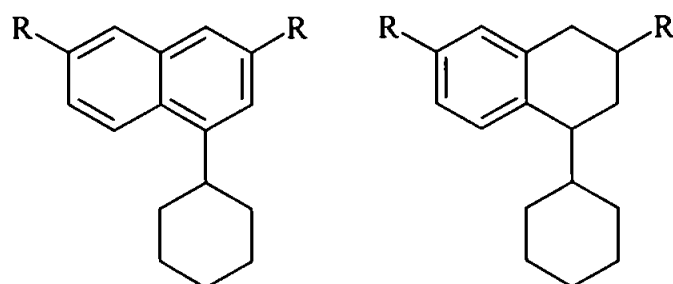


Figure 7. Structures suggested as typical UCM components. (Thomas, 1995)

The work of the above authors has increased the current knowledge of UCMs. However, some problems were experienced in recovering all of the products from the RuO_4 oxidation of hydroaromatic molecules (see Chapter 4, Method Development).

It is vital to account for all of the oxidation products, since a mass balance approach is essential in deriving a more complete composition for UCMs, especially if the oxidative degradation technique is to be developed for use in optimisation of refinery models.

Therefore the problems of loss of oxidation products must be overcome before the RuO₄ oxidation of feedstocks can be used as an analytical tool.

1.3 Aims of the present study.

The purpose of the present study was to enable better characterisation of heavy petroleum feedstocks in order to optimise a fundamental model of FCC operation and hence enhance production of refined oil fractions of high economic value.

Heavy petroleum fractions are, by definition, highly complex mixtures of hydrocarbons largely unresolved by modern instrumental techniques. Oxidative degradation of unresolved complex mixtures of hydrocarbons (UCMs) has previously been of use in furthering the elucidation of aliphatic and, to a certain extent, aromatic UCMs. In particular, RuO₄ oxidation has shown promise as a selective degradation technique that could effectively make aromatic UCMs more amenable to characterisation.

For instance, Thomas (1995) used RuO₄ to examine aromatic UCMs from several heavy petroleum fractions and was able to propose the structures such as those shown in Figure 7 as 'typical' aromatic UCM components. However, problems experienced with the incomplete recovery of oxidation products from hydroaromatic structures have so far limited the usefulness of RuO₄ oxidation in the retro-structural analysis of aromatic UCMs. The study of Thomas (1995) highlighted the need for a more detailed examination of the oxidation of hydroaromatic compounds and a critical appraisal of the RuO₄ method in order to maximise recovery of oxidation products and to achieve mass-balance.

Also, since the purpose of the present study was to improve the BP Amoco FCC computer model, it was necessary to determine whether data that could feasibly be obtained from the RuO₄ oxidation of feedstocks would actually have some effect on the predictions of the model.

Thus, these somewhat disparate requirements for UCM characterisation, if studied in a coherent programme of research, could lead to improvements in the refining of crude oil, with all the economic and environmental benefits that would entail. This could only be realised by integration of the results of some very specific aims;

- Examination of the effects of changing inputs of feedstock compositional data on the operation and sensitivity of a fluidised catalytic cracker (FCC) computer model, (Chapter 3).
- Investigation of improved oxidation methods of characterisation of complex oil feedstocks in order to provide more complete and appropriate data for input into FCC computer model, (Chapter 4).
- Optimisation of the above methods by careful calibration using synthetic model feedstock hydrocarbons. A number of hydrocarbons were therefore synthesised herein specifically for this purpose, (Chapters 5 & 6).

2 *Experimental*

This chapter describes the practical aspects of the study in detail, from synthesis of model compounds to their oxidation and analysis.

2.1 Reagents and consumables

Organic solvents used were of HPLC grade from Rathburns (Walkerburn, Scotland). The purity of solvents was monitored by rotary evaporation of 100 mL solvent to 1 mL and analysis by GC and GCMS. New bottles of solvents were invariably found to be 'clean', but older bottles were rejected if any compounds other than solvent were present, (*e.g.* phthalate plasticisers).

De-ionised water was obtained from a MilliQ system.

Sodium-dried diethylether and toluene were prepared by extruding sodium wire into a 2.5L bottle of HPLC grade solvent.

Anhydrous sodium sulphate, silica, Fuller's Earth, cotton wool and sand were all pre-extracted by with DCM (Soxhlet 24 h).

Silica (Aldrich, 60-100 mesh) was activated at 120°C overnight (18 h), cooled in a dessicator and the required deactivation achieved by adding the appropriate percentage of de-ionised water and homogenisation by shaking (mechanical shaker, 1 h).

Alumina (Merck, 60-100 mesh) was activated at 450°C overnight (18 h), cooled in a dessicator and the required mass of de-ionised water added for the desired deactivation. Homogenisation was by mechanical shaker (1 h).

All glassware was cleaned by soaking in a bath of 2% Decon (24 h), rinsing under hot tap water, then distilled water followed by drying overnight in an oven at 120°C.

Glassware and glass storage vials were solvent-rinsed prior to use.

Argentation TLC plates were prepared on acetone-washed 20cm x 20cm plates and spread with an aqueous slurry of silica gel (Merck 60G kieselgel). The plates were dried (120°C ~1 h) and pre-eluted with a 10% w/v solution of silver nitrate in acetonitrile. The plates were re-activated prior to use and stored in the dark.

2.2 Analyses

2.2.1 Gas Chromatography (GC)

GC analysis was carried out on a Hewlett Packard (HP) 5890 Series II gas chromatograph equipped with a 12m x 0.25mm i.d. wall coated open tubular (WCOT) fused silica capillary column coated with methylsilicone stationary phase (HP-1, Hewlett Packard). Hydrogen carrier gas with flame ionisation detection was used, with samples introduced by a HP 6370 autosampler into a split/splitless injector (typically splitless, purge valve closed for 90s).

The GC oven was typically programmed from 40°C - 300°C at 5°C min⁻¹, held 10 min.

The signal from the detector was fed *via* a Philips PU 6030 data capture unit to a personal computer running Unichem 4880 chromatography data software (v1.11, Unicam Ltd., Cambridge). Quantification of analytes was performed off-line using internal standards and response factors where obtainable.

2.2.2 Gas Chromatography Mass Spectrometry (GCMS)

Two instruments were used for GCMS analysis; a Hewlett Packard MSD 5970 Chemstation interfaced with a HP 5890 gas chromatograph fitted with a 12 m x 0.25 mm i.d. WCOT capillary column with 100% methylsilicone stationary phase (HP-1, Hewlett Packard) with helium carrier gas.

A Finnigan MAT GCQ Mass Spectrometer was also used, interfaced with a Finnigan MAT GCQ gas chromatograph having a split/splitless injector and 25m x 0.25mm i.d. WCOT with 5% phenylsilicone / 95% methylsilicone stationary phase (DB5, J & W Scientific) column with helium carrier gas.

Typical GC programmes for GCMS analyses were 40 – 300°C @ 5°C min⁻¹, held 10 min, or 40 – 300°C @ 10°C min⁻¹, held 10 min.

2.2.3 Infrared Spectroscopy (IR)

A Brüker IFS-66 FTIR spectrometer was used to obtain infrared spectra. Liquid samples were analysed as thin films between NaCl windows. Solid samples were determined as KBr discs. Spectra were background subtracted.

2.2.4 Nuclear Magnetic Resonance Spectroscopy (NMR)

¹³C, DEPT and ¹H NMR spectra of samples (~50 mg dissolved in deuterated chloroform) were recorded using a Jeol 270MHz high resolution FT-NMR spectrometer.

2.3 Ruthenium tetroxide oxidation

2.3.1 Original apparatus

The apparatus used for preliminary ruthenium tetroxide oxidations was the unmodified apparatus described by Thomas (1995).

The system consisted of an oxidation vessel seated in a water bath (Figure 8). A constant flow of nitrogen was used to flush gases and volatiles produced by the oxidation through the first trap (pyridine/ethanol) to a CO₂ trap. The system was closed for the duration of the oxidation, typically 24 h.

A detailed critical examination of each stage of the original oxidation procedure, including the work-up of the oxidation products, can be found in Chapter 4.

The first vessel, a 2-neck 25 mL round bottomed flask (rbf) contained the reaction mixture: a slow stream of nitrogen was introduced *via* a short Pasteur pipette held in a thermometer adapter – a Teflon liner was used to avoid contact of the reaction mixture with the silicone washer. The gas was directed over the surface of the oxidation mixture, flushing any gaseous oxidation products through a micro-condenser and into the first Dreschel bottle containing an equal-volume mixture of pyridine and ethanol.

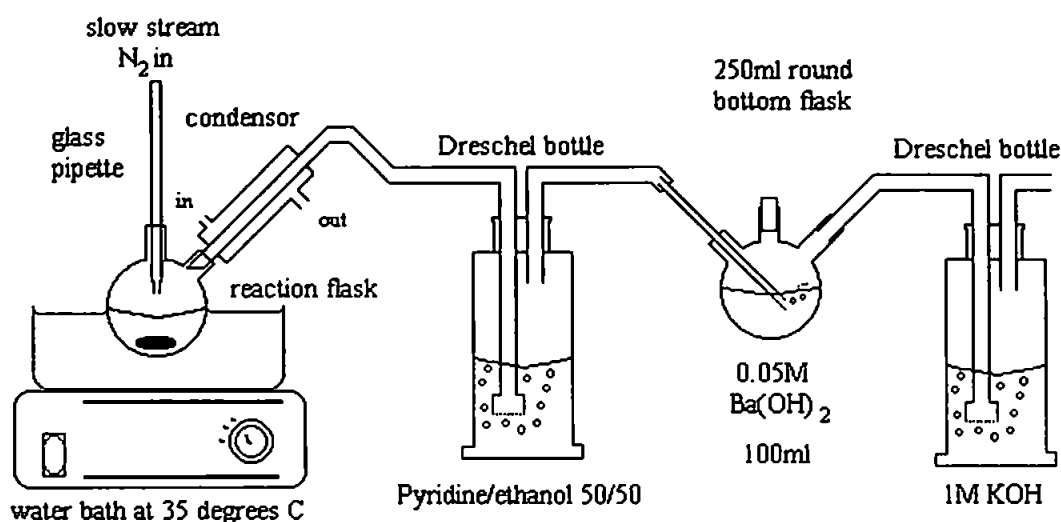


Figure 8. Original apparatus for ruthenium tetroxide oxidation.

The gas flow was then directed into the CO_2 trap. The trap consisted of a 250 mL 3-neck rbf, filled with 100.00 mL aqueous 0.1M $Ba(OH)_2$ (BDH, England, used as supplied). The nitrogen/ CO_2 was bubbled through the solution using a glass Pasteur pipette held in the left-hand neck by a thermometer adapter. The vertical neck was stoppered for the duration of the oxidation. A final Dreschel bottle containing aqueous 1M KOH completed the set-up, preventing air from entering the CO_2 trap. Connections between the flasks and Dreschel bottles were made using flexible silicone tubing.

An oxidation was initiated by adding the substrate (in chloroform solution) to the oxidation flask once the apparatus and reagents were in place. The flask was then closed and left stirring at 35°C for 24 hours.

2.3.1.1 CO_2 determination.

On completion of the 24 h period, the CO_2 trap was removed and the contents immediately titrated vs. 0.1M $HCl_{(aq)}$. Two indicators were used; phenolphthalein turning clear to pink, when the excess $Ba(OH)_2$ had been neutralised, and screened methyl orange

turning green to violet when the solid precipitate of BaCO_3 had completely reacted with the HCl. The difference between the two titres gave the titre for the amount of BaCO_3 produced. It was important that the titration was made slowly as the solid BaCO_3 took some time (with stirring) to dissolve.

2.3.2 Work-up of oxidation products

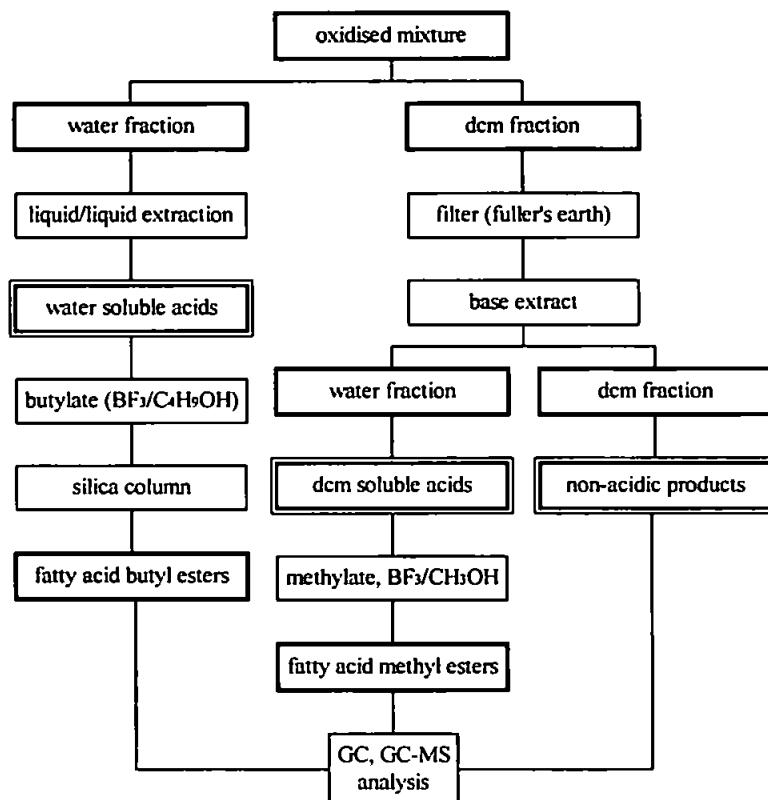


Figure 9. Steps of the post-oxidation work-up.

The contents of the oxidation flask were poured into a separating funnel holding ~30 mL de-ionised water. The oxidation flask was rinsed with ~2 mL each of de-ionised water and dichloromethane (DCM). The Teflon flea was removed.

At this point, the DCM fraction was yellow, indicating the presence of RuO_4 . Once the solid sodium periodate was all dissolved, the DCM fraction turned gradually green then black, indicating a change in oxidation state of the ruthenium. As soon as the active ruthenium species were absent (i.e. no yellow colour), hexanoic acid and pentadecanoic acid (10 mg each as a solution in ethanol) were added as internal standards.

The lower DCM layer was removed, and the aqueous layer extracted with 2 x 5 mL portions of DCM. The combined DCM fraction was then back-washed with 3 x 5 mL portions of de-ionised water and the water washings combined with the aqueous fraction.

2.3.2.1 Water-soluble fraction

The aqueous fraction was acidified to pH 2, then placed in a liquid/liquid extractor and extracted with diethylether (300 mL) for 24 h. The subsequent ethereal extract often contained a significant amount of water and required drying using anhydrous sodium sulphate before it could be rotary evaporated to ~2 mL. The extract was then transferred to a 3 mL Reacti-vial® and the remaining solvent removed under a stream of nitrogen.

The water-soluble fraction was then derivatised for analysis by GC. BF₃/butanol 1 mL (Supelco) was added to the contents of the Reacti-vial®, the vial was then closed (plastic cap and Teflon coated rubber septum) and sonicated for a few minutes to encourage dissolution of the contents. The Reacti-vial® was then heated (80°C, 30 min) in an oven. On cooling, the contents were transferred to a separating funnel using 3 x 2 mL DCM, washed with 3 x 100 mL de-ionised water to remove as much butanol as possible and dried with anhydrous sodium sulphate.

Remaining traces of butanol were removed by passing the mixture through a 5% w/w deactivated silica column (~5g silica, 25 x 1cm column, prepared as a slurry in DCM), using 3 column volumes of DCM. The DCM eluent was then rotary evaporated and remaining solvent removed with a stream of nitrogen.

The sweet-smelling butyl esters were then examined using GC and GCMS.

2.3.2.2 DCM fraction.

The DCM fraction was first dried with anhydrous sodium sulphate. Colloidal ruthenium species (greeny-black) were then removed by vacuum filtration through a layer of

Fuller's Earth. The Fuller's Earth was prepared by stirring 1-2g with ~10 mL DCM in a small beaker, then pouring quickly onto a GF/A glass fibre filter paper held in a 7cm Büchner funnel. The filtrate was colourless, indicating the complete removal of the ruthenium species.

The DCM fraction was then base-extracted in order to separate the acidic oxidation products from the non-acidic oxidation products and any unoxidised substrate. The filtered DCM fraction was transferred to a small rbf, the solvent was removed *via* rotary evaporation and ~10 mL of a solution of 10% (w/v) KOH in methanol was added to the flask. A condenser was fitted and the mixture gently refluxed (10 min). On cooling, the contents of the flask were poured into a separating funnel, the flask was rinsed with DCM then de-ionised water. The non-acidic products were extracted into DCM, leaving the DCM-soluble acids in the aqueous fraction as the potassium salts. The aqueous fraction was then acidified to pH 1, and the acids extracted into DCM.

The non-acidic fraction was dried with anhydrous sodium sulphate and the DCM removed (rotary evaporation, nitrogen stream) prior to analysis by GC and GCMS.

The acid fraction was dried with anhydrous sodium sulphate, transferred to a small rbf for rotary evaporation to a few millilitres. The remaining solvent was removed under a stream of nitrogen – using the original rbf.

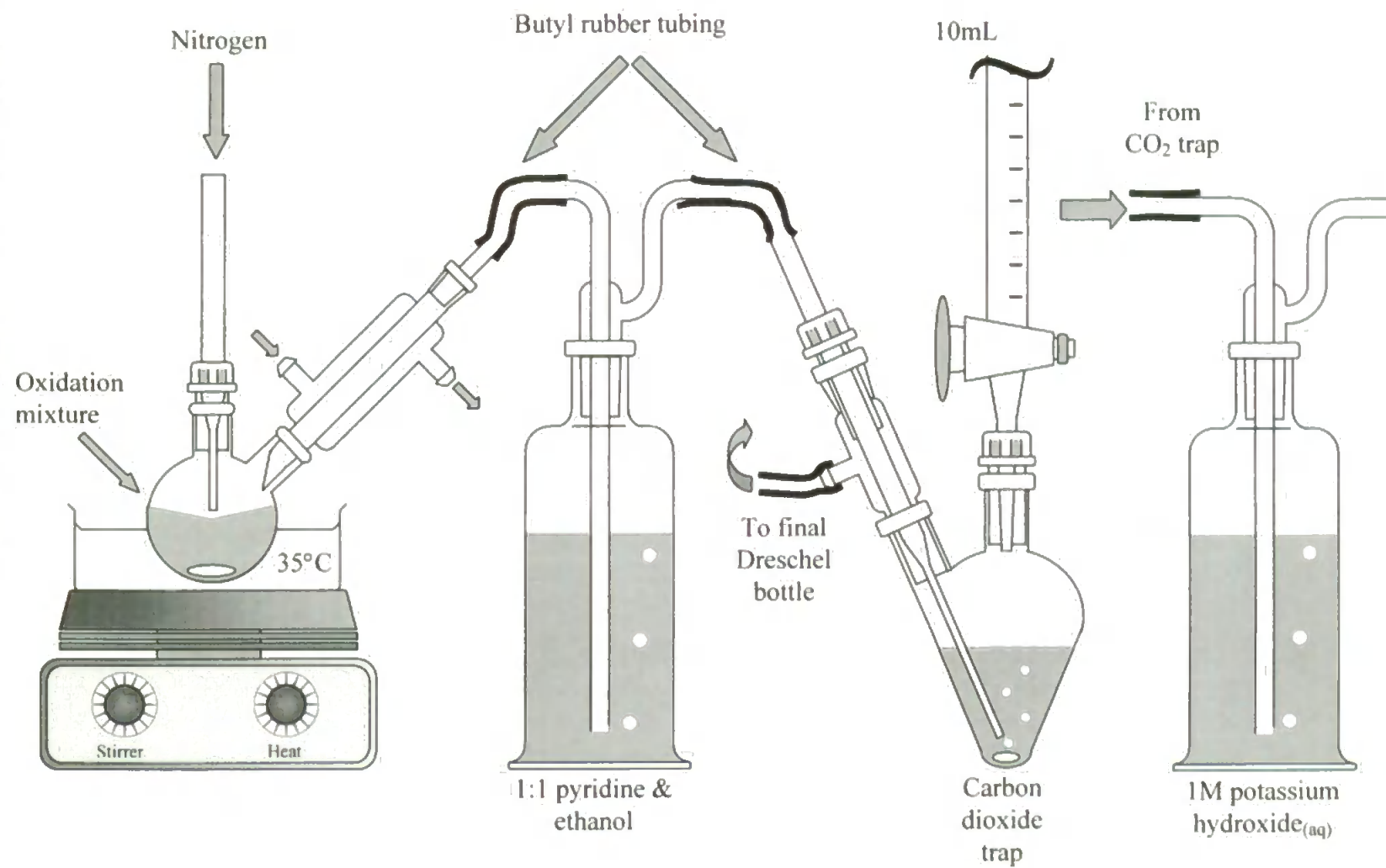
The free acids were methylated prior to analysis by GC and GCMS. Methylation was achieved using a solution of 14% BF₃ in methanol (~10 mL, Aldrich) added to the rbf containing the DCM soluble acids. A condenser was fitted and the mixture gently refluxed (10 min). The contents of the flask were then transferred to a small separating funnel where an excess of de-ionised water was added to neutralise the methylation reagents. The methyl esters were extracted into 3 x 2 mL portions of DCM, back-washed with 2 x 10 mL de-ionised water and dried with anhydrous sodium sulphate. The DCM

fraction was then rotary evaporated and remaining solvent removed using a stream of nitrogen. The derivatised acids were then examined by GC and GC-MS.

2.3.3 Modified apparatus for ruthenium tetroxide oxidations.

Figure 10 shows the modified oxidation apparatus. The major improvement to the apparatus for the oxidation was the new CO₂ trapping system (discussed in Chapter 4, Method Development). The new trap allowed determination of CO₂ *in-situ* without exposing the system to air, thus minimising errors due to incursion of atmospheric CO₂. The oxidation vessel and contents remained largely unmodified. However, the RuCl₃.6H₂O was now more easily added as a solution in de-ionised water. Exactly 1.00 mL of a 2.6 mgmL⁻¹ solution was added once the system has been purged with nitrogen (10 min) to remove trapped air. Purging minimised errors in CO₂ determination due to the presence of atmospheric CO₂. CO₂ trapped before oxidation commenced was neutralised with sodium methoxide solution from the burette (colour change yellow to blue). The RuCl₃.6H₂O solution was then added by syringe *via* the neck holding the N₂ supply to the oxidation vessel.

Figure 10. Modified apparatus for ruthenium tetroxide oxidations.



On leaving the reaction vessel the nitrogen/carbon dioxide stream first encountered the pyridine/ethanol trap, then bubbled through the CO₂ trap. A full description of the CO₂ trap and its development is given in Chapter 4 (Method Development). A 50 mL 2-neck pear-shape flask held an excess of CO₂ absorption solution (~10 mL) comprising a 3:1:3 mixture of ethanol, benzylamine and dioxane, with thymol blue added as an indicator. A thermometer adapter retained a 10 mL volumetric burette in the vertical neck. The burette held ~0.2M sodium methoxide in 3:1 toluene/methanol. A rubber bung in the top of the burette adequately prevented evaporation over the 24 h period of the oxidation.

The sodium methoxide stock solution was made up from analytical grade sodium methoxide (BDH), first dissolved in methanol, then the correct amount of toluene added. The stock solution was regularly standardised against benzoic acid in 3:1 toluene/methanol to account for small amounts of atmospheric CO₂ absorbed during storage. During the oxidation the CO₂ absorption solution was stirred continuously (Teflon flea) to avoid formation of a CO₂-saturated layer.

The final 1M KOH trap provided an air lock, preventing air from re-entering the system. Connections between the four flasks were now made using flexible butyl rubber tubing, in place of the silicone tubing used previously by Thomas (1995).

2.3.3.1 CO₂ determination

At the end of the 24 h period, the rubber bung was removed from the top of the burette held in the CO₂ trap. The contents of the trap (bright yellow) were then titrated with the sodium methoxide (previously standardised) to the endpoint (royal blue). The mixture was stirred during the titration.

2.3.3.2 Work-up of oxidation products

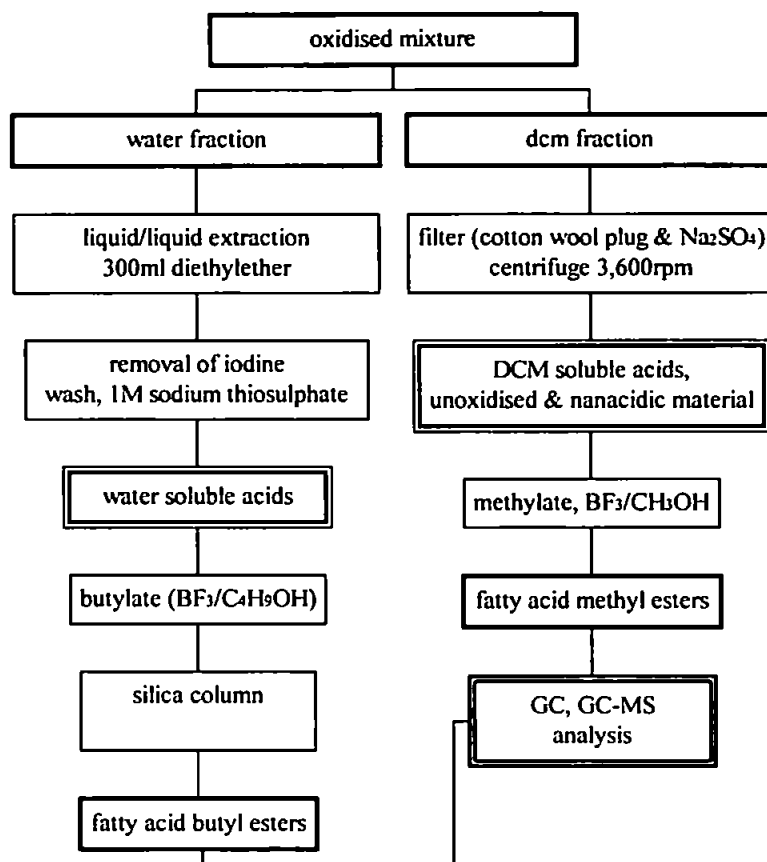


Figure 11. Work-up of oxidation products - schematic.

2.3.3.3 Water-soluble fraction

The aqueous fraction of the oxidation products was largely treated as explained previously (section 2.3.2.1 Water-soluble fraction), although it was observed that iodine (from the breakdown of sodium periodate) was present in significant quantities after liquid/liquid extraction. In order to remove any iodine present, 10 mL of a 1M aqueous solution of sodium thiosulphate was added to the first water wash after the water-soluble acids had been butylated. This removed iodine to the aqueous phase, which was discarded.

2.3.3.4 DCM fraction

The DCM fraction was dried with anhydrous sodium sulphate. The majority of the colloidal ruthenium was removed by a combination of filtering through a small column of finely ground sodium sulphate and centrifuging at 3,600 rpm (20 min). The small amount of ruthenium remaining did not interfere with subsequent stages of the work-up or analysis.

The DCM-solubles were then methylated for analysis. The removal of the base extraction step greatly simplified the work-up, and helped to reduce losses of oxidation products during work-up.

The methylation procedure was simplified by replacing the laborious refluxing step with a technique adapted from the butylation procedure used. After the DCM fraction had been filtered and centrifuged, the volume was reduced to a few mL (rotary evaporation). The DCM solubles were then transferred to a 3 mL Reacti-vial® where the remaining solvent was removed under a stream of nitrogen. 14% BF₃/methanol (~2 mL, Supelco) was added to the vial which was then closed and heated to 60°C in an oven (30 min). The contents of the vial were then transferred to a small separating funnel containing de-ionised water (~10 mL), extracted into DCM (3 x 2 mL portions) and back-washed with de-ionised water (2 x 10 mL portions). The solvent was removed by rotary evaporation and nitrogen stream.

2.4 Organic Synthesis of model UCM compounds.

6-Cyclohexyltetralin, 1-*n*-nonyl-7-cyclohexyltetralin (with 1-*n*-nonyl-7-cyclohexylnaphthalene as a co-product), and 1-(3'-methylbutyl)-7-cyclohexyltetralin were synthesised, essentially using the methods developed with Wraige (1997; Figure 12).

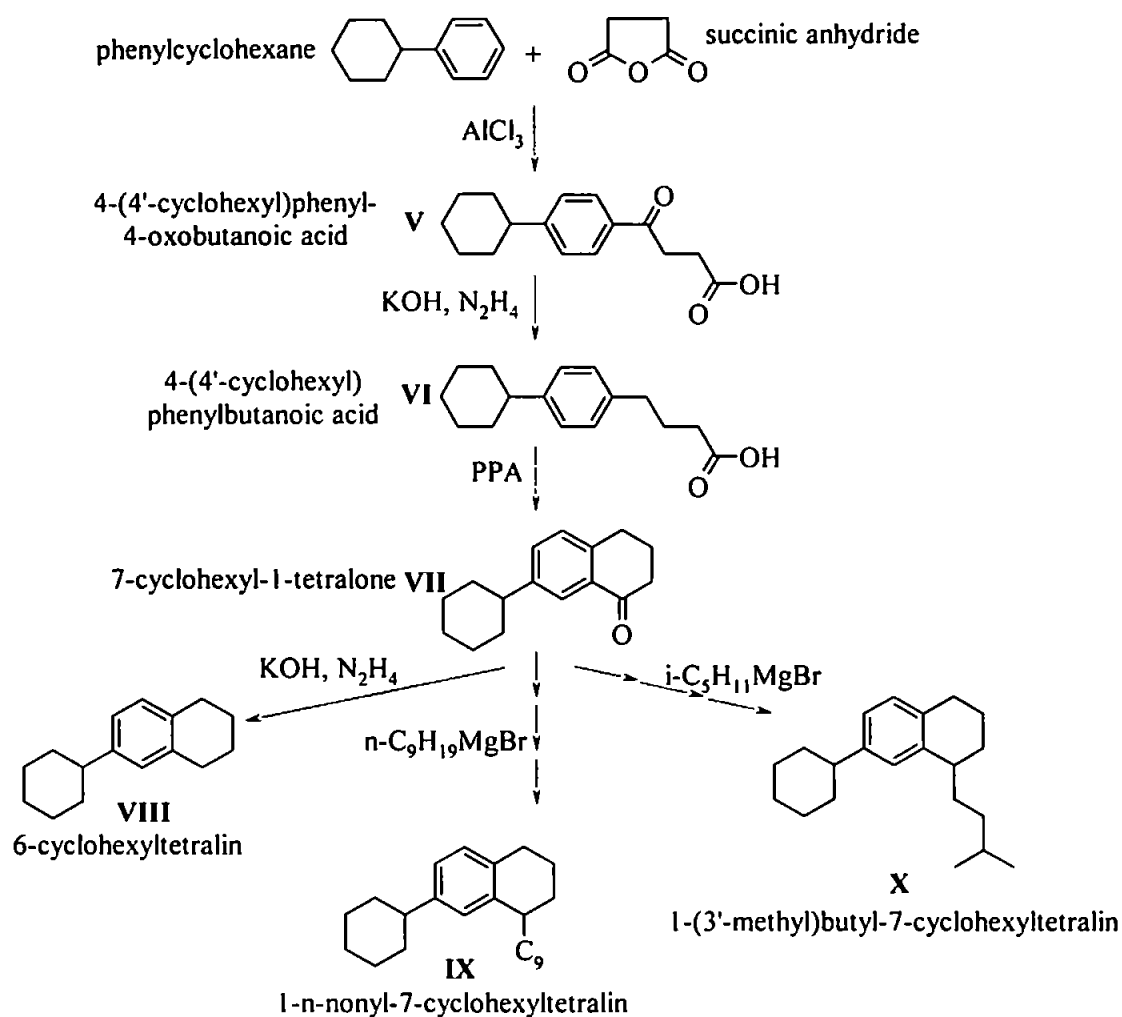
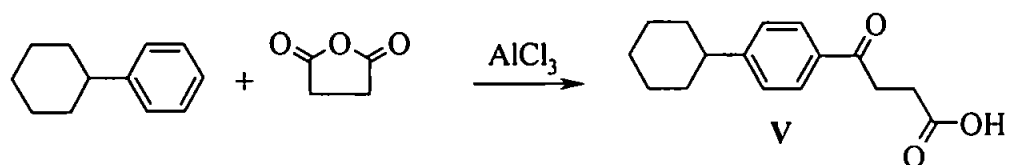


Figure 12. Scheme for the preparation of alkyl substituted cyclohexyltetralins.

2.4.1 Preparation of 4-phenyl-(4'-cyclohexyl)-4-oxobutanoic acid (V)



Preparation of 4-phenyl-(4'-cyclohexyl)-4-oxobutanoic acid (V) was achieved using Friedel-Crafts acylation of phenylcyclohexane. General details of Friedel-Crafts reactions can be found in March (1992) and Vogel (1989).

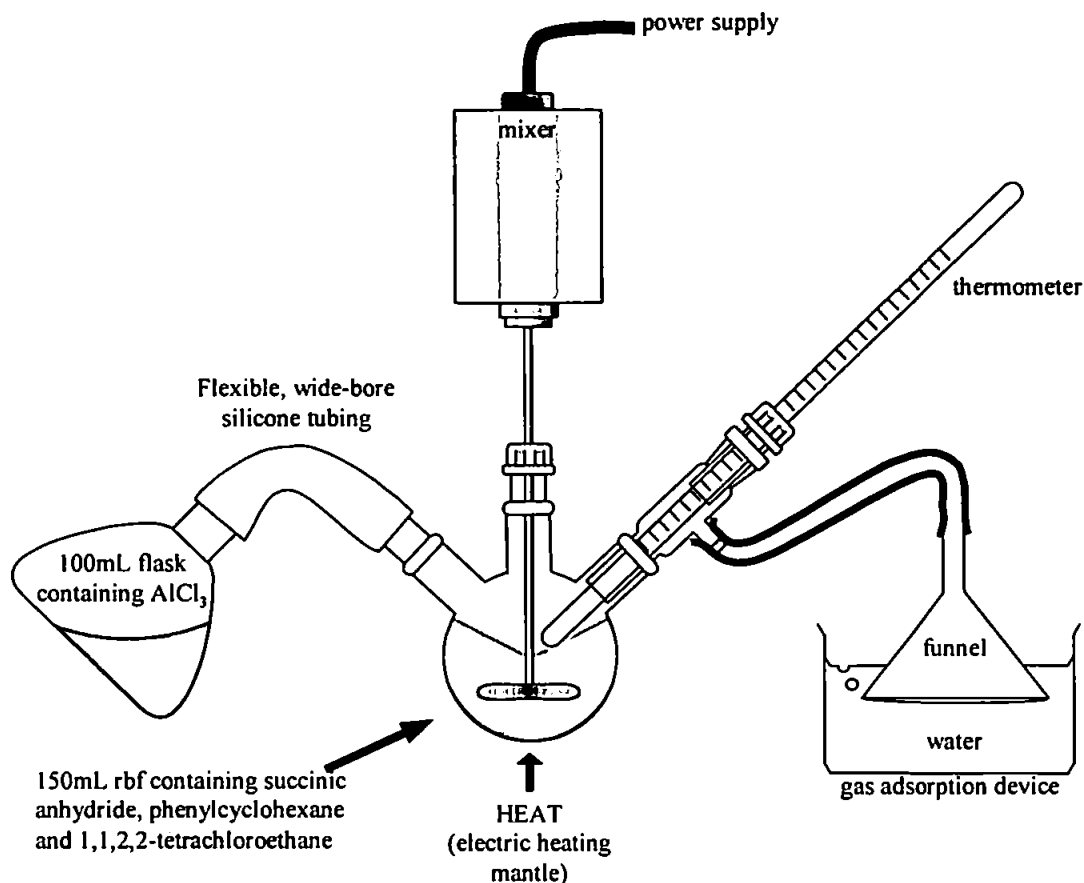


Figure 13. Apparatus for the Friedel-Crafts acylation of phenylcyclohexane.

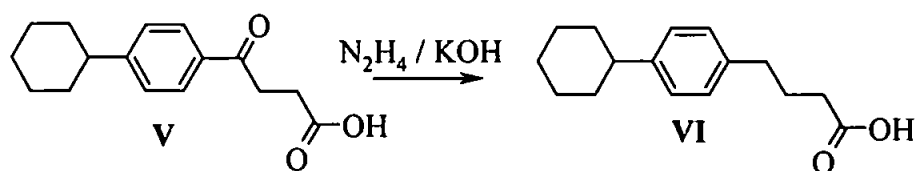
The apparatus was assembled as above (Figure 13). Typically, phenylcyclohexane (0.1 mol, 16.00 g), succinic anhydride (0.12 mol, 12.00 g) and 60 mL 1,1,2,2-tetrachloroethane were placed in the rbf, heated (80°C) and stirred to dissolve the succinic anhydride. AlCl_3 (0.24 mol, 32.00 g) was finely ground in a pestle and mortar and placed in the 100 mL flask attached to the rbf. Once the succinic anhydride was fully dissolved, the mixture was allowed to cool to room temperature. Portions of the AlCl_3 were added slowly with vigorous stirring. The temperature of the mixture was monitored and kept below 80°C by slowing the addition of AlCl_3 . The mixture was observed to turn orange then dark red during the addition of AlCl_3 . The mixture was stirred for a further 30 min, then poured carefully onto ice held in a 300 mL glass beaker and stirred with a

glass rod (HCl fumes were evolved). 150 mL of 2:1 water : conc. HCl was carefully stirred into the mixture.

The contents of the beaker were transferred to a 500 mL rbf equipped for distillation. The mixture was steam distilled, extra water being added from an addition funnel to maintain ~300 mL liquid in the flask. 1,1,2,2-tetrachloroethane was separated from the distillate collected and ~95% of the solvent was recovered from the mixture in ~3 h. Colour changes of the organic layer observed during steam distillation were light yellow – yellowish green – dark green and finally beige on cooling. The hot mixture was poured into a 500 mL beaker before cooling.

The crude 4-phenyl-(4'-cyclohexyl)-4-oxobutanoic acid (V) formed a solid mass with Al₂O₃ (from the hydrolysis of AlCl₃) entrained on cooling. Most of the aqueous layer was removed and the mass of crude product was dissolved by boiling with 5% NaOH_(aq). At this point the solution was a dark brown, thus decolourising carbon (1 g) was added and the solution filtered hot. Conc. HCl was then added dropwise with stirring until the supernatant was acidic (litmus). The finely divided mixture of crude product and Al₂O₃ was filtered and water washed before adding ~200 mL of 1M NaCO₃ to dissolve the 4-phenyl-(4'-cyclohexyl)-4-oxobutanoic acid (V). Al₂O₃ was then filtered off and discarded. The remaining filtrate was treated with conc. HCl dropwise until no further precipitate formed. The creamy yellow crumb-like precipitate was filtered, water washed and dried overnight (40°C). The mass of product was 22.5g, giving a yield of 87%. Purity by GC was 95%.

2.4.2 Preparation of 4-phenyl(4'-cyclohexyl)butanoic acid (VI)



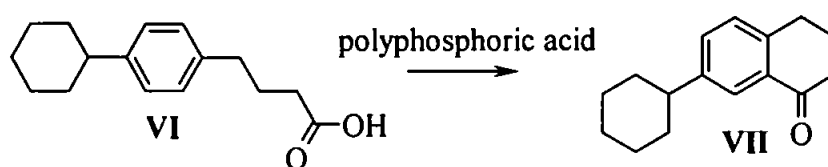
Preparation of 4-phenyl(4'-cyclohexyl)butanoic acid (VI) was achieved using the Huang-Minlon adaptation of the Wolff-Kishner reduction (Huang-Minlon, 1946).

Typically, KOH (0.1 mol, 6 g) and diethylene glycol (40 mL) were placed in a 3-neck 100 mL rbf equipped with reflux condenser and thermometer. The mixture was heated (electric heating/stirring mantle) and stirred until the KOH dissolved. 4-Phenyl-(4'-cyclohexylbenzene)-4-oxobutanoic acid (V, 0.048 mol, 12.47 g) and hydrazine hydrate (98% pure, 0.07 mol, 3.6 mL) were added and the mixture refluxed (~136°C) for 1 h. The reflux condenser was replaced with distillation apparatus and the mixture distilled until the temperature of the liquid in the flask reached the boiling point of diethylene glycol (241 – 248°C). The reflux condenser was then replaced and the mixture refluxed for a further 4 h.

When the mixture was cool enough to handle with gloves it was poured onto ice in a 200 mL beaker. The contents were then acidified (Congo red) by dropwise addition of conc. HCl. The aqueous layer was decanted off and discarded. Clean water was added and the contents left stirring overnight.

The sticky brown solid was removed from the beaker and dissolved in diethyl ether (100 mL, 200 mL conical flask). Decolourising carbon (~1 g) and Na₂SO₄ (~5 g) was added and the mixture boiled gently for 1 min by placing the flask in a bowl of hot water. Filtration of the mixture yielded a pale yellow solution which was rotary evaporated to remove the solvent. A clear brown oil (10.8 g) was obtained as the crude product giving a yield of 91.5%. Purity by GC was 98%.

2.4.3 Preparation of 7-cyclohexyl-1-tetralone (VII)

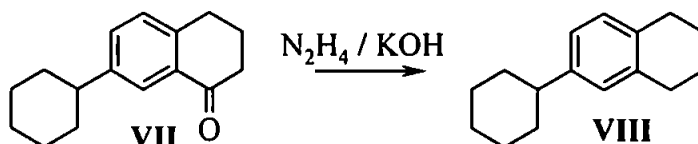


Preparation of 7-cyclohexyl-1-tetralone (VII) was achieved using hot polyphosphoric acid (PPA); *e.g.* March, 1992; Vogel, 1989.

Typically, PPA (26.5 g) was heated in a glass beaker on a hotplate (90°C). 4-Phenyl(4'-cyclohexyl)butanoic acid (VI, 0.044 mol, 10.8 g) was also heated (~70°C) and added quickly to the PPA. The brown mixture was stirred with a glass rod for ~30 min after which a further 22g hot PPA was added. The mixture was stirred for a further 5 min after which the beaker was removed from the hotplate and the contents allowed to cool to ~60°C. Crushed ice (~100 g) was added to the contents of the beaker and stirred until a thick brown oil separated from the aqueous layer. The contents of the beaker were then transferred to a 500 mL separating funnel. Portions of diethylether (3 x 50 mL) were used to extract the oil from the aqueous layer. The combined diethylether extracts were washed (5% NaOH_(aq) 2 x 50 mL) followed by washing with water until the washings were neutral. The orange coloured diethylether solution was dried (Na₂SO₄) then rotary evaporated to remove as much diethylether as possible. The crude product, 7-cyclohexyl-1-tetralone (VII), was a thick red/brown oil, with a characteristic smell.

The yield of 7-cyclohexyl-1-tetralone (VII) was 89%. Purity by GC was >90%.

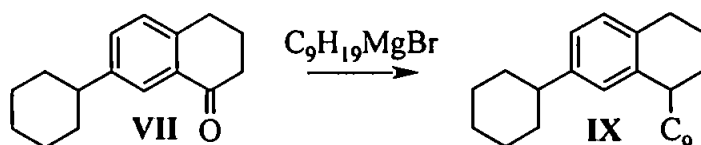
2.4.4 Preparation of 6-cyclohexyltetralin (VIII)



The preparation of 6-cyclohexyltetralin (VIII) followed the same procedure for the reduction of a ketone described in section 2.4.2 (Preparation of 4-phenyl(4'-cyclohexyl)butanoic acid (VI)).

Purification was effected by column chromatography (elution through 5% deactivated silica with 3 column volumes of pentane) the yield of 99+% pure product (by GC) was 3g (99%). 6-Cyclohexyltetralin is a colourless, odourless, viscous liquid.

2.4.5 Preparation of 1-n-nonyl-7-cyclohexyltetralin (IX)



A 3-neck, 100 mL rbf was fitted with an addition funnel, condenser and nitrogen line. All glassware, magnesium turnings (0.1 mol, 2.4 g) and Teflon flea were dried in an oven at 120°C for at least an hour. The glassware was assembled hot, and the N₂ flow established before it had cooled. This ensured that no moisture was present in the reaction vessel. The tops of the condenser and addition funnel were fitted with drying tubes filled with calcium chloride.

Diethylether (25 mL, Na dried) was placed in the rbf with the magnesium *via* the addition funnel. 1-Bromononane (0.1 mol, 21.07g, AnalaR, Aldrich) was dissolved in diethylether (25 mL, Na dried) and placed in the addition funnel. 5 mL of the bromononane solution was then added to the rbf. The rbf was gently heated and stirred (electric heating mantle/stirrer). After 10-20 minutes a cloudy precipitate was observed, indicating the formation of the Grignard reagent C₉H₁₉MgBr. The remainder of the bromononane solution was added dropwise, with continued stirring. The heat of the reaction kept the mixture refluxing gently. The rate of addition of the bromononane was varied to keep the mixture just refluxing. The mixture was now a black/grey cloudy solution. Once all the bromononane solution was added, the mixture was left to reflux for ~½ h. 7-Cyclohexyl-1-tetralone (VII, 0.033 mol, 7.5 g) was dissolved in diethylether (25 mL, Na dried) and placed in the addition funnel. The 7-cyclohexyl-1-tetralone (VII) solution was added

dropwise and the flow controlled to keep the mixture refluxing gently. The mixture was kept refluxing for 1-1½ hours, by which time the mixture in the rbf was viscous and mustard coloured. On cooling, the mixture was poured onto ice and neutralised with saturated NH₄Cl solution. The organic products were extracted into diethylether and washed with de-ionised water (2 x 25 mL). The mass of crude product after rotary evaporation was ~20g. A significant amount of diethylether still entrained within the mixture (by smell) made it impossible to calculate the yield of crude product.

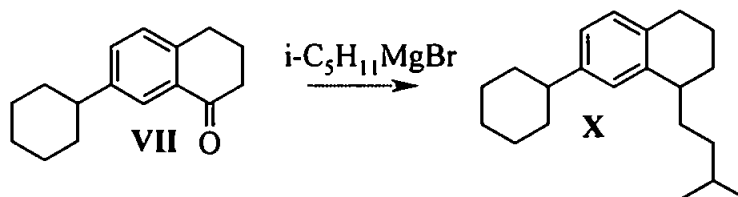
The crude product consisted of octadecane, 7-cyclohexyl-1-tetralone (VII), 1-*n*-nonyl-7-cyclohexyltetralin (IX), 1-*n*-nonyl-7-cyclohexylnaphthalene (XI) and 1-methyl-7-cyclohexyltetralin.

Large-scale open column chromatography was used to separate the mixture. Several large-scale columns were used: 70cm x 3cm i.d. Holding 115g 1.5% deactivated alumina, packed as a slurry in hexane and eluted with hexane. 1-1.5g of crude product applied to each column. Fractions were collected in 8 mL glass vials and solvent removed with a nitrogen stream. GCMS examination of selected fractions showed separation by number of aromatic rings; octadecane was unretained, 1-*n*-nonyl-7-cyclohexyltetralin (IX) eluted before 1-*n*-nonyl-7-cyclohexylnaphthalene (XI).

The monoaromatic fractions were shown to consist of three main components; unsubstituted 6-cyclohexyltetralin (VIII), 1-methyl-7-cyclohexyltetralin and 1-*n*-nonyl-7-cyclohexyltetralin (IX), with the nonyl homologue making up the majority (~50%). Rather than attempt a further separation of these components it was decided to use the fraction since an examination of the oxidation behaviour of such a mixture might prove informative.

The diaromatic fractions were largely 1-*n*-nonyl-7-cyclohexylnaphthalene (XI, 90+% by GC), with impurities of the unsubstituted and methyl homologues present in only some of the fractions. The purest fractions were combined and used in the oxidation studies.

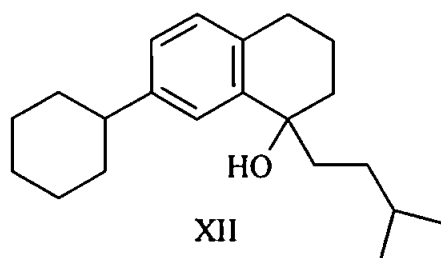
2.4.6 Preparation of 1-(3'-methylbutyl)-7-cyclohexyltetralin (X)



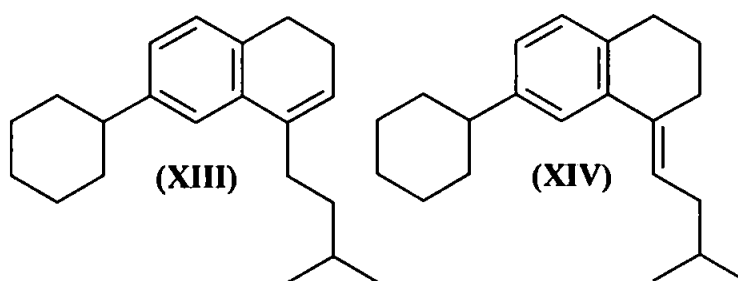
Glassware as described above for Grignard reactions was assembled straight from the oven, with Mg turnings (0.012 mol, 0.29g, freshly made) and a Teflon flea in place. A flow of nitrogen was established. Diethylether and toluene (25 mL, 1:1 mixture, both Na dried) was added to the flask. 1-Bromo-3-methylbutane (0.012 mol, 1.83 g) and a small crystal of iodine was dissolved in a further 25 mL of the 1:1 diethylether and toluene mixture, and ~5 mL of this mixture added to the flask. After ~5 minutes of gentle heating and stirring a grey precipitate was observed. The remaining 1-bromo-3-methylbutane solution was added drop-wise over a period of 10-20 minutes. After this time it was observed that all of the Mg turnings had disappeared, leaving a brown liquid with a grey precipitate. 7-cyclohexyl-1-tetralone (VII, 0.008 mol, 1.83 g) was dissolved in diethylether and toluene (25 mL 1:1 mixture) and placed in the addition funnel. The substrate was added slowly whilst stirring the mixture. When no apparent reaction was observed, gentle heat was applied and the mixture refluxed for ½ hour.

On cooling, the mixture was poured onto ~100 mL ice in a 500 mL beaker and hydrolysed with sat. NH_4Cl (100 mL). A white precipitate was observed on contact of the reaction mixture with the water/ice. A yellow/brown organic layer separated and was drawn off. The aqueous fraction was transferred to a separating funnel and extracted with

diethylether (2 x 10 mL). The combined diethylether fractions were dried with Na_2SO_4 and rotary evaporated to remove the solvents. The yield of crude product was not calculated due to the large amount of diethylether still present in the mixture. The crude product was 93% pure, excluding toluene, and was identified by IR and GCMS as the tertiary alcohol (XII).



The alcohol was dehydrated by refluxing with a x2 molar excess of orthophosphoric acid (15 min). The cooled mixture was then transferred to a separating funnel where sat. NaCl (5 mL) was added to neutralise any remaining acid. The crude alkene products were then extracted into diethylether (2 x 10 mL), and purified by passing through a large open glass column (45cm x 2.5cm i.d.) of fully deactivated silica. GC analysis of the alkene products (~600 mg) showed two major peaks due to alkene isomers (XIII & XIV, 75% and 13% respectively).



Portions of the alkene mixture were hydrogenated using palladium coated carbon (5% Pd) as follows. Pd/C (40-50 mg) was weighed into an 8 mL glass vial, hexane (6 mL) was added and H_2 bubbled through for 20 minutes. After this period, alkene mixture (100-130 mg) was added to the vial using a syringe and left for 2 h. Further hexane was

added to maintain the level of solvent at ~6 mL. After 2 hours, the solution was filtered through a cotton wool plug in a Pasteur pipette and the solvent removed using a stream of nitrogen. GC analysis of the hydrogenation products showed 100% conversion of the alkenes to the desired product.

3 Computer Modelling of FCC Operation.

Methods of modelling FCC refinery operations are reviewed and the results of modelling experiments with oil company oil characterisation and FCC models are described.

3.1 Introduction

Computer models play a vital part in optimising the efficiency (and ultimately the profits) of many modern industrial processes. The refining industry takes full advantage of the advances in modern computing and is continually developing and improving such computer models, with the aim of predicting accurately the effects of changes in the operation of refinery processes.

Van der Eijk *et al.* (1990) state that ideally such a refinery model “should reflect as closely as possible the physical and chemical processes involved. This in turn calls for chemical resolution at the molecular level.” Whilst this kind of resolution may be possible for the simpler processes in a refinery where the feedstocks are relatively simple mixtures of light hydrocarbons, for processes as complex as FCC, even 10 years after the above review, this is still a considerable challenge.

FCC has been described as the ‘workhorse’ of the refining industry (Al-Enezi & Elkamel, 2000), and as such it is in the refiner’s interest to maximise product and profit from a FCC unit.

Various approaches to modelling refinery processes can be taken. The simpler so-called ‘correlative approach’, where bulk properties of the feed are correlated to product yields and properties is attractive because it requires relatively little analysis or computing power. Al-Enezi *et al.* (1999) presented correlations for the FCC process based on bulk properties of the feed and yields of 11 products, using data from the literature and from pilot and commercial plants. Their correlations gave improved predictions over previously published correlations, and had the advantage that they could be integrated with general refinery software used for planning and scheduling purposes.

The same research group (Al-Enezi & Elkamel, 2000) have also developed a neural network that models the FCC process, taking bulk properties of the feedstock and

predicting yields of 11 product and the Carbon residue¹ value. The authors compared their model to previous correlations and also to a commercial FCC simulator. Each time the neural network gave significantly better predictions.

The alternative approach to modelling is use of a 'first principles' approach. That is, taking individual components of a feedstock and determining exactly how they will react under given conditions. Such fundamental models are far more complex than those used in the correlative approach, requiring detailed information on every aspect of the FCC unit, including a complete composition of the feedstock, catalyst properties and FCC conditions. The major problem here of course, is the feedstock composition. Typical FCC feedstocks are highly complex mixtures of hydrocarbons, with metals and other heteroatoms, and complete molecular analysis has so far proved beyond the scope of modern analytical methods (reviewed in Chapter 1 – Introduction).

In such fundamental models the method of describing the feedstock has been determined by the current analytical limitations, early models resorted to 'lumping' – where the many individual components of a feedstock are grouped into measurable categories defined by compound classes or boiling range. These 'lumps' are then connected by simplified reaction networks. Improving analytical techniques have refined the 'lumps' somewhat, but the fact remains that insufficient data exists in the 'lumped' models to forecast small changes in product properties. Quann & Jaffe (1992), introduce their own modification of the lumping technique based on molecular information, so-called 'Structure Oriented Lumping', or SOL. The approach has been developed further to include 3,000 molecular species and 30,000 elementary chemical reactions (Christensen *et al.*, 1999). This new

¹ Carbon Residue – The amount of solid left behind when a sample is pyrolysed in an inert gas. Often given as Conradson carbon residue (CCR) or Micro carbon residue (MCR) referring to the specific equipment and conditions employed, (Gray, 1994).

model can accurately predict bulk yields and also gives good predictions of product composition.

The advantage of using fundamental models over correlative models is that the molecular nature of the data used in fundamental models enables the molecular composition of products to be predicted, and as the precise composition of products becomes more vital for legislative and environmental reasons, such information is desirable.

3.1.1 FCC Modelling at BP

Similar to the SOL approach, the fundamental model used by BP uses a set of 'pseudo-components' to describe the feedstock composition. Pseudo-components are model compounds that reflect the structures of hydrocarbons likely to be found in FCC feedstocks. Liguras & Allen (1989) proposed describing a mixture using hundreds of pseudo-components derived from a set of typical routine analytical data. The model at BP has been under continuous development, and now uses detailed data as outlined in the figure below.

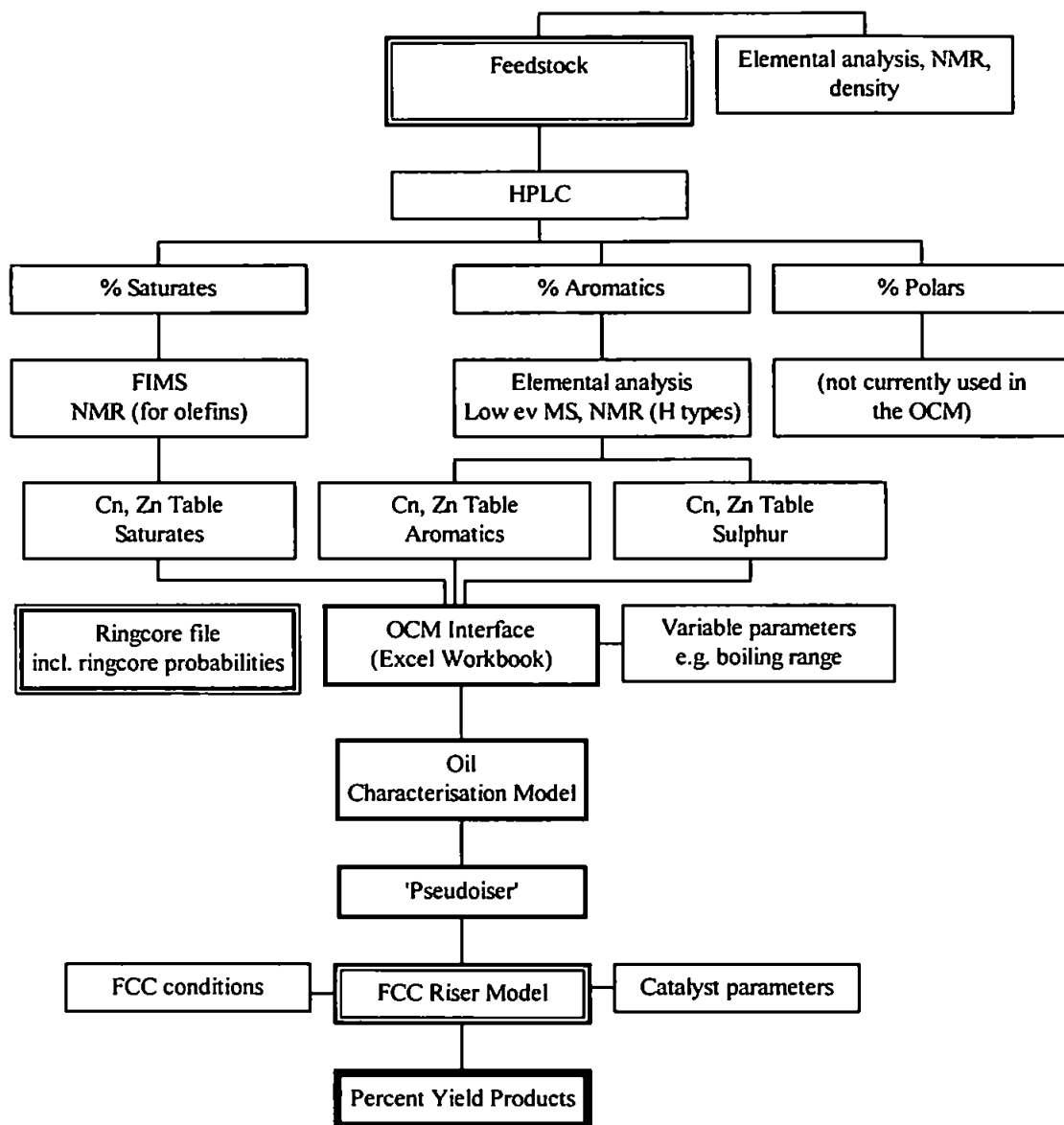


Figure 14. Analytical inputs to the Sunbury Riser Model.

3.1.2 The Oil Characterisation Model (OCM)

The Oil Characterisation Model is a preliminary step in the FCC modelling used at BP. From measured data plus the 'ringcore file', the OCM produces a number of files describing the sample. These files are then used by the 'pseudoiser' (see section 3.1.3) to derive a set of pseudo-components and their relative concentrations, which then are used in the Sunbury Riser Model (SRM).

The OCM is an application program written *in-house* at BP. Put simply, the OCM contains algorithms that take mass spectrometry data and predict physical and chemical properties of the feedstock sample.

Properties predicted by the model include simulated distillation² (sim-dis) data, bulk density and percent aromatic and benzylic hydrogen. These properties can be compared with measured data to ascertain the accuracy of the OCM's prediction of feedstock composition.

The user interacts with the OCM through the 'OCM Interface', a Microsoft® Excel workbook that contains macros which receive the input data and run the OCM. The user is able to vary a series of parameters giving further information on the sample; these too are used by the OCM and will affect the predictions.

The 'ringcore file' is an important input to the OCM. It is a database of the structures of 104 unsubstituted hydrocarbons containing from 1 to 5 aromatic and condensed fused rings. These are the building blocks used by the OCM in generating a picture of feedstock composition (hence the term, *ring-core*). Saturated, aromatic and hydroaromatic structures are included, along with sulphur and nitrogen homologues.

Over thirty parameters that together make up a complete description of the ringcore are included in the ringcore file. Such parameters include number of carbon atoms, Z number, total number of rings, number of aromatic rings, and the numbers of carbon and hydrogen atoms in different environments.

Within the restrictions outlined by the user and the ringcore file, the OCM uses the building block ringcores to construct all the molecules possible by adding alkyl substituents and using alkyl chains to join two or more ringcores. Physical properties of

² Simulated distillation is a widely used gas chromatography technique that recreates the large-scale atmospheric distillation of a feedstock, giving information on its composition.

this mixture of substituted ringcores are calculated by the OCM and sim-dis data is constructed.

Also contained in the ringcore file is a probability for each ringcore. Expressed as a number between one and zero, the probability represents the concentration of individual ringcores. As well as individual probabilities, a grouped probability for hydroaromatics, aromatics, saturates, sulphur and nitrogen can be set *via* the OCM Interface. If there is no prior knowledge of sample history, the probability of each ringcore is set to one; this is called the 'equal probabilities' assumption.

Probabilities for ringcores can be adjusted by examining the process history of the feed. For example, a feed that has been hydrotreated is known to contain a higher proportion of hydroaromatic compounds due to the hydrogenation of aromatic rings. The use of such modified ringcore files has been shown to improve accuracy.

What is ultimately needed however, is a more detailed characterisation of the sample in order to determine the *actual* concentrations of each ringcore; for the largely chromatographically unresolved compounds of real feedstocks, theoretically this could be achieved by analysis of the RuO₄ oxidation products. This will be explained in more detail in section 3.2.

3.1.3 The 'pseudoiser'

'Pseudoisation' is the next step to the SRM. Data produced by the OCM is used to derive the concentration of a set of pseudo-components. There are 94 pseudo-components in the database including aromatic and hydroaromatic structures and also cyclic and acyclic alkanes.

Of six text files produced by the OCM, the 'ring-table file' is used by the 'pseudoiser'. The ring-table file contains matrices of the number of rings vs. the number of aromatic rings for different boiling range 'cuts'. This is used by macros in the 'pseudoiser' Excel

Workbook to calculate a concentration for each of the pseudo-components.

3.1.4 Sunbury Riser Model (SRM)

The newly generated pseudo-component set is entered into the BP model of FCC operation; the Sunbury Riser Model. As previously mentioned, the SRM is a fundamental model, using data for numerous chemical reactions including rate constants and other physical parameters. FCC operating conditions (e.g. temperature and pressure) and catalyst properties (including percent recovery and poisoning rates) are also specified. All of these parameters may be varied, allowing for different catalysts and operating conditions. Thus the effect of these parameters on SRM predictions can be examined.

The SRM calculates the percent yield of products (*i.e.* gas, diesel etc.) that would be achieved under the prescribed conditions. Predicted yields are then compared with real data to determine the accuracy of the model.

3.2 Using data from RuO₄ oxidations

Ideally, analysis of a feedstock would replace the OCM and pseudoiser steps with an analytically (rather than computationally) determined composition of the feedstock. This does not necessarily mean a determination of every species in the mixture, but enough structural and quantitative information for the SRM to accurately model the cracking processes and so predict accurate yields of FCC products. In the meantime however, RuO₄ oxidation of feedstocks should theoretically enable a more accurate calculation of the ringcore probabilities to be made, enabling a more accurate set of pseudo-components to be constructed.

It is therefore necessary to convert data obtained from RuO₄ analyses into a set of ringcore possibilities. The connection between fragments of RuO₄ oxidised aromatic hydrocarbons (*i.e.* various carboxylic acids) and the ringcores is used to generate a new

set of ringcore probabilities.

A simple view of ruthenium tetroxide oxidation is currently assumed, *i.e.* that all aromatic carbons are oxidised to carbon dioxide, and that the only products are the theoretically predicted carboxylic acids. When oxidised by ruthenium tetroxide, a ringcore will produce one or more carboxylic acids and a quantity of CO₂ depending on the number of aromatic carbons. Since the OCM only uses the ringcores specified in the ringcore file, it must also be assumed that the sample only contains molecules derived from those ringcores.

A large proportion of molecules in a feedstock are likely to produce monocarboxylic acids on oxidation as a result of alkyl substitutions on an aromatic portion of a molecule. These provide no information on the structure of the ringcore.

The types of poly-carboxylic acids that are produced from hydroaromatic structures are shown in Figure 15. It must be noted that these are not the only potential sources of poly-carboxylic acids from the oxidation of a complex mixture of hydrocarbons. Figure 16 indicates alternative routes to the formation of poly-carboxylic acids.

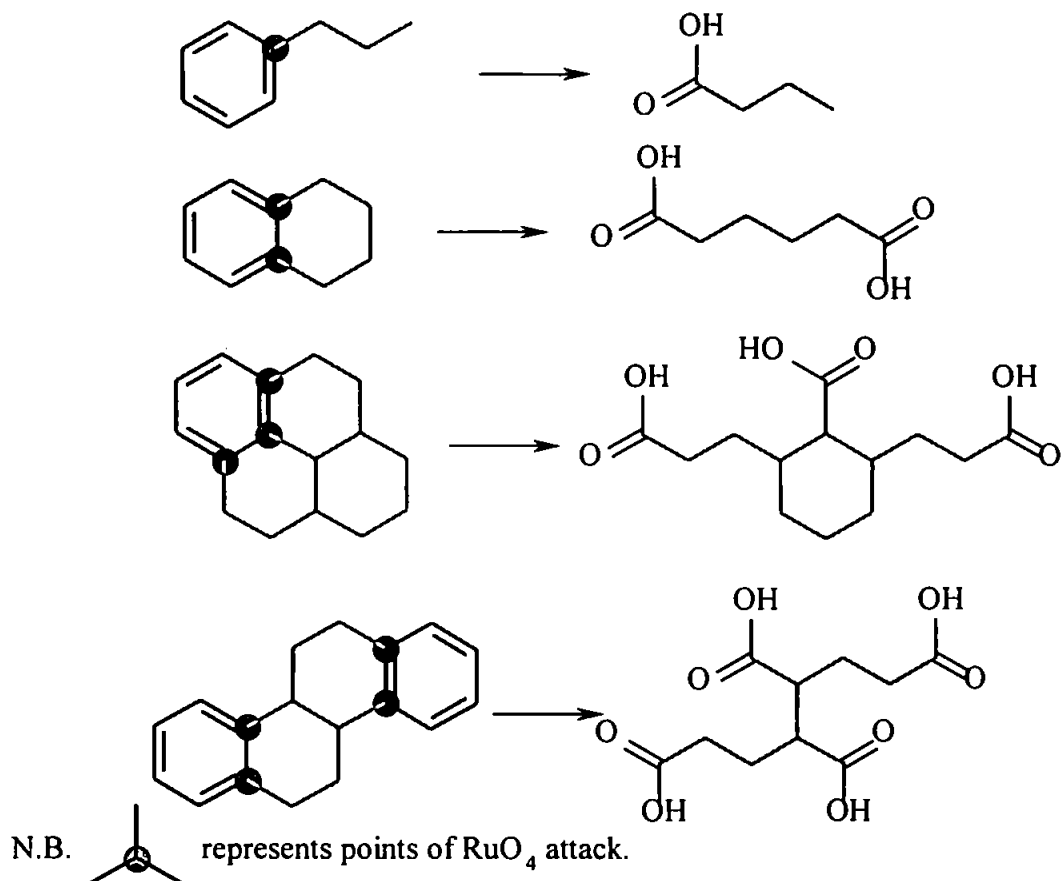


Figure 15. Carboxylic acids produced on RuO_4 oxidation of selected ringcores from the ringcore file.

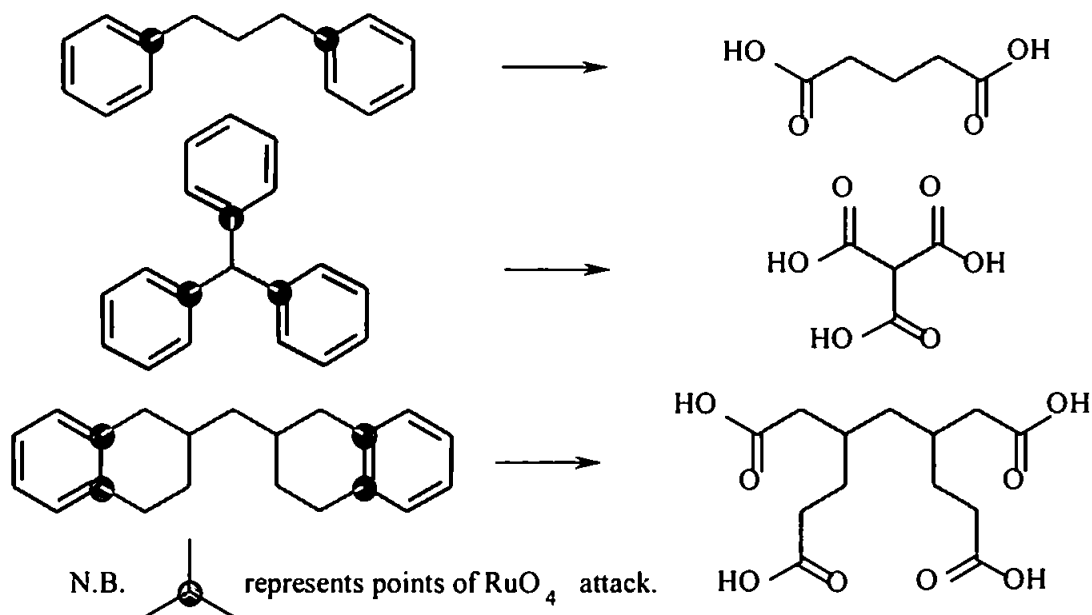


Figure 16. Examples of potential sources of di-, tri- and tetracarboxylic acids from two or more ringcores joined by alkyl bridges.

3.3 Using pseudo- RuO₄ oxidation data to generate new ringcore files.

In order to determine the influence of the extra information that could be determined using RuO₄ oxidation of feedstocks, new ringcore probabilities were calculated from a hypothetical distribution of carboxylic acids that could be produced if a feedstock were oxidised by ruthenium tetroxide.

Macros were written in Microsoft Excel that would take analytical data and calculate a new set of ringcore probabilities, based on the knowledge of which ringcores would produce what type of carboxylic acids upon RuO₄ oxidation. The macros were written by the author during a visit to the BP Research and Engineering Centre, Sunbury-on-Thames.

Two systems were constructed to determine the level of detail required of an analysis. For example, detailed GCMS analysis could determine Z number, number of carboxylic acid groups, molecular mass of products and so on, whereas a simple HPLC analysis could simply give proportions of di-, tri- and tetra-carboxylic acids (e.g. by ion exclusion chromatography – reviewed in Further Work, Chapter 7). If both analyses produce data which have the same effect on the model predictions then common sense (and economy) dictates that the minimum expense and effort be expended for maximum result, and the least detailed (least expensive) analytical technique is adopted.

The Excel Workbook contained two worksheets that had a list of all the possible acids produced from each ringcore. The first worksheet simply distinguishes between the number of carboxylic acid groups in the molecule (*i.e.* di-, tri- and tetracarboxylic acids). This is called ‘simple acid’ information. The second worksheet distinguishes between the number of condensed rings as well as the number of carboxylic acid groups - referred to as ‘complex acid’ information. This reflects two levels of detail that could be achieved in the analysis of the oxidation products.

Each worksheet contained a specially designed macro which requested the percent concentration of each type of acid found. This then generated a new ringcore file from a template. The new ringcore probabilities are calculated as shown below.

$$\frac{\% \text{ acid found}}{100} = \text{ringcore probability}$$

For example, if tetracarboxylic acids made up 5% of the total acidic fraction;

$$\frac{5}{100} = 0.05 \text{ (ringcore probability)}$$

Therefore, a ringcore that would produce a particular acid on oxidation would be given the corresponding probability. Where a ringcore produces more than one acidic molecule on oxidation only the larger is taken into account, since that is likely to be the more specific acid for that ringcore. Figure 3 gives a summary of the procedures involved in using oxidation data for OCM experiments.

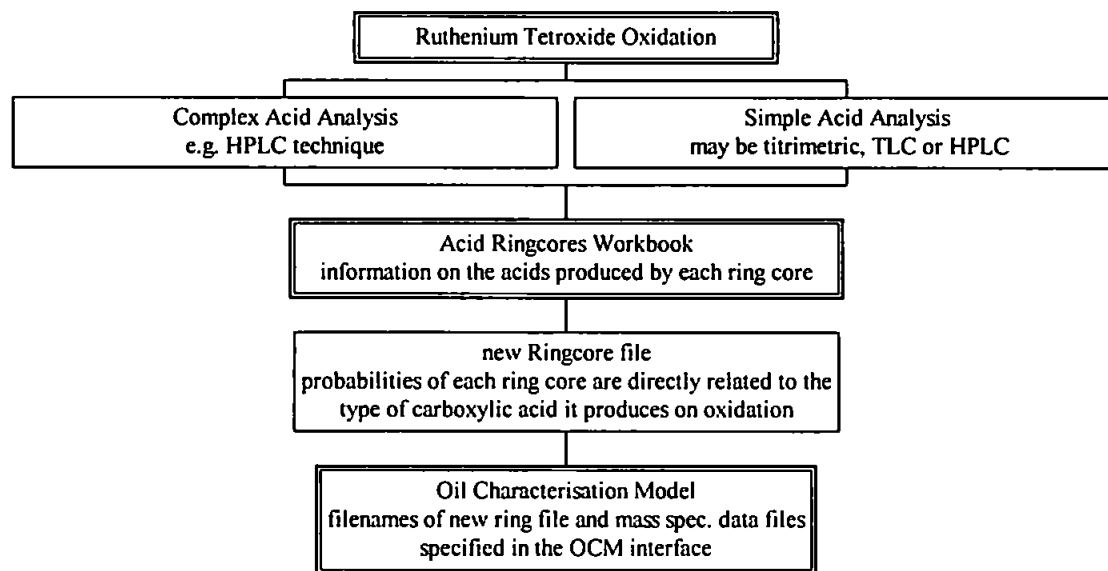


Figure 17. Integrating data from RuO₄ oxidations into the Oil Characterisation Model.

3.3.1 The new ringcore files

The distribution of acid types was varied in order to reflect possible extremes of feedstock composition. It should be pointed out at this stage that accuracy was not an aim

of this exercise; since the hypothetical data on acid distribution is effectively arbitrary, no attempt was made to produce figures close to any actual data. The purpose of this exercise was simply to determine the *influence* of the ringcore files on the OCM predictions, and also to determine the extent to which other OCM parameters influence the OCM predictions. The data used to create the new files are shown in Table 2 and Table 3.

| type of acid | Ringcore file name | | | |
|-------------------|--------------------|-------------------|-------------------|-------------------|
| | complex acid 1 | complex acid 2 | complex acid 3 | complex acid 4 |
| alkyl di-acid | 50 | 50 | 40 | 10 |
| 1 ring di-acid | 30 | 20 | 20 | 10 |
| 2 ring di-acid | 10 | 10 | 10 | 10 |
| 3 ring di-acid | 5 | 3 | 5 | 10 |
| 4 ring di-acid | 5 | 5 | 5 | 10 |
| alkyl tri-acid | 0 | 2 | 5 | 10 |
| 1 ring tri-acid | 0 | 1 | 5 | 10 |
| 2 ring tri-acid | 0 | 1 | 3 | 10 |
| 3 ring tri acid | 0 | 1 | 2 | 10 |
| alkyl tetra-acid | 0 | 3 | 3 | 4 |
| 1 ring tetra-acid | 0 | 1 | 1 | 3 |
| 2 ring tetra-acid | 0 | 1 | 1 | 3 |

Table 2. Values used to generate the 'complex acid' ringcore files (% of total).

| | Ringcore file name | | | |
|--------------|--------------------|---------------|---------------|---------------|
| type of acid | simple acid 1 | simple acid 2 | simple acid 3 | simple acid 4 |
| di-acid | 100 | 90 | 80 | 35 |
| tri-acid | 0 | 5 | 15 | 35 |
| tetra-acid | 0 | 5 | 5 | 30 |

Table 3. Values used to generate the 'simple acid' ringcore files (% of total).

The newly generated ringcore files were used then in computer model experiments using the OCM. Table 4 shows the significant parameters that may be changed in the OCM interface sheet. This study looked briefly at the effect of changing some of these parameters as a gauge to determine the relative significance of changing the ringcores files as described above.

| parameter | value | comment |
|----------------------------------|-------------|---|
| number of ringcores per molecule | one or two | Allows for more complex molecules to be constructed by the OCM. |
| minhydron flag | off | Kept in the off position (see text). |
| degree of substitution | 0 → 1 | The proportion of substitutable carbon that is substituted, within the maximum and minimum range. |
| maximum substitutions | constant 12 | |
| minimum substitutions | constant 2 | |
| probability hydroaromatic | constant 1 | More accurately regulated by the ringcore file. |
| ringcore filename | - | MH1, MH2, MH3 or sa1, sa2, sa3, sa4, ca1, ca2, ca3, ca4 from the simple/complex acid information. |

Table 4. Summary of important parameters input to the OCM.

The parameter 'number of ringcores per molecule' is interesting; when specified as two the OCM is 'allowed' to join two ringcores together to make larger molecules using carbon chains from C₀ to the maximum allowable number of carbons, within the given

boiling range and other restrictions. This means that using two 'ringcores per molecule' will allow the OCM to construct molecules like those suggested by Thomas (1995) as average UCM components and those synthesised and oxidised using RuO₄ for this study.

The 'degree of substitution' parameter (variable from 0 → 1) indicates the proportion of substitutable carbon on a ringcore that is substituted by the OCM.

The 'minhydron flag' is a setting that minimises the amount of aromatic hydrogen calculated by the OCM. The algorithm takes all the isomers of a particular Z number and uses the ringcore with the least aromatic hydrogen. Only that ringcore is used in the OCM calculations. In preliminary work with the OCM the 'minhydron flag' (when turned on) had the effect of overshadowing the effect of any other changes made, so for this study it was kept in the 'off' position, allowing unrestricted aromaticity.

The 'probability hydroaromatic' (variable from 0 → 1) is a global 'concentration' set for all of the hydroaromatic ringcores in the ringcore file. It takes the ringcore concentration in the ringcore file and multiplies it by the 'probability hydroaromatic' value. Concentrations for hydroaromatics, as well as the other ringcores are calculated more finely using the detailed input data (*i.e.* the simple/complex acid information), so this type of gross adjustment is unnecessary. The probability of hydroaromatics was kept at 1.

3.4 Results and Discussion

Table 5 shows a summary of 35 experiments using the oil characterisation model (OCM). Results from these runs were then put through the 'pseudoiser'. A selection of pseudocomponent sets were then input to the Sunbury riser model (SRM).

As well as the ringcore files generated herein, three ringcore files in use at BP (MH1, MH2 and MH3) were used for comparison. Ringcore file MH1 used the 'equal probabilities' assumption; *i.e.* assuming all the ringcores are of equal concentration in the feedstock. Consequently, the ringcore probability is set to 1 for each ringcore. Ringcore

file MH2 had the probability of all hydroaromatic ringcores reduced to 0.1. Ringcore file MH3 had some ringcore probabilities reduced to 0.1, selected on the basis of analytical data and knowledge of the process history of the feedstock being modelled.

| | one ringcore per molecule | | | | | two ringcores per molecule | | | | |
|-----|---------------------------|------|------|------|------|----------------------------|------|------|------|------|
| | degree of substitution | | | | | | | | | |
| | 0.00 | 0.25 | 0.50 | 0.75 | 1.00 | 0.00 | 0.25 | 0.50 | 0.75 | 1.00 |
| MH1 | ✓ | ✓ | ✓✓ | ✓ | ✓ | | ✓ | ✓✓ | ✓ | ✓ |
| MH2 | ✓ | ✓ | ✓✓ | ✓ | ✓ | | | | | |
| MH3 | ✓ | ✓ | ✓ | ✓ | ✓ | | | | | |
| sa1 | | | ✓ | | | | | ✓✓ | | |
| sa2 | | | ✓ | | | | | ✓✓ | | |
| sa3 | | | ✓ | | | | | ✓✓ | | |
| sa4 | | | ✓ | | | | | ✓✓ | | |
| ca1 | | | ✓ | | | | | ✓✓ | | |
| ca2 | | | ✓ | | | | | ✓✓ | | |
| ca3 | | | ✓ | | | | | ✓✓ | | |
| ca4 | | | ✓ | | | | | ✓✓ | | |

✓ = OCM and 'pseudoiser' ✓✓ = OCM, 'pseudoiser' and SRM

Table 5. Summary of experiments on the OCM and 'pseudoiser'.

The intention here was to determine whether, and to what extent data from the analysis of RuO₄ oxidation products of feedstocks via the ringcore file would influence predictions of the OCM, 'pseudoiser' and the SRM. If a large influence was observed, the whole rationale of pursuing RuO₄ oxidation as a tool for the molecular analysis of feedstocks would be fully justified, but no such quantitative investigations appear to have been made prior to this study.

3.4.1 The OCM

The OCM calculates many parameters that describe the oil composition. Many are used in the 'pseudoiser', others are used for comparison with measured data to determine the accuracy of the OCM predictions. Of these parameters, the bulk density and percentages of aromatic and benzylic hydrogen were chosen as indicators of change in the OCM predictions.

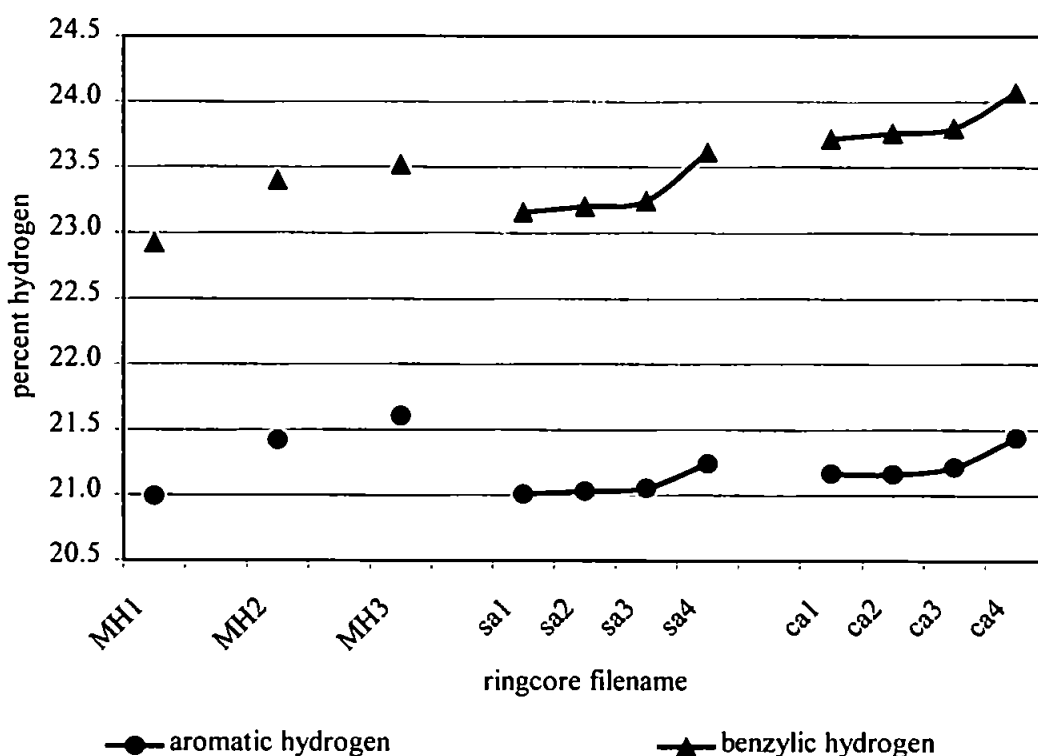
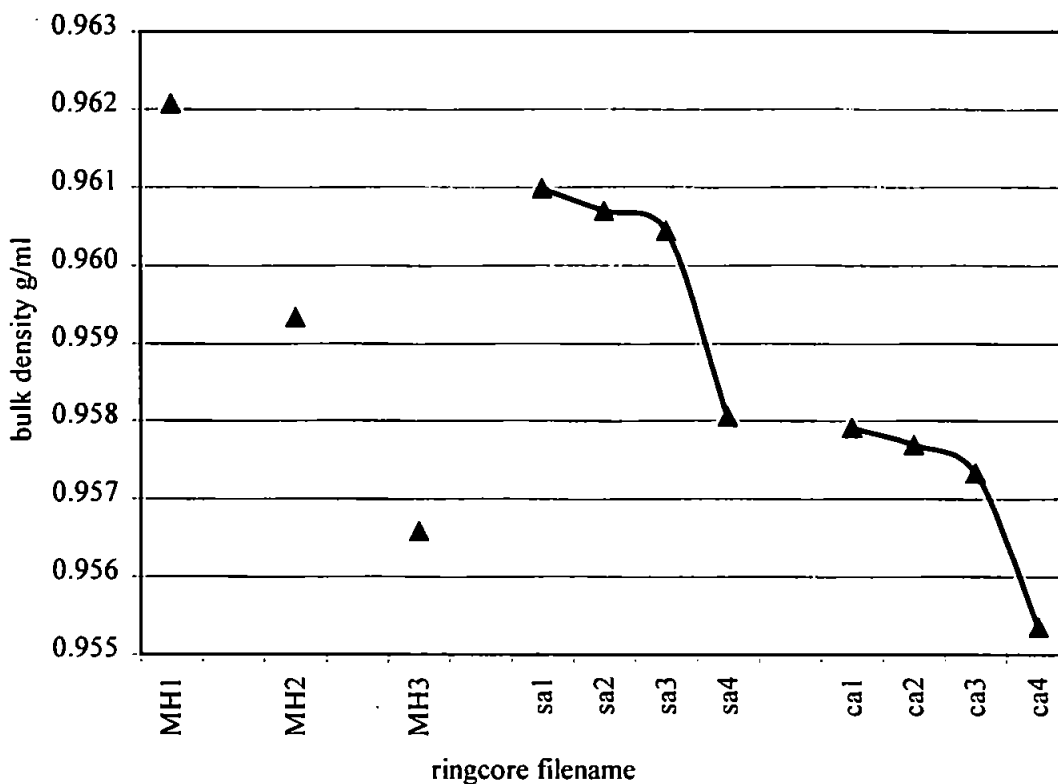


Figure 18. The effect of different ringcore files on predicted aromatic and benzylic hydrogen (sa-n = 'simple acid' ringcore file n, ca-n = 'complex acid' ringcore file).

Figure 18 shows the effect of the ringcore file on predicted aromatic and benzylic hydrogen. For this set of experiments the number of ringcores per molecule allowed was one. The BP ringcore files (MH n) show an increase in both aromatic and benzylic hydrogen (MH1→MH2→MH3) of about 0.7%. This perhaps reflects the increase in aromatic moieties as a result of lower ringcore probabilities for hydroaromatic ringcores.

Similarly, the ringcore files generated herein (ca-*n* & sa-*n*) showed an increase of about 0.5% for aromatic hydrogen and 1% for benzylic hydrogen.



*Figure 19. The effect on predicted bulk density of different ringcore files (sa-*n* = 'simple acid' ringcore file *n*, ca-*n* = 'complex acid' ringcore file), the degree of substitution is a constant 0.5, one ringcore per molecule.*

Figure 19 shows the effect of the different ringcore files on the predicted bulk density. The ringcore files MH1, MH2 and MH3 show a decrease in bulk density as the file-number increases (MH1→MH3). Likewise the 'simple' and 'complex acid' ringcore files.

The negative trends observed in bulk density correspond to the positive trends in aromaticity indicated by aromatic and benzylic hydrogen.

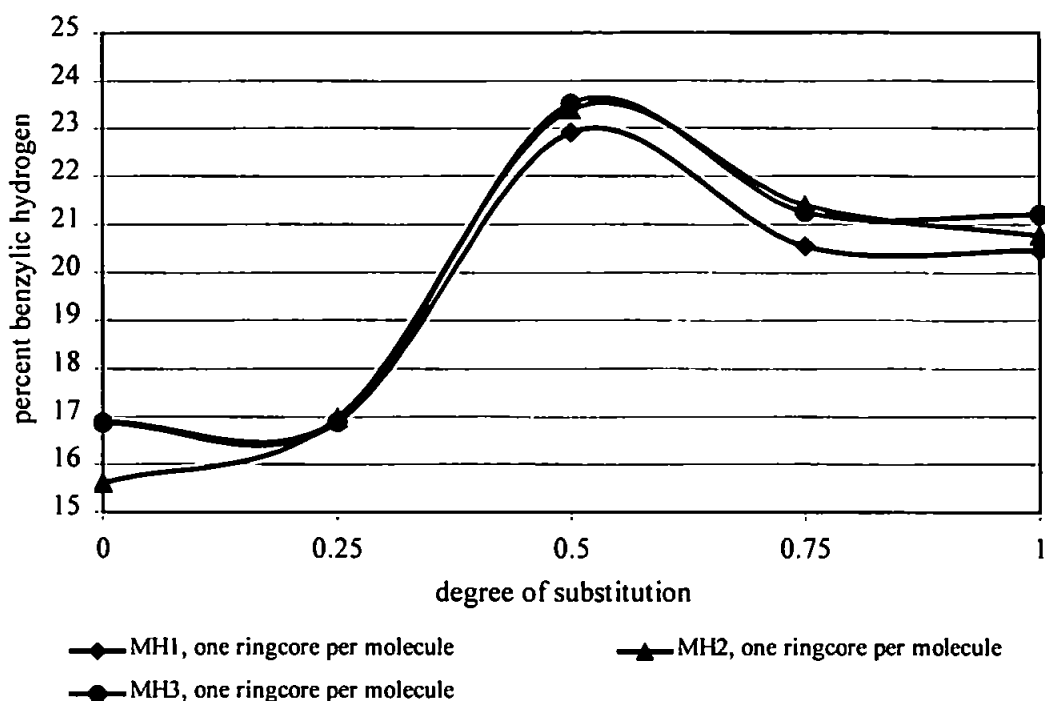


Figure 20. The effect of increasing the degree of substitution on predicted benzylic hydrogen.

Figure 20 shows the effect of changing the degree of substitution when the three BP ringcore files were used in the OCM. For all three ringcore files a marked increase from ~16 to ~23% is observed at 0.5 degrees of substitution that is maintained at ~21% benzylic hydrogen at degrees of substitution of 0.75 and 1.00. A similar but negative pattern is observed for aromatic hydrogen (not shown). To keep the experiment relatively simple it was decided not to vary the degree of substitution for experiments using the 'simple acid' and 'complex acid' ringcore files, but to keep it at a constant 0.5.

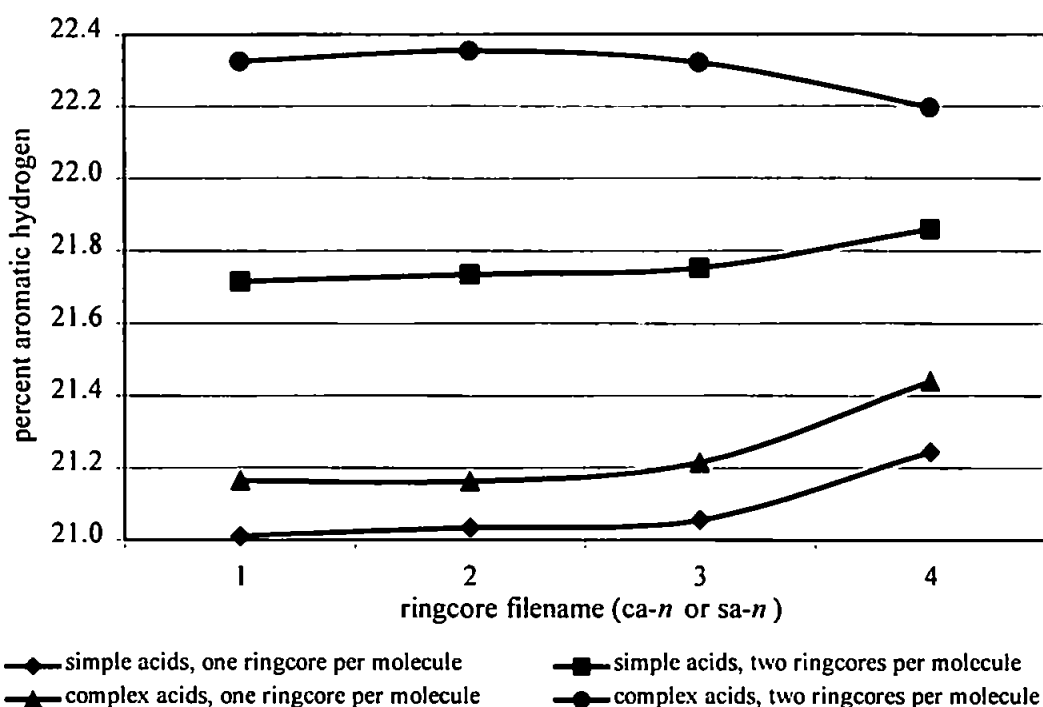


Figure 21. The effect on predicted aromatic hydrogen of allowing more than one ringcore per molecule in the OCM. Degree of substitution 0.5 constant.

Figure 21 shows that several factors influence the predicted % aromatic hydrogen; two sets of ringcore files were used in the OCM (ca-n and sa-n) and each was calculated allowing either one or two ringcore per molecule.

The two sets of experiments allowing only one ringcore per molecule show an increase of ~0.3% as the ringcore file number increases (equivalent to ~1% of the total aromatic hydrogen).

The effect of increasing the number of ringcores per molecule from one to two consistently increases the aromatic hydrogen by between 0.5% and 2.5%.

Similar trends in the predicted benzylic hydrogen were also observed (not shown).

3.4.1.1 Discussion

Results from the experiments on the OCM detailed above clearly show that the ringcore files generated herein (ca-n, sa-n) do indeed influence the OCM predictions at least as

much as those produced by the BP ringcore files. The observed changes in aromatic and benzylic hydrogen and also the bulk density would be expected in turn to have a similar influence on the distribution of pseudocomponents.

3.4.2 The 'pseudoiser'

Data from all of the experiments on the OCM were fed into the pseudoiser which produced a set of pseudocomponents for each run. There are 100 pseudocomponents in the set, from hydrogen to substituted six-ring aromatics and hydroaromatics, each with a different concentration. The pseudocomponent set is the 'feedstock' input to the FCC model; the SRM. Changes in the concentration of individual pseudocomponents would obviously affect 'feedstock' behaviour in the FCC, so observed changes in pseudocomponents generated from the 'simple' and 'complex acid' ringcore files would mean significant changes in the ratios of products produced by the FCC model. That is, in the economic value of the FCC product.

Pseudocomponent nomenclature is relatively straight forward; the name of each gives the number of carbon atoms and an indication of the number and arrangement of rings in the 'molecule'. Figure 22 illustrates this.

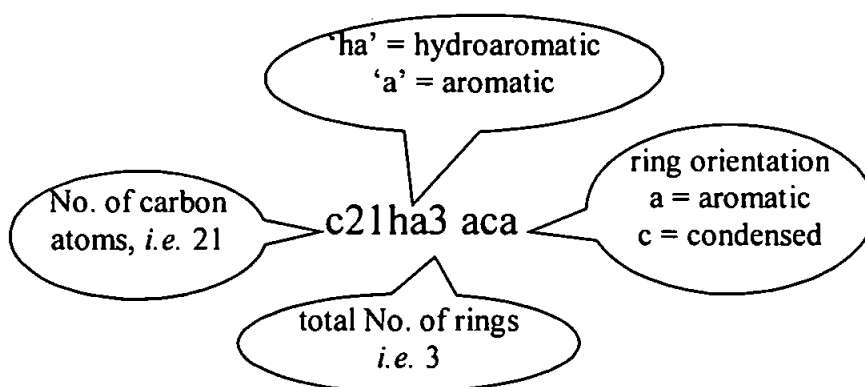


Figure 22. Pseudocomponent nomenclature.

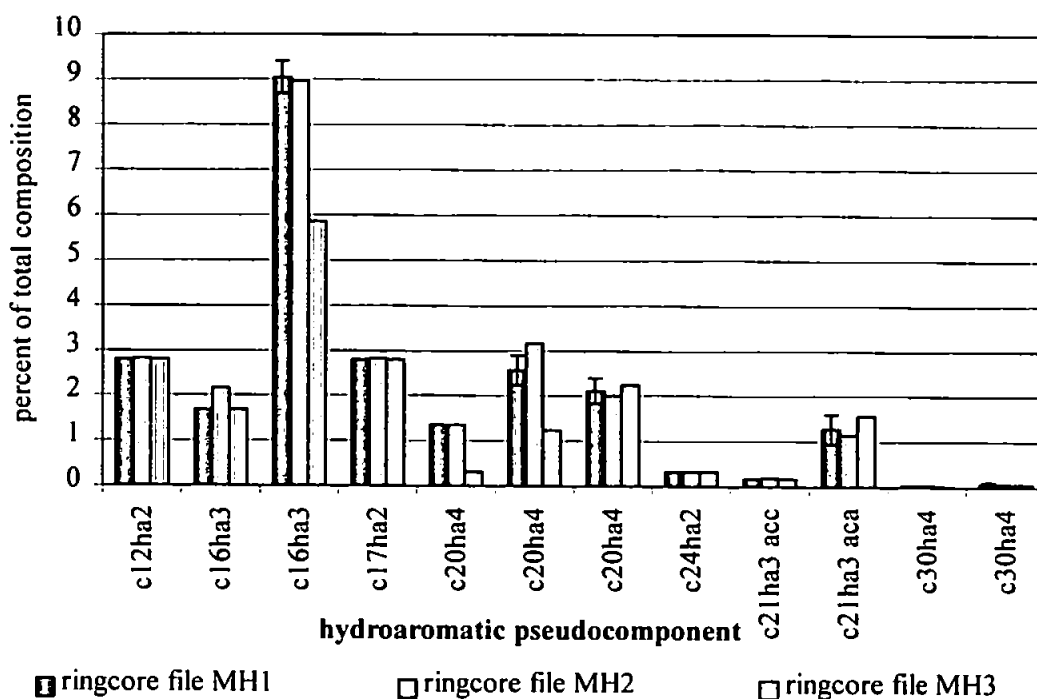


Figure 23. The effect on selected hydroaromatic pseudocomponent concentrations of different ringcore files and changing degree of substitution. Values are averages of five experiments with varying degrees of substitution from 0 to 1. Error bars show \pm one standard deviation (nil for MH2 and MH3).

Figure 23 shows the hydroaromatic pseudocomponent concentration varying with ringcore file – in this case the BP ringcore files MH1, MH2 and MH3. Degree of substitution is also varied, although this only has an effect on the pseudocomponent concentrations for experiments using ringcore file MH1.

The hydroaromatic content of the pseudocomponent set for these experiments varied from 19% (MH3) to 27% (MH2); a substantial difference of 8%.

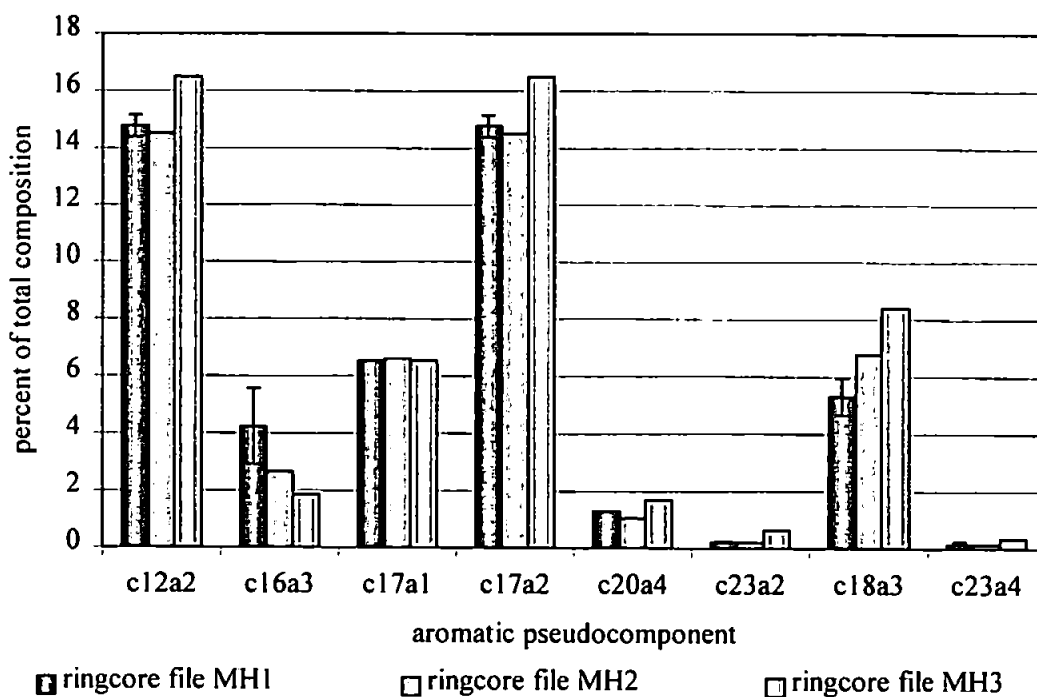


Figure 24. The effect on selected aromatic pseudocomponent concentrations of different ringcore files and changing degree of substitution. Values are averages of five experiments with varying degrees of substitution from 0 to 1. Error bars show \pm one standard deviation (nil for MH2 and MH3).

Figure 24 shows the effect on aromatic pseudocomponents of the BP ringcore files and changing degree of substitution. As the figure shows, concentrations vary considerably with ringcore file, but again only ringcore file MH1 shows any change in pseudocomponent concentrations with changing degree of substitution. The aromatic content of the pseudocomponent sets for these experiments is between 45% (MH1) and 55% (MH3) of the total; a difference of 10%.

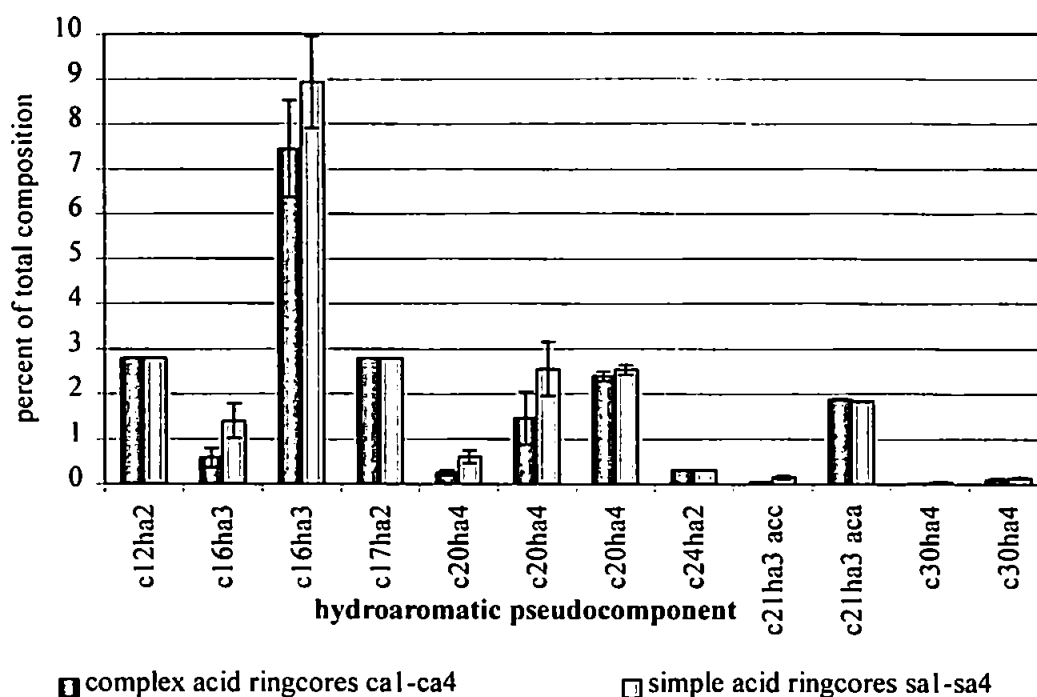


Figure 25. The effect on selected hydroaromatic pseudocomponent concentrations of different ringcore files. Values are averages of results using four ringcore files, with a degree of substitution of 0.5 and allowing one ringcore per molecule. Error bars show values \pm one standard deviation between the four ringcore files.

Figure 25 shows the hydroaromatic pseudocomponent concentrations varying with the ringcore files generated herein. The standard deviation shows that the ringcore files have quite an effect on the pseudocomponent concentrations, with the pseudocomponents c16ha3 and c20ha4 showing marked variation.

N.B. Several pseudocomponents have the same designation (*i.e.* c20ha4) but are distinguished in the pseudoiser and SRM as having different degrees of aromaticity. For example, pseudocomponent No. 25, 'c20ha4' = dodecahydrochrysene, pseudocomponent No. 26, also 'c20ha4' = hexahydrochrysene and pseudocomponent No. 27, also 'c20ha4' = dihydrochrysene.

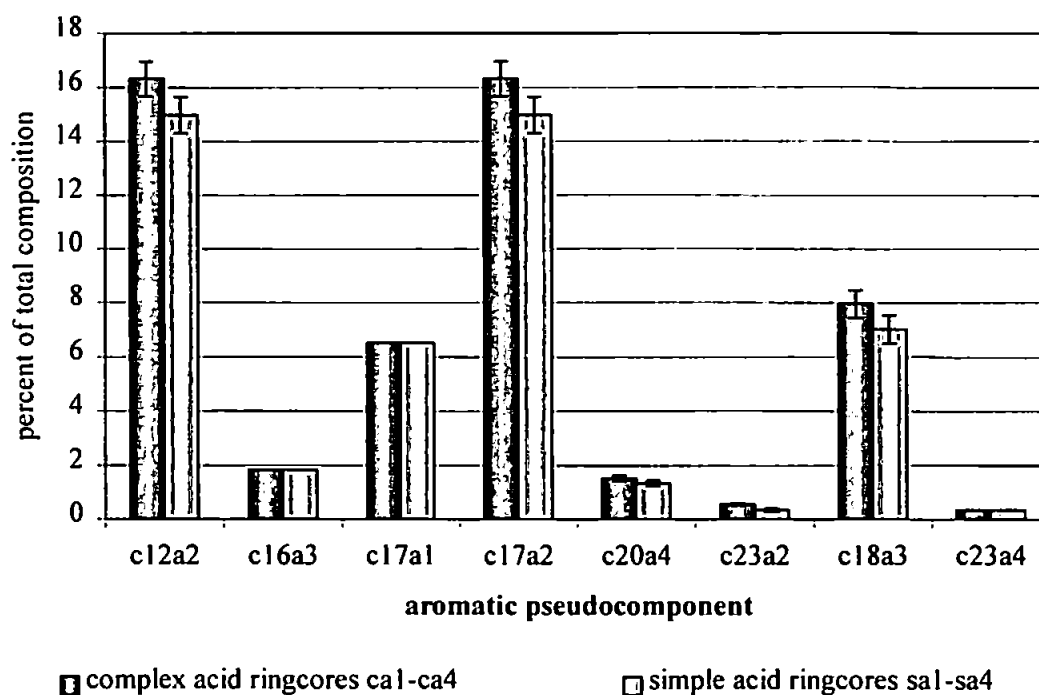


Figure 26. The effect on selected aromatic pseudocomponent concentrations of different ringcore files. Values are averages of results using four ringcore files, with a degree of substitution of 0.5 and allowing one ringcore per molecule. Error bars show values \pm one standard deviation across the four ringcore files.

Figure 26 shows the aromatic pseudocomponent concentrations varying with the ringcore files ca1-4 and sa1-4. Three pseudocomponents in particular are influenced by the ringcore files; c12a2, c17a2 and c18a3. An increase in larger pseudocomponents at the expense of smaller ones (e.g. c12a2, naphthalene) \rightarrow c18a3, a phenanthrene) would have a significant effect on the products predicted by the SRM.

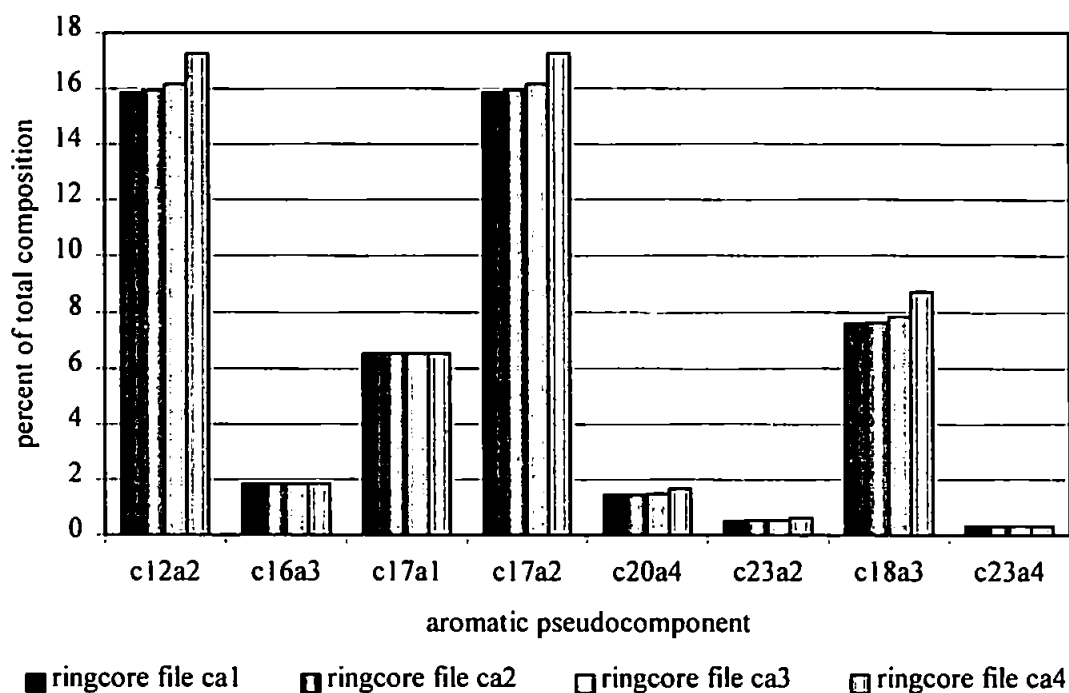


Figure 27. The effect of ringcore files ca1 to ca4 on the aromatic pseudocomponent concentrations with 0.5 degrees of substitution and allowing one ringcore per molecule.

Figure 27 shows the influence of individual ringcore files ca1 to ca4 on the aromatic pseudocomponent concentration. The trend observed for the pseudocomponents c12a2, c17a2 and c18a3 reflects the earlier observations of aromatic hydrogen predicted by the OCM (Figure 21). The total aromatic content for ringcore file ca1 is 50%, increasing to 54% for ringcore file ca4, a significant increase of 4%.

3.4.2.1 Discussion.

The use of different ringcore files has shown a marked influence on the pseudocomponent concentrations for both the BP ringcore files and the hypothetical 'simple' and 'complex acid' ringcore files generated herein. The effect of these changes are reflected on the SRM predictions of FCC products, could now be investigated.

3.4.3 The SRM.

A selection of pseudocomponent sets was submitted for input to the SRM (Table 5).

Catalyst and FCC operational parameters remained constant.

The SRM calculated yields of individual pseudocomponents and grouped these into five distillation fractions and coke.

| Distillation fraction | Number of pseudocomponents | From... | To... |
|----------------------------|----------------------------|-------------------------|--|
| Dry gas | 4 | H ₂ | C ₂ alkanes |
| Liquid petroleum gas (LPG) | 6 | C ₃ alkanes | C ₄ alkanes |
| Cat. cracked spirit (CCS) | 39 | C ₅ alkanes | C ₁₀ alkanes |
| Light cycle oil (LCO) | 16 | C ₁₃ alkanes | 3-ring aromatics and hydroaromatics |
| Heavy cycle oil (HCO) | 35 | C ₂₀ alkanes | 5-ring aromatics and 6-ring hydroaromatics |
| Coke | 0 | - | - |

Table 6. Distribution of pseudocomponents in the distillation fractions predicted by the SRM.

The relative economic value of these products varies considerably, especially when the crude oil prices are high. It is vital for refineries to maximise yields of useful high value products like LPG and cat. cracked spirit and to minimise yields of less useful, low value products. Table 7 shows a summary of the uses and value of the various products obtained from an FCC unit.

| FCC product | Composition | Use | Market value, \$/bbl* |
|----------------------------|--------------------------------------|---------------------------------------|-----------------------|
| Dry gas | Hydrogen | Refinery fuel | - |
| Liquid petroleum gas (LPG) | Butane & propane | Fuel | 146 |
| Cat. cracked spirit (CCS) | light hydrocarbons | Gasoline base stock | 187 |
| Light cycle oil (LCO) | middle hydrocarbons, high % aromatic | Poor quality diesel (highly aromatic) | 173 |
| Heavy cycle oil (HCO) | heavy hydrocarbons | Fuel oil | 20 |
| Coke | Carbon | Burnt off catalyst in FCC. | - |

*bbl = barrel = 42 US gallons. Prices shown are weekly averages, OPIS (2000).

LPG – average of propane, iso-butane and n-butane, Conway LPG market.

CCS – ‘naphtha’ feedstock (the best equivalent), U.S. Gulf Coast market.

LCO – ‘lt. Cycle’ feedstock, U.S. Gulf Coast market.

HCO – ‘Residual fuel’ 3% sulphur, high pour, New York Harbour cargo.

Table 7. Summary of uses and value of products obtained from an FCC unit.

Table 8 shows a summary of the changes made to input data files to the SRM.

| ringcore file | ringcores per molecule | degree of substitution |
|--------------------|------------------------|------------------------|
| MH1 | 1 and 2 | 0.5 |
| MH2 | 1 | |
| sa1, sa2, sa3, sa4 | 2 | |
| ca1, ca2, ca3, ca4 | | |

Table 8. Summary of experiments on the SRM.

Figure 28 shows the distribution of products predicted by the SRM. The values are averages predicted from 11 experiments on the SRM, using ringcore files MH1, MH2, ca1 to ca4 and sa1 to sa4. Figure 29 shows the product values in terms of the daily production from a 30,000 BPD FCC unit.

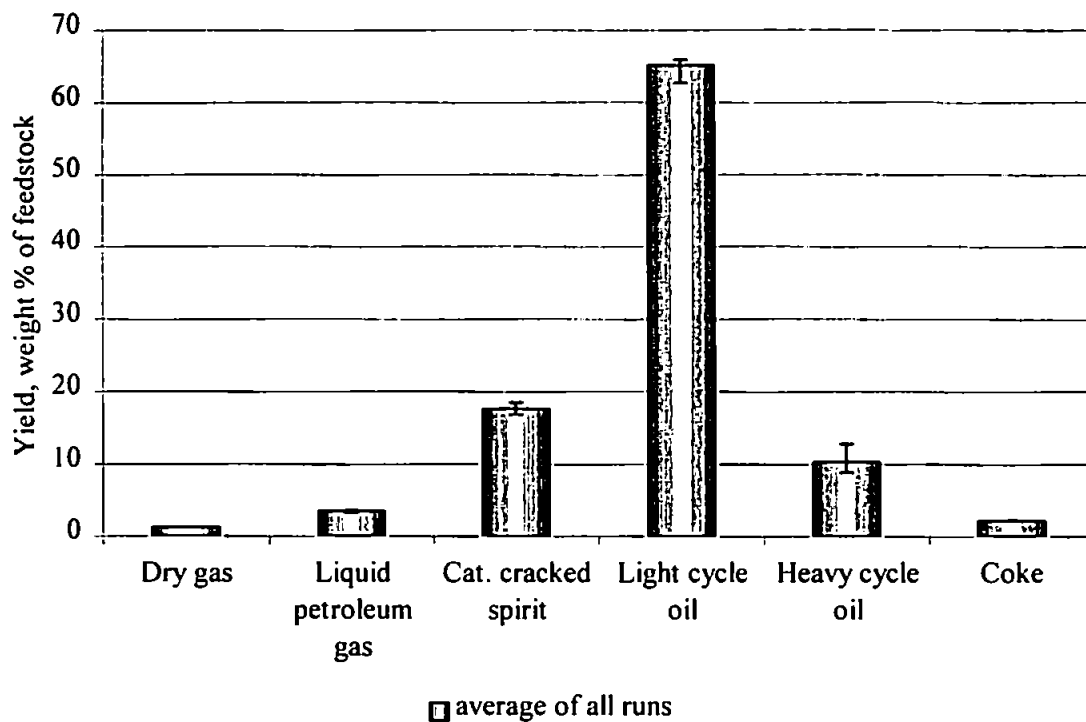


Figure 28. The percentage yields of products predicted by the SRM. The values are average of all experiments on the SRM. Error bars show maximum and minimum of the predicted range.

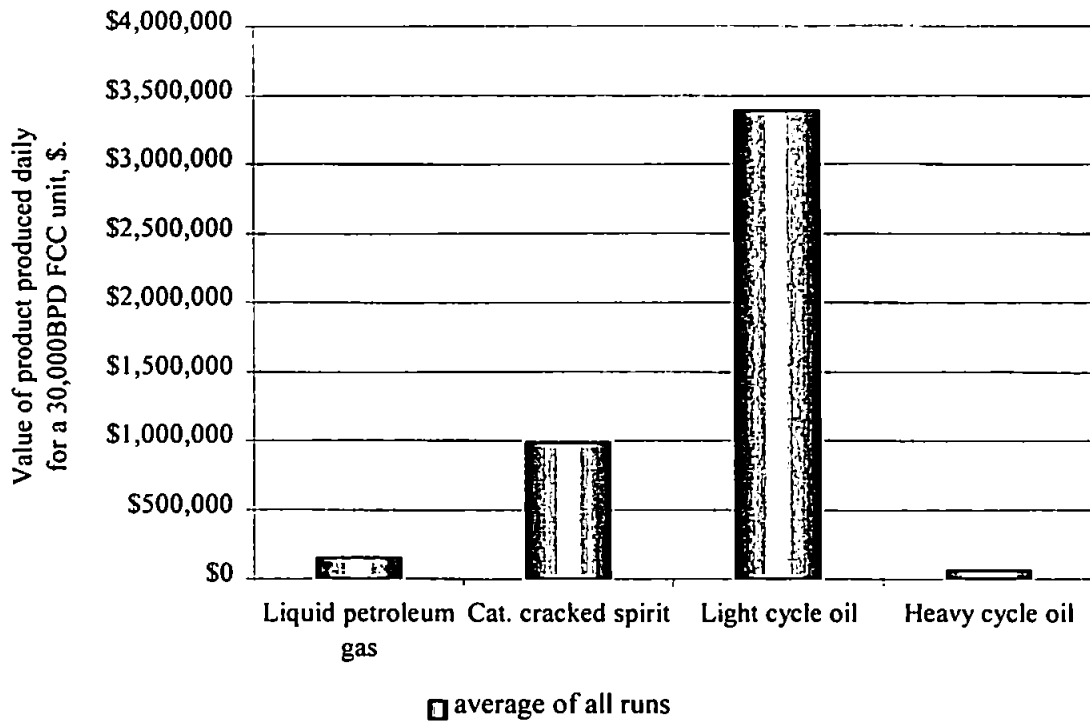


Figure 29. Value of products produced daily by a 30,000 BPD FCC unit, expressed in terms of their current market price, (see Table 7), average of all SRM experiments.

Table 9 to Table 13 give details of the effects of different ringcore files and some OCM parameters on product yields as predicted by the SRM.

| Product | Yield, % weight of feedstock | | | |
|---------------------|------------------------------|-----------------------------|-----------------------|------------|
| | MH1 1 RC per molecule | MH1 2 RC per molecule | Difference | |
| | | | % of average yield | Value*, \$ |
| Dry gas | 1.26 | 1.25 | 1.22 | - |
| Liquid propane gas | 3.32 | 3.42 | -3.13 | 4,792 |
| Cat. cracked spirit | 17.63 | 17.92 | 0.53 | 5,177 |
| Light cycle oil | 62.69 | 63.51 | -3.93 | 133,192 |
| Heavy cycle oil | 12.83 | 11.67 | 21.18 | 13,374 |
| Coke | 2.28 | 2.24 | 2.44 | - |

* = Value per day's production from a 30,000 BPD FCC unit.

Table 9. The effect of increasing the number of 'ringcores per molecule' allowed on product yields predicted by the SRM

| Product | Yield, % weight of feedstock | | | |
|---------------------|------------------------------|-------|----------------------------|------------|
| | Experiment results | | Difference between results | |
| | MH1 | MH2 | % of average yield | Value*, \$ |
| Dry gas | 1.26 | 1.25 | -0.77 | - |
| Liquid propane gas | 3.32 | 3.42 | 3.06 | 4,686 |
| Cat. cracked spirit | 17.63 | 17.92 | 1.60 | 15,766 |
| Light cycle oil | 62.69 | 63.51 | 1.30 | 43,948 |
| Heavy cycle oil | 12.83 | 11.67 | -9.44 | 5,962 |
| Coke | 2.28 | 2.24 | 1.76 | - |

* = Value per day's production from a 30,000 BPD FCC unit.

Table 10. The effect of the ringcore files MH1 and MH2 on product yields predicted by the SRM.

| Product | Yield, % weight of feedstock | | | | | |
|---------------------|------------------------------|-------|-------|-------|----------------------------|------------|
| | Experiment results | | | | Difference between results | |
| | sa1 | sa2 | sa3 | sa4 | % of average yield | Value*, \$ |
| Dry gas | 1.24 | 1.24 | 1.24 | 1.23 | 0.74 | - |
| Liquid propane gas | 3.45 | 3.46 | 3.47 | 3.55 | 3.07 | 1,645 |
| Cat. cracked spirit | 17.14 | 17.12 | 17.14 | 16.92 | 1.26 | 41,877 |
| Light cycle oil | 65.57 | 65.53 | 65.48 | 65.38 | 0.28 | 14,451 |
| Heavy cycle oil | 10.39 | 10.43 | 10.46 | 10.71 | 3.13 | 3,380 |
| Coke | 2.22 | 2.22 | 2.21 | 2.19 | 1.14 | - |

* = Value per day's production from a 30,000 BPD FCC unit.

Table 11. The effect of the 'simple acid' ringcore files on product yields predicted by the SRM.

| Product | Yield, % weight of feedstock | | | | | |
|---------------------|------------------------------|-------|-------|-------|----------------------------|------------|
| | Experiment results | | | | Difference between results | |
| | ca1 | ca2 | ca3 | ca4 | % of average yield | Value*, \$ |
| Dry gas | 1.24 | 1.24 | 1.24 | 1.25 | 0.52 | - |
| Liquid propane gas | 3.57 | 3.57 | 3.56 | 3.53 | 1.07 | 4,704 |
| Cat. cracked spirit | 17.75 | 17.84 | 17.93 | 18.52 | 4.25 | 12,404 |
| Light cycle oil | 65.84 | 65.86 | 65.82 | 65.58 | 0.43 | 9,608 |
| Heavy cycle oil | 9.38 | 9.28 | 9.23 | 8.89 | 5.35 | 1,977 |
| Coke | 2.22 | 2.22 | 2.22 | 2.23 | 0.81 | - |

* = Value per day's production from a 30,000 BPD FCC unit.

Table 12. The effect of the 'complex acid' ringcore files on product yields predicted by the SRM.

| Product | Yield, % weight of feedstock | | | |
|---------------------|------------------------------|----------------------|----------------------------|------------|
| | Experiment results | | Difference between results | |
| | Average simple acid | Average complex acid | % of average yield | Value*, \$ |
| Dry gas | 1.24 | 1.24 | 0.34 | - |
| Liquid propane gas | 3.48 | 3.56 | 2.23 | 3,418 |
| Cat. cracked spirit | 17.08 | 18.01 | 5.29 | 52,110 |
| Light cycle oil | 65.49 | 65.77 | 0.43 | 14,650 |
| Heavy cycle oil | 10.50 | 9.19 | -13.27 | 8,377 |
| Coke | 2.21 | 2.22 | 0.50 | - |

* = Value per day's production from a 30,000 BPD FCC unit.

Table 13. The difference between the 'simple acid' and 'complex acid' ringcore files in terms of product yields predicted by the SRM.

The tables above are summarised in Figure 30. The chart shows that changing inputs to the SRM to reflect the additional information provided by a theoretical RuO₄ oxidation of

FCC feedstocks has an influence of between -13% and 5% of individual product yields for the SRM. A difference of 1% to a particular FCC product can mean a significant difference in the economic yield of FCC products, so the influences of RuO₄ data on the predicted FCC yields would be of great economic value, as suggested by the data shown in Figure 31.

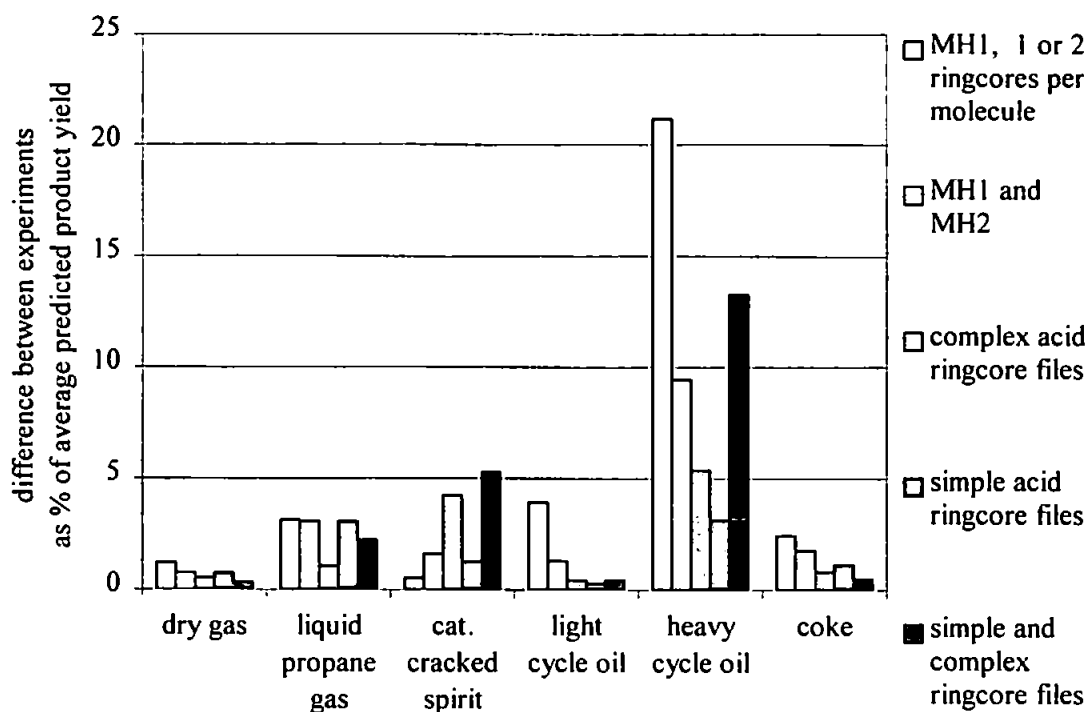


Figure 30. The difference between selected SRM experiments expressed as a percent of the average product yield

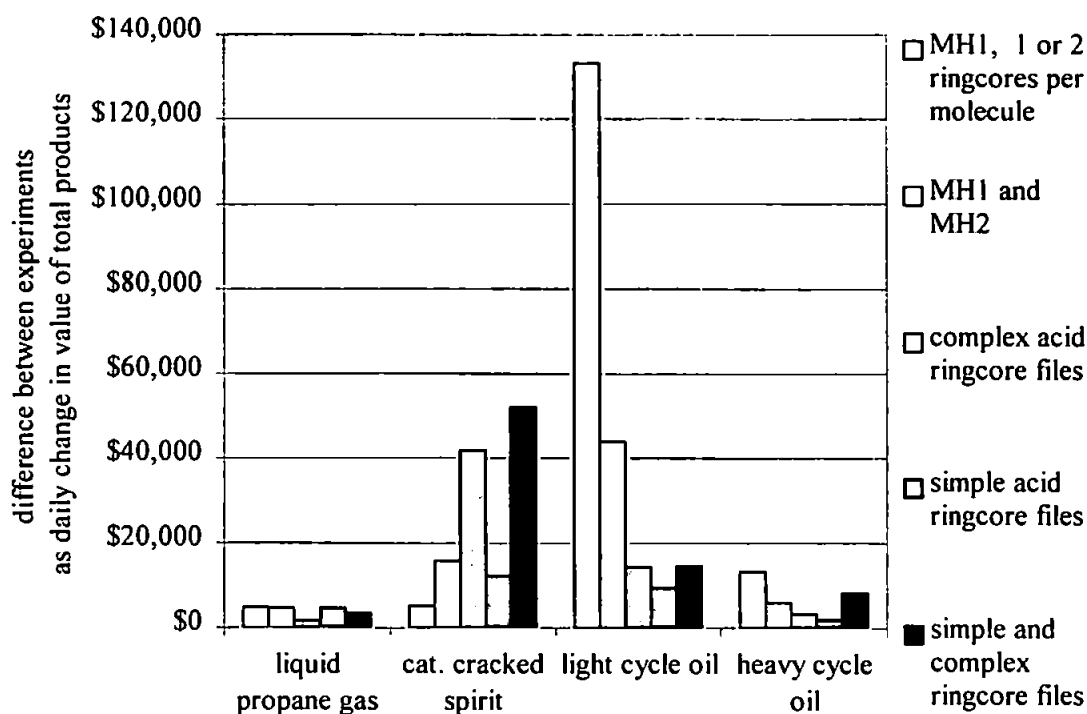


Figure 31. The influence of selected SRM experiments on the value of products produced daily by a 30,000 BPD FCC unit, expressed as their market value (see Table 7).

3.5 Conclusion

Computational experiments with simulated acid compositions suggest that significant effects on modelling feedstock composition would result from use of the different acids ('complex' and 'simple') data. Those in turn would affect predicted products of FCC operation. Using average market prices for such refined fractions, economically significant *daily* differences in FCC operation are predicted.

The data has therefore justified the need for a detailed analytical description of the acids produced in reality by RuO₄ oxidation of FCC hydrocarbon feedstocks (UCMs).

4 *Method Development*

A critical appraisal of, and subsequent improvements made to, the RuO₄ oxidation and work-up procedures are discussed.

4.1 Introduction

The RuO₄ oxidation method originally used by Revill (1992), (modified from the methods of Stock & Tse, 1983 and Boucher *et al.*, 1991) to oxidise unresolved complex mixtures of hydrocarbons later underwent further modifications (Thomas, 1995, after Standen, 1992; Standen and Eglinton 1992) to incorporate a mass-balance approach whereby water soluble products, DCM soluble products and CO₂ were each determined. However, even the modified method of Thomas (1995) did not allow optimal recoveries of these fractions (see Table 14 below) particularly when hydroaromatics were oxidised. Other workers have also reported poor recovery of RuO₄ oxidation products from hydroaromatics such as tetralin (Djerassi & Engle, 1953, cited in Lee and van den Engh, 1973; Spitzer & Lee, 1974).

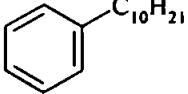
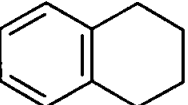
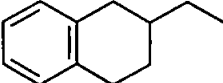
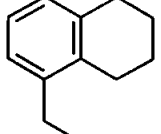
| Compound | DCM % | CO ₂ % | Water % | Total % | Unaccounted (%) |
|--|--------|-------------------|---------|---------|-----------------|
|  1-Phenyldecane | 74 | 26 | 0 | 100 | 0 |
| | 72 | 31 | 0 | 103 | -3 |
| | 68 | 31 | 0 | 99 | 1 |
| Mean | 71.3 | 29.3 | 0 | 101.6 | -0.6 |
| σ_{n-1} | 3.1 | 2.9 | 0 | 2.1 | - |
| Theory | 69 | 31 | 0 | 100 | - |
|  Tetralin | 1 | 29 | 1 | 31 | 69 |
| | 5 | 39 | 5 | 49 | 51 |
| | 5 | 39 | 3 | 47 | 53 |
| Mean | 4 | 36 | 3 | 42 | 58 |
| σ_{n-1} | 2.3 | 5.8 | 2.0 | 9.8 | - |
| Theory | 0 | 40 | 60 | 100 | - |
|  2-Ethyltetralin | 1 | 29 | <1 | 31 | 69 |
| | Theory | 0 | 33 | 67 | 100 |
|  5-Ethyltetralin | 28 | 21 | 2 | 51 | 49 |
| | Theory | 0 | 25 | 75 | 100 |

Table 14. Products of RuO₄ oxidation of 1-phenyldecane, tetralin, 2-ethyltetralin and 5-ethyltetralin. Thomas (1995).

4.2 Method evaluation

To recap briefly (a more detailed discussion appears in Chapter 1), the principle of the RuO₄ method for UCM hydrocarbon characterisation is that water soluble products reflect oxidation products of short chain substituents of the aromatic ring (*via ipso – C* oxidation), DCM soluble products reflect longer chain and alicyclic substituents and CO₂ reflects ‘aromaticity’ (unsubstituted aromatic carbons). As an illustration, 5-ethyl-2-heptyltetralin may be considered:

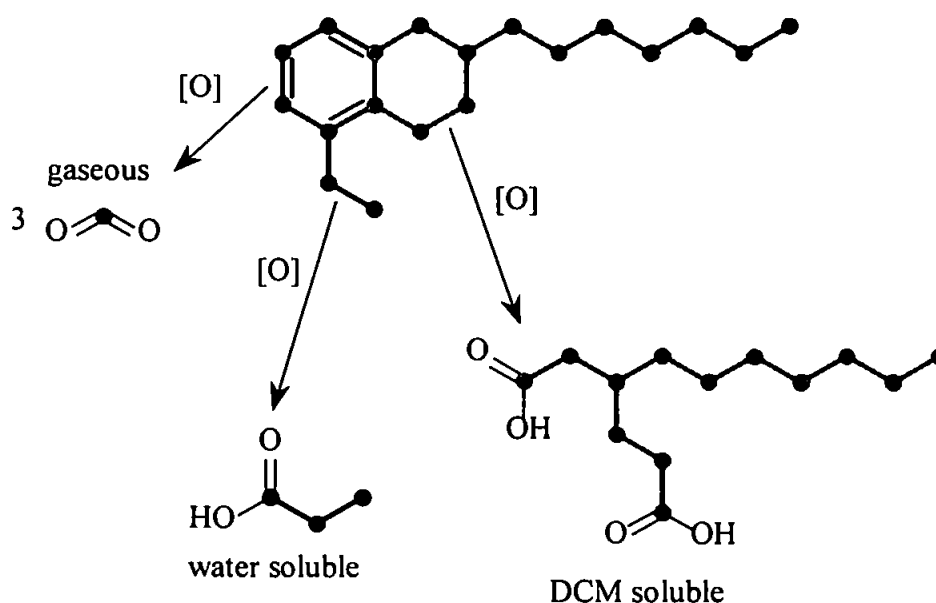


Figure 32. Ruthenium tetroxide oxidation of 5-ethyl-2-heptyltetralin.

The recovery of oxidation products from the RuO₄ oxidation of tetralin were re-investigated herein (Table 15 and Figure 33) in quadruplicate experiments. A mean total recovery of $53.1 \pm 9.5\%$ compares well with the 58% recovery of Thomas (1995), but whereas Thomas (1995) experienced losses of water soluble products alone, the results from the present study showed approximately equal losses from the water soluble fraction (hexanedioic acid) and of carbon dioxide. Thomas (1995) speculated that loss of

water soluble acids might be due to further oxidation of dicarboxylic acids to shorter acids. This is a possibility, and indeed, chain shortening of acids both in the DCM soluble and water soluble fractions was observed in the present study (detailed in Chapter 6). A corresponding increase in the amount of CO₂ measured was not observed in this study, or by Thomas (1995) but this may be due to inefficiencies of the CO₂ trapping system (reviewed in section 4.3.1).

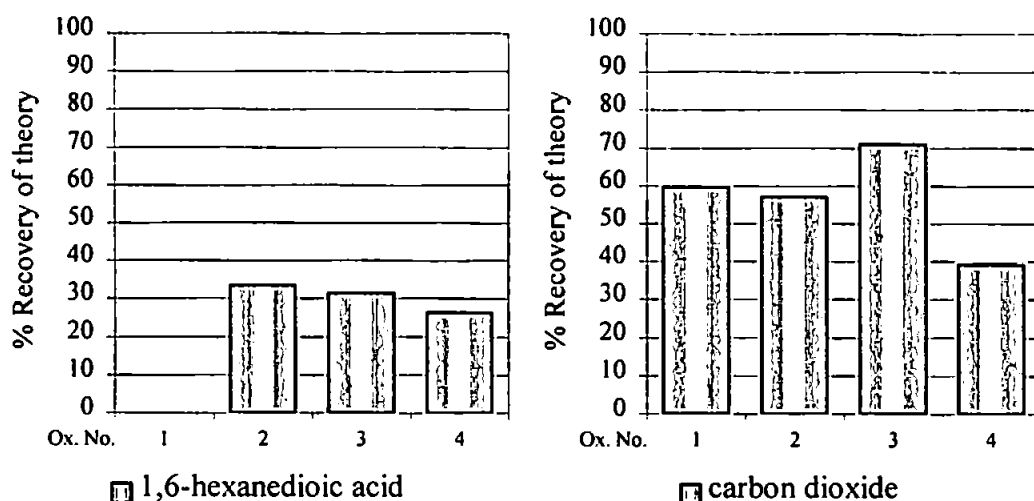


Figure 33. Recovery of products from the ruthenium tetroxide oxidation of tetralin.

| Oxidation No. | Recovery (% of theory) | | Unaccounted |
|----------------|------------------------|-----------------|-------------|
| | 1,6-Hexanedioic acid | CO ₂ | |
| 1 | - | 23.9 (60) | - |
| 2 | 33.5 (56) | 22.9 (57) | 43.7 |
| 3 | 31.5 (54) | 28.4 (71) | 40.2 |
| 4 | 26.3 (44) | 15.7 (39) | 58.1 |
| Mean | 30.4 (54) | 22.7 (57) | 47.3 |
| σ_{n-1} | 3.7 (6) | 5.3 (13) | - |
| Theory | 60.0 | 40.0 | - |

Table 15. Products recovered from four repeat oxidations of tetralin (this study).

It was therefore concluded that an evaluation of all of the steps in the RuO₄ oxidation procedure currently in use, from CO₂ trapping to the work-up of oxidation products was required. The aims were to maximise recovery of oxidation products and to simplify the RuO₄ oxidation.

Figure 34 shows the existing procedures. Each process shown in a grey box was closely examined to identify sources of losses of oxidation products, and to examine alternatives for simplification.

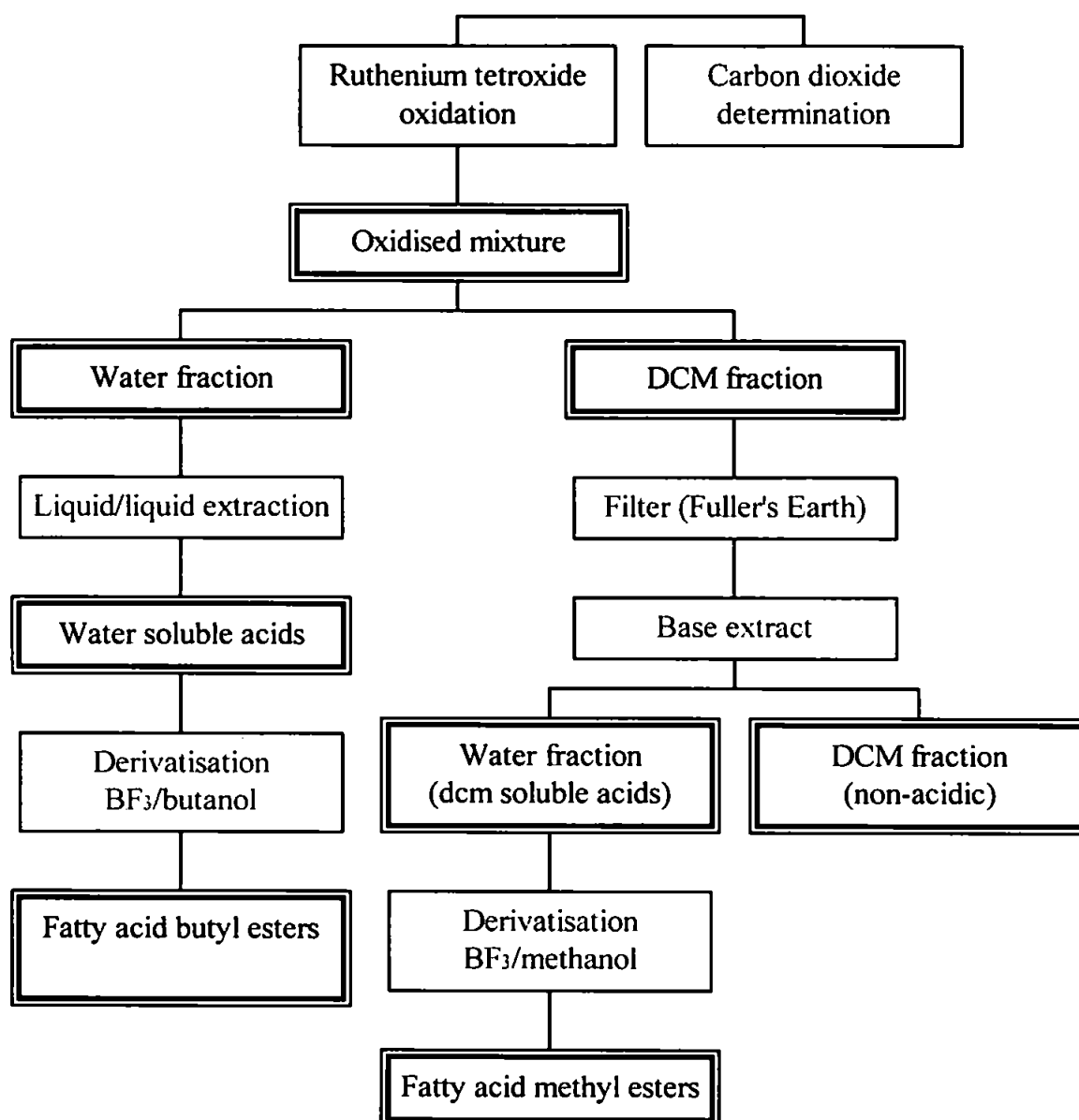


Figure 34. Work-up procedure for ruthenium tetroxide oxidation products (after Thomas, 1995).

4.3 Method developments

4.3.1 Carbon dioxide determination

Accurate and precise determination of the carbon dioxide produced in RuO_4 oxidations of UCM hydrocarbons is vital for the mass balance approach to be taken in the present study. Carbon dioxide also provides an important measure of 'aromaticity' (or strictly of unsubstituted aromatic carbons).

Data given in Figure 33 show that only half the CO_2 expected from the oxidation of tetralin was observed. The standard deviation of measurements was large. Consequently, an investigation of the accuracy and precision of the CO_2 trapping system of Thomas (1995) was undertaken, starting with measurement of the efficiency of the $\text{Ba}(\text{OH})_2$ trap.

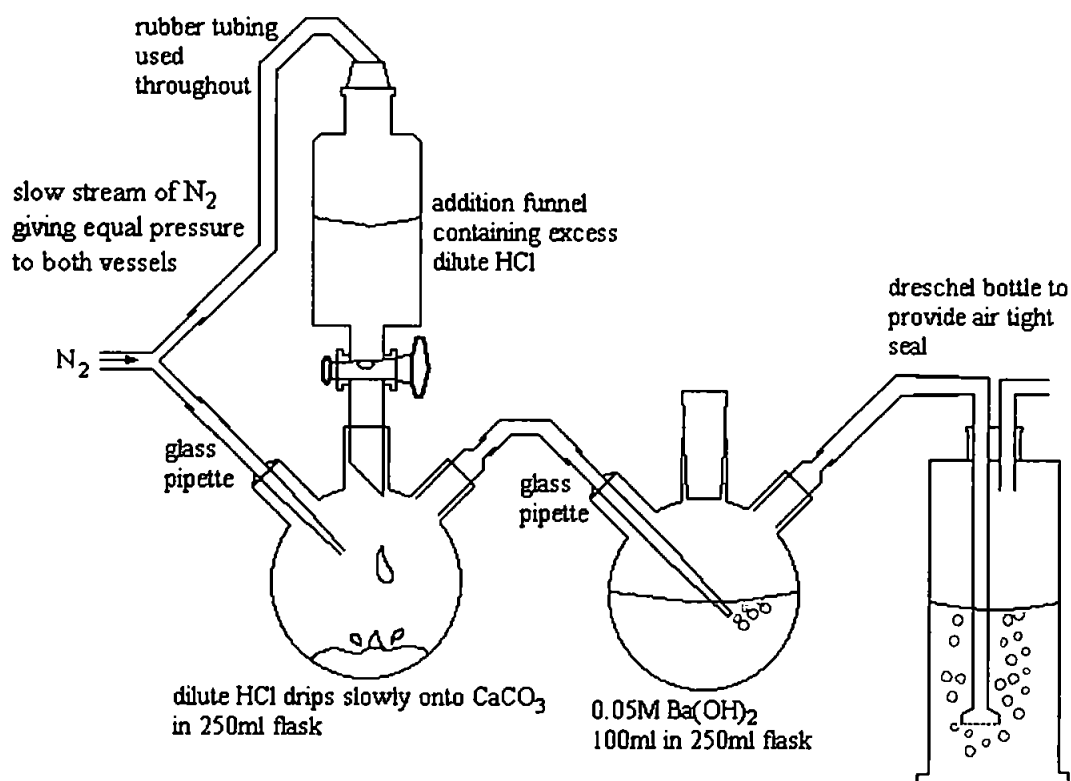


Figure 35. Diagram showing the original apparatus for the determination of CO_2 trap efficiency (after Thomas, 1995).

Figure 35 shows the apparatus used by Thomas (1995) to trap CO₂ and in preliminary studies herein to measure CO₂ trap efficiency. An experiment was designed to mimic the conditions experienced during oxidation. Dilute HCl was dripped onto accurately weighed CaCO₃ slowly enough to take approximately 24 hours for all the HCl to be dispensed. The CO₂ produced was allowed to bubble through Ba(OH)₂ (aq) and the contents were titrated vs. 0.1M HCl (ConvoL™) when all of the CaCO₃ had dissolved.

The CO₂ trap efficiency was measured in triplicate giving efficiencies of 100%, 60% and 60%. Thomas (1995) measured CO₂ trap efficiency at 73% (number of replicates unknown).

Use of the CO₂ trap indicated some obvious problems. The N₂/CO₂ stream was introduced into a round bottomed flask containing 0.05M Ba(OH)₂ using a glass Pasteur pipette. The tip of the pipette was necessarily narrow to minimise the size of the bubbles produced, thus increasing the surface area of the bubble exposed to the Ba(OH)₂. The narrow tip often became temporarily blocked with barium carbonate (BaCO₃), only unblocking when sufficient pressure was built up. This caused variation in the flow of gas and in the size of the bubbles produced. The efficiency of the trap probably varied considerably during 24 h.

In fact a review of the literature reveals that, perhaps surprisingly, the accurate determination of CO₂ is not a trivial exercise. Carbon dioxide is not particularly soluble in water. Van Nieuwenburg and Hegge (1951) state that the “quantitative absorption of carbon dioxide in aqueous solutions of baryta (Ba(OH)₂) either requires a very large excess of baryta or the use of complicated absorption vessels, or both.”

Clearly neither a very large excess of Ba(OH)₂(aq) or “complicated” absorption vessels were being used for the determination of CO₂ during the RuO₄ oxidation conducted by Thomas (1995).

4.3.1.1 Organic solvents for CO₂ absorption.

Blom and Edelhausen (1955) report that organic solvents are much more efficient at dissolving CO₂ than inorganic solutes. The method of Van Nieuwenburg and Hegge (1951) using a mixture of aniline, ethanol and Ba(OH)₂ is attractive, but would not solve pipette blocking/unblocking problems. Instead, an absorption medium where no solid precipitate is formed would be ideal. Such a method was described by Patchornik and Shalitin (1961) and this was therefore adopted, with modifications, for the present study. Carbon dioxide was absorbed in a mixture of ethanol, benzylamine and dioxane (ratio 3:1:3 respectively). In this system CO₂ reacts with the benzylamine to form a soluble salt which can then be titrated directly with sodium methoxide:

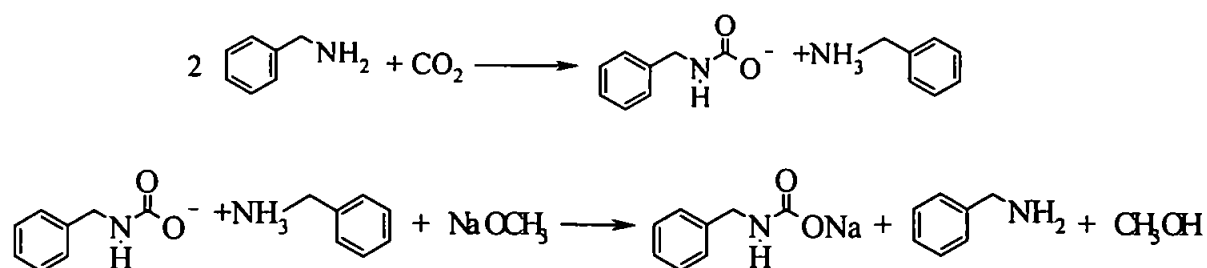


Figure 36 shows the apparatus used to test the efficiency of the new CO₂ trap.

The absorption solution was placed in a pear-shaped flask to give extra depth. The solution was stirred during both the oxidation step and during titration to prevent formation of a CO₂ saturated layer. Stirring also had the effect of breaking up bubbles and keeping them under the surface of the liquid for a longer period of time. All of these factors helped to increase the time allowed for CO₂ absorption before bubbles of N₂/CO₂ escaped the absorption solution.

A burette sealed by a rubber bung and filled with sodium methoxide solution was put in place before the start of the oxidation to prevent atmospheric CO₂ entering the vessel during titration. The solution was then titrated with sodium methoxide at the end of the

experiment. Thymol blue was used as an indicator. A very sharp yellow to blue endpoint was observed.

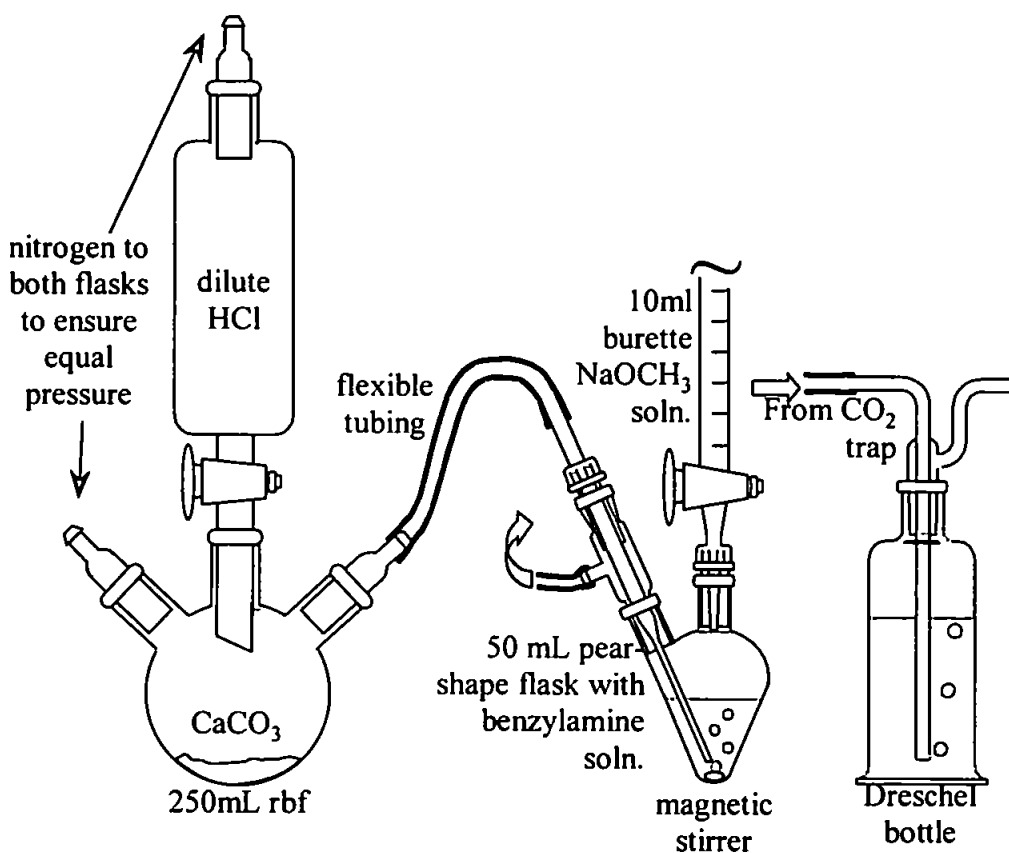


Figure 36. Apparatus for testing the efficiency of the benzylamine CO₂ trap.

4.3.1.2 Silicone tubing

Silicone tubing used to connect the vessels of the RuO₄ oxidation apparatus together were found to be permeable to carbon dioxide (personal communication, Dr. Snape, Brixham Environmental Laboratory, Astra Zeneca Ltd.). During long-term experiments (24 h to several days) a significant proportion of CO₂ was lost due to diffusion through silicone tubing (Snape, pers. Comm.). Butyl rubber was found to be a suitable alternative since it was flexible but impermeable to CO₂.

4.3.1.3 Results

To measure the efficiency of the new apparatus two experiments were carried out. For both, the apparatus was as shown in Figure 36. CO₂ was generated as described in section 4.3.1, *i.e.* by dropping dilute HCl onto a weighed amount of CaCO₃ in a 250 mL rbf. The system was first purged (30 min) with N₂ to remove atmospheric CO₂ from the system. The absorption solution was neutralised (observed as a green solution one drop before the final end-point) before CO₂ production commenced.

In the first experiment, CO₂ was generated over a period of 20 min after which the solution was left stirring for a further 60 min then titrated. In the second experiment the CO₂ was generated over a period of 24h, as in a typical oxidation situation. Table 16 shows the results of the two experiments.

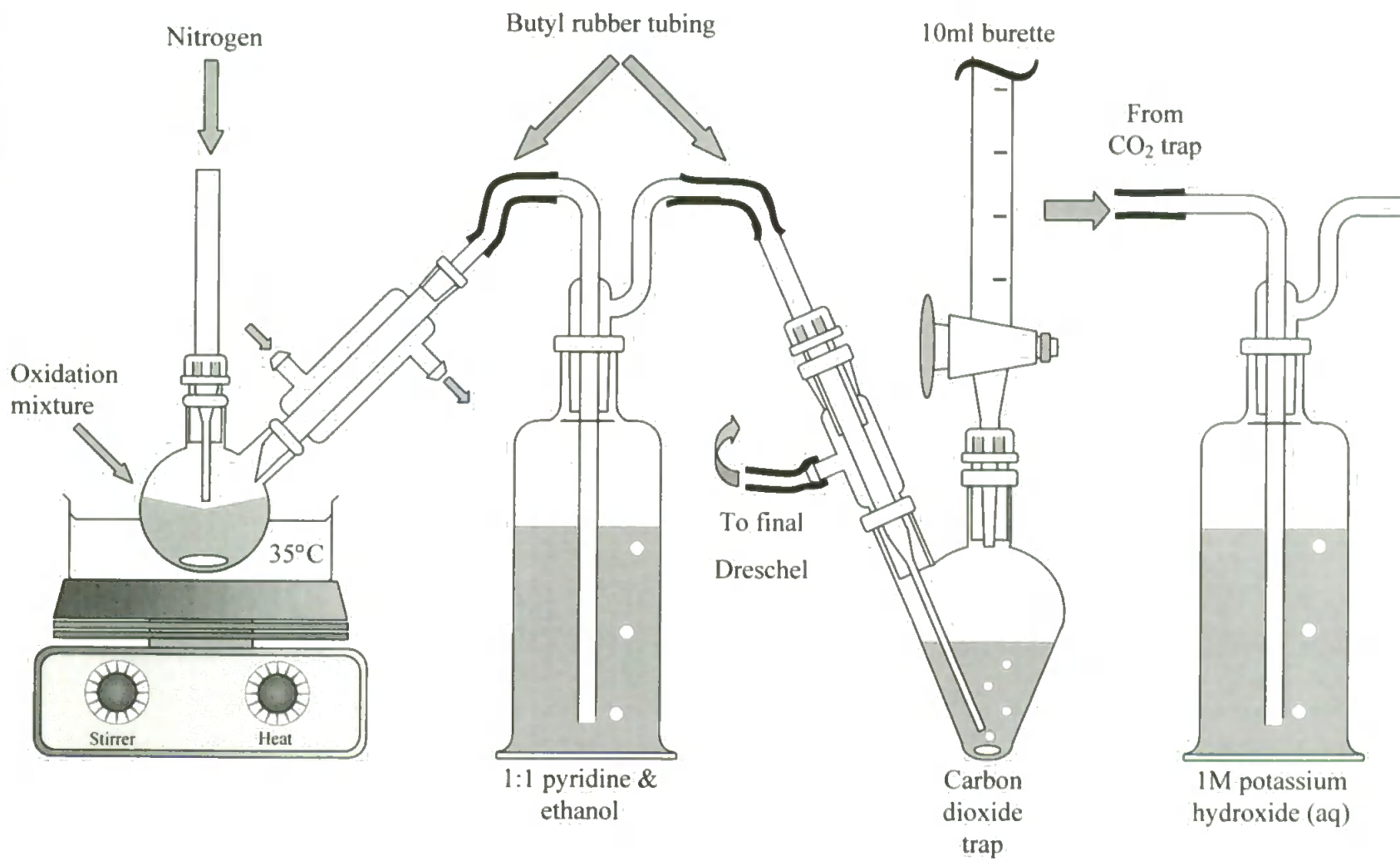
| Experiment | Replicate No. | CO ₂ Observed | Mean | Std. Dev. |
|---------------|---------------|--------------------------|-------|-----------|
| 1 (20 min) | 1 | 95.94 | 92.14 | 4.12 |
| | 2 | 92.72 | | |
| | 3 | 87.77 | | |
| 2 (24 h) | 1 | 86.11 | 89.85 | 4.22 |
| | 2 | 86.21 | | |
| | 3 | 95.09 | | |
| | 4 | 89.59 | | |

Table 16. Results of two experiments to test the efficiency of the benzylamine CO₂ trap. Observed CO₂ is expressed as percent of expected.

The results show an improvement on the aqueous Ba(OH)₂ CO₂ trap, both in terms of accuracy and of precision. The standard deviations for both experiments were very similar but the mean percent CO₂ observed is slightly lower for the 24 h experiment. This may be due to leakage of gas from ground glass joints over the 24 h period. Sealing joints with silicone grease would no doubt prevent leakage but may have contaminated the oxidation mixture. The small amount of leakage observed was deemed acceptable.

The apparatus for oxidation using ruthenium tetroxide is shown in Figure 37.

Figure 37. Modified apparatus for the RuO_4 oxidations of hydrocarbons.



4.3.2 Liquid/liquid extraction of water-soluble acids.

The liquid/liquid extraction step was used by Thomas (1995) to extract water soluble acids produced on oxidation of aromatic UCMs into an organic solvent before derivatisation and analysis by gas chromatography. Figure 38 shows the apparatus used. Liquid/liquid extraction works by directing condensed solvent (diethylether) into the inner glass column, which exits through the sinter at the bottom extracting anything slightly soluble as it bubbles up through the water sample and returns to the rbf where the cycle is repeated.

Obviously the solvent used must be less dense than water and be polar enough to extract the water-soluble organic compounds in a reasonable time. The disadvantages of using this system are many; water is sparingly soluble in diethylether – so after 24 h of extraction the few mL of water at the bottom of the rbf is likely to have a significant amount of the extracted water-soluble products in it. The procedure is time-consuming – requiring 24 h for the extraction, then drying (Na_2SO_4) and rotary evaporation of the large amount of diethylether, the volume of solvent required is relatively large, and more importantly, volatile compounds (such as low molecular weight carboxylic acids) may be lost due to evaporation, both from the extraction procedure itself (as in Soxhlet extraction –Ali (1994) and Wraige (1997) review losses from various extraction procedures) and rotary evaporation.

4.3.2.1 Experiments and results.

Repeat extraction of three acids (propanedioic, ethylpropanedioic and hexanedioic acid) was carried out using the apparatus shown in Figure 38. Each acid (10-15 mg) was dissolved in de-ionised water (~80 mL), acidified to pH 2 (conc. HCl) and placed in the liquid/liquid extractor. Diethylether (~300 mL) was placed in the 500 mL rbf and heated

until boiling vigorously (using anti-bumping granules). The acid solution was extracted for 24 h. After 24 h the diethylether solution was dried (~20 g Na₂SO₄ in the rbf) and the solvent removed (rotary evaporation). The acids were then derivatised using BF₃/C₄H₉OH and analysed by GC as the butyl esters. Ethyl octanoate was used as an external standard, added after the butylation stage.

A control was prepared by derivatising a mixture of the three carboxylic acids with BF₃/C₄H₉OH and analysing by GC. Response factors of the butyl esters with respect to ethyl octanoate were measured by repeat injection of the control (Table 18).

The percentage recovery of acids is shown in Table 17:

| Acid | Extraction experiment No. | | | | | Mean | σ _{n-1} |
|-------------------|---------------------------|-------|-------|------|-------|-------|------------------|
| | 1 | 2 | 3 | 4 | 5 | | |
| Propanedioic | 77.2 | 136.2 | 29.6 | 30.6 | 29.8 | 60.7 | 46.9 |
| Ethylpropanedioic | 83.2 | 130.0 | 121.9 | 84.9 | 100.4 | 104.1 | 21.3 |
| Hexanedioic | 86.6 | 26.8 | n.d. | 21.3 | 85.8 | 55.1 | 36.0 |

n.d. = not detected

Table 17. Percentage recovery of acids by liquid/liquid extraction into diethylether.

As can be seen from Table 17, the recoveries of the three acids were very erratic. No reasonable explanation can be put forward for such inconsistent recoveries.

Attempts were made to replace this step with a solid phase extraction (SPE) procedure, but initial experiments were unsuccessful due to irreversible adsorption of the acids onto the extraction media. Time constraints did not allow further development of a SPE procedure. The existing liquid/liquid extraction procedure was therefore retained but the loss of acids was to be compensated for by addition of an internal standard (hexanoic acid) immediately after oxidation, *preceding* the liquid/liquid extraction step.

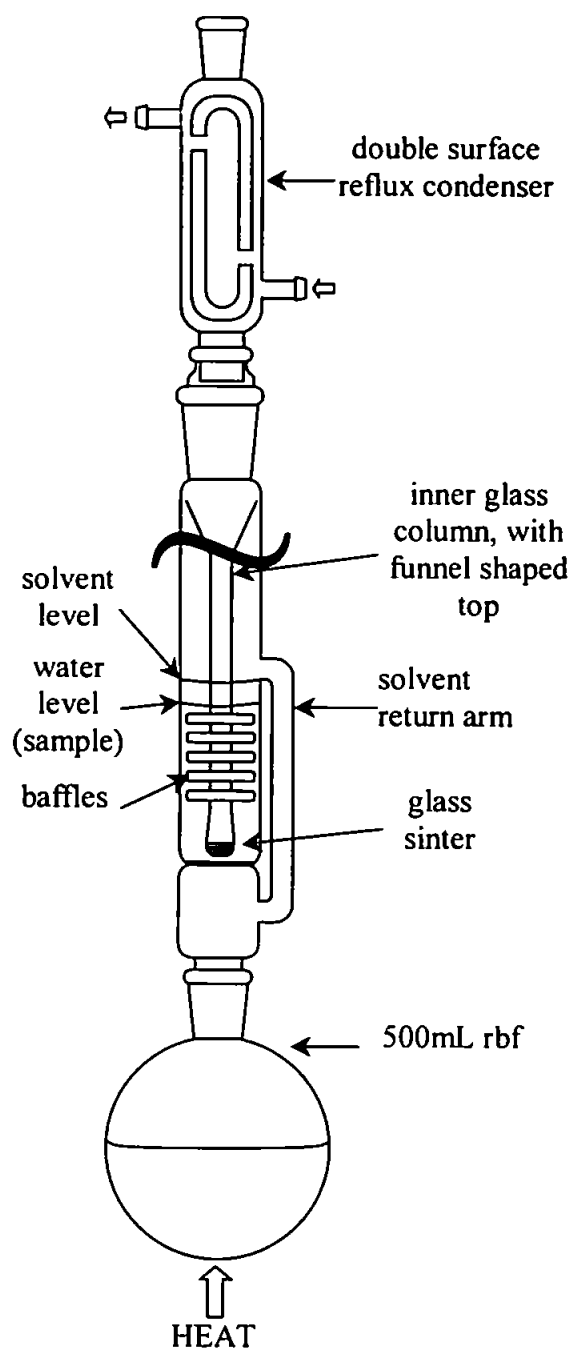


Figure 38. Liquid/liquid extraction apparatus.

| Compound | ethyloctanoate | propanedioic acid | 2-ethylpropanedioic acid | 1,6-hexanedioic acid |
|-----------------|----------------|-------------------|--------------------------|----------------------|
| Response factor | 1.00 | 1.62 | 1.56 | 1.58 |

Table 18. Response factors of dicarboxylic acids with respect to ethyloctanoate.

4.3.3 Fuller's Earth filtration of colloidal ruthenium salts.

Fuller's earth was used by Thomas (1995) as a filtration aid to remove colloidal ruthenium from the DCM fraction of oxidation products. However, losses may be encountered if carboxylic acids adsorb to Fuller's earth irreversibly.

This could not explain the low recovery of reaction products from the oxidation of tetralin (Table 14 and Table 15), since short chain carboxylic acids are found in the water fraction after oxidation. However, any step that may actively remove reaction products is not desirable, and should be replaced.

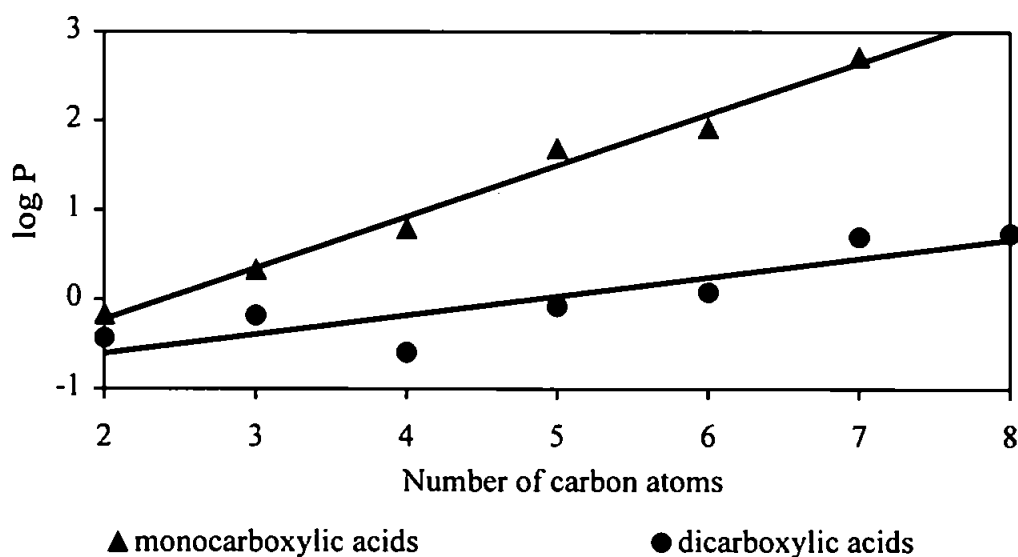


Figure 39. The octanol/water partition coefficients ($\log P$) for monocarboxylic and α - ω -dicarboxylic acids (Klopman et al., 1994)

Figure 39 shows the partition coefficients of monocarboxylic and α - ω -dicarboxylic acids in octanol/water ($\log P$). Higher numbers signify an increasing affinity for octanol, indicating decreasing polarity. Dicarboxylic acids are significantly more polar than monocarboxylic acids. Thus it would be expected that dicarboxylic acids may adsorb more strongly than monocarboxylic acids to a surface more polar than the solvent.

An experiment to determine the extent to which carboxylic acids adsorb to Fuller's Earth was thus undertaken.

4.3.3.1 Results.

From a stock solution (in DCM) of 4 carboxylic acids (pentadecanoic, tetracosanoic, 1,10-decanedioic and 1,24-tetracosanedioic acids), aliquots were taken (5-10 mg each acid) and filtered (7cm Büchner funnel) through either GF/A glass fibre filter paper, or 2 g Fuller's Earth supported on GF/A paper. The filter medium was rinsed with an equal volume of fresh DCM after filtering the acid mixture. Immediately after filtration, an internal standard (hexadecanoic acid) was added to the filtrate.

The filtrate was then rotary evaporated, blown down (N_2), derivatised ($BF_3/MeOH$) and analysed by GC. The experiment was carried out in triplicate. As a control, one aliquot of the acid mixture was simply blown down (N_2), methylated and analysed by GC.

Figure 40 demonstrates quite clearly that dicarboxylic acids adsorb in quantity (~90%) to Fuller's Earth. A significant proportion of monocarboxylic acids also adsorbed (~20%).

The acids apparently adsorb quite strongly, since the Fuller's Earth from one experiment was extracted with DCM (Soxhlet, 24 h) and only trace amounts of the monocarboxylic acids and no dicarboxylic acids were observed in the extract.

Thus an alternative method of removing the colloidal ruthenium was obviously required.

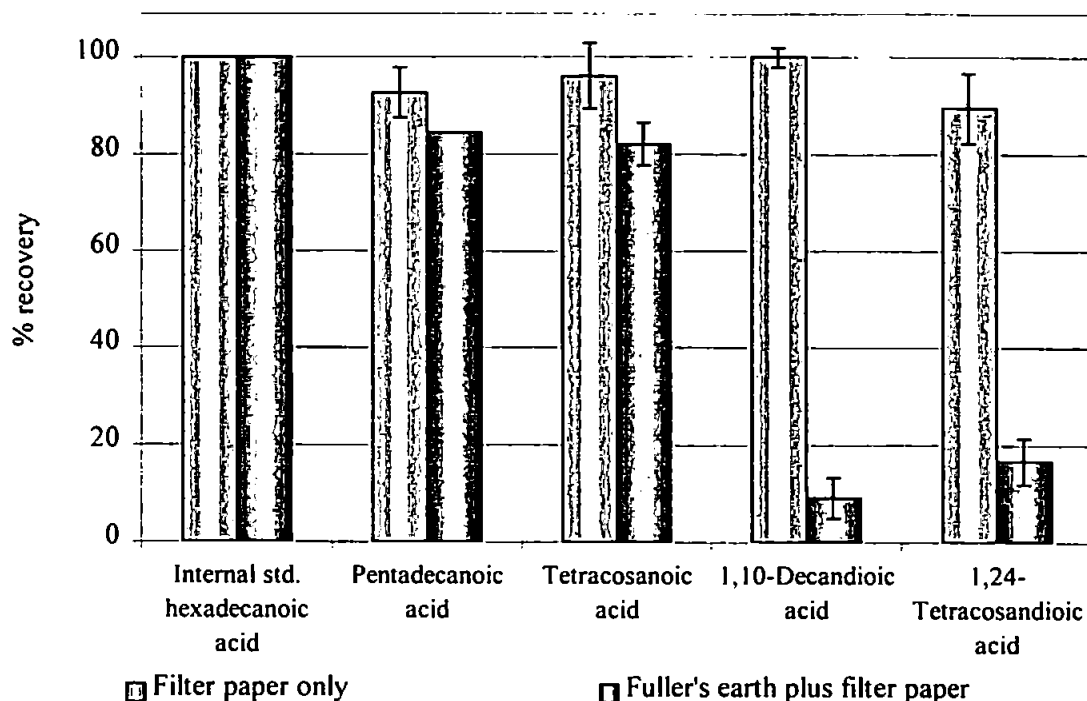


Figure 40. Recovery of mono- and dicarboxylic acids filtered through Fuller's Earth. Values are averages ($n = 3$), error bars show \pm one standard deviation.

4.3.3.2 Removal of colloidal ruthenium salts.

Alternative methods of removing colloidal ruthenium from an organic phase might involve ultra-fine filtration or centrifugation.

Solvent extraction of metals from aqueous solution has been used for decades in the analysis of metals. The principle was appealing since it could be incorporated into existing washing steps of the oxidation work-up.

Gandon *et al.*, (1993) outlined a procedure for the removal of radioactive ruthenium complexes from aqueous nuclear waste. This involved the formation and co-precipitation of a ruthenocyanide complex with copper ferrocyanide. The procedure is simple and the formation of the ruthenocyanide species is instantaneous.

Once the solid co-oxidant NaIO_4 in the reaction mixture has been dissolved, the speciation of ruthenium in the dichloromethane fraction is unknown. The yellow RuO_4 is unstable, and soon changes colour to a dark green/black.

Ruthenium was extracted from dichloromethane into an aqueous layer by the addition of a few crystals of (yellow) potassium ferrocyanide. The shift was observed as a change in the colour of the two phases; the dark green colour transferred from the organic phase to the aqueous, leaving a colourless organic phase, conveniently indicating the absence of ruthenium.

However, it was also found that by simply passing the DCM fraction through a small column of ground Na_2SO_4 most of the colloidal ruthenium salts were removed. Any small amounts of remaining ruthenium salts had no apparent effect on the subsequent work-up and quantification of the DCM-soluble oxidation products. It was therefore decided not to use the solvent extraction step in order to keep the work-up procedure as simple as possible.

4.3.4 Base extraction.

Since this developmental study was concerned with the oxidation of single compounds or simple mixtures the oxidation products were likely to be fairly simple mixtures themselves. The base extraction step was therefore deemed unnecessary at this stage, thus simplifying the work-up in terms of effort and time. In future oxidation studies, it would be worthwhile developing a SPE method, since this would require no reflux step and would use much less solvent.

4.3.5 Micro-scale derivatisation procedures.

The original methylation procedure used to derivatise DCM-soluble acids before GC and GCMS analysis (see section 2.3.3.4, Chapter 2) involved a cumbersome reflux step. The

procedure was quicker and used less reagent if carried out in a sealed Reacti-vial™ (as for the butylation of water-soluble acids).

4.4 Summary and Conclusions.

This chapter has presented a number of improvements to many aspects of the RuO₄ oxidation and work-up procedures. The replacement of the carbon dioxide trap with an organic solvent-based method is an important development. This is indicated by the significantly improved recoveries of CO₂ from the RuO₄ oxidation of tetralin (Table 19). The recovery of CO₂ from the oxidation of tetralin using the new organic solvent trapping system compares favourably with the initial experiment where CO₂ was generated by the addition of HCl to CaCO₃ (Table 19).

| | CO ₂ trap evaluation using CaCO ₃ (24 h) ^a | Oxidation of tetralin | |
|----------------|---|---|--|
| | | Before method development ^b | After method development ^c |
| mean | 89.9 | 56.7 | 82.2 |
| σ_{n-1} | 4.2 | 13.1 | 2.9 |

^a – see Table 16, n = 4

^b – see Table 15, n = 4

^c – see Table 23, n = 8

Table 19. Recovery of carbon dioxide from the RuO₄ oxidation of tetralin before and after method development.

The removal of the Fuller's Earth filtration step is another significant improvement and while the solvent extraction of previously insoluble ruthenium by-products looked promising, a simple filtration through ground Na₂SO₄ proved sufficient – a procedure which was already deemed necessary to the work-up.

Further work is needed to develop an alternative to liquid/liquid extraction, although extraction of water-soluble oxidation products into an organic solvent may be unnecessary if an HPLC method were used to analyse the water soluble fraction.

The base extraction procedure was omitted for this study, although the oxidation of real samples such as feedstocks would require such a step. A suitable SPE method could be developed as an alternative.

These promising modifications were tested by oxidation of a number of synthetic 'model' UCM hydrocarbons. Details of these syntheses are presented in the Chapter 5, and of the oxidations in Chapter 6.

5 Synthesis of UCM model hydrocarbons.

Hydrocarbons suggested by Thomas (1995) as typical UCM components were unavailable commercially and so were synthesised herein. 6-Cyclohexyltetralin, 1-(3'-methylbutyl)-7-cyclohexyltetralin, 1-*n*-nonyl-7-cyclohexyltetralin and 1-*n*-nonyl-7-cyclohexylnaphthalene were prepared in gram quantities and fully characterised by GCMS, IR and NMR techniques. Analysis showed the synthesised hydrocarbons to be relatively pure (80+%) except for 1-*n*-nonyl-7-cyclohexyltetralin which was a simple mixture (53%) with 6-cyclohexyltetralin (22%) and 1-methyl-7-cyclohexyltetralin (11%).

5.1 Synthesis of substituted cyclohexyltetralins

Several studies have postulated 'average' or model structures for aromatic UCM hydrocarbons, usually on the basis of the identification of oxidation products, followed by a 'retro-structural' analysis (reviewed by Thomas, 1995). Whilst Gough (1989) proposed alkylbenzene structures with branched side-chains *e.g.* (I),

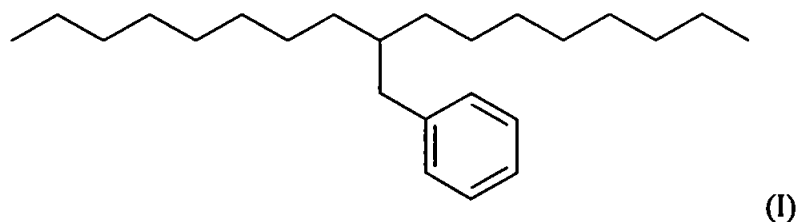


Figure 41. T-branched alkylbenzene structure proposed by Gough (1989) as typical aromatic UCM component.

most subsequent studies have concluded that the oxidation products are more consistent with alkylated alicyclic aromatics such as alkyltetralins. Thus Revill (1992), Thomas (1995) and Warton (1999) all considered that the branched carboxylic acids produced from ruthenium tetroxide oxidations of aromatic UCMs were indicative of alkyltetralins and similar compounds *e.g.* (II).

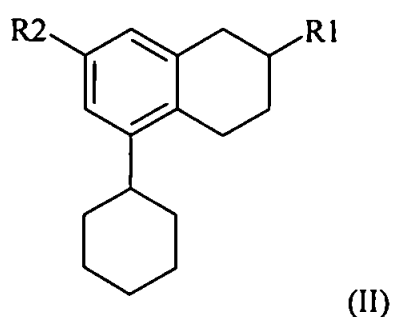


Figure 42. Substituted alkyltetralin proposed by Thomas (1995) as 'average' monoaromatic UCM component.

On the basis of the studies of Thomas (1995), Wraige (1997) synthesised a 'model' or 'average' aromatic UCM component, 1-*n*-propyl-7-cyclohexyltetralin (III) and assayed

the toxicity of the compound to the mussel, *Mytilus edulis* in order to investigate the environmental effects of aromatic UCM hydrocarbons.

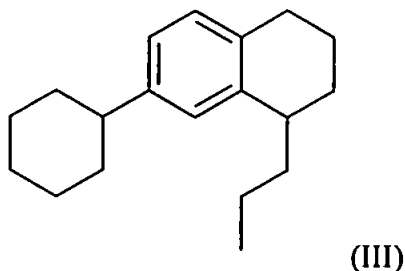


Figure 43. 1-*n*-propyl-7-cyclohexyltetralin, synthesised by Wraige (1997) to study the environmental impact of UCM hydrocarbons.

However, the oxidative studies of the model hydrocarbon advocated by Thomas (1995) were not made by Wraige (1997) and only enough pure 1-*n*-propyl-7-cyclohexyltetralin (III) was synthesised for the mussel assays. Therefore in the present study, the aim was to synthesise several new model aromatic UCM hydrocarbons in quantities large enough for thorough structural characterisation and for subsequent oxidative studies.

This chapter presents the synthetic strategy and full characterisation of the intermediates and products. Full details of the synthetic procedures involved are presented in Chapter 2.

5.2 Substituted cyclohexyltetralins

The compounds suggested by Thomas (1995) as possible models of UCM hydrocarbons have the general structure 1-alkyl-7-cyclohexyltetralin (IV), where R represents straight chain or branched alkyl groups. For the present study, straight chain and branched homologues with R = H, *i*-C₅H₁₁ and *n*-C₉H₁₉ were synthesised in order that the effects of RuO₄ oxidation of tetralin-based structures with different substituents could be investigated.

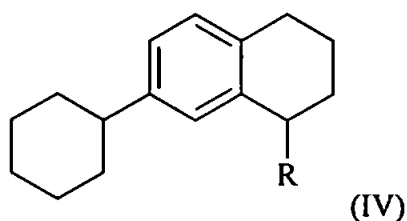


Figure 44. General structure of 1-alkyl-7-cyclohexyltetralins - proposed model UCM monoaromatic hydrocarbons.

The synthesis of 6-cyclohexyltetralin ($R = H$) was a joint project between the author and Wraige (1997). Full details of the synthesis of compounds where $R = H$, $i\text{-C}_5\text{H}_{11}$ and $n\text{-C}_9\text{H}_{19}$ are described herein.

Experimental details of the syntheses can be found in Chapter 2. The structures and purity of synthetic intermediates and the final products were determined by GC, GC-MS, IR and NMR. In interpreting the MS, IR and NMR spectra, correlation charts and tables of chemical shift data were consulted (*e.g.* Smith and Busch, 1999; Stuart, 1996; Breitmaier, 1993).

5.3 Synthetic strategy

Figure 45 shows a schematic of the chosen synthetic route. This route follows the well-known Haworth synthesis of aromatic hydrocarbons (March, 1992; Vogel, 1989). The first step involved the formation of a keto-acid (V) *via* a Friedel-Crafts acylation. The keto-acid (V) was then reduced (*via* a Clemmensen reduction) and the resulting carboxylic acid (VI) cyclised to give a cyclic ketone (VII). The tetralone (VII) was then further reduced to the hydrocarbon (VIII), or used as the substrate in a Grignard reaction to make compounds such as IX and X.

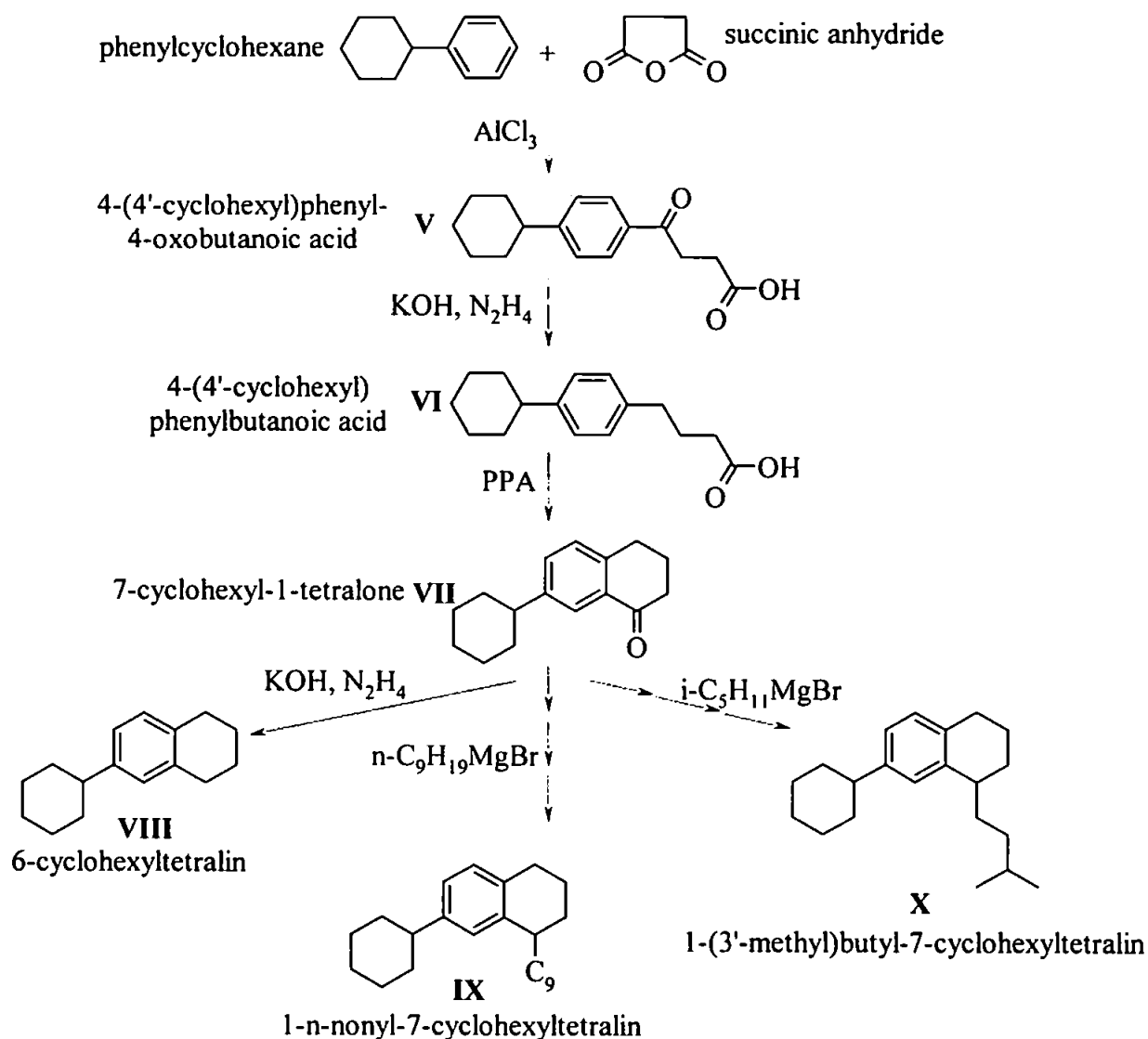


Figure 45. Scheme for the synthesis of substituted cyclohexyltetralins. (PPA = polyphosphoric acid)

5.4 Preparation of 4-(4'-cyclohexylphenyl)-4-oxobutanoic acid (V).

It was initially intended that the carboxylic acid (VI) be synthesised *via* a Friedel-Crafts alkylation of phenylcyclohexane with γ -butyrolactone, thus avoiding the first step shown in Figure 45. Mosby (1952) and Truce & Olsen (1952) reported syntheses involving the condensation of various γ -lactones and aromatic hydrocarbons with reasonable success. Truce & Olsen also found that by increasing the proportion of aluminium chloride to

lactone, the acid was cyclised *in-situ* producing the cyclic ketone, thus eliminating several steps of the Haworth synthesis.

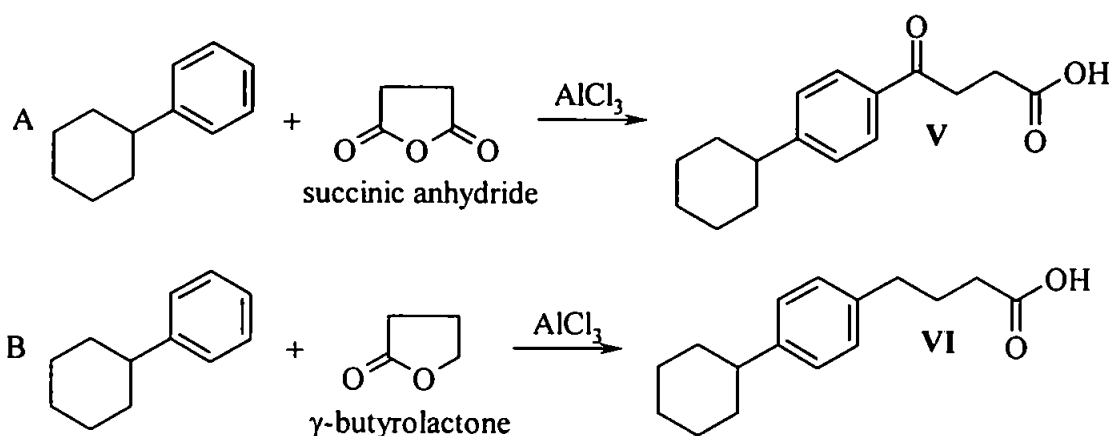


Figure 46. Friedel-Crafts reactions; A = acylation, B = alkylation.

More recently however, Eisenbraun *et al.* (1971) compared the acylation route (A, Figure 46) to the alkylation route (B, Figure 46) and found several problems with the latter. Variable yields according to reaction conditions and the *in-situ* isomerisation of products led the authors to conclude that the more conventional acylation route was the most satisfactory. Preliminary experiments made herein tended to support this. Following the acylation reaction (B, Figure 46) using γ -butyrolactone, a wide range of undesired products was observed, with a very low yield (4%) of the desired carboxylic acid (VI). The difficulty in separating the minimal amount of product from the reaction matrix made the alkylation route impractical. It was therefore decided that although the acylation route might take longer, it would provide more satisfactory yields of more pure products. The chosen procedure followed a typical Friedel-Crafts acylation as described in various texts (*e.g.* March, 1992; Vogel, 1989). In the acylation of benzene and substituted benzenes (*e.g.* phenylcyclohexane) an excess of the substrate is used as the solvent, for larger hydrocarbons the solvent generally used is nitrobenzene which has beneficial

effects on product yields, and reduces the destructive effect of AlCl_3 by formation of a complex (Berliner, 1949).

Therefore nitrobenzene was used as a solvent in the first acylations carried out herein. However the complete removal of the solvent from the product was a problem due to the low volatility (Bp. nitrobenzene 201-211°C). Another solvent - 1,1,2,2-tetrachloroethane (Bp. 147°C) having the same beneficial properties as nitrobenzene (Berliner, 1949) was employed in subsequent acylations with greater success; product yields were as good as with nitrobenzene, and the solvent was readily removed by steam distillation.

$\text{Al}(\text{OH})_3$ produced on hydrolysis of the AlCl_3 was removed by dissolving the crude product (V) in a solution of Na_2CO_3 (forming the sodium salt) and filtering off the solid $\text{Al}(\text{OH})_3$. At this stage, coloured impurities were largely removed by boiling the sodium salt of the keto-acid (V) with decolourising carbon followed by hot filtration.

5.4.1 Characterisation of 4-(4'-cyclohexylphenyl)-4-oxobutanoic acid (V)

5.4.1.1 GCMS

A total ion current (TIC) chromatogram of the crude keto-acid (V) as the trimethylsilyl (TMS) derivative is shown in Figure 47. Integration of the peak areas showed the crude keto-acid (V) to be 99% pure, thus further purification was deemed unnecessary.

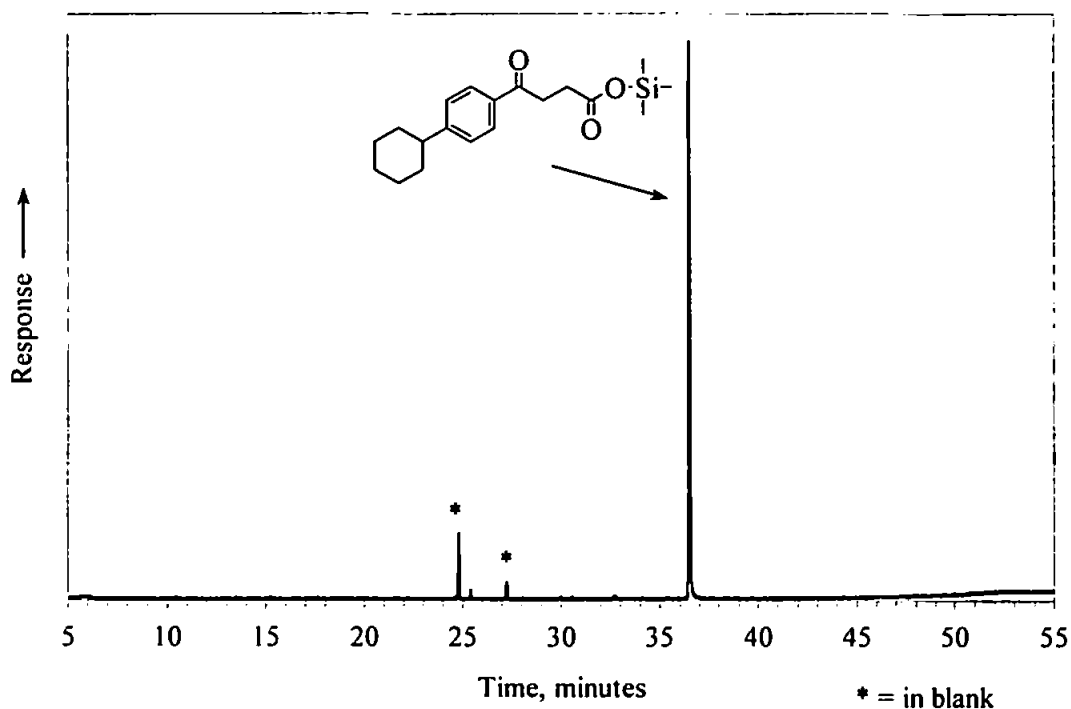


Figure 47. TIC chromatogram of 4-phenyl(4'-cyclohexyl)-4-oxobutanoic acid (V) TMS ester. GC = 12m HP1, 40 – 300°C @ 5°C min⁻¹, held 10 min.

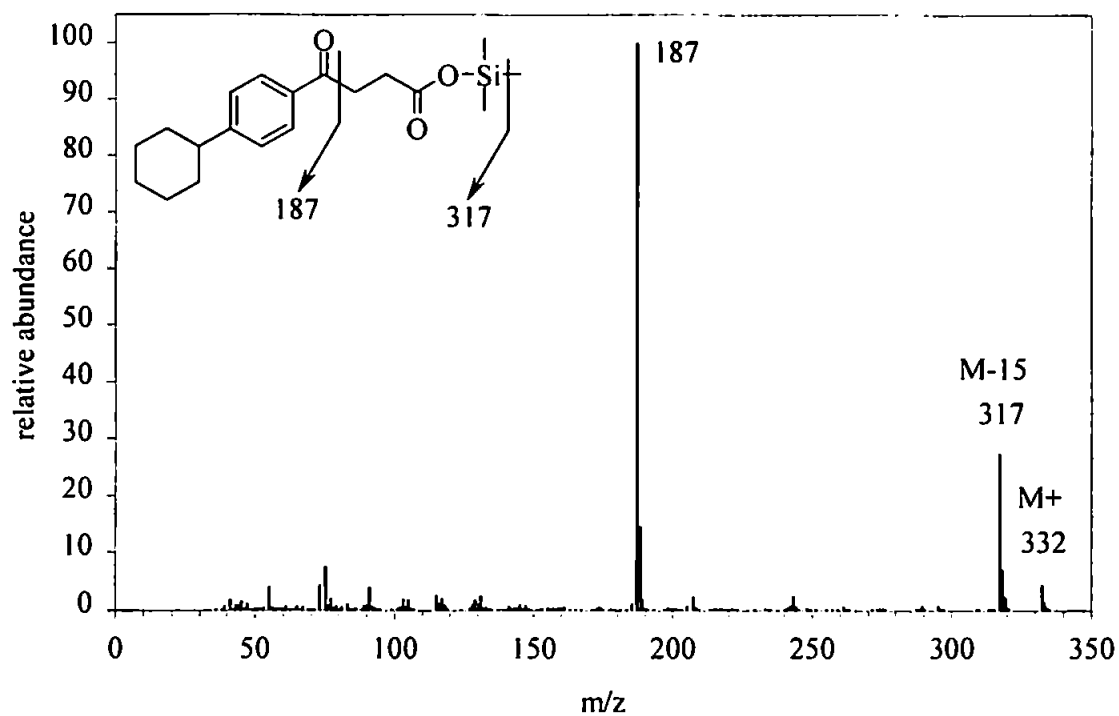


Figure 48. Mass spectrum of 4-phenyl(4'-cyclohexyl)-4-oxobutanoic acid (V) TMS ester.

The mass spectrum of the keto-acid (V, Figure 48, as the TMS ester) confirmed the structure; giving the M^+ ion at m/z 332, $M-15$ at m/z 317 corresponding to the loss of a methyl group from the TMS group. The labile nature of the methyl groups on the TMS group accounts for the relatively low intensity of the molecular ion. The ion at m/z 187 corresponds to a loss of 145 mass units, accounted for by benzylic cleavage to leave the cyclohexylbenzoyl fragment.

5.4.1.2 IR

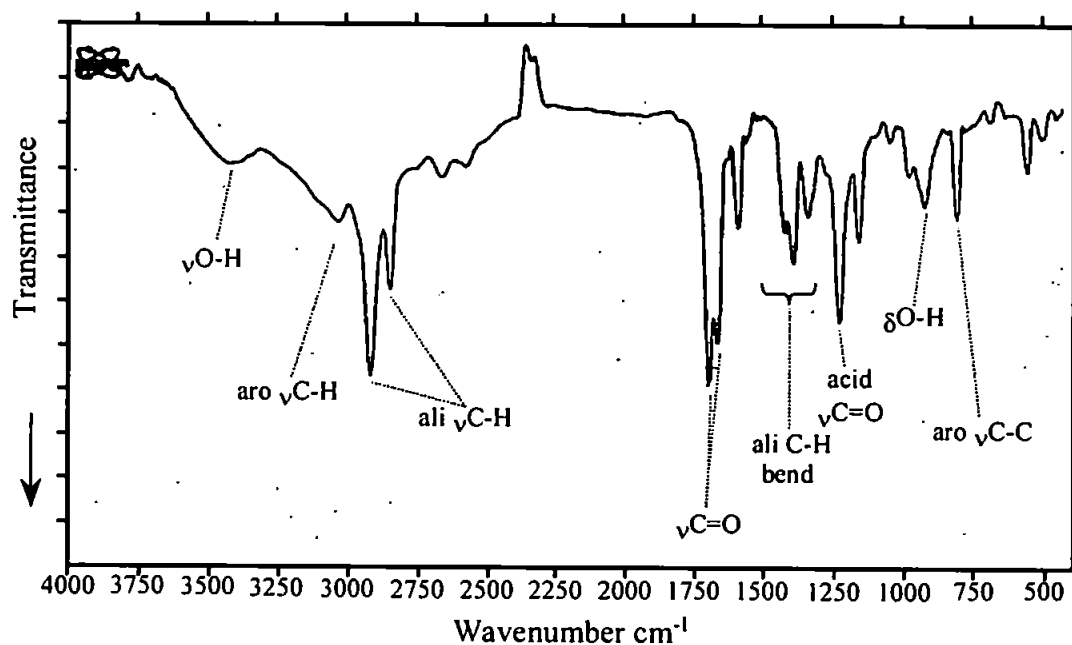


Figure 49. Infrared spectrum of 4-phenyl(4'-cyclohexyl)-4-oxobutanoic acid (V); KBr disk.

The infrared spectrum of the keto-acid (V, Figure 49) shows all the expected features; two strong bands at 2924 and 2853 cm^{-1} indicating aliphatic C-H stretching, a weaker, broader band at 3038 cm^{-1} indicating the aromatic C-H stretch, and superimposed on top of these is the very broad O-H stretch due to the hydrogen bonded carboxylic -OH group. The other dominant features of this spectrum are the two strong bands at 1679 and 1709 cm^{-1} due to the ketone carbonyl and the carboxylic carbonyl groups respectively.

Peaks in the region below 1600 cm^{-1} may tentatively be assigned as due to C-C stretch in the aromatic ring (*para*- substituted at 819 cm^{-1}), aliphatic C-H bend (~ 1350 to $\sim 1500\text{ cm}^{-1}$), the C-O stretch of the carboxylic acid group (~ 1200 to $\sim 1300\text{ cm}^{-1}$) and the O-H bend of the acid group (938 cm^{-1}).

5.4.1.3 NMR

Interpretation of the ^{13}C NMR spectrum of the keto-acid (V, Figure 50) was relatively straightforward; the only tertiary aliphatic resonance at 44 ppm is the tertiary carbon in the cyclohexyl ring (C4). This is confirmed by the DEPT spectrum (Figure 51), where carbon C4 is above the baseline, and therefore must be tertiary or methyl, and the other aliphatic peaks are below the baseline and are therefore secondary CH_2 carbons. Aromatic carbons, being further downfield are found between 120 and 160 ppm. The two *ipso* carbons C5 and C8 are further deshielded by their substituents (especially the adjacent carbonyl) and are found at 134 and 154 ppm (identified by their absence in the DEPT sequence spectrum). The remaining aromatic carbons C6 and C7 are found at 127 and 128 ppm. The characteristic feature of this spectrum is however the two carbonyl resonances, the acid carbonyl C12 found at 178 ppm and the ketone carbonyl C9 found at 197 ppm.

The ^1H NMR spectrum of 4-phenyl(4'-cyclohexyl)-4-oxobutanoic acid (V, Figure 52) showed two doublets between 7 and 8 ppm corresponding to aromatic hydrogens H6 and H7. The resonance due to H4 (attached to the only tertiary carbon) was observed downfield from the other cyclic hydrogens at 2.5 ppm due to proximity to the benzene ring. The cyclic methylene hydrogens were observed between 1 and 2 ppm and the remaining hydrogens H10 and H11 (both adjacent to carbonyls) were observed at 2.8 and 3.3 ppm. Integration of the peaks confirms the assignments.

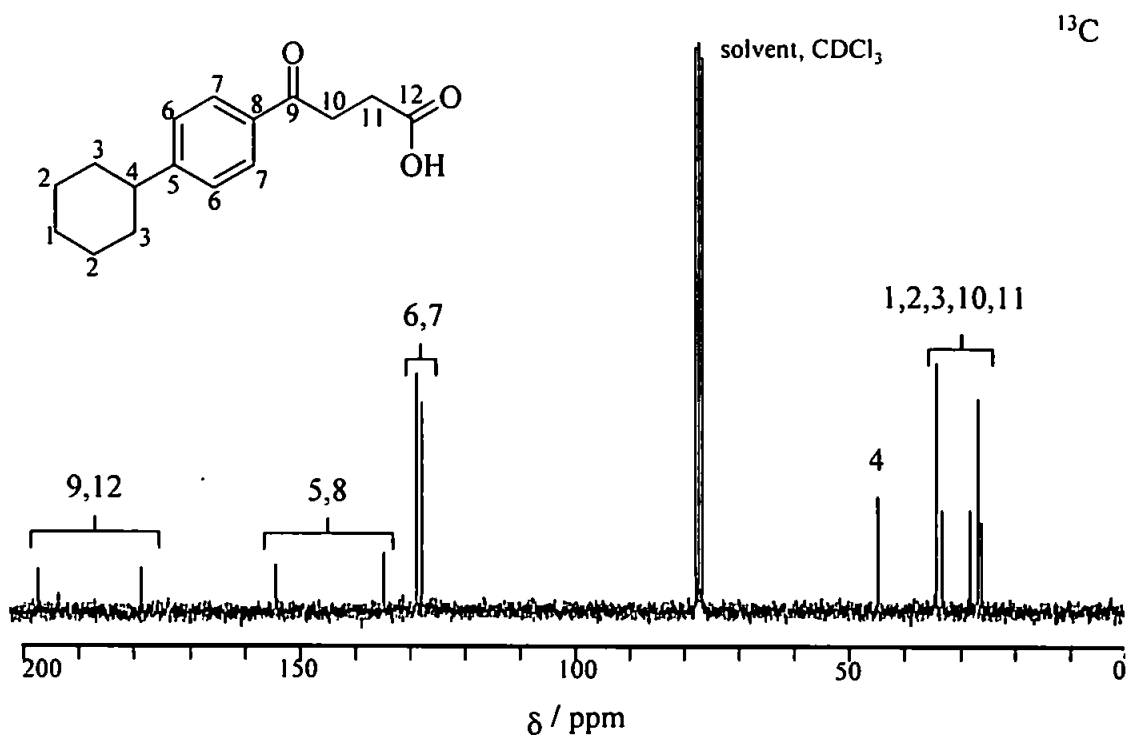


Figure 50. ¹³C NMR spectrum of 4-phenyl(4'-cyclohexyl)-4-oxobutanoic acid (V).

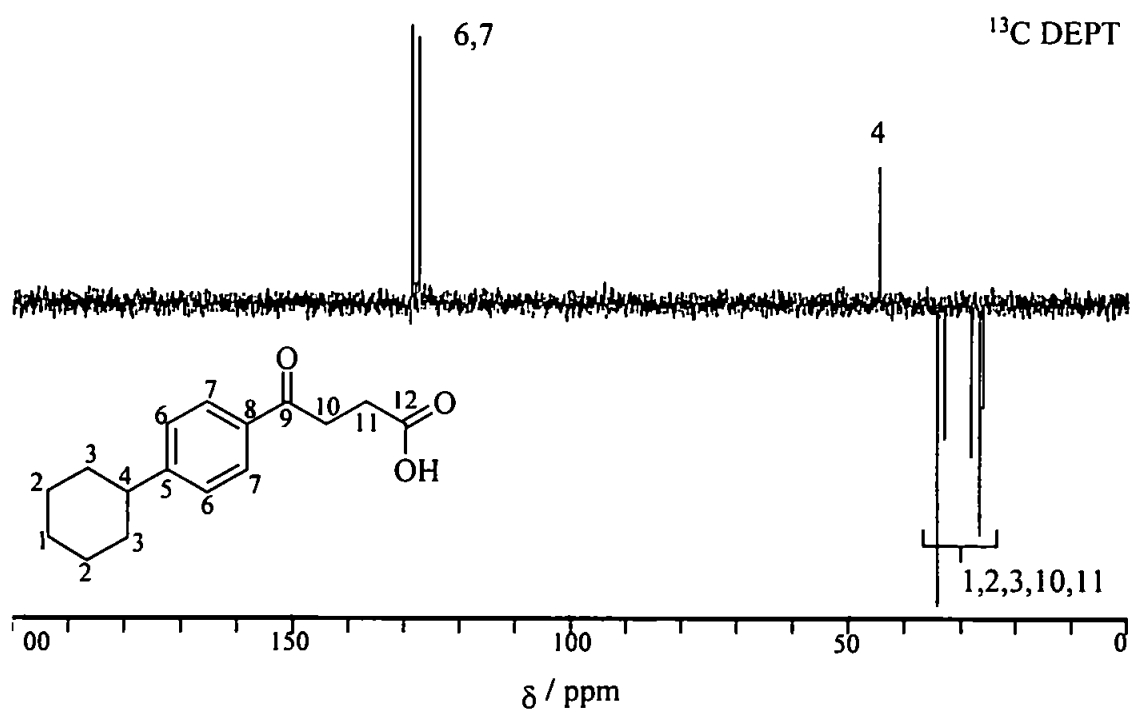


Figure 51. DEPT NMR spectrum of 4-phenyl(4'-cyclohexyl)-4-oxobutanoic acid (V).

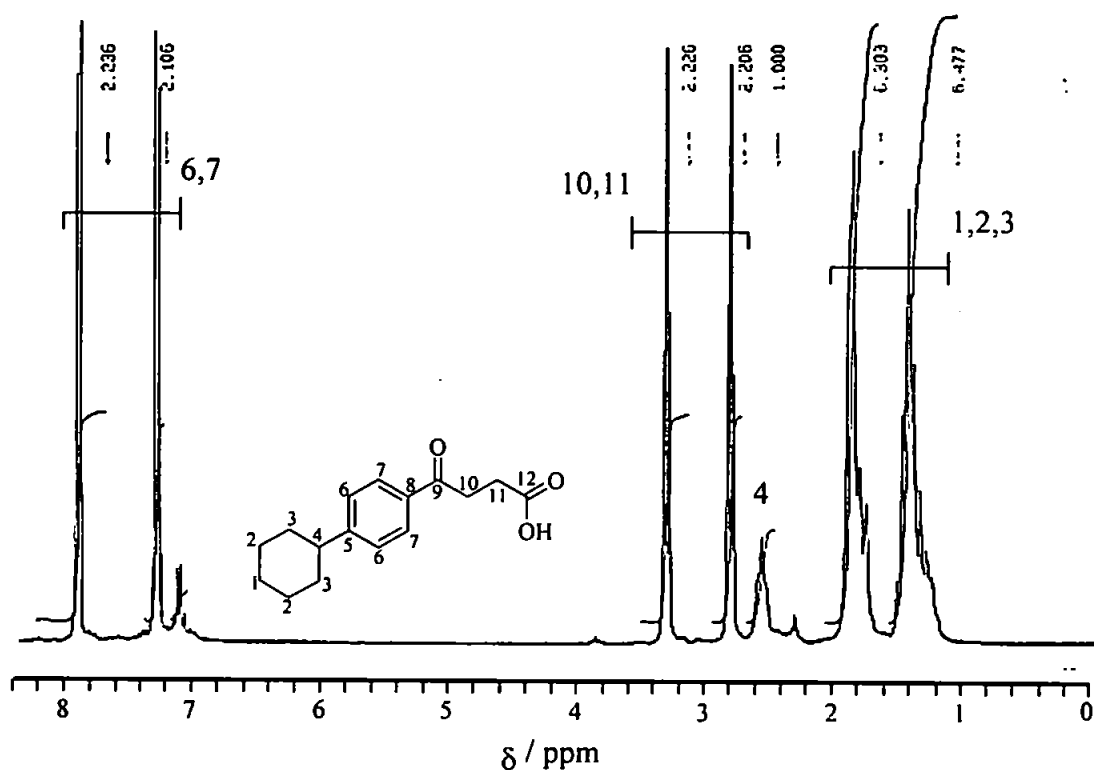


Figure 52. ¹H NMR spectrum of 4-phenyl(4'-cyclohexyl)-4-oxobutanoic acid (V).

5.5 Preparation of 4-(4'-cyclohexylphenyl)butanoic acid (VI).

The second step in the synthetic scheme involved the reduction of the ketone group of keto acid V to a methylene group to give acid VI. There are various established methods of achieving this including the Clemmensen reduction and the Wolff-Kishner reduction. Of the two, the Huang-Minlon modification of the Wolff-Kishner reduction (Huang-Minlon, 1946) was chosen since the Clemmensen reduction is unsuitable for high molecular weight compounds (Vogel, 1989). The Huang-Minlon-Wolff-Kishner reduction involved formation of the hydrazone of II and subsequent decomposition to give the methylene group.

5.5.1 Characterisation of 4-(4'-cyclohexylphenyl)butanoic acid (VI).

5.5.1.1 GCMS

The TIC chromatogram of the crude product (III, Figure 53, TMS ester) showed the high purity of the product after purification using decolourising carbon. Integration of the peak areas show the purity to be 90%. There was one major impurity (~10%) observed at a retention time of 13.3 min. The mass spectrum of the acid (Figure 54) showed the relatively weak molecular ion at m/z 318, along with the intense ion at m/z 303 corresponding to M-15, *i.e.* loss of a methyl from the TMS group. Cleavage of the butanoate substituent between the second and third carbon in the chain resulted in the alkene cation at m/z 186. Cleavage at the esteric carbon gave the COOTMS⁺ ion at m/z 117.

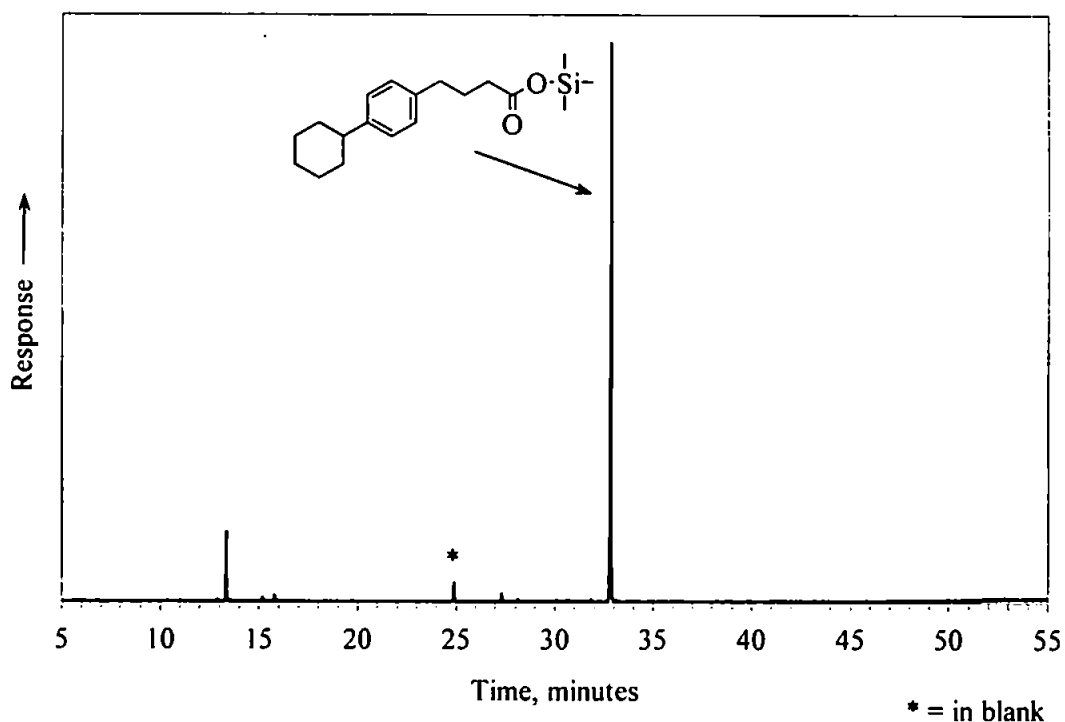


Figure 53. TIC chromatogram of 4-phenyl(4'-cyclohexyl)butanoic acid (VI) TMS ester. GC = 12m HP1, 40 – 300°C @ 5°C min⁻¹, held 10 min.

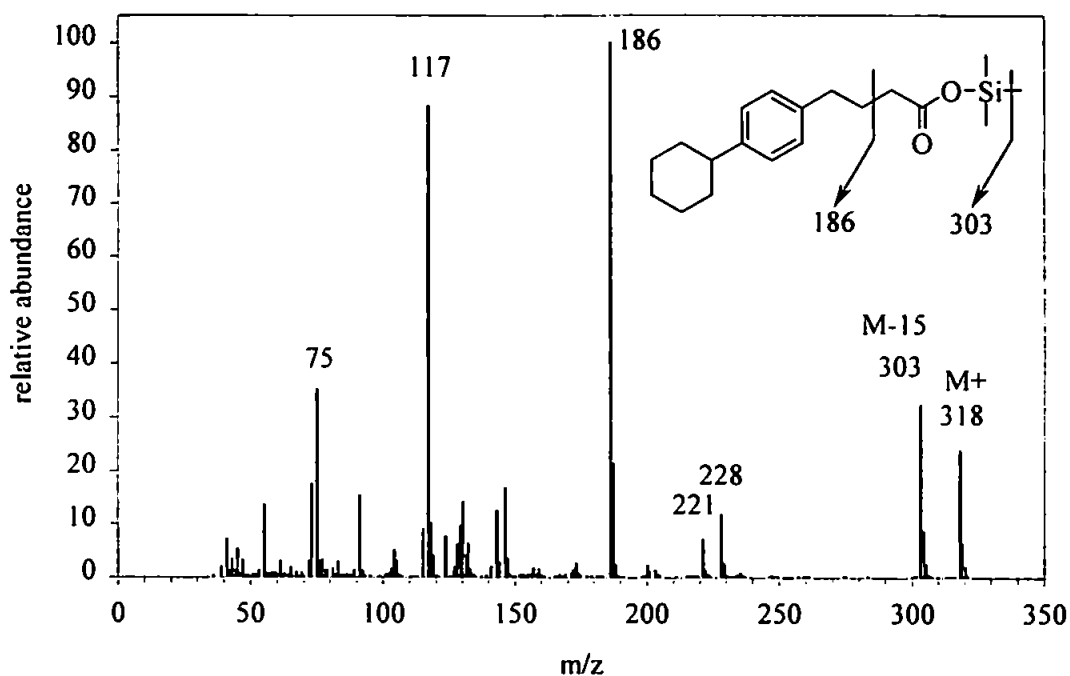


Figure 54. Mass spectrum of 4-phenyl(4'-cyclohexyl)butanoic acid (VI) TMS ester.

The impurity (10% by area) observed at 13.3 min in the TIC is an unidentified compound. The mass spectrum is shown in Figure 55. The mass spectrum shows a possible molecular ion at m/z 314 with a loss of M-15 (-CH₃ from TMS?). The molecule has at least one TMS group (characteristic ion at m/z 73) indicating a carboxylic acid or hydroxyl group.

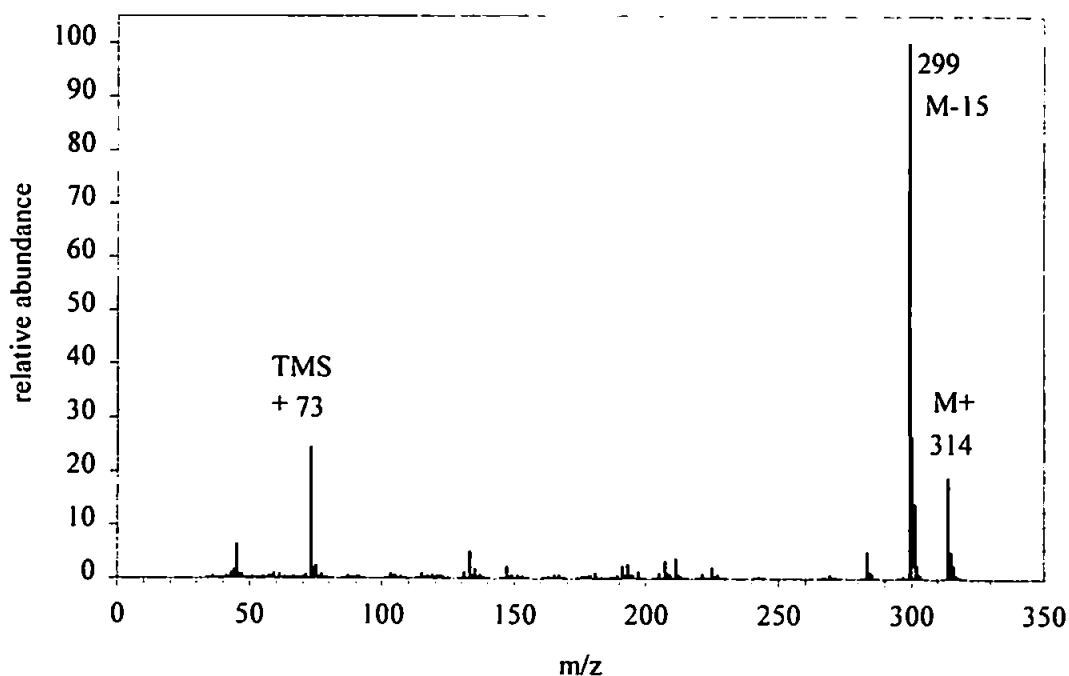


Figure 55. Mass spectrum of impurity in 4-phenyl(4'-cyclohexyl)butanoic acid (VI).

5.5.1.2 IR

The infrared spectrum of the crude product (Figure 56) shows the features expected of the desired acid; the broad O-H stretch is still evident dominating the $3400\text{-}3000\text{ cm}^{-1}$ region. Also observed are two aliphatic C-H stretches found at 2925 and 2854 cm^{-1} respectively. The strong peak at 1708 cm^{-1} shows the acidic carbonyl, no other carbonyl stretches are observed indicating the complete reduction of the keto-acid (II) to the acid. Peaks in the region below 1600 cm^{-1} are less intense in this spectrum, but may be due to aromatic C-C stretching (~ 1450 to $\sim 1650\text{ cm}^{-1}$) and aliphatic C-H bending (~ 1350 to $\sim 1500\text{ cm}^{-1}$).

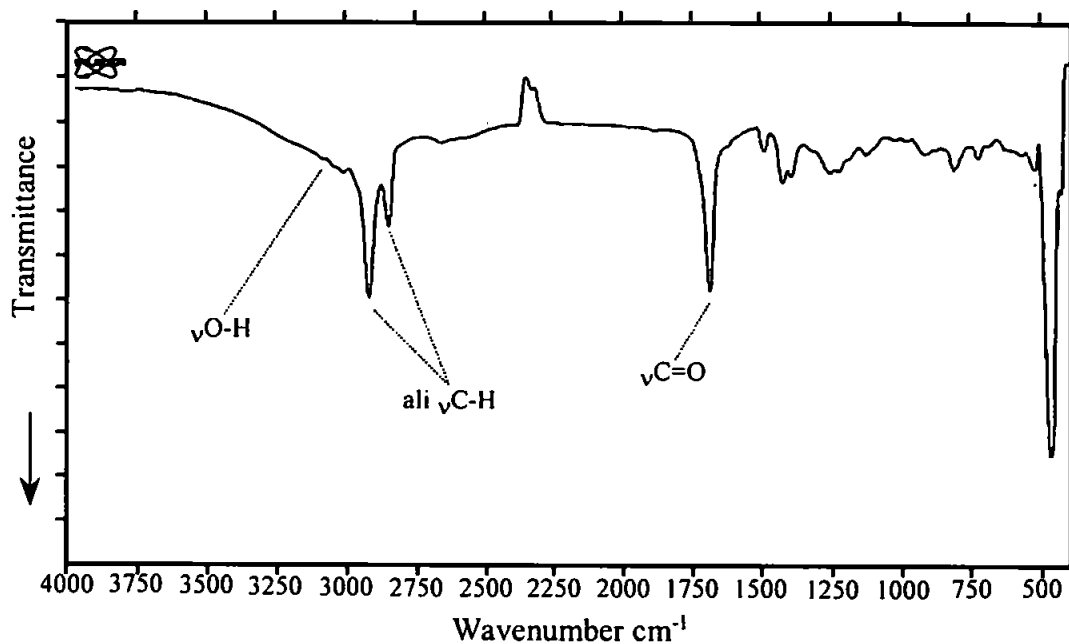


Figure 56. Infrared spectrum of 4-phenyl(4'-cyclohexyl)butanoic acid (VI); KBr disk.

5.5.1.3 NMR

The ¹³C NMR spectrum of the crude acid was similar to that of the keto-acid (II) described in the previous section. Six aliphatic resonances were now observed between 20 and 40 ppm (the peak at 34.5 was a doublet); these correspond to the hydrogens on the cyclohexyl ring, and the three CH₂ groups on the butanoic acid substituent, (C9, C10 and C11).

The tertiary carbon (C4) on the cyclohexyl ring, was again found at 44 ppm, the equivalent pairs of aromatic carbons (C6 and C7) at 126 and 128 ppm, their intensity reflecting the number of carbons in the environments. The aromatic *ipso* carbons (C5 and C8) are found at 145 and 138 ppm, C8 can be assigned by the upfield shift in comparison with the ¹³C spectrum of the keto-acid (II) now that it was no longer deshielded by the keto-carbonyl.

The remaining acidic carboxylic carbon (12) was again at 179 ppm. These assignments are confirmed by the DEPT sequence NMR spectrum (Figure 58).

The ^1H NMR spectrum together with assignments is shown in Figure 59. The singlet in the aromatic region (7.3 ppm) represents hydrogens H6 and H7 and the acidic hydrogen was observed far downfield at 11.5 ppm. The aliphatic H9, H10 and H11 are assigned by their relative proximity to the carboxylic acid group and the benzene ring.

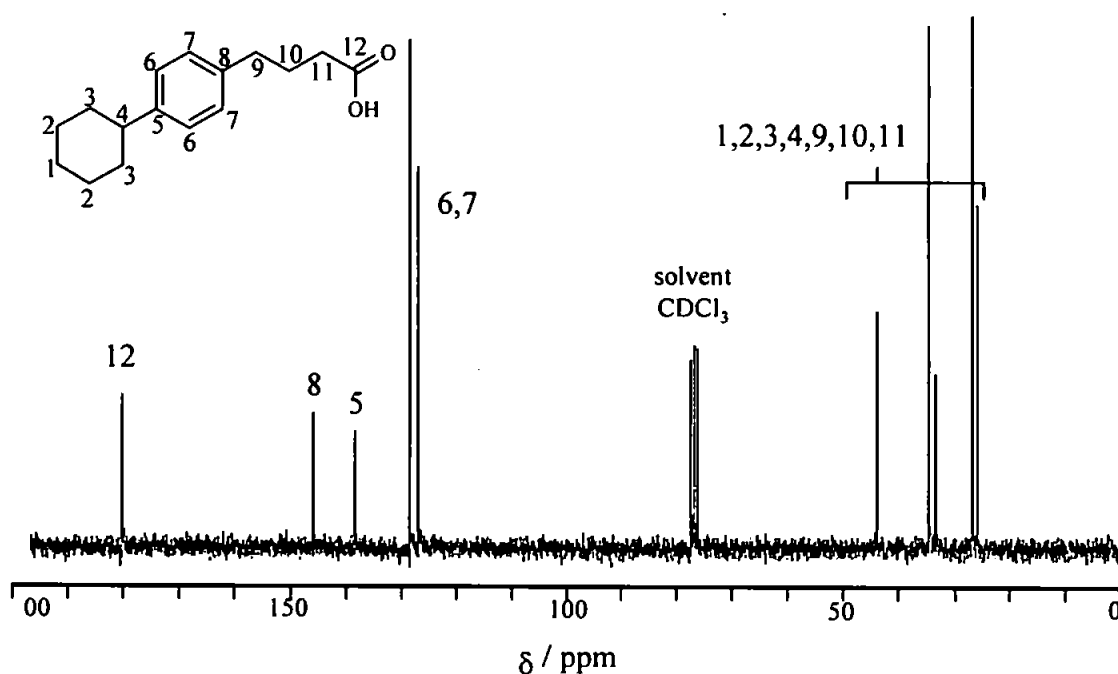


Figure 57. ^{13}C NMR spectrum of 4-phenyl(4'-cyclohexyl)butanoic acid (VI).

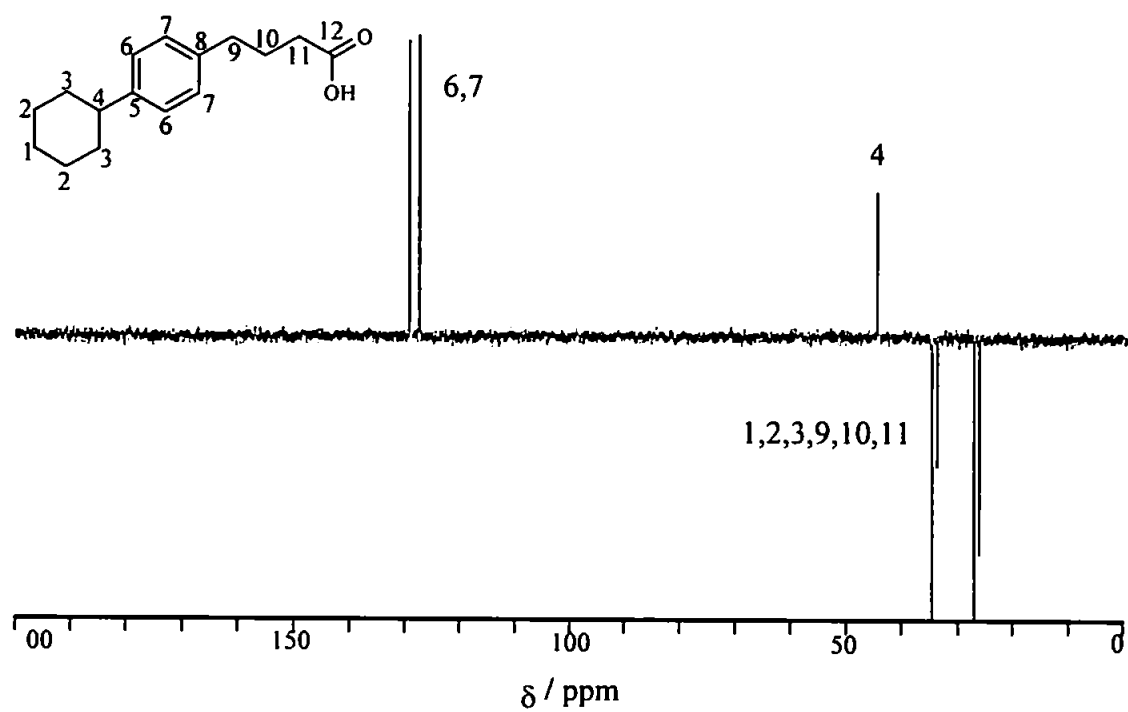


Figure 58. DEPT NMR spectrum of 4-phenyl(4'-cyclohexyl)butanoic acid (VI).

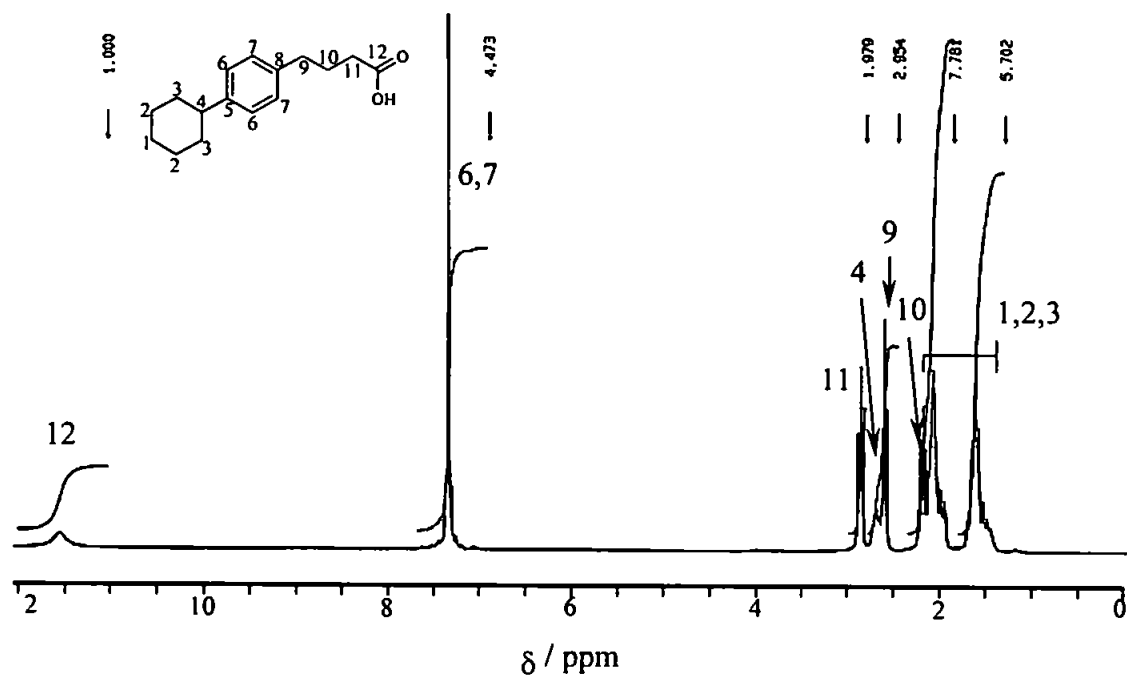


Figure 59. ^1H NMR spectrum of 4-phenyl(4'-cyclohexyl)butanoic acid (VI).

5.6 Preparation of 7-cyclohexyl-1-tetralone (VII).

The third step of the synthetic route was the cyclisation of the acid (VI) to tetralone (VII). This was achieved using a method described by Snyder and Werber (1955), where the carboxylic acid (VI) is dissolved in hot polyphosphoric acid and stirred vigorously. The tetralone was recovered by extraction into diethylether.

5.6.1 Characterisation of 7-cyclohexyl-1-tetralone (VII).

5.6.1.1 GCMS

The TIC chromatogram (Figure 60) showed a product with high purity; integration of peak areas indicated this to be 97%.

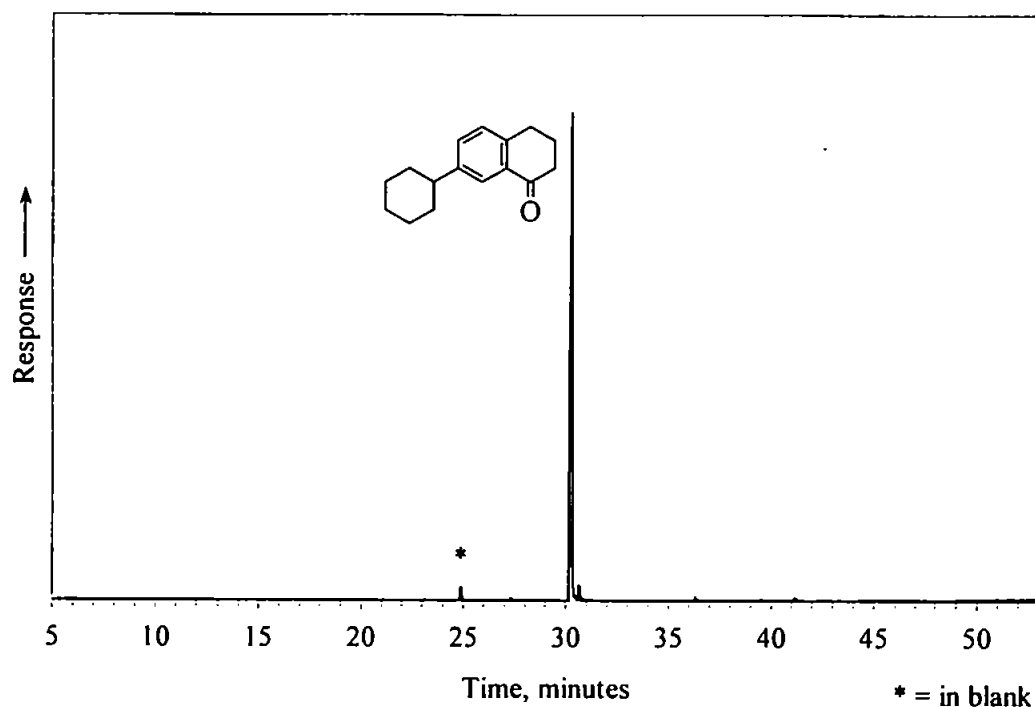


Figure 60. TIC chromatogram of 7-cyclohexyl-1-tetralone (VII). GC = 12m HP1, 40 – 300°C @ 5°C min⁻¹, held 10 min.

The mass spectrum of 7-cyclohexyl-1-tetralone is shown in Figure 61. The molecular ion is observed at m/z 228 (base peak). The ion at m/z 200 represents a loss of 28; since

parity is retained a neutral molecule has been eliminated; either carbon monoxide (as shown in the spectrum) or ethene. Ethene may be eliminated through an E₂ type elimination; similar to a McLafferty rearrangement, but CO is the most likely loss from a cyclohexanone compound. A₁ cleavage of the cyclohexyl ring is likely to contribute to the abundances of the ion at m/z 185, corresponding to a loss of 43 *i.e.* C₃H₇.

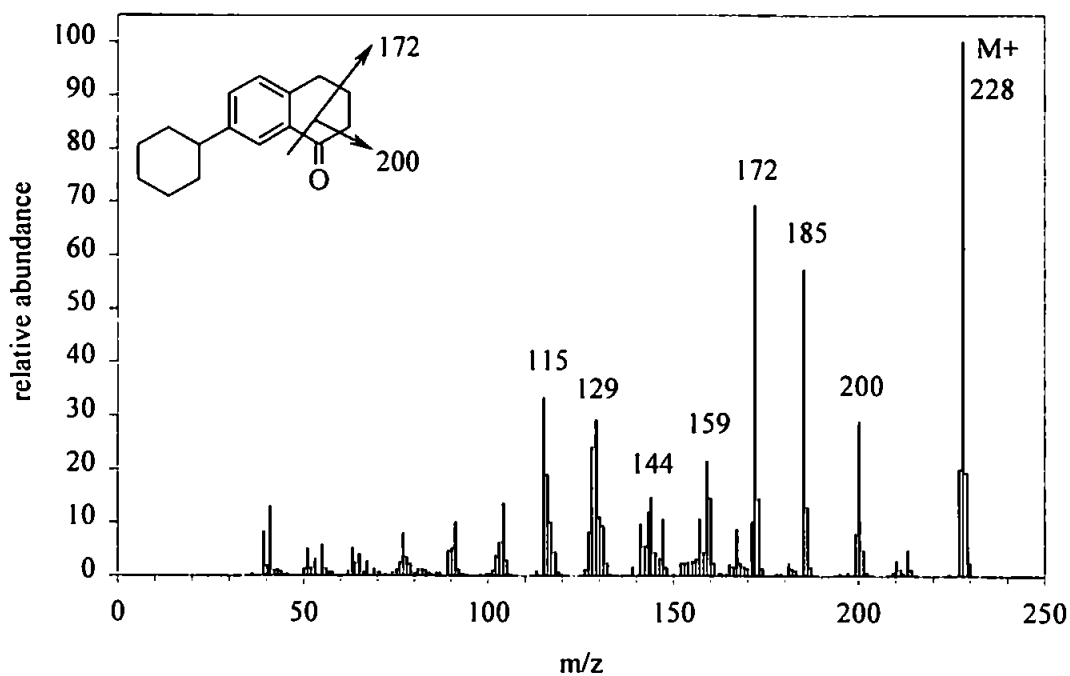


Figure 61. Mass spectrum of 7-cyclohexyl-1-tetralone (VII).

5.6.1.2 IR

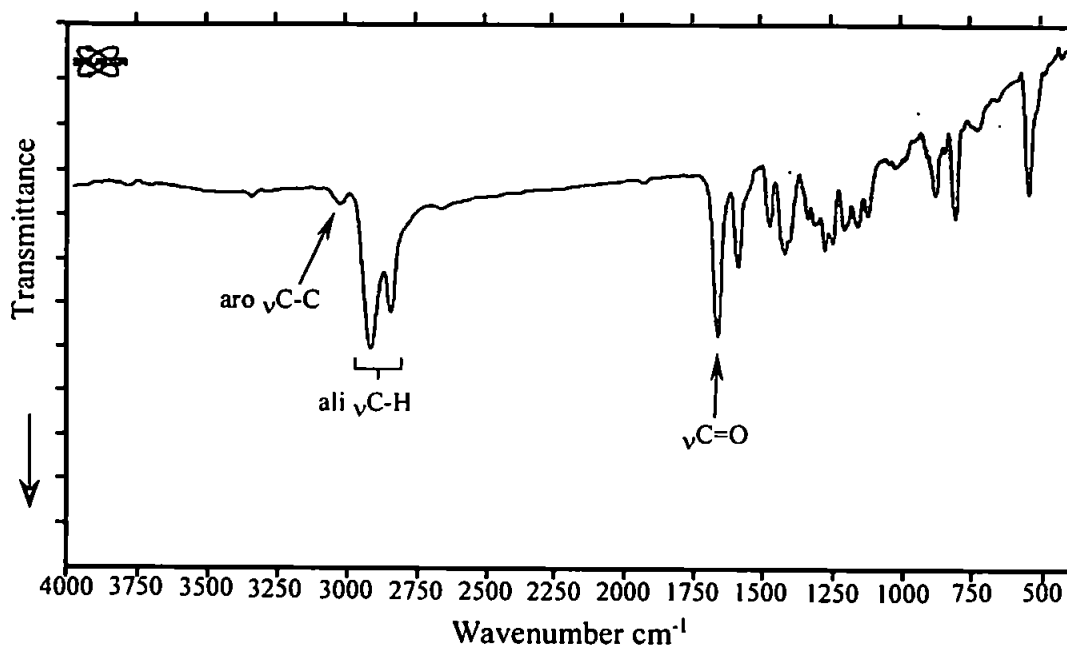


Figure 62. Infrared spectrum of 7-cyclohexyl-1-tetralone (VII).

The infrared spectrum of the crude tetralone (Figure 62) again showed the spectral bands expected from aliphatic and aromatic features. From the aliphatic portion of the molecule the strong C-H stretches at 2923 and 2850 cm⁻¹ and the weaker band at 3032 cm⁻¹ due to the aromatic C-H stretch were visible. The single carbonyl absorption was observed at 1680 cm⁻¹ plus a series of peaks below 1600 cm⁻¹ that cannot easily be assigned, but are likely to be accounted for by aromatic C-C stretching and aliphatic C-H bending as previously discussed.

5.6.1.3 NMR

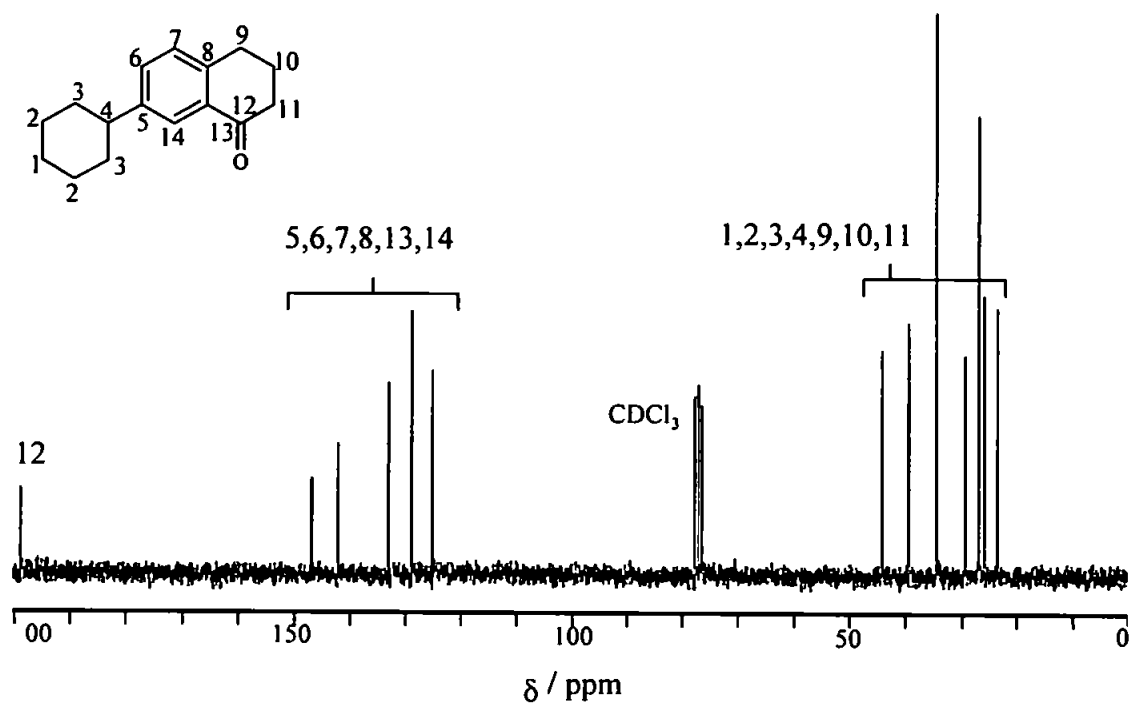


Figure 63. ^{13}C NMR spectrum of 7-cyclohexyl-1-tetralone (VII).

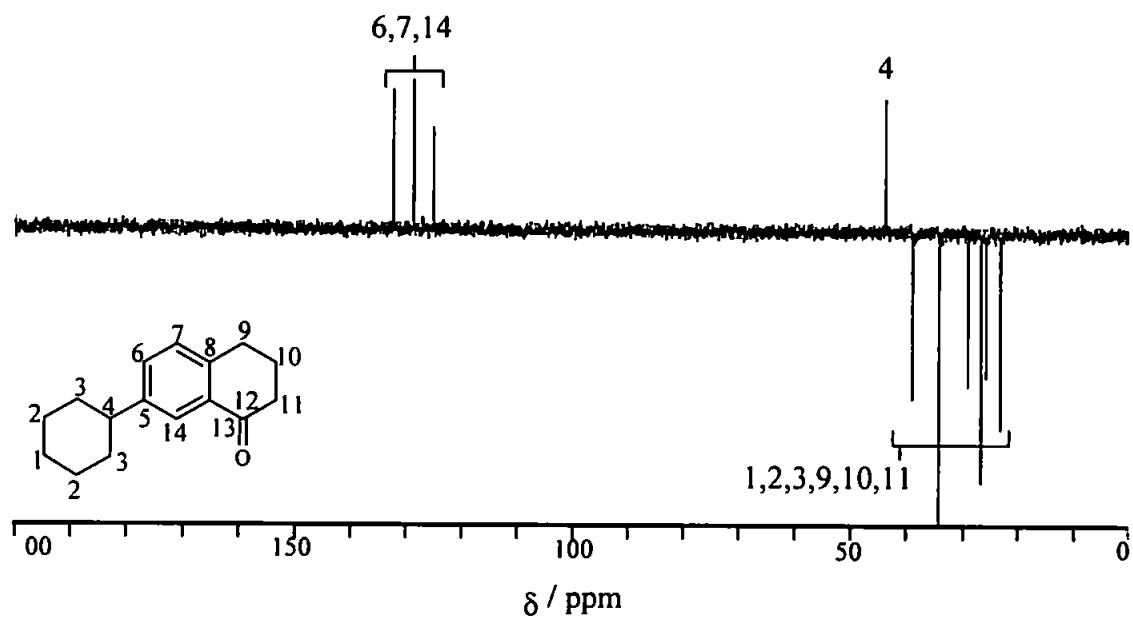


Figure 64. DEPT NMR spectrum of 7-cyclohexyl-1-tetralone (VII).

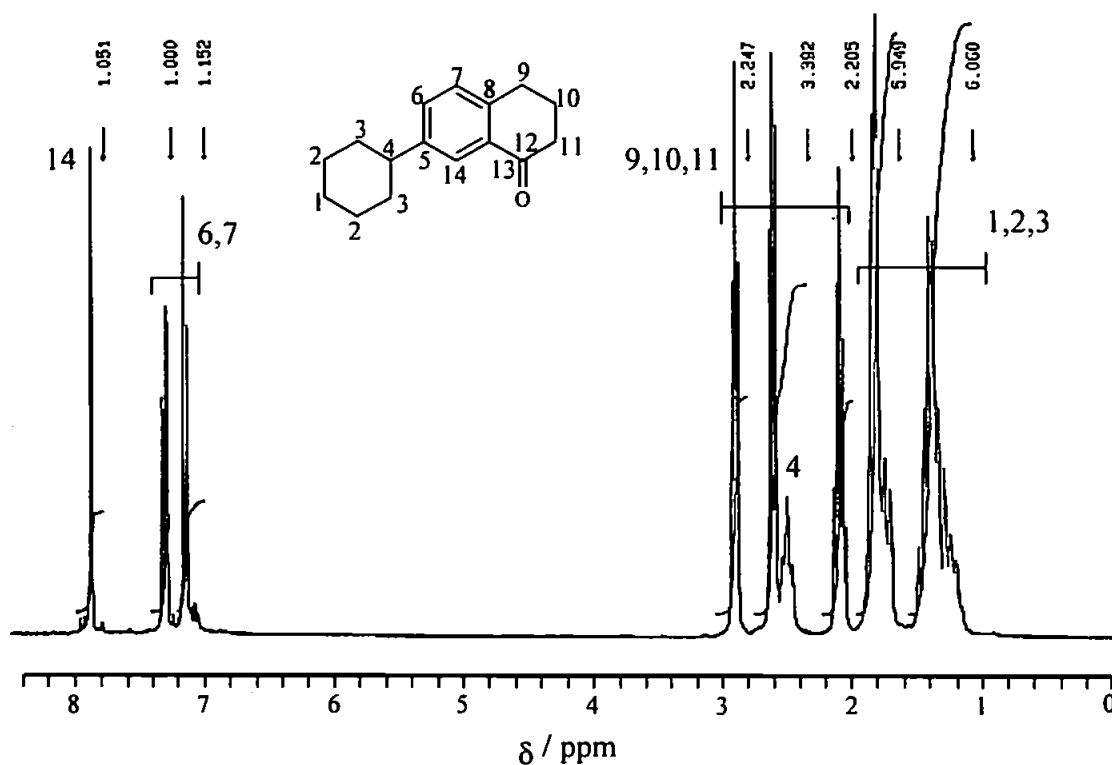


Figure 65. ¹H NMR spectrum of 7-cyclohexyl-1-tetralone.

The ¹³C NMR spectrum (Figure 63) showed 14 resonances; the carbonyl resonance was shifted far downfield to 198 ppm, the three aromatic *ipso* carbons (C5, C8 and C13) are found at 146, 141 and 132 ppm, distinguished from the unsubstituted aromatic carbons (C6, C7 and C14) by the DEPT sequence (Figure 64). Likewise, the tertiary carbon C4 was identified at 44 ppm, the carbons 2 and 3 are tentatively identified by the increased intensity of the peaks at 26 and 34 ppm. The remaining aliphatic carbons (C1, C11, C12 and C13) are observed in the region between 20 and 40 ppm.

The ¹H NMR spectrum (Figure 65) showed the aromatic hydrogens between 7 and 8 ppm, the hydrogen H14 being further downfield due to the shielding effect of a carbonyl in a β position. The aliphatic hydrogens were observed below 3 ppm; H4, H9, H10 and H11 were slightly further downfield due to the proximity of both the carbonyl and the benzene ring. Integration of the peak areas confirmed the assignments.

5.7 Preparation of 6-cyclohexyltetralin (V).

6-Cyclohexyltetralin (V) was prepared from the tetralone (VII) simply by repeating the Huang-Minlon-Wolff-Kishner reduction as described in section 5.5, thus reducing the ketone group to a methylene group.

5.7.1 Characterisation of 6-cyclohexyltetralin (V).

5.7.1.1 GCMS

The TIC chromatogram in Figure 66 shows the purity of 6-cyclohexyltetralin (V) to be 98%.

The mass spectrum (Figure 67) showed the abundant molecular ion at m/z 214. The ion m/z 171 was of almost equal intensity and corresponded to a loss of 43, typical of the simple cleavage of aliphatic chains. Loss of C_3H_7 (*i.e.* 43) from the fused saturated ring would result in the cyclohexyl substituted tropylium ion m/z 171. This probably accounts for the high intensity. Less intense peaks at M-15, M-29 and M-57 are also observed, along with the tropylium ion; m/z 91.

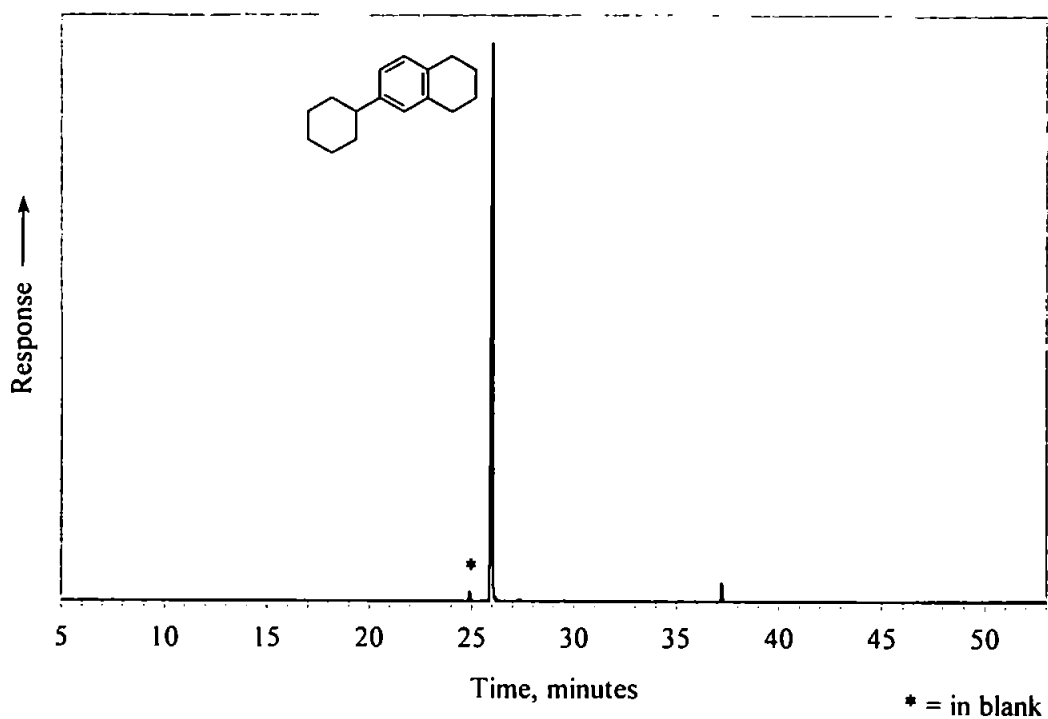


Figure 66. TIC chromatogram of 6-cyclohexyltetralin (V). GC = 12m HP1, 40 – 300°C @ 5°C min⁻¹, held 10 min.

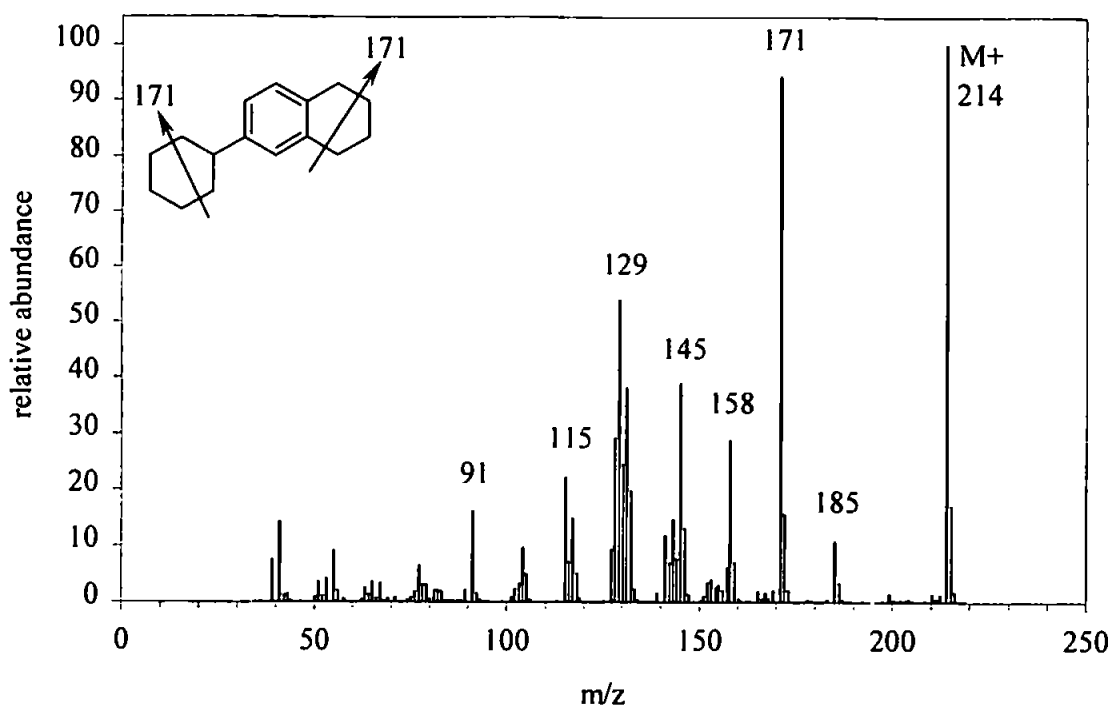


Figure 67. Mass spectrum of 6-cyclohexyltetralin (V).

The mass spectrum of the impurity observed at 37.2 min (Figure 68) was tentatively identified as 1,7-dicyclohexyltetralin (mass 296). It shows features of the mass spectrum of 6-cyclohexyltetralin *i.e.* ions at m/z 171 and 145. A loss of 83 (corresponding to a cyclohexyl fragment) was observed, giving an ion at m/z 213; possibly a 6-cyclohexyltetralin ion.

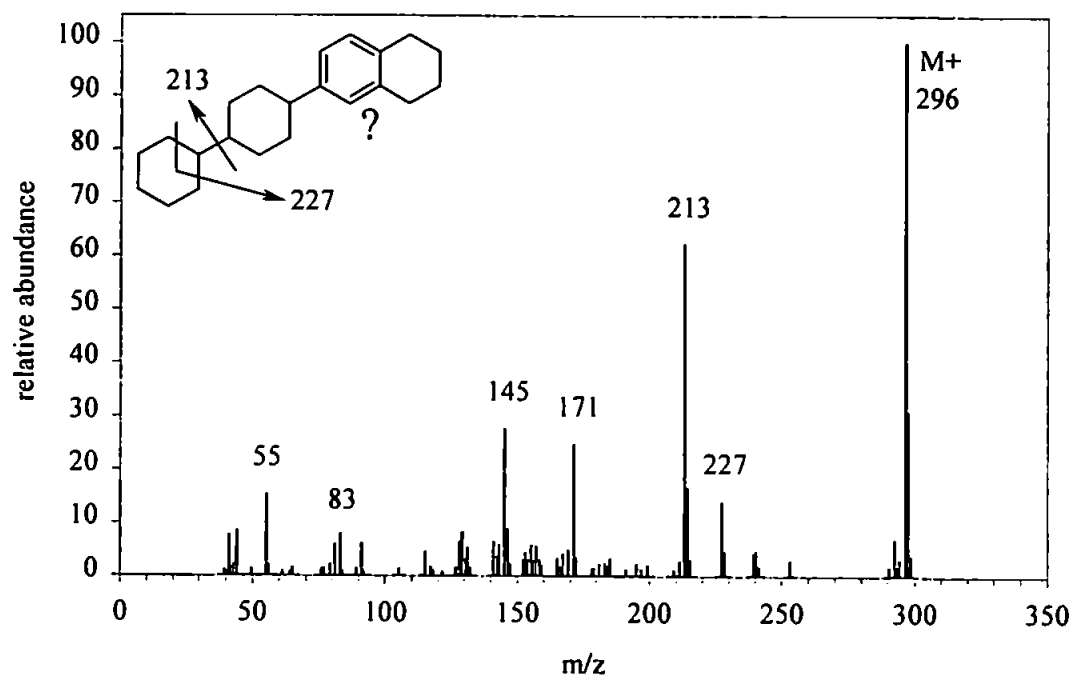


Figure 68. Mass spectrum of (tentatively) 6-(4'-cyclohexylcyclohexyl)tetralin).

5.7.1.2 IR

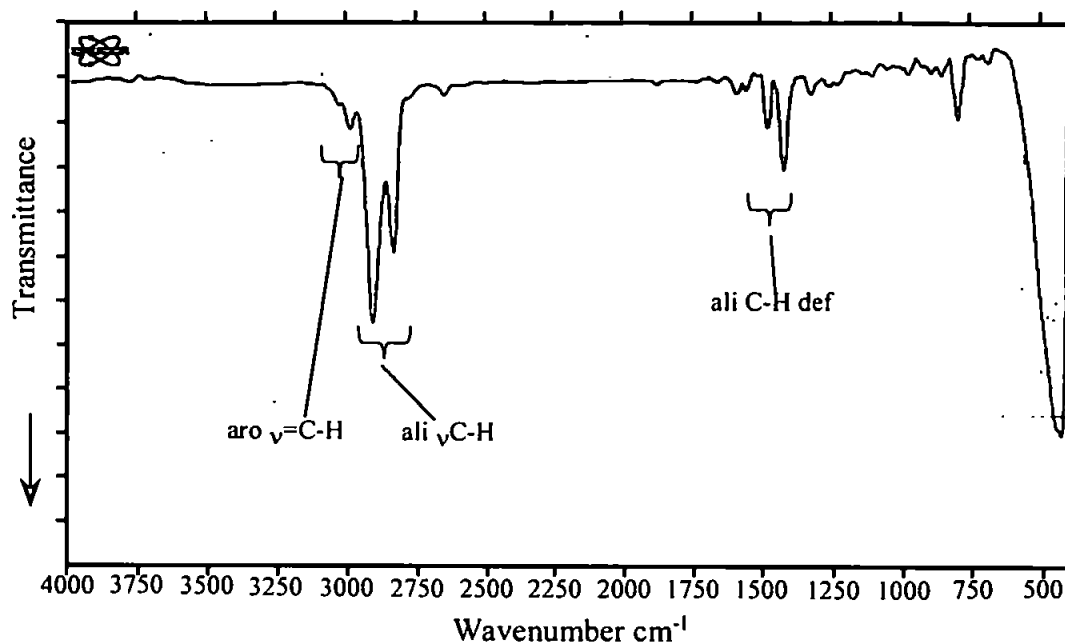


Figure 69. Infrared spectrum of 6-cyclohexyltetralin (V).

The infrared spectrum of 6-cyclohexyltetralin was relatively simple (Figure 69); the aliphatic C-H stretches were observed at 2924 and 2850 cm⁻¹, along with the aromatic C-H stretches at 3001 cm⁻¹. The group of bands around 1450 cm⁻¹ is likely to be due to C-H deformations of CH₂ and CH₃ groups in the molecule. The absorption still observed at 816 cm⁻¹ was probably due to the aromatic substitution, though it is difficult to interpret with the complex substitution pattern.

5.7.1.3 NMR

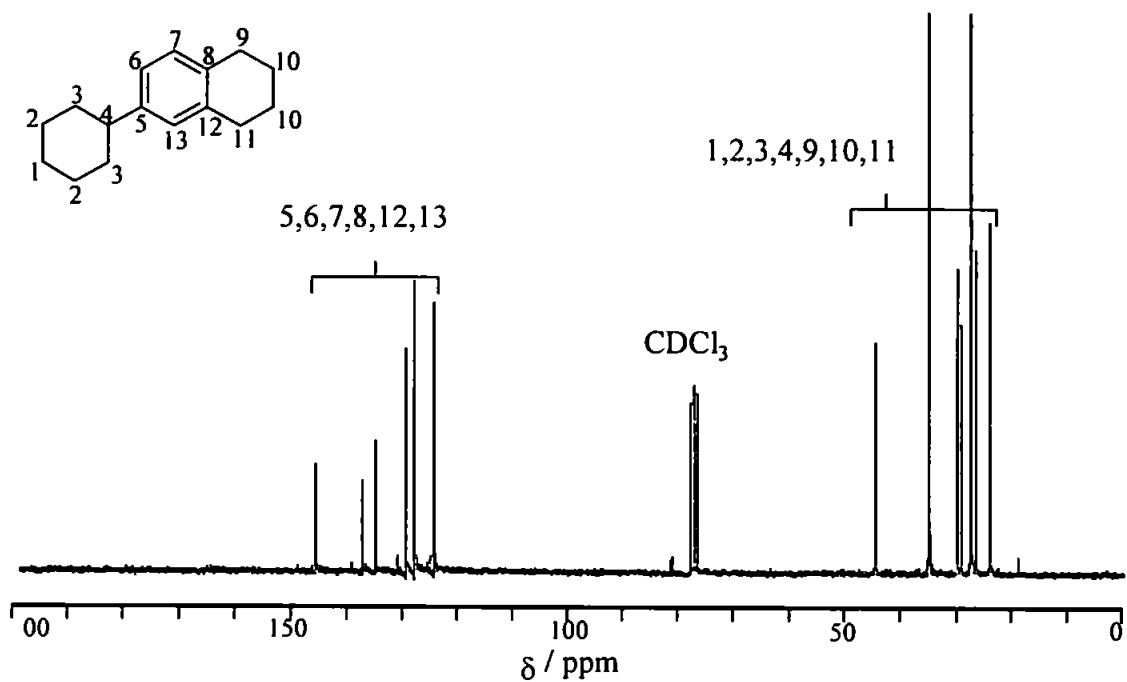


Figure 70. ^{13}C NMR spectrum of 6-cyclohexyltetralin (V).

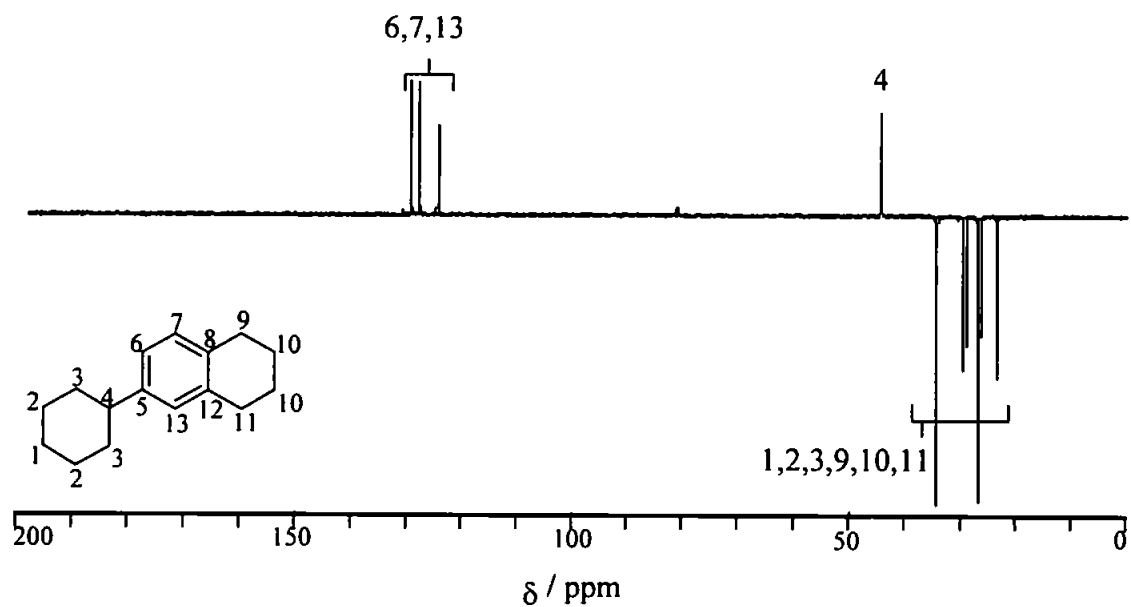


Figure 71. DEPT NMR spectrum of 6-cyclohexyltetralin (V).

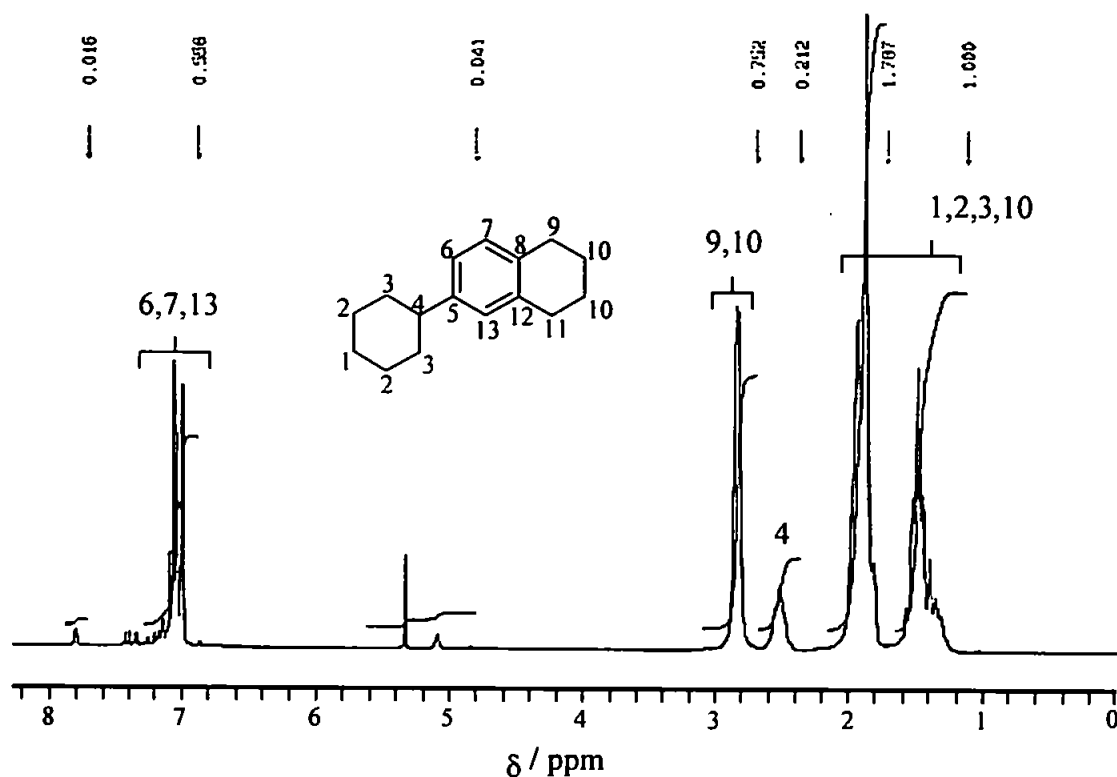


Figure 72. ^1H NMR spectrum of 6-cyclohexyltetralin (V).

The ^{13}C NMR spectrum of 6-cyclohexyltetralin is shown in Figure 70. The aromatic *ipso* carbons (C5, C8 and C12) are observed between 130 and 150 ppm, the remaining aromatic carbons (C6, C7 and C13) are found between 120 and 130 ppm. The tertiary carbon (C4) is found as usual at 44 ppm and the carbons C2 and C3 (34 and 26 ppm) are distinguished from the other aliphatic carbons by their increased intensity, although the other equivalent CH_2 (C10) is not distinguished by an increased intensity. The other aliphatic carbons are found in the region between 20 and 30 ppm. The DEPT sequence spectrum (Figure 71) confirmed these assignments.

The ^1H NMR spectrum (Figure 72) was reasonably simple, with no downfield shifts due to carbonyls observed. The three aromatic hydrogens were observed around 7 ppm, the hydrogen 4 was still observed at 2.5 ppm with hydrogens C9 and C10 at 2.9 ppm. The remaining aliphatic hydrogens C1, C2, C3 and C10 were observed below 2 ppm. Small

resonances observed at 7.8, 5.1 and 5.4 ppm are probably due to small amounts of impurities in the compound.

5.8 Preparation of 1-alkyl-7-cyclohexyltetralins (VIII, IX and X).

A Grignard reaction is widely used to add alkyl groups to tetralones (e.g. March, 1992; Vogel, 1989). As illustrated in Figure 73, this involves the formation of the alkylmagnesium halide *in-situ*, which can then react with the substrate. This reaction produces the tertiary alcohols in reasonable yields. The alcohols may then be dehydrated *via* acid-catalysed dehydration, producing an isomeric mixture of alkenes. The alkenes are hydrogenated to the hydrocarbon using hydrogen gas with Adam's catalyst.

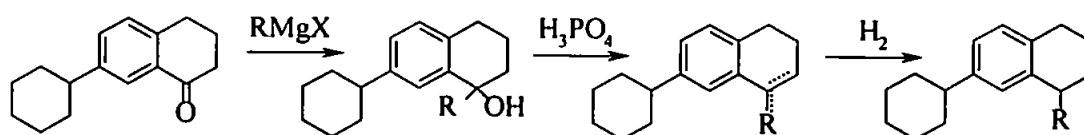


Figure 73. The Grignard addition of alkyl groups to 7-cyclohexyl-1-tetralones and subsequent dehydration and hydrogenation to 1-alkyl-7-cyclohexyltetralins.

5.9 Preparation of 7-cyclohexyl-1-n-nonyltetralin (IX)

A Grignard reaction was used to add an *n*-nonyl chain to 7-cyclohexyl-1-tetralone (VII). Examination of the reaction products however showed none of the expected tertiary alcohol. Products observed were nonane (from nonyl magnesium bromide), octadecane from a Würtz-type coupling of two nonyl magnesium bromide molecules (March 1985) and 7-cyclohexyl-1-tetralone (VII), either unreacted material, or more likely formed in an enolisation³ reaction. Two hydrocarbons, identified as 7-cyclohexyl-1-*n*-nonyltetralin (the eventual target compound; VI) and 7-cyclohexyl-1-*n*-nonylnaphthalene were also

³ Enolisation; where the substrate donates an alpha hydrogen to the Grignard reagent. On hydrolysis, the enolate ion formed is converted back to the original ketone.

observed as major products. The IR spectrum of the crude product (Figure 74) showed no bands corresponding to -OH stretching or C-O stretching.

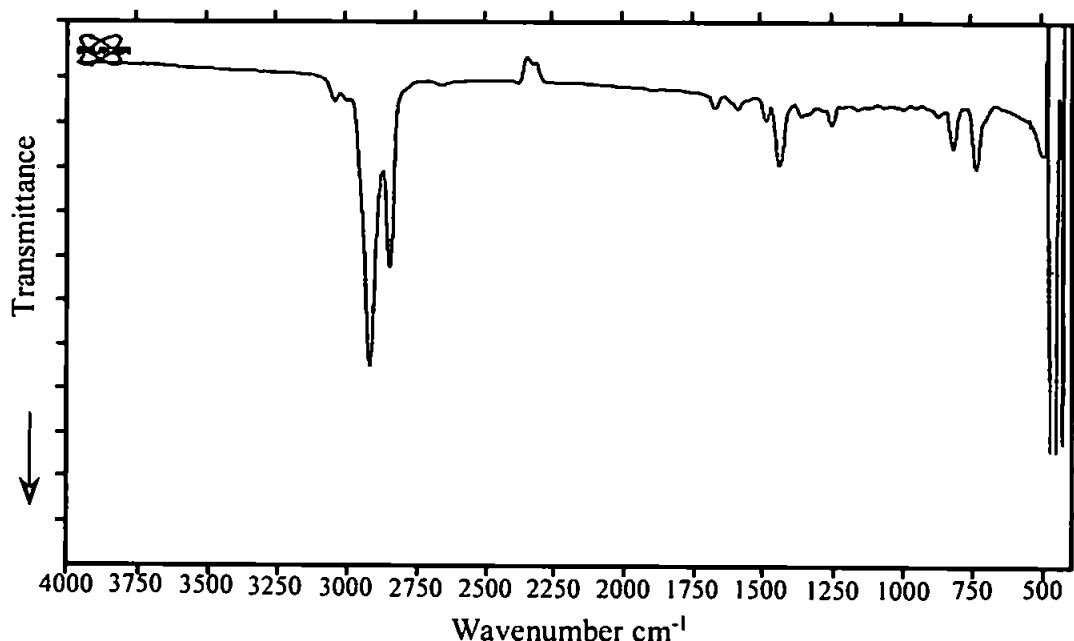


Figure 74. Infrared spectrum of the crude product obtained on the Grignard addition of $\text{C}_9\text{H}_{19}\text{MgBr}$ to 7-cyclohexyl-1-tetralone (VII), thin film, NaCl windows.

It is believed that the reaction mixture overheated during the Grignard reaction and the alcohol formed was dehydrated *in-situ*. It is not known how the target compound 7-cyclohexyl-1-*n*-nonyltetralin was formed in the reaction mixture in such quantity. The aromatic product 1-*n*-nonyl-7-cyclohexylnaphthalene may have been formed by the aromatisation of the alkene produced on the dehydration of the tertiary alcohol.

An attempt was made to remove octadecane from the reaction mixture by vacuum distillation. This proved unsuccessful, as the mixture 'bumped' violently on heating, making distillation near impossible. The recovered reaction mixture had a composition similar to the undistilled mixture, with the addition of several other compounds; mainly 6-cyclohexyltetralin (VIII), 2-cyclohexylnaphthalene, and a compound identified as 7-cyclohexyl-1-methyltetralin. Identifications were made on the basis of mass spectral data.

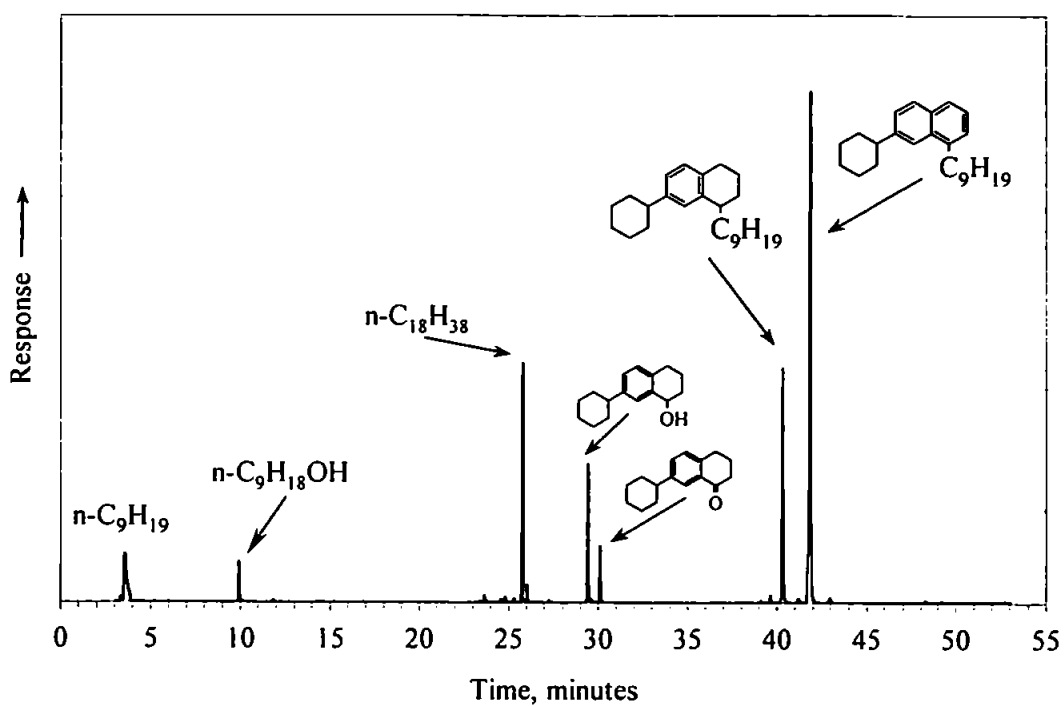


Figure 75. TIC chromatogram of the mixture obtained from the Grignard addition of a nonyl-chain to 7-cyclohexyl-1-tetralone (VII). GC = 12m HP1, 40 – 300°C @ 5°C min⁻¹, held 10 min.

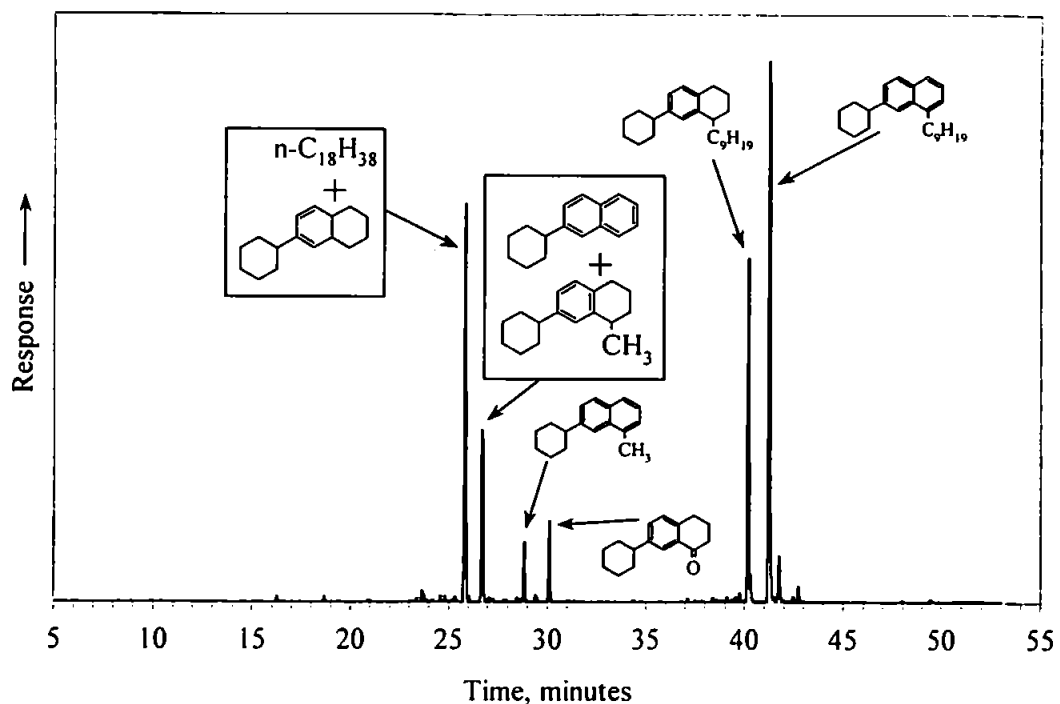


Figure 76. TIC of the mixture obtained from the Grignard addition of a nonyl-chain to 7-cyclohexyl-1-tetralone (VII) after attempted vacuum distillation. GC = 12m HP1, 40 – 300°C @ 5°C min⁻¹, held 10 min.

The TIC chromatograms of the mixture before and after vacuum distillation are shown in Figure 75 and Figure 76.

It is unsure how 1-methyl-7-cyclohexyltetralin came to be in the reaction products. Methylbromide present in the bromononane used to make the Grignard reagent would produce this result and would not be detected by GC purity checks of reagents since it would elute with the solvent front.

The mixture (Figure 76) was separated by argentation thin layer chromatography (Ag^+ TLC, mobile phase pentane, 0.25 mm adsorbent layer) into three fractions; alkanes (R_f 0.82-1.00, Figure 77), monoaromatics (R_f 0.65-0.82, Figure 78) and diaromatics (R_f 0.1-0.65, Figure 79). Unfortunately, large scale Ag^+ TLC (1 mm adsorbent layer) proved cumbersome and overlap of the mono- and di-aromatic fractions was a recurring problem (as illustrated in Figure 79).

Open-column chromatography using alumina as the adsorbent was more successfully employed to separate the mixture (see Chapter 2).

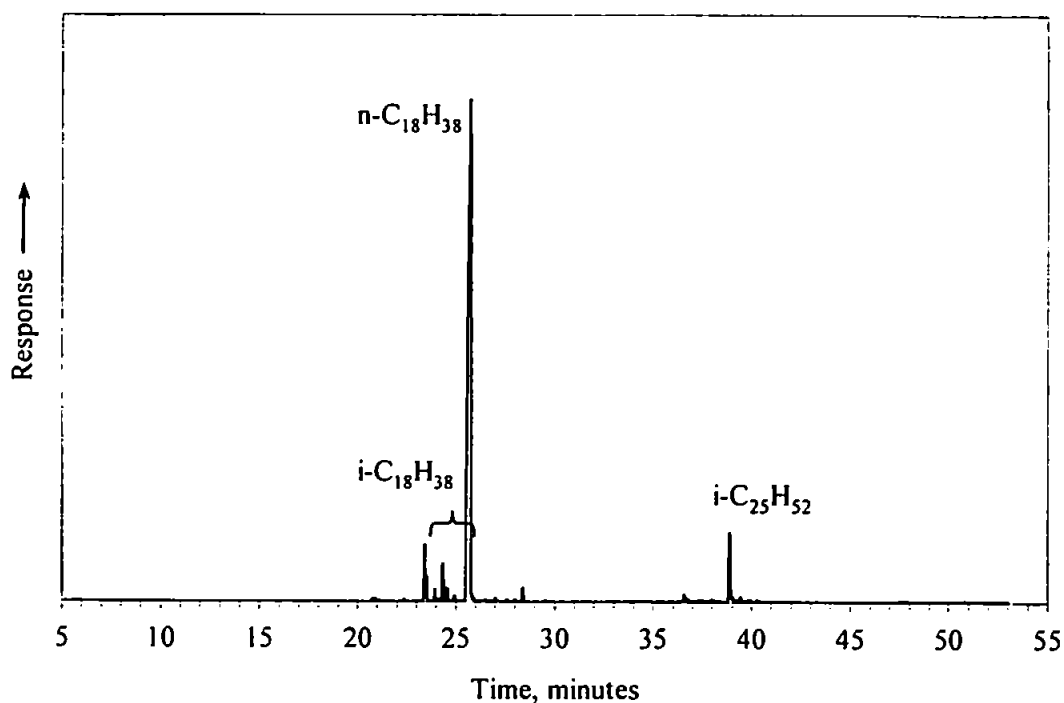


Figure 77. TIC chromatogram of alkane fraction (R_f 0.82-1.00) from the Ag^+ TLC separation of the products from the Grignard addition of $n-C_9H_{19}$ to 7-cyclohexyl-1-tetralone (VII). GC = 12m HP1, 40 – 300°C @ 5°C min⁻¹, held 10 min.

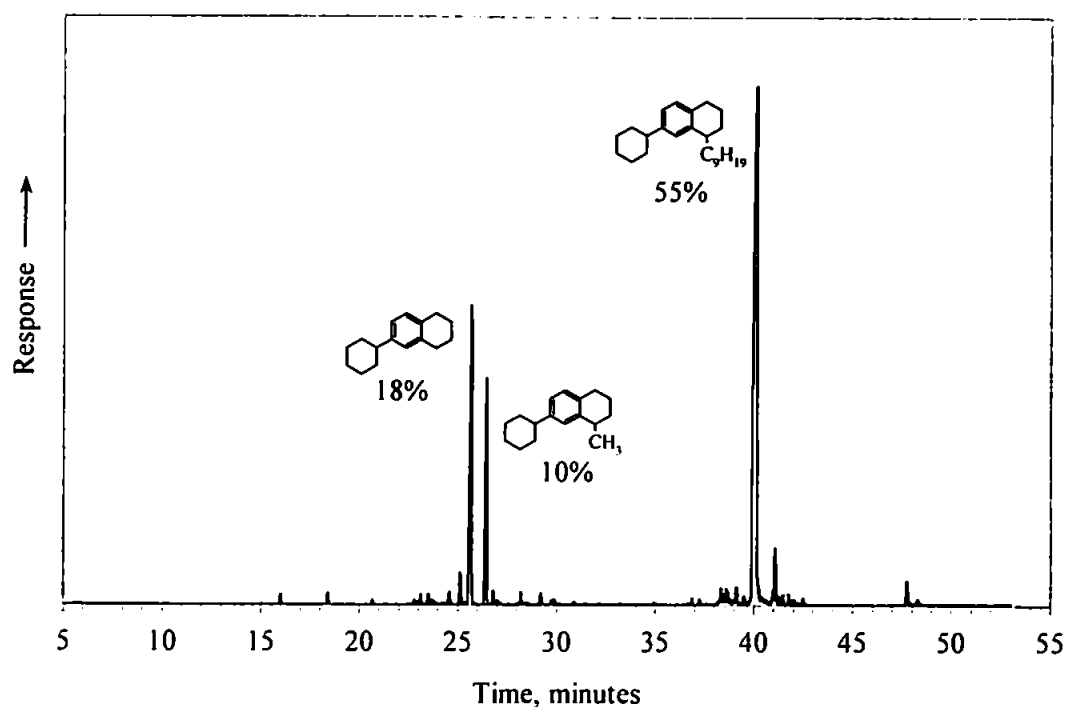


Figure 78. TIC chromatogram of the monoaromatic fraction (R_f 0.65-0.82) from the Ag^+ TLC separation of the products from the Grignard addition of $n-C_9H_{19}$ to 7-cyclohexyl-1-tetralone (VII). GC = 12m HP1, 40 – 300°C @ 5°C min⁻¹, held 10 min.

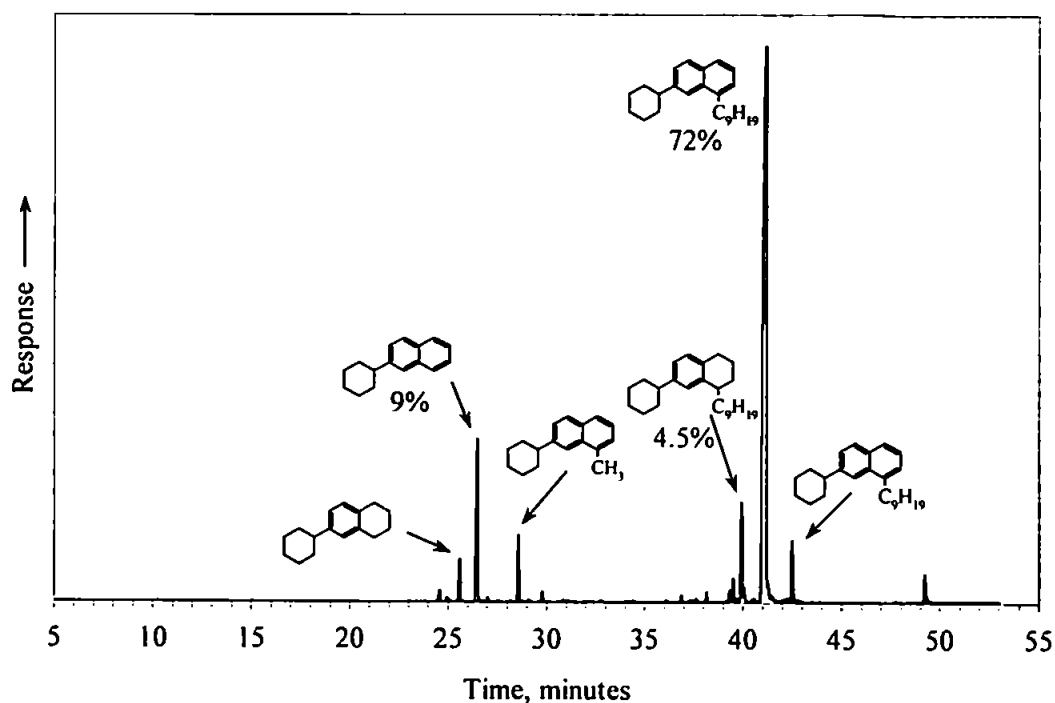


Figure 79. TIC chromatogram of the di-aromatic fraction (R_f 0.1-0.65) from the Ag^+ TLC separation of the products from the Grignard addition of $n-C_9H_{19}$ to 7-cyclohexyl-1-tetralone (VII). GC = 12m HP1, 40 – 300°C @ 5°C min^{-1} , held 10 min.

The monoaromatic fraction obtained from open column chromatography was a mixture of 6-cyclohexyltetralin, 7-cyclohexyl-1-methyltetralin and 7-cyclohexyl-1-nonyltetralin. The diaromatic fraction was largely 7-cyclohexyl-1-nonylnaphthalene. The formation of these simple mixtures of proposed UCM hydrocarbons may prove to be useful in the study of the RuO_4 oxidation of simple mixtures.

5.9.1 Characterisation of 7-cyclohexyl-1-nonyltetralin (IX).

5.9.1.1 GCMS

The TIC of the monoaromatic fraction obtained from open column chromatography is shown in Figure 80 (*c.f.* similar fraction from Ag^+ TLC; Figure 78). The composition of the mixture is shown in Table 20.

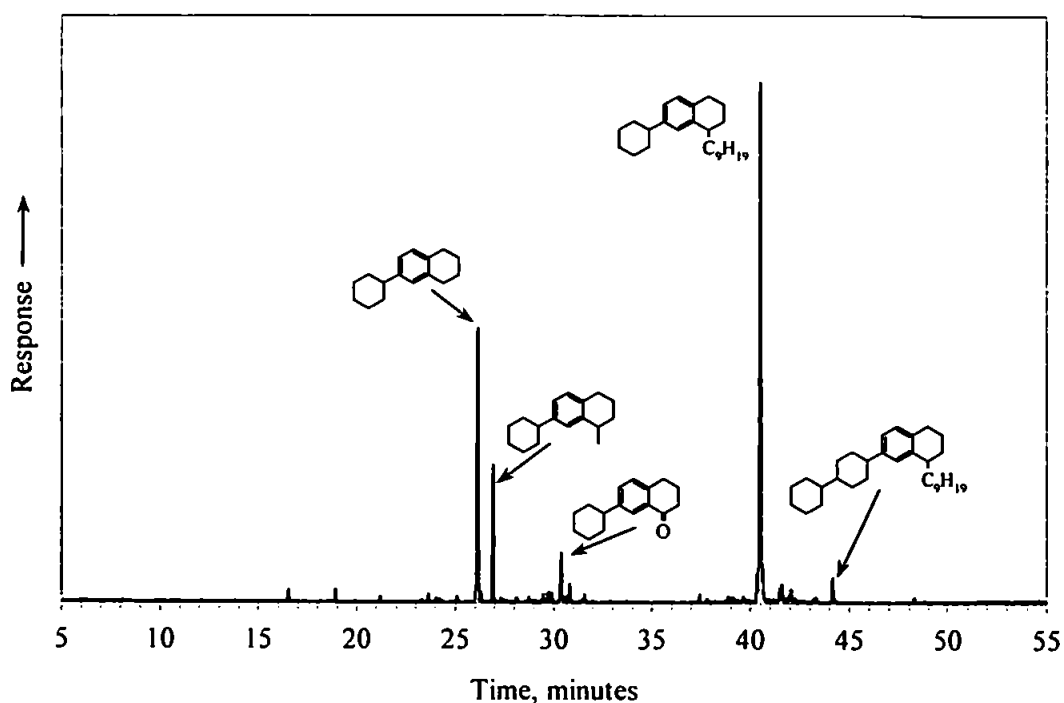


Figure 80. TIC chromatogram of the monoaromatic fraction obtained from open column chromatography of the crude product of the Grignard reaction to produce 1-n-nonyl-7-cyclohexyltetralin (IX). GC = 12m HP1, 40 – 300°C @ 5°C min⁻¹, held 10 min.

| compound | percent of total (by peak area) |
|--|------------------------------------|
| 1-n-nonyl-7-cyclohexyltetralin (VI) | 52.7 |
| 6-cyclohexyltetralin (V) | 22.4 |
| 1-methyl-7-cyclohexyltetralin | 10.6 |
| 7-cyclohexyl-1-tetralone (VII) | 4.0 |
| possible 1-n-nonyl-7-(4'-cyclohexyl)cyclohexyltetralin | 2.1 |

Table 20. Composition of monoaromatic fraction from open column chromatography of crude product obtained from the Grignard reaction of 7-cyclohexyltetralone + C₉H₁₉MgBr.

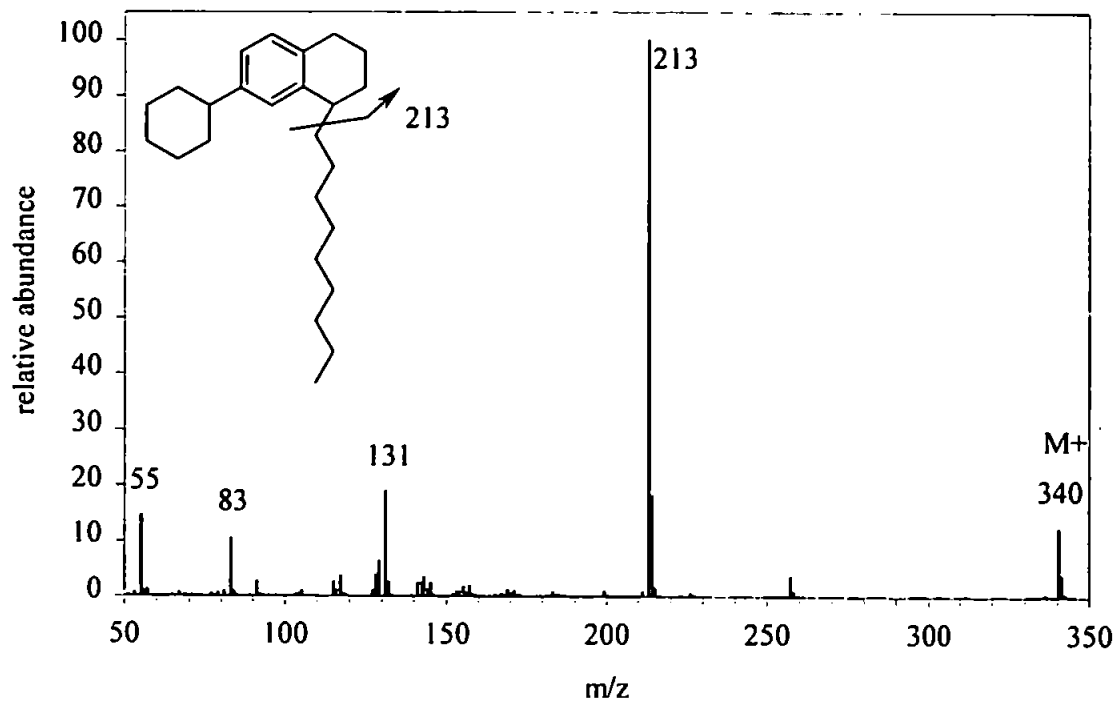


Figure 81. Mass spectrum of 1-n-nonyl-7-cyclohexyltetralin (IX).

5.9.1.2 IR

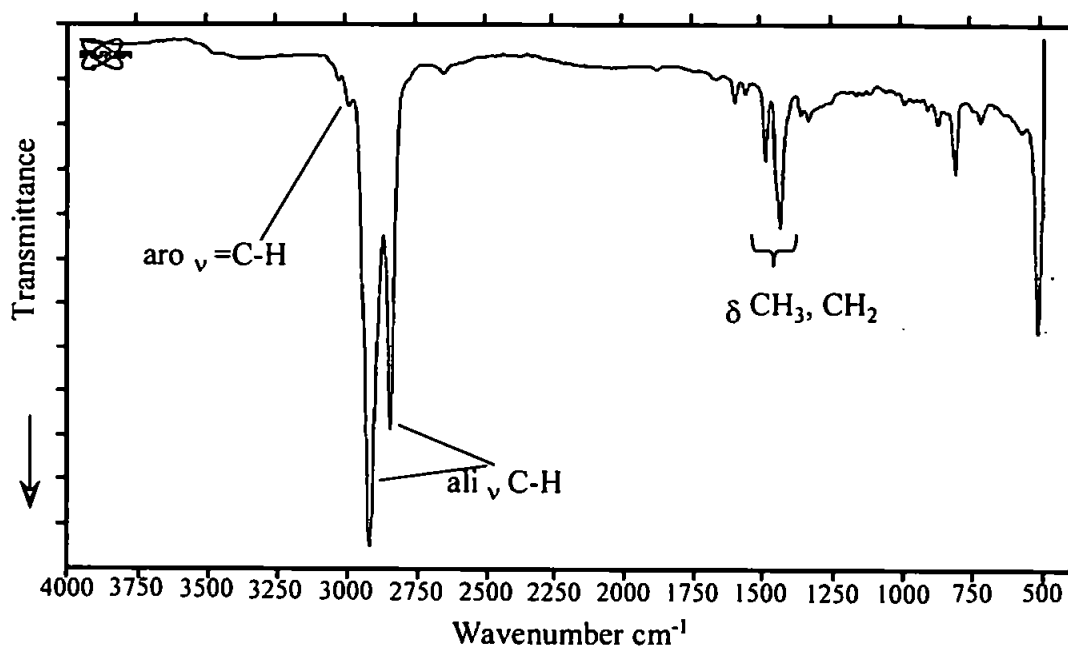


Figure 82. IR spectrum of the monoaromatic fraction containing 1-n-nonyl-7-cyclohexyltetralin (LX).

The IR spectrum of the monoaromatic fraction is shown in Figure 82, and greatly resembles that of 6-cyclohexyltetralin (Figure 69). The higher relative intensity of the aliphatic C-H stretches observed between 2750 and 3000 cm^{-1} indicated the increase in aliphatic carbon due to the nonyl group.

5.9.1.3 NMR

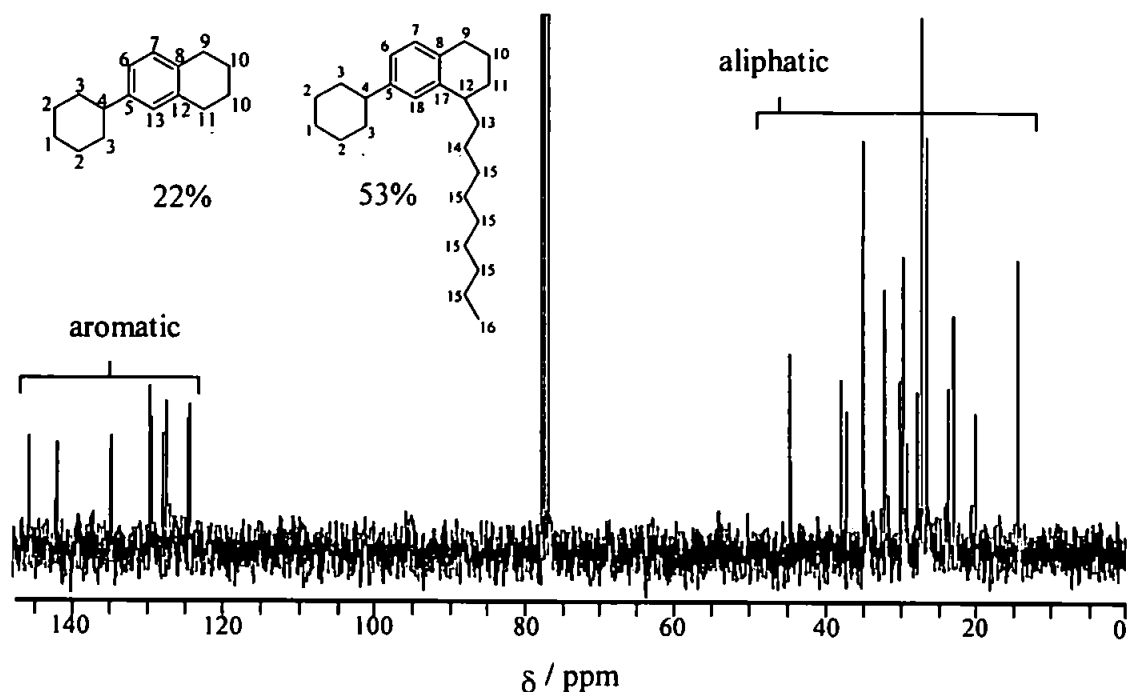


Figure 83. ^{13}C NMR spectrum of a mixture containing 53% 1-*n*-nonyl-7-cyclohexyltetralin (VI), 22% 6-cyclohexyltetralin (V) and 11% 1-methyl-7-cyclohexyltetralin.

The ^{13}C NMR spectrum of the monoaromatic fraction is shown in Figure 83. Resonances due to 1-methyl-7-cyclohexyltetralin are likely to be very weak compared to the other components in the mixture.

10 resonances were observed between 120 and 150 ppm corresponding to aromatic carbons. Aromatic carbons in all three components of the mixture were likely to show comparable chemical shifts since the compounds are structurally similar. The resonances observed below 50 ppm were due to the aliphatic carbons of the compounds. The single resonance observed at 14 ppm was likely to correspond to the methyl carbon 16 on 1-*n*-nonyl-7-cyclohexyltetralin (VI) because of the small chemical shift, the DEPT sequence spectrum confirmed this. The DEPT sequence (Figure 84) showed six resonances in the aromatic region between 120 and 130 ppm corresponding to the six

aromatic carbons in the two major components of the mixture. Note the arrangement of the six aromatic resonances in three pairs reflects the small change in the aromatic carbon resonances due to the addition of a *n*-nonyl group. Carbon C4 in both compounds was found at 43 ppm (a doublet) while the tertiary carbon C12 in the nonyl homologue (marked C₉ 12) was observed at 35 ppm. The low intensity resonance observed at 32 ppm (marked *) was probably due to the tertiary carbon in the methyl homologue.

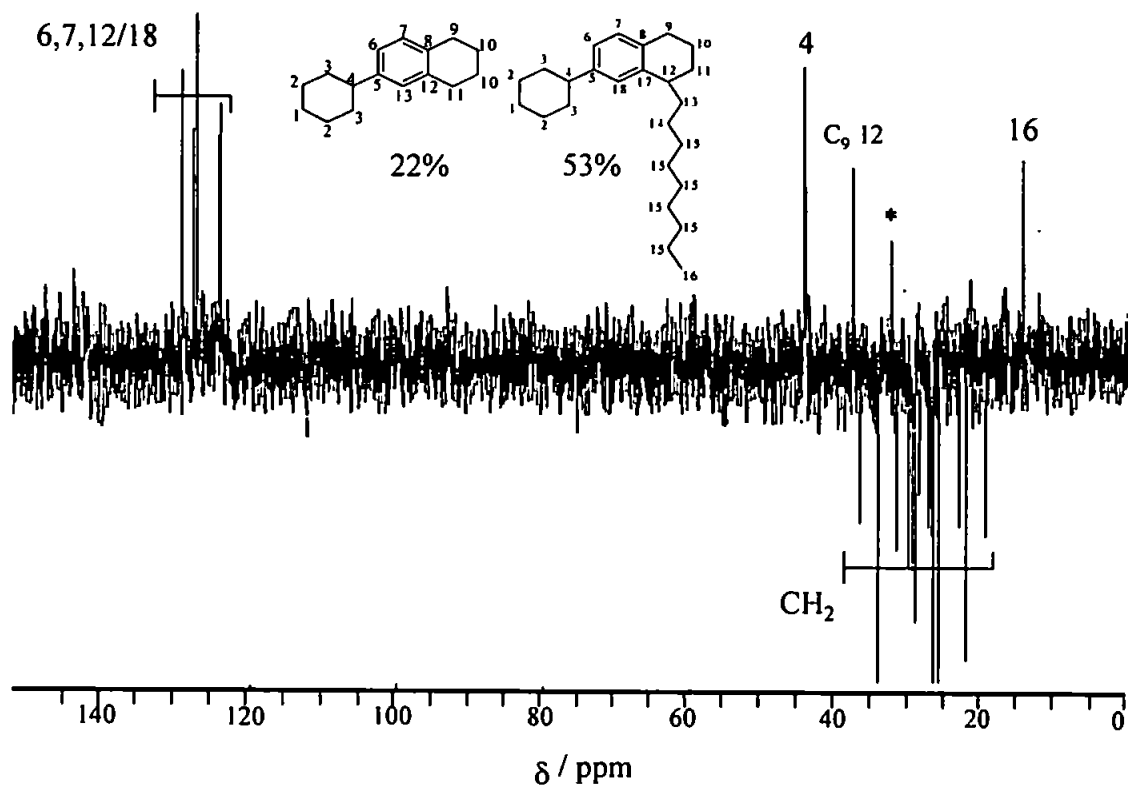


Figure 84. DEPT NMR spectrum of a mixture containing 53% 1-*n*-nonyl-7-cyclohexyltetralin (VI), 22% 6-cyclohexyltetralin (V) and 11% 1-methyl-7-cyclohexyltetralin.

The ¹H NMR spectrum of the mixture showed aromatic resonances around 7 ppm. The peak at 2.5 ppm corresponds to the tertiary C-H (H4) as observed in the ¹H spectrum of 6-cyclohexyltetralin (Figure 72) and (H12) on the nonyl homologue, while the peak at 2.8 ppm was due to H9 and H11 on 6-cyclohexyltetralin and H9 on 1-*n*-nonyl-7-cyclohexyltetralin. The peak at 0.9 ppm corresponds to the methyl H on the nonyl

homologue (H16) and the large peaks between 1 and 2 ppm are due to the numerous methylene H in the compounds. Integration of the peaks tended to confirm the assignments.

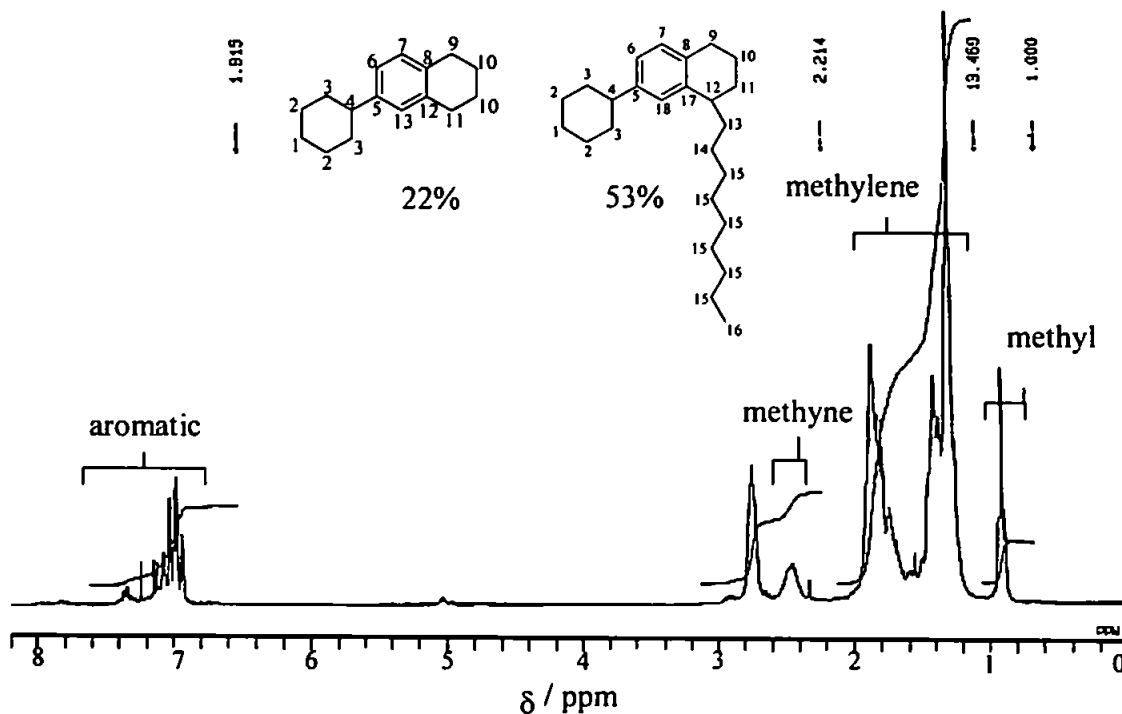


Figure 85. ^1H NMR spectrum of a mixture containing 53% 1-*n*-nonyl-7-cyclohexyltetralin (VI), 22% 6-cyclohexyltetralin (V) and 11% 1-methyl-7-cyclohexyltetralin.

5.9.2 Characterisation of 1-*n*-nonyl-7-cyclohexylnaphthalene (XI).

5.9.2.1 GCMS

The TIC chromatogram of the diaromatic fraction obtained from open column chromatography of the crude product showed the relative purity of 1-*n*-nonyl-7-cyclohexylnaphthalene (XI) to be 92% by peak area. Major impurities were 2-cyclohexylnaphthalene (1%), a compound tentatively identified as 1-*n*-nonyl-7-(4'-cyclohexyl)cyclohexylnaphthalene (2%) and two compounds (5%) whose mass spectra were virtually identical to that of 1-*n*-nonyl-7-cyclohexylnaphthalene (XI, probably structural isomers).

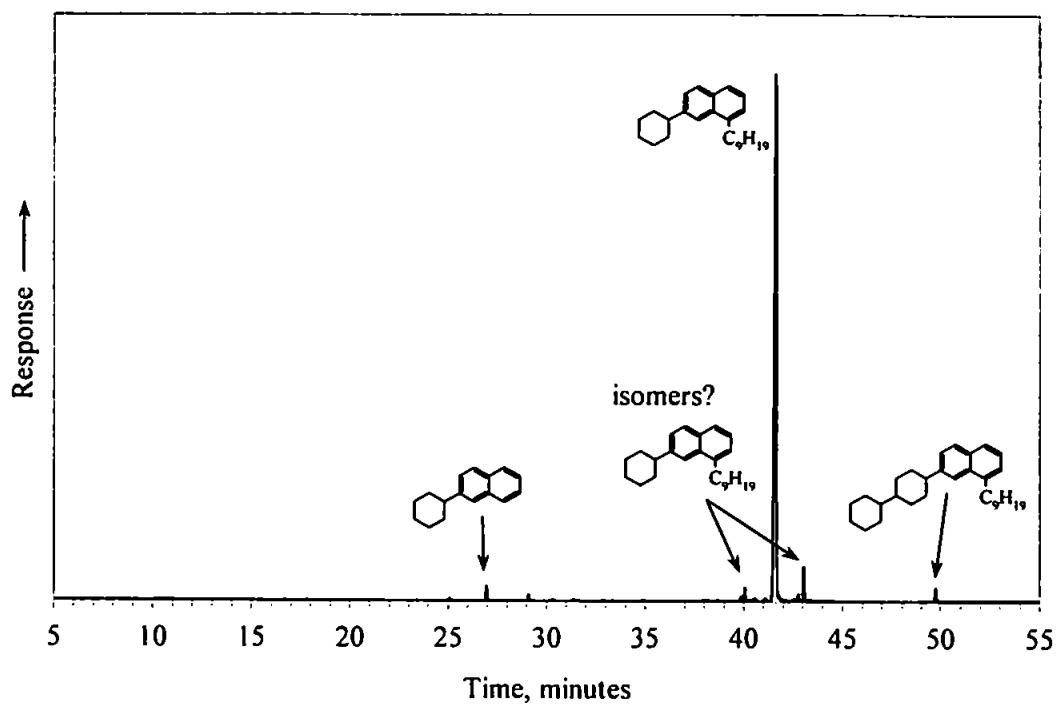


Figure 86. TIC chromatogram of the diaromatic fraction obtained from open column chromatography on the crude product obtained from the Grignard reaction to produce 1-*n*-nonyl-7-cyclohexyltetralin (IX). GC = 12m HP1, 40 – 300°C @ 5°C min⁻¹, held 10 min.

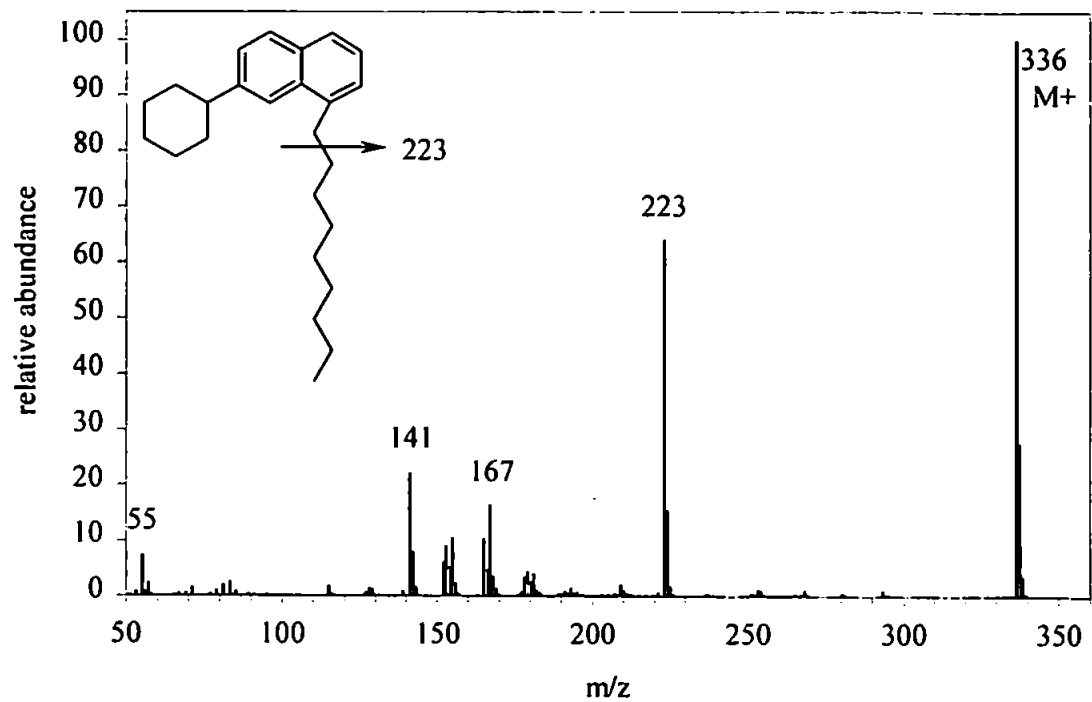


Figure 87. Mass spectrum of 1-n-nonyl-7-cyclohexylnaphthalene (XI).

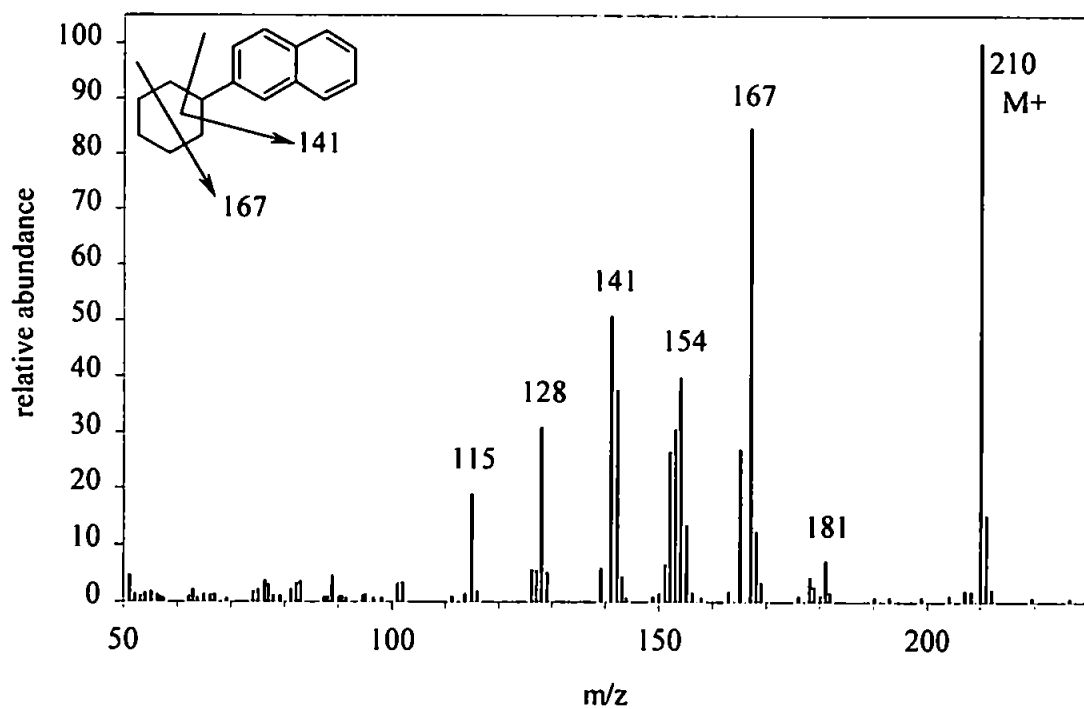


Figure 88. Mass spectrum of 2-cyclohexylnaphthalene.

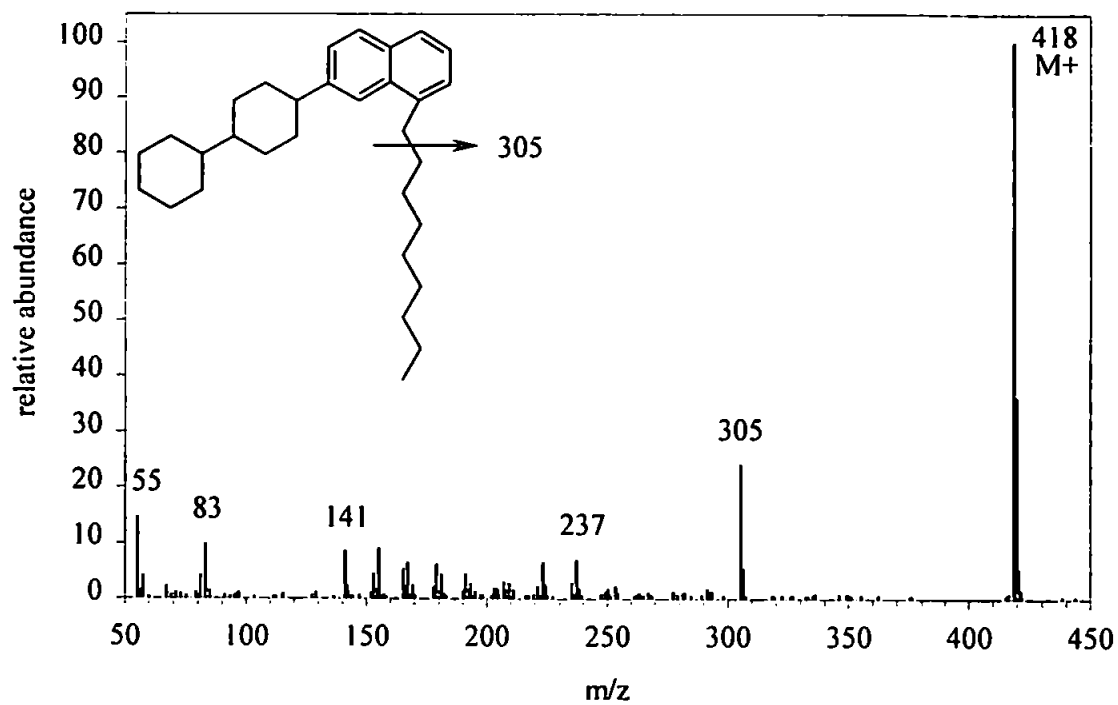


Figure 89. Mass spectrum of (tentatively) 1-n-nonyl-7-(4'-cyclohexylcyclohexyl)naphthalene.

5.9.2.2 IR

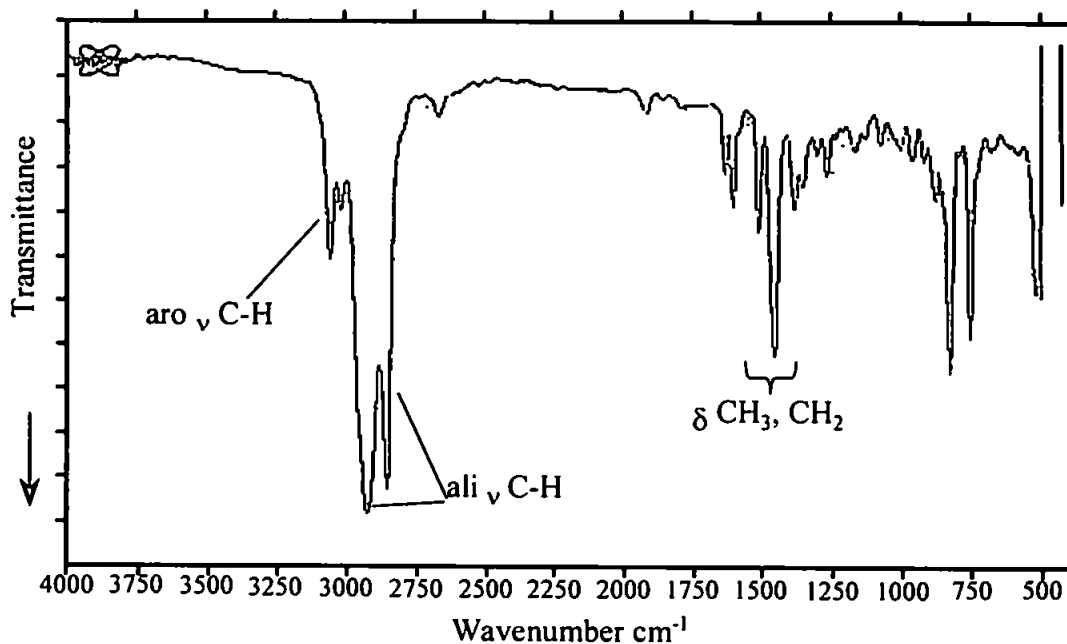


Figure 90. Infrared spectrum of 1-*n*-nonyl-7-cyclohexylnaphthalene(XI); thin film, NaCl windows.

Compared to the IR spectrum of the monoaromatic fraction (Figure 82), the IR spectrum of 1-*n*-nonyl-7-cyclohexylnaphthalene (XI, Figure 90) showed more intense bands between 3000 and 3100 cm⁻¹ (=C-H stretch), 1680 and 1600 cm⁻¹ (C=C stretch) and below 1000 cm⁻¹ (out of plane -C-H bending), probably due to the greater proportion of aromatic carbon in the molecule. A greater number of bands in the fingerprint region (*i.e.* below 1500 cm⁻¹) where aromatic and alkene bands are to be found are also observed.

5.9.2.3 NMR

The ¹³C NMR spectrum of 1-*n*-nonyl-7-cyclohexylnaphthalene (Figure 91) showed the expected ten naphthyl resonances in the region 120 to 150 ppm. The methyl carbon C15 was observed at 15 ppm and the only tertiary carbon was observed further downfield at 45 ppm. The CH₂ resonances are observed between 20 and 40 ppm.

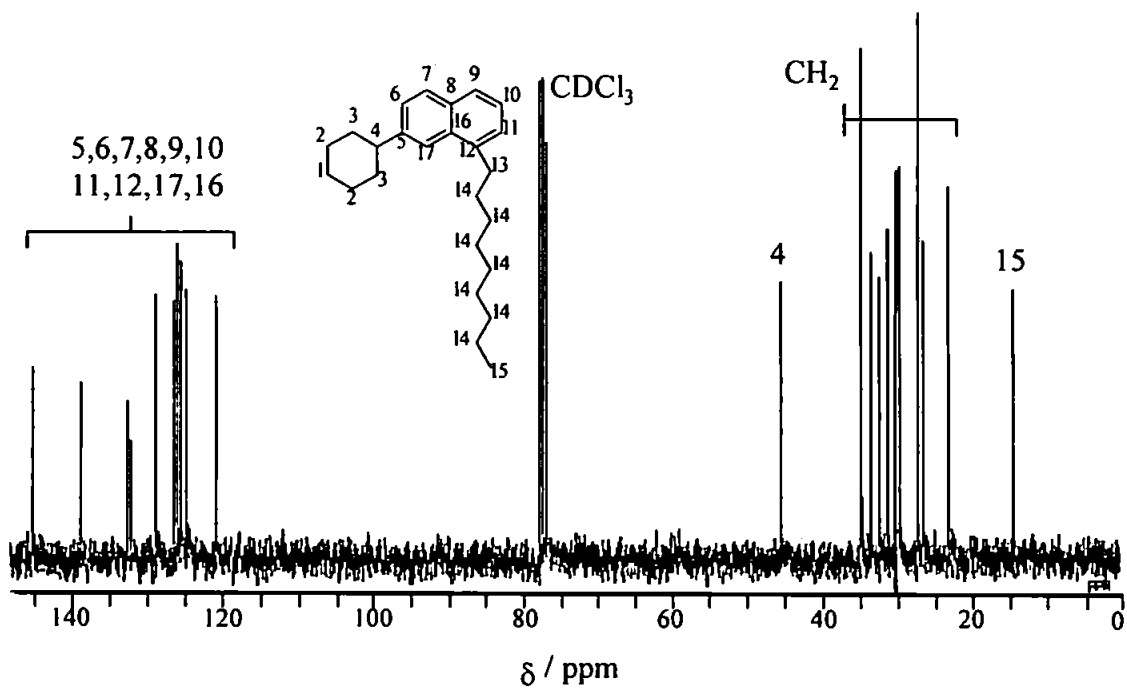


Figure 91. ^{13}C NMR spectrum of 1-n-nonyl-7-cyclohexyltetralin.

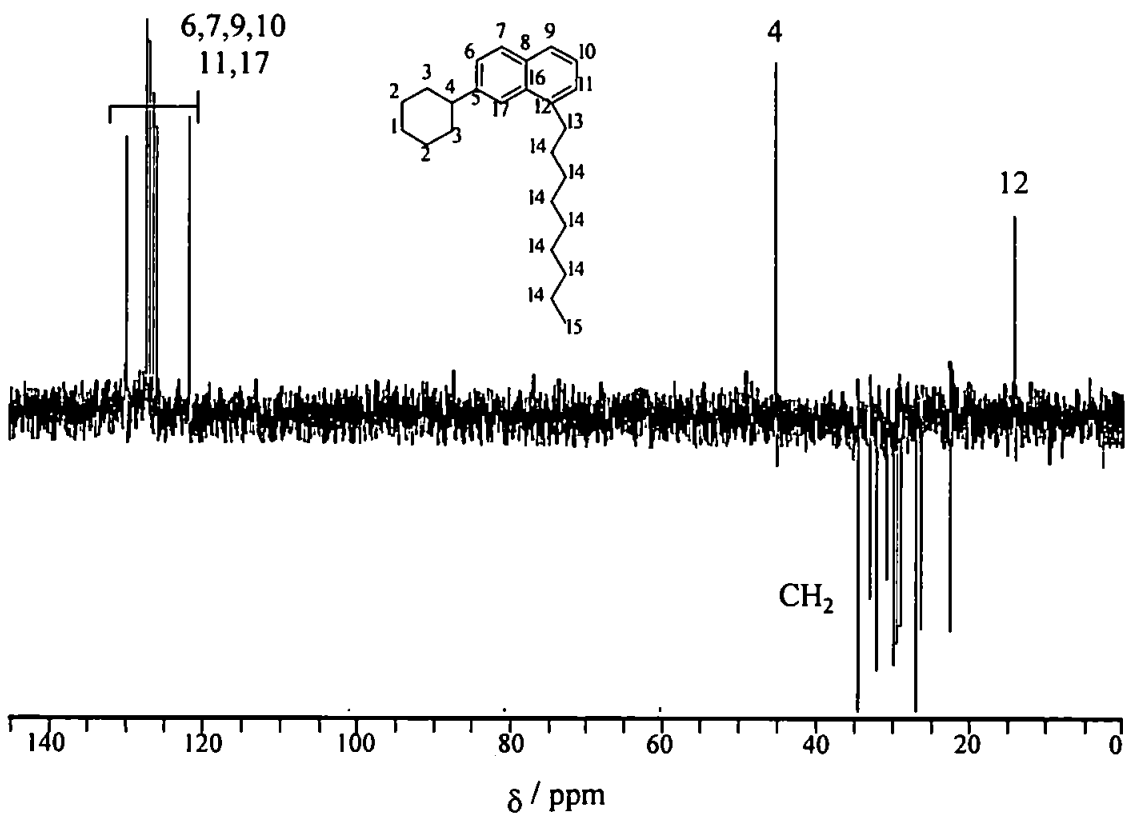


Figure 92. DEPT NMR spectrum of 1-n-nonyl-7-cyclohexyltetralin.

The DEPT spectrum (Figure 92) confirmed the assignments and showed which of the aromatic resonances were unsubstituted.

The ^1H NMR spectrum of 1-*n*-nonyl-7-cyclohexylnaphthalene showed more resonances in the aromatic region between 7 and 8 ppm when compared to the ^1H NMR spectrum of the monoaromatic fraction (Figure 85). A corresponding decrease in the methylene resonances was also observed. Methyl and methyne resonances were assigned by comparison with previous spectra. Peak integration confirmed these assignments.

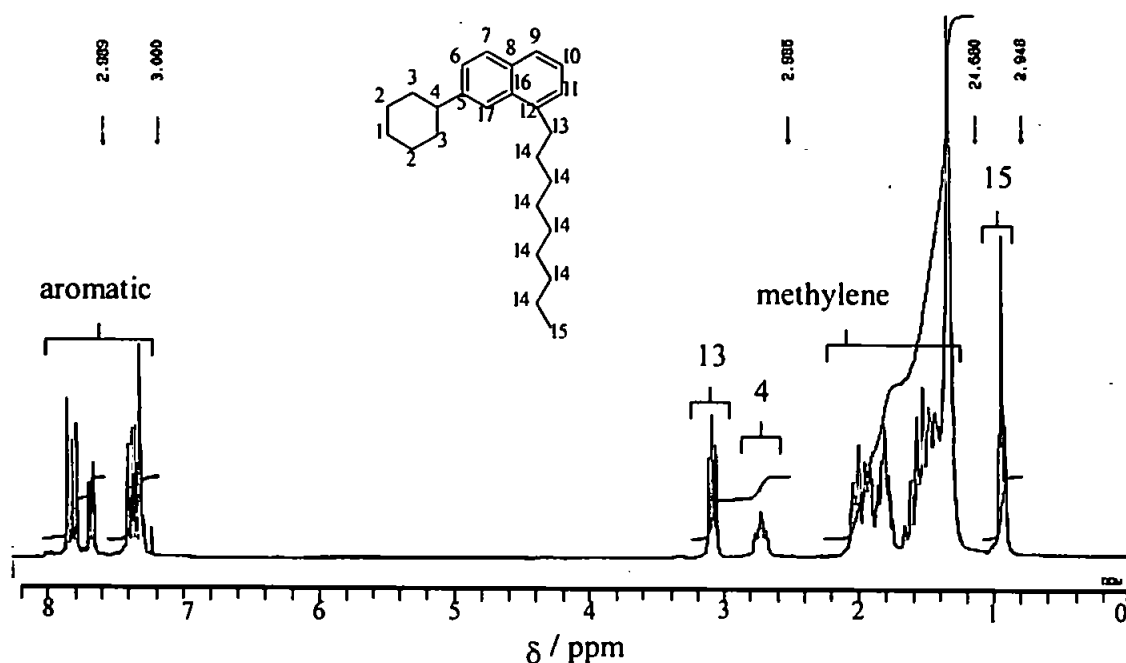


Figure 93. ^1H DEPT NMR spectrum of 1-*n*-nonyl-7-cyclohexylnaphthalene.

5.9.3 Preparation of 1-(3'-methylbutyl)-7-cyclohexylnaphthalene (X).

Several attempts were made to attach a branched substituent to 7-cyclohexyl-1-naphthalene (VII). However, formation of Grignard reagents from 2-methyl-1-bromopropane (XII), 2-methyl-2-bromopropane (XIV) and 2-iodobutane (XIII) were unsuccessful.

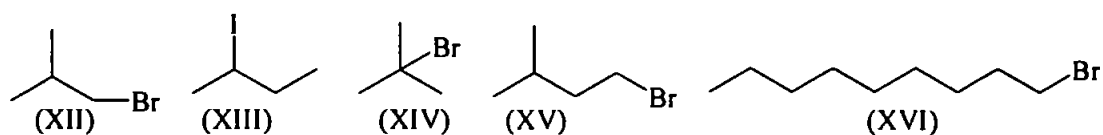


Figure 94. Compounds used in the attempted formation of Grignard reagents.

Modifications to the method were made in an attempt to initiate the reaction, namely adding freshly scraped magnesium, a small crystal of iodine to initiate the formation of the Grignard reagent and using sodium-dried toluene in an equal mixture with diethylether as an alternative solvent. None of these attempts were successful.

With hindsight, the failure of these attempts was perhaps predictable; an examination of the standard organic texts show that the steric hindrance of a tertiary butyl group promotes side reactions, enolisation in particular, in which the original starting material is recovered on hydrolysis of the reaction products. Indeed, the major product from such attempts was 7-cyclohexyl-1-tetralone (VII) *i.e.* the starting material.

It was consequently decided to use a longer alkane chain, with a branch point distant from the halogen atom to reduce steric interference. Thus the formation of the Grignard reagent from 1-bromo-3-methylbutane (XV) was successful and 1-(3'-methylbutyl)-7-cyclohexyltetralin (X) was prepared.

5.9.3.1 Characterisation of 1-(3'-methylbutyl)-7-cyclohexyltetralin (X).

5.9.3.1.1 GCMS

The TIC of 1-(3'-methylbutyl)-7-cyclohexyltetralin (X) is shown in Figure 95. The purity of the product was 82% by peak area. The impurities were 6-cyclohexyltetralin (4%), a possible isomer of 1-(3'-methylbutyl)-7-cyclohexyltetralin (X, 3%) and a compound tentatively identified as 1-(3'-methylbutyl)-7-(4'-cyclohexylcyclohexyl) tetralin (X, 5%, mass spectrum; Figure 97).

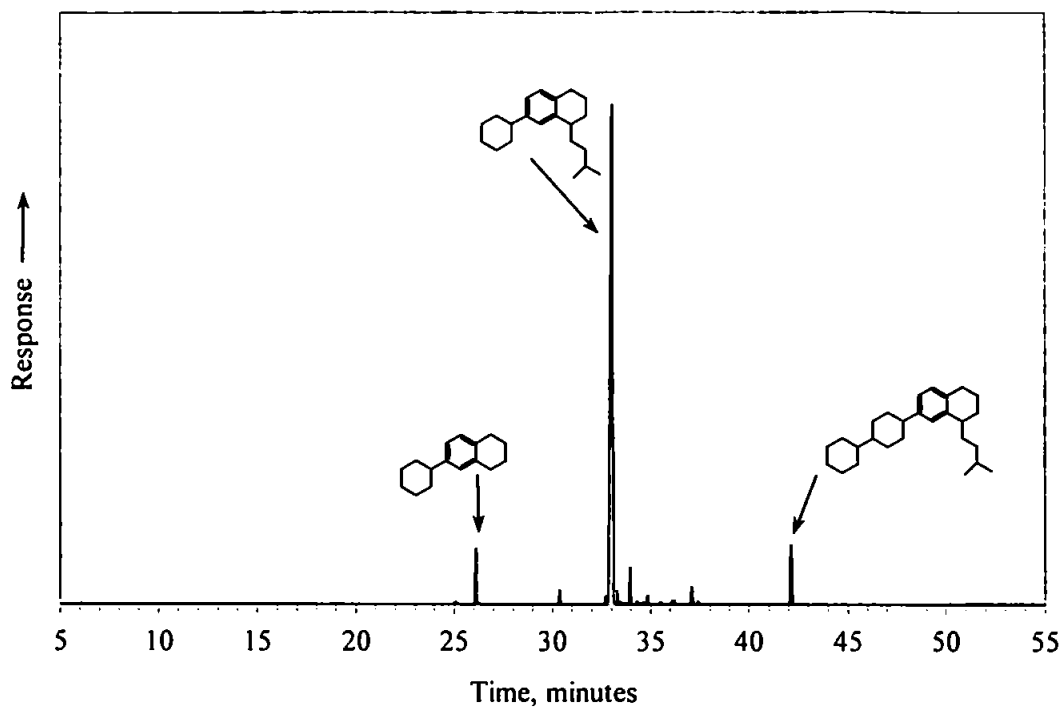


Figure 95. TIC chromatogram of 1-(3'-methylbutyl)-7-cyclohexyltetralin (X). GC = 12m HP1, 40 – 300°C @ 5°C min⁻¹, held 10 min.

The mass spectrum of 1-(3'-methylbutyl)-7-cyclohexyltetralin (X) is shown in Figure 96. The molecular ion is observed at m/z 284 and loss of the 3-methylbutyl fragment gives the 6-cyclohexyltetralin ion at m/z 213.

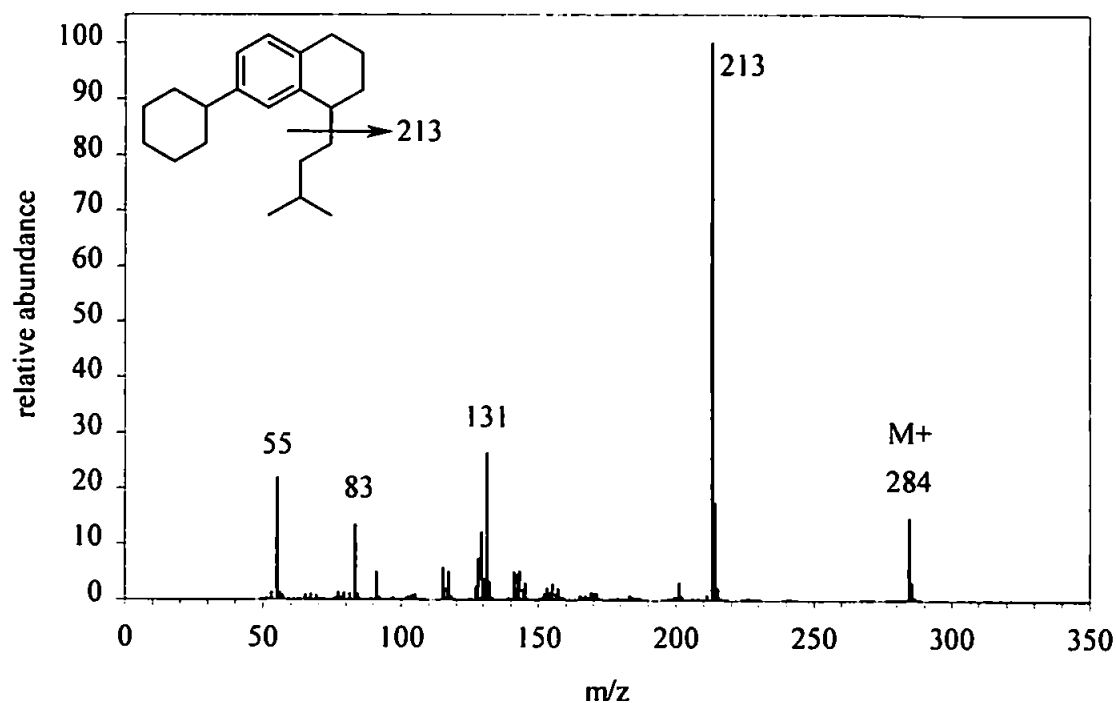


Figure 96. Mass spectrum of 1-(3'-methylbutyl)-7-cyclohexyltetralin (X).

The mass spectrum of 1-(3'-methylbutyl)-7-(4'-cyclohexylcyclohexyl)tetralin (X, Figure 97), showed $M^{+\bullet}$ at m/z 366. Loss of the first cyclohexyl fragment resulted in the ion at m/z 283 (plus the cyclohexyl fragment at m/z 83) while loss of the 3-methylbutyl fragment gave the major ion at m/z 295. Two ions at m/z 81 and 83 possibly showed sequential loss of cyclohexyl fragments from the structure shown.

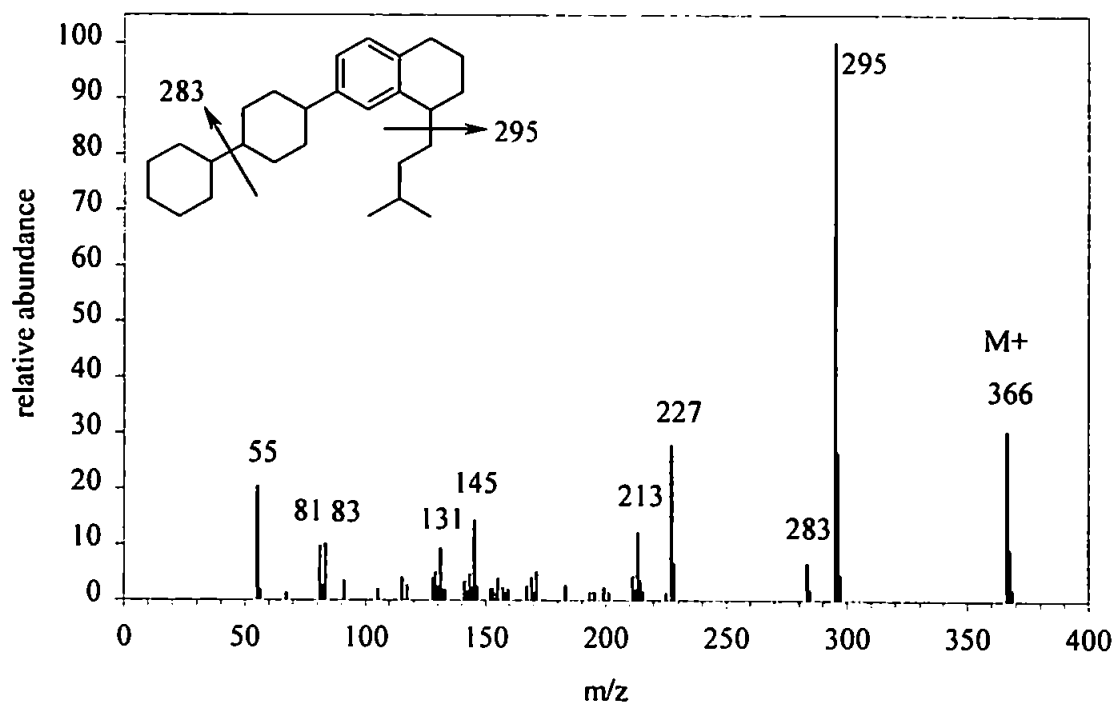


Figure 97. Mass spectrum of (tentatively) 1-(3'-methylbutyl)-7-(4'-cyclohexylcyclohexyl)tetralin.

5.9.3.1.2 IR

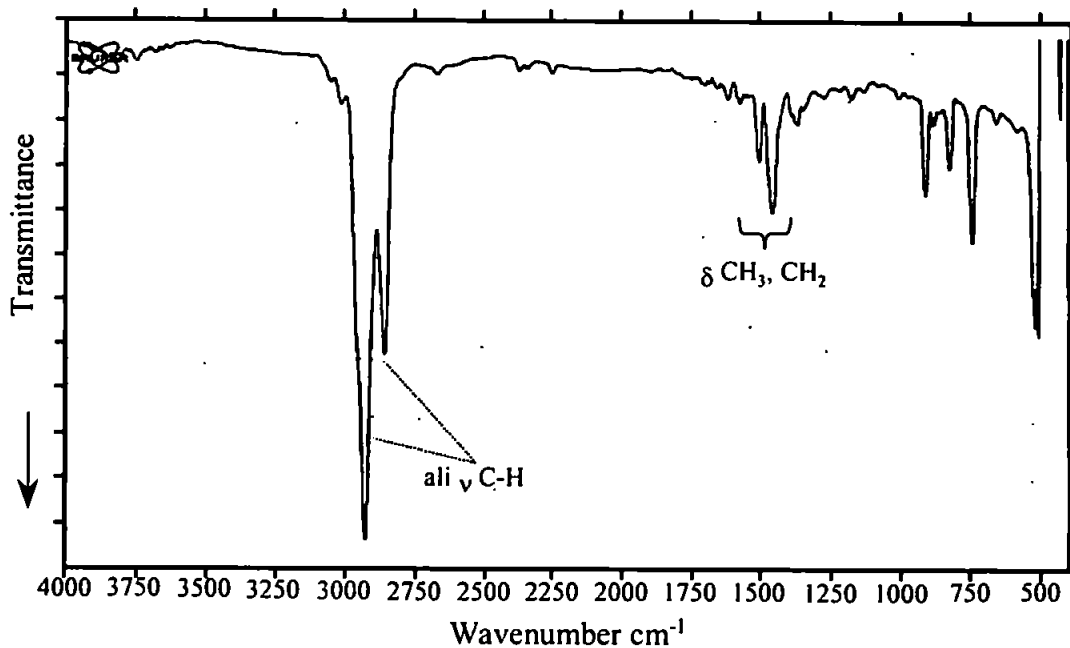


Figure 98. Infrared spectrum of 1-(3'-methylbutyl)-7-cyclohexyltetralin (X).

The infrared spectrum of 1-(3'-methylbutyl)-7-cyclohexyltetralin is shown in Figure 98. The spectrum was relatively simple. Intense aliphatic C-H stretches were observed between 2750 cm^{-1} and 3000 cm^{-1} . The two bands in the region around 1500 cm^{-1} were difficult to assign since both CH_3 , CH_2 and aromatic absorptions are found in this region.

5.9.3.1.3 NMR

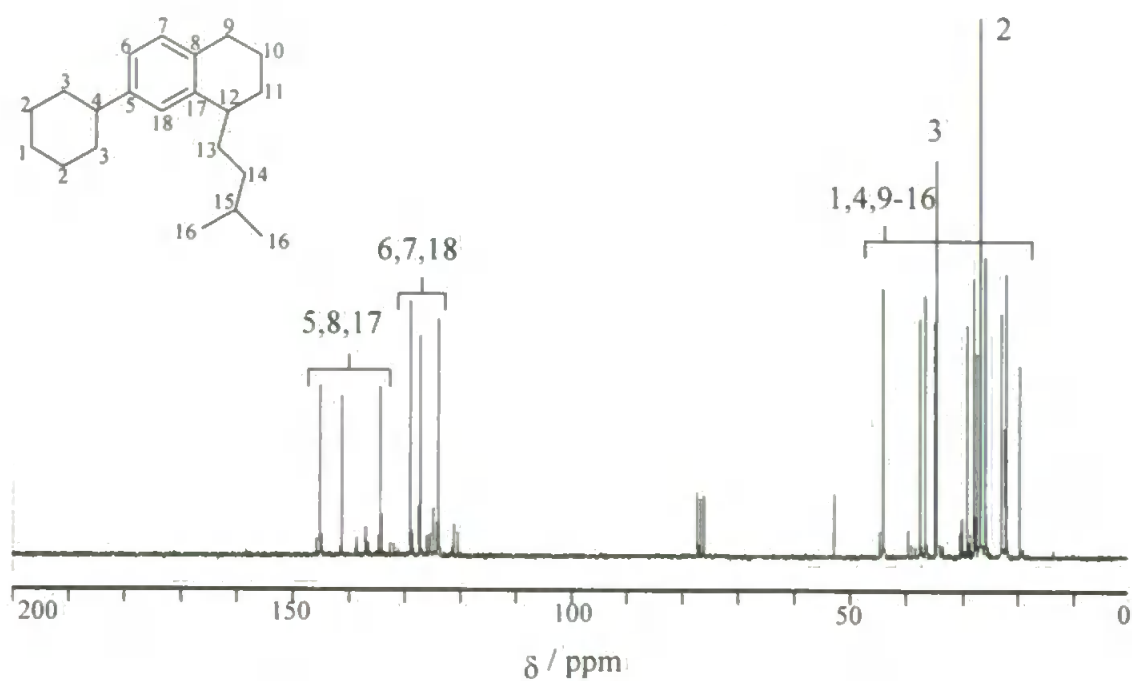


Figure 99. ^{13}C NMR spectrum of 1-(3'-methylbutyl)-7-cyclohexyltetralin (X).

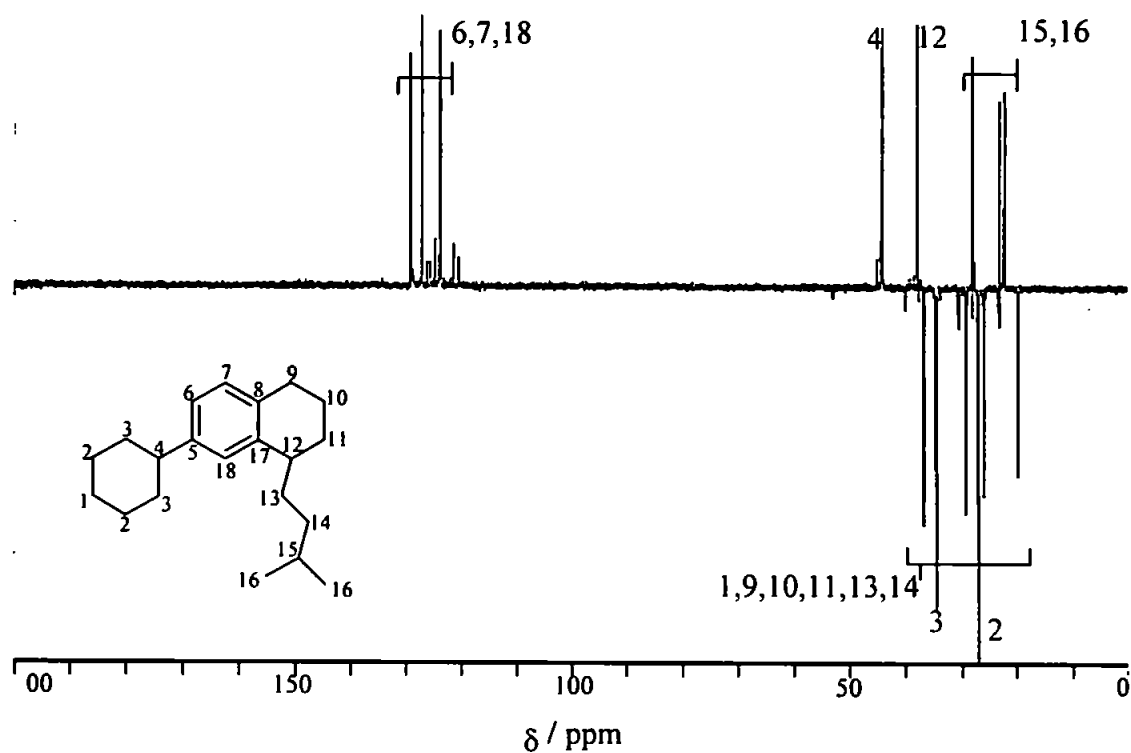


Figure 100. DEPT NMR spectrum of 1-(3'-methylbutyl)-7-cyclohexyltetralin (X).

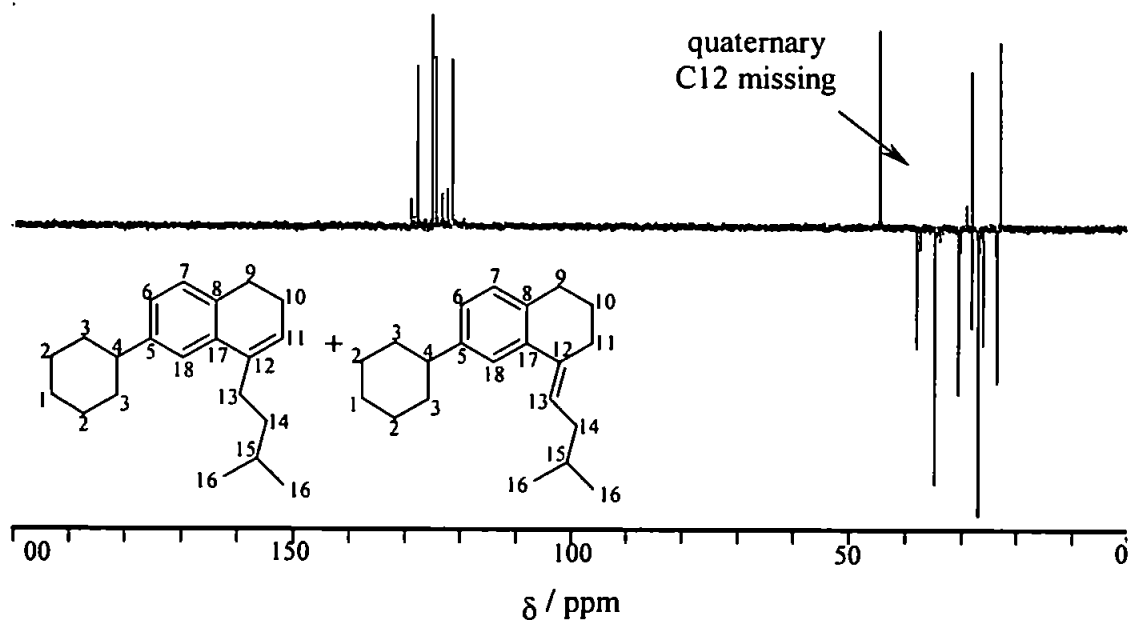


Figure 101. DEPT NMR spectrum of alkene precursors to 1-(3'-methylbutyl)-7-cyclohexyltetralin (X).

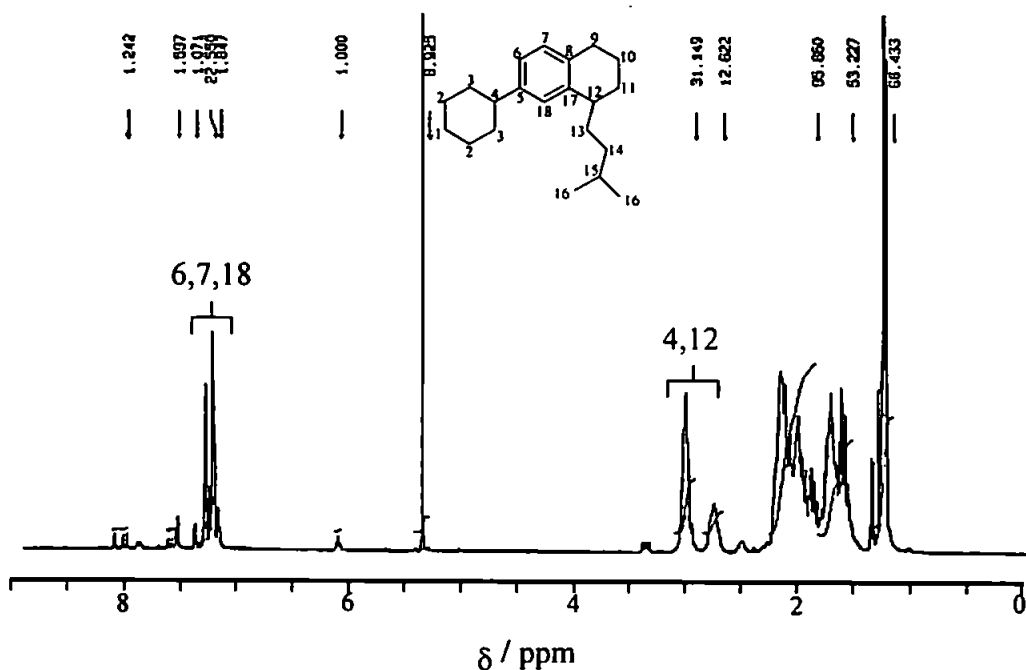


Figure 102. ^1H NMR spectrum of 1-(3'-methylbutyl)-7-cyclohexyltetralin (X).

Figure 99 and Figure 100 show the ^{13}C and DEPT NMR spectra. The six downfield resonances corresponding to aromatic carbons were assigned according to the DEPT spectrum where *ipso* carbons are not observed. Of the aliphatic carbons, C3 and C2 are assigned on the basis of their higher relative intensities and by comparison with ^{13}C NMR spectra of the precursors of this compound (II, VI and X). The resonance due to carbon C3 is further downfield than C2 because of the closer proximity to the aromatic ring. Carbon C4 is assigned by comparison with previous spectra and the DEPT spectrum. The carbon C12 is assigned because of its absence in the DEPT spectrum of the precursor alkenes (Figure 101), since the presence of double bonds on carbons 11=12 and 12=13 means carbon C12 was quaternary and therefore absent in a DEPT sequence spectrum. Small resonances observed in both spectra were probably due to impurities in the sample. The ^1H NMR spectrum showed a greater number of resonances in the aliphatic region (*i.e.* below ~ 4 ppm) corresponding to the hydrogens on the iso-pentyl substituent. There

were now two resonances observed at 2.8 and 3 ppm corresponding to hydrogens H4 and H12 bonded to tertiary carbons adjacent to the benzene ring.

5.10 Summary

6-Cyclohexyltetralin (V) was successfully synthesised in gram quantities (Table 21) and fully characterised. 1-*n*-nonyl-7-cyclohexyltetralin (VI) was also successfully synthesised, along with the aromatic homologue 1-*n*-nonyl-7-cyclohexylnaphthalene (Table 21). The fact that these two compounds were in simple mixtures with (mainly) 6-cyclohexyltetralin (V) and 1-methyl-7-cyclohexyltetralin, though not planned, could nonetheless prove to be of benefit for subsequent RuO₄ oxidation studies. RuO₄ oxidations of simple mixtures of known compounds has not been reported in the literature.

Synthesis of a branched C₄ cyclohexyltetralin was unsuccessful, and reasons for this have been given. Synthesis of a C₅ branched homologue; 1-(3'-methylbutyl)-7-cyclohexyltetralin (X) was successful and the product was fully characterised.

A summary of the compounds synthesised is shown in Table 21;

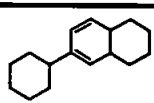
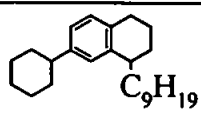
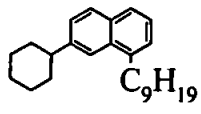
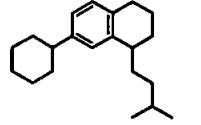
| Compound | yield | GC purity | structure |
|---|-------|-----------------|--|
| 6-cyclohexyltetralin | > 3g | 98 % | VIII  |
| 1-nonyl -7-cyclohexyltetralin | ~ 1g | 53% see text | IX  |
| 1-nonyl-7-cyclohexylnaphthalene | ~ 1g | 92% | XI  |
| 1-(3'-methylbutyl)-7-cyclohexyltetralin | ~0.4g | 82 % | X  |

Table 21. Summary of model UCM hydrocarbons synthesised.

The model UCM hydrocarbons synthesised herein have not been made before and extend the range of 1-alkyl-7-cyclohexyltetralins synthesised in association with Wraige (1997). The oxidation of such novel compounds should provide valuable insights into the behaviour of complex mixtures of aromatic hydrocarbons (*i.e.* aromatic UCMs) when oxidised by RuO_4 , and further elucidate the complex range of products obtained from such oxidations.

6 Ruthenium Tetroxide Oxidation of Synthetic Model UCM components.

A mass-balance approach to the oxidation of model UCM components synthesised herein and a *retro*-structural reconstruction of observed oxidation products is presented.

Compounds oxidised in replicate were tetralin (n = 8), 6-cyclohexyltetralin (n = 10), 1-(3'-methyl)butyl-7-cyclohexyltetralin (n = 4), 1-*n*-nonyl-7-cyclohexyltetralin (as a mixture with 6-cyclohexyltetralin and 1-methyl-7-cyclohexyltetralin, n = 5) and 1-*n*-nonyl-7-cyclohexylnaphthalene (n = 3).

Both the predicted oxidation products and products from the over oxidation of primary oxidation products ('chain-shortening') were observed for the hydroaromatics.

6.1 Introduction.

Chapter 4 presented the method development for the ruthenium tetroxide oxidation of hydrocarbons. Chapter 5 presented details of the synthesis of some model UCM hydrocarbons proposed by Thomas (1995) on the basis of detailed Ion Cyclotron Resonance Mass Spectrometry (ICRMS) *retro*-structural analysis of RuO₄ oxidation products from several feedstocks. This chapter presents results from the oxidation of the model UCM hydrocarbons

The selective nature of RuO₄ oxidation has led to its use in attempts to elucidate the structure of complex organic matter. Previous substrates studied have included *e.g.* kerogens (Boucher *et al.*, 1990, 1991; Standen *et al.*, 1991, 1992), biodegraded crude oils (Revill, 1992; Thomas, 1995; Warton, 1999; Warton *et al.*, 2000), bitumens (Strausz and Lown, 1991; Mojelsky *et al.*, 1985; Mojelsky *et al.*, 1992), asphaltenes (Trifilieff, 1987), coals (Stock and Tse, 1983; Stock *et al.*, 1985; Stock and Wang, 1986; Olsen and Diehl, 1984; Olsen *et al.*, 1987) and refinery feedstocks (Thomas, 1995).

However, foundation studies of the oxidation of individual aromatic hydrocarbons by RuO₄ have been limited to a few simple compounds such as 1-phenylpropane, tetralin (Stock and Tse, 1983), C₀, C₁ and C₄ naphthalenes (Spitzer and Lee, 1974), 2- and 5-ethyltetralin and 9-ethylfluorene (Thomas 1995). These studies have rarely, if ever, been carried out in replicate. Hence no statistics for reproducibility are available. These are essential if the method is to be used for routine characterisation of feedstocks as proposed herein (reviewed in Chapter 1).

As discussed, the RuO₄ oxidation of hydroaromatic molecules (*e.g.* alkyltetralins) is possibly not as straightforward as that of simple aromatics (*e.g.* alkylbenzenes). Significant losses of expected oxidation products were observed by Thomas (1995) and previously (Djerassi and Engle, 1953; Stock and Tse, 1983). The oxidation of

ethyltetralins (Thomas, 1995) showed 100% conversion (*i.e.* no ethyltetralin was observed in the oxidation products) and most of the expected CO₂ (80+%) was recovered but only a fraction of the other expected oxidation products was observed (Table 22).

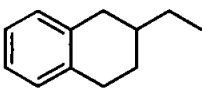
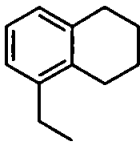
| Compound | % Observed | | | | unaccounted |
|--|------------|-----|-----------------|-------|-------------|
| | Water | DCM | CO ₂ | total | |
|  2-Ethyltetralin | <1 | 1 | 29 | 31 | 69 |
|  5-Ethyltetralin | 2 | 28 | 21 | 51 | 49 |

Table 22. Ruthenium tetroxide oxidation of ethyltetralins (Thomas, 1995).

The fact that RuO₄ oxidation of relatively simple hydroaromatic compounds gives such poor results may have significant consequences for the analysis of products from the oxidation of complex mixtures. If no water soluble products were observed from the oxidation of hydroaromatic compounds, then it might be assumed that dicarboxylic acids were the products of the oxidation of two aromatic rings joined by an alkyl chain *i.e.*;

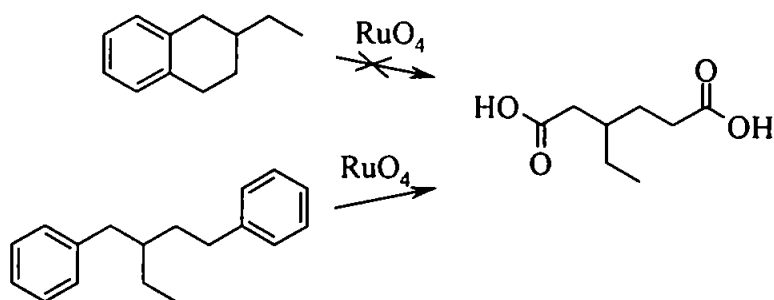


Figure 103. Possible inference from Thomas' (1995) results of the oxidation of 2-ethyltetralin.

However, preliminary work herein (Chapter 4, Method Development) and the findings of Stock and Tse (1983) and Spitzer and Lee (1974) have shown that the lack of water

soluble oxidation products experienced by Thomas (1995) was likely to be exacerbated by experimental factors. This prompted the method developments described in Chapter 4. Indeed, the need for a mass balance approach to the *retro*-structural analysis of complex mixtures is paramount. Each fraction of the oxidation products (CO₂, water-soluble and DCM-soluble products) gives important information about the sample which is unattainable by any one instrumental technique. The *retro*-structural *mass balance* analysis of more complex (especially diaromatic and hydroaromatic) compounds is vital in order to fully understand and exploit oxidation products from RuO₄ oxidation of complex mixtures of aromatic hydrocarbons and make RuO₄ oxidation a useful tool in their elucidation.

6.2 *Results and Discussion.*

Replicate oxidations of model UCM hydrocarbons were carried out using the improved method described in Chapters 2 and 4.

Calculations of carbon dioxide result from determinations with an average CO₂ trap recovery of $90 \pm 4\%$ ($n = 4$).

Quantification of water-soluble products was intended to be made using an internal standard (2-ethylpropanedioic acid) added immediately after the oxidation. This acid was chosen because it showed the most consistent recovery from the liquid/liquid extraction procedure (mean 104% recovery, see Section 4.3.2). However, examination of the water-soluble fractions of eight oxidations showed preferential loss of the internal standard. A further carboxylic acid - hexanoic acid was chosen for subsequent oxidations, but this was found to partition between the water and DCM fractions. Consequently, quantification of water soluble products was finally achieved by spiking the water-soluble fractions (derivatised as the *n*-butyl esters) with ethyl octanoate. A liquid/liquid extraction efficiency of 73% for the water soluble oxidation products was

calculated from a previous experiment (Section 4.3.2). Quantification of the DCM-soluble fraction was achieved using pentadecanoic acid as a true internal standard.

Response factors were not used in calculations since reference compounds were not available for many of the oxidation products (*e.g.* 2-*n*-nonyl-1,6-hexanedioic acid).

Blank oxidations were carried out as a control ($n = 3$) and showed the presence of only the internal standards.

6.2.1 RuO_4 oxidation of tetralin.

In order to test further the method developments made in the RuO_4 oxidation procedure (Chapter 4) several repeat oxidations of tetralin were carried out ($n = 8$).

Expected products from the oxidation of tetralin would be 4 mol CO_2 and 1 mol 1,6-hexanedioic acid as shown in Figure 104, though several workers have shown that 1-tetralone and 1,5-pentanedioic acid are also significant products (Spitzer and Lee, 1974; Stock and Tse, 1983; Olson and Diehl, 1984).

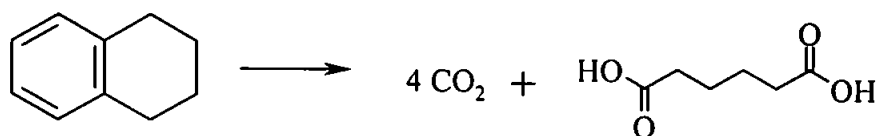


Figure 104. Expected products from the RuO_4 catalysed oxidation of tetralin.

Table 23 and Figure 106 show the oxidation products recovered. Recovered 1,5-pentanedioic acid (as 1,6-hexanedioic acid equivalent) was included in the figures for 1,6-hexanedioic acid, since it was believed to originate from the further oxidation of 1,6-hexanedioic acid. Several workers reported 1,5-pentanedioic acid as a significant product of the oxidation of tetralin structures (Spitzer and Lee, 1974; Stock and Tse, 1983; Olson and Diehl, 1984).

The 'expected' figures of 40 and 60% for carbon dioxide and hexanedioic acid respectively simply refer to the proportion of original carbon atoms from tetralin *i.e.*

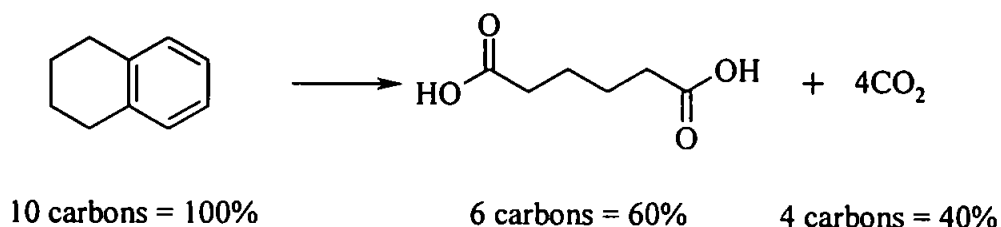


Figure 105. Calculation of 'expected' values for the oxidation products of tetralin.

| Oxidation No. | Recovery (% of expected) | | Unaccounted |
|----------------|--------------------------|-----------------|-------------|
| | 1,6-Hexanedioic acid | CO ₂ | |
| 1 | 27.8 (46) | 32.7 (82) | 39.5 |
| 2 | 44.8 (75) | 5.8 * (15) | 49.3* |
| 3 | 45.0 (75) | 33.3 (83) | 21.7 |
| 4 | 36.5 (61) | 34.1 (85) | 29.4 |
| 5 | 40.3 (67) | 33.2 (83) | 26.5 |
| 6 | 34.8 (58) | 33.0 (83) | 32.1 |
| 7 | 39.0 (65) | 30.2 (76) | 30.8 |
| 8 | 35.2 (59) | 33.5 (84) | 31.4 |
| Mean | 37.9 (63) | 32.9 (82) | 30.2 |
| σ_{n-1} | 1.3 (10) | 1.3 (3) | 5.5 |
| Expected | 60.0 | 40.0 | - |

* = outlier not included in calculations.

Table 23. Recovery of products from the ruthenium tetroxide oxidation of tetralin.

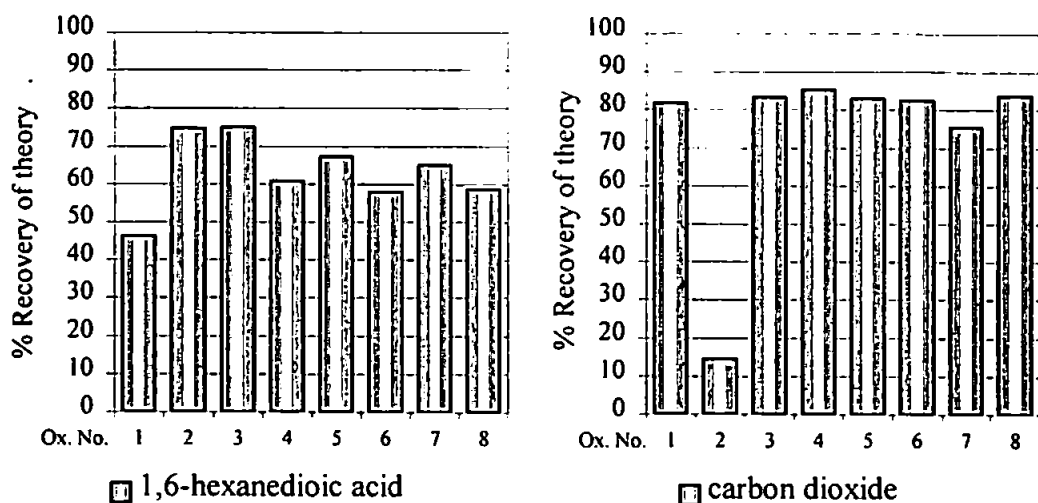


Figure 106. Recovery of products from the RuO_4 oxidation of tetralin.

GCMS analysis of the water-soluble fraction (as the *n*-butyl esters) of the oxidation products of tetralin showed the major product to be 1,6-hexanedioic acid but with a significant amount of 1,5-pentanedioic acid and a trace of 1,4-butanedioic acid (Figure 107). Other minor components observed in the chromatogram were unidentified.

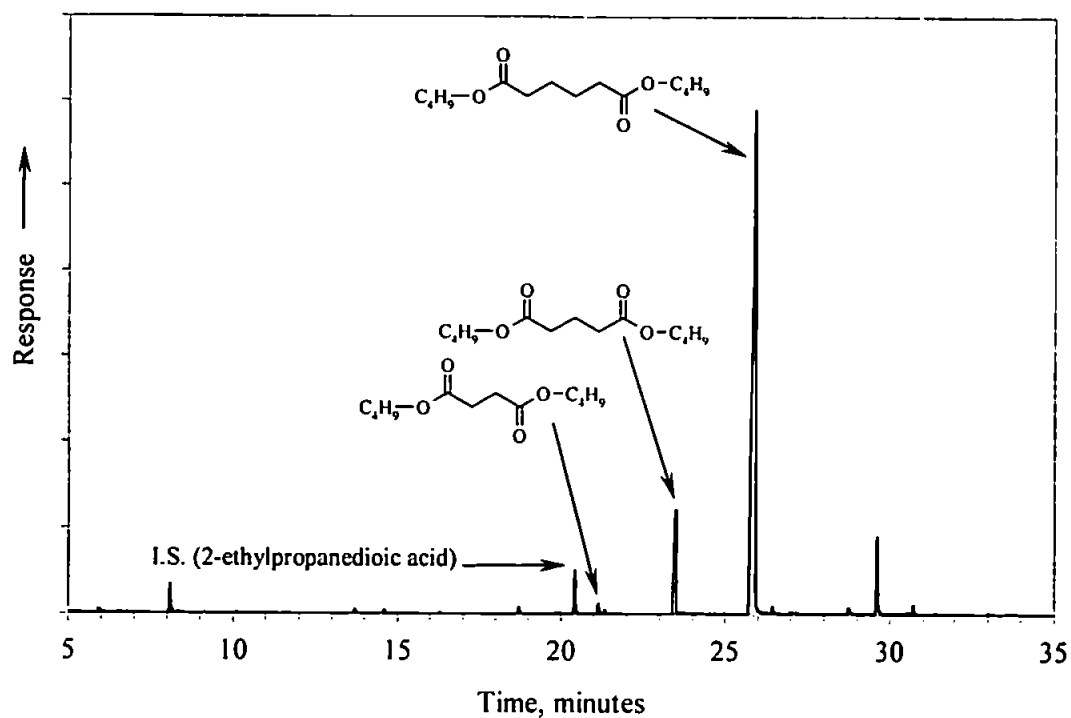


Figure 107. Partial TIC chromatogram of the water-soluble products from the RuO_4 oxidation of tetralin (as *n*-butyl esters, Oxidation No. 10). GC = 25m DB5, 40-300°C @ 5°C min^{-1} , held 10 min.

From Table 23 it is obvious that recovery of carbon dioxide with the modified trap has indeed led to an improvement over previous studies (Thomas, 1995) However, recovery of 1,6-hexanedioic acid still remains at about half that expected even allowing for chain-shortening. No oxidation products or unoxidised tetralin were observed in the DCM fraction.

6.2.2 RuO_4 oxidation of 6-cyclohexyltetralin.

The expected products from the ruthenium tetroxide oxidation of 6-cyclohexyltetralin were 1,6-hexanedioic acid, cyclohexane carboxylic acid and 3 mol CO_2 (Figure 108).

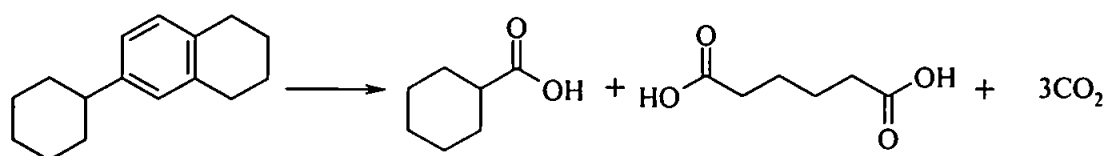


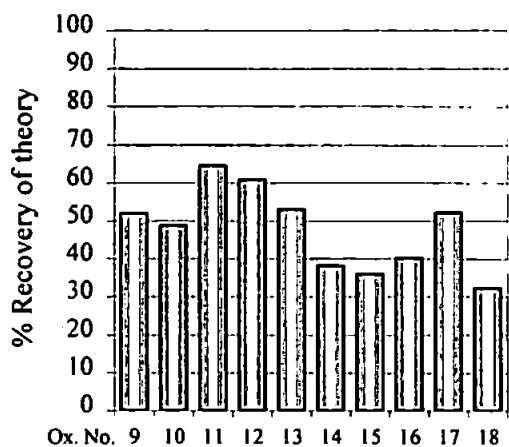
Figure 108. Theoretical products from the RuO_4 oxidation of 6-cyclohexyltetralin.

Table 24 and Figure 109 show the recovery of products from 10 repeat oxidations of 6-cyclohexyltetralin. As with hexanoic acid, cyclohexane carboxylic acid partitions between the aqueous and DCM phase during the oxidation work-up. Consequently cyclohexane carboxylic acid was quantified in both phases and the two quantities combined.

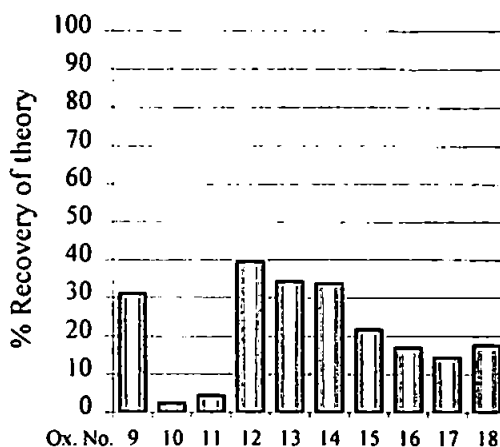
Good recoveries of carbon dioxide were again observed (Figure 109, Table 24). However, recovery of hexanedioic acid was on average half that expected and recovery of cyclohexane carboxylic acid was highly variable (range 1–17%, theory = 43.8%).

| Oxidation No. | Recovery (% of theory) | | | Unaccounted |
|----------------|------------------------|-----------------------------|-----------------|-------------|
| | 1,6-Hexanedioic acid | Cyclohexane carboxylic acid | CO ₂ | |
| 9 | 19.5 (52) | 13.6 (31) | 18.6 (99) | 48.3 |
| 10 | 18.3 (49) | 1.0 (2) | 25.1 (134) | 55.6 |
| 11 | 24.2 (65) | 1.9 (4) | 17.7 (94) | 56.2 |
| 12 | 22.8 (61) | 17.3 (40) | 17.3 (92) | 42.7 |
| 13 | 19.9 (53) | 15.0 (34) | 15.8 (84) | 49.3 |
| 14 | 14.3 (38) | 14.8 (34) | 15.7 (84) | 55.2 |
| 15 | 13.5 (36) | 9.5 (22) | 20.2 (107) | 56.8 |
| 16 | 15.1 (40) | 7.4 (17) | 25.8 (137) | 51.7 |
| 17 | 19.6 (52) | 6.3 (14) | 17.6 (94) | 56.5 |
| 18 | 12.1 (32) | 7.7 (18) | 18.9 (101) | 61.3 |
| Mean | 19.7 (48) | 12.6 (22) | 19.2 (103) | 53.4 |
| σ_{n-1} | 7.0 (11) | 11.6 (13) | 3.3 (19) | 5.4 |
| Theory | 37.5 | 43.8 | 18.8 | - |

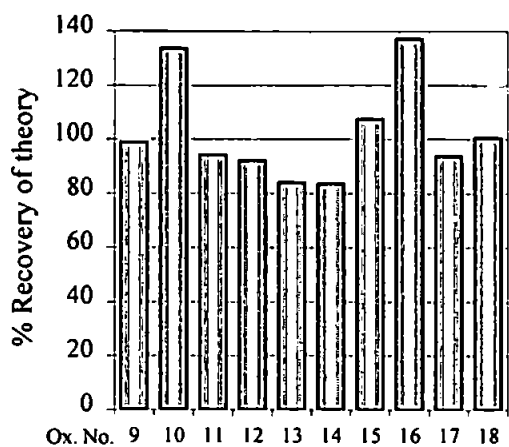
Table 24. Recovery of identified products from the RuO₄ oxidation of 6-cyclohexyltetralin.



1,6-hexanedioic acid



cyclohexane carboxylic acid



carbon dioxide

Figure 109. Recovery of identified products from the ruthenium tetroxide oxidation of 6-cyclohexyltetralin.

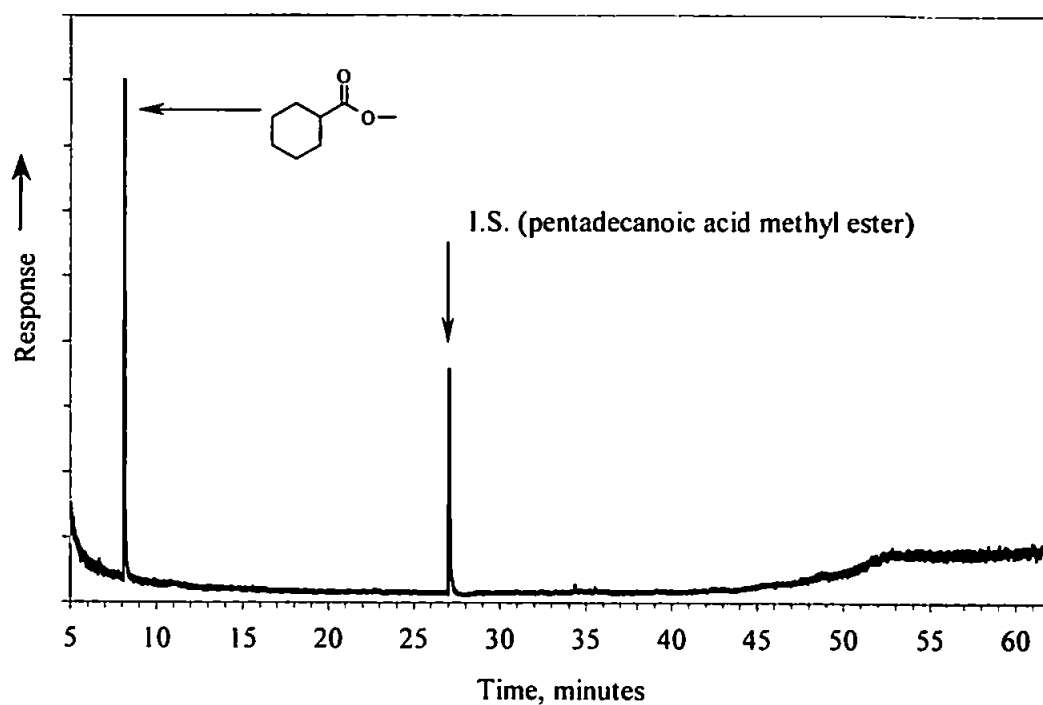


Figure 110. TIC chromatogram of the DCM-soluble products from the oxidation of 6-cyclohexyltetralin (as methyl esters, Oxidation No. 12). GC = 25m DB5, 40-300°C @ 5°C min⁻¹, held 10 min.

Figure 110 shows the TIC chromatogram of the DCM-soluble oxidation products (as methyl esters) from one of the oxidations of 6-cyclohexyltetralin. No other DCM-soluble products were observed.

The low recoveries of water soluble oxidation products (~50% of that expected) are consistent with the oxidation products of tetralin. The variable recoveries of cyclohexane carboxylic acid may be due to losses by evaporation and/or by further oxidation of the carboxylic acid group.

The further oxidation of cyclohexane carboxylic acid has not been reported in the literature, but RuO₄ oxidation of the cyclohexyl ring may produce 1,6-hexanedioic acid (Figure 111), or possibly cyclohexanone.

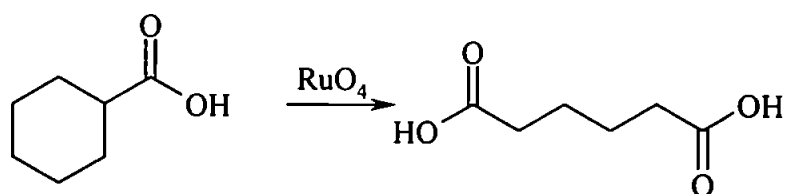


Figure 111. Postulated product from the further oxidation of cyclohexane carboxylic acid.

No other products that may originate from further oxidation of cyclohexane carboxylic acid were observed, although cyclohexanone would elute with the solvent front under the GC conditions used.

6.2.3 RuO_4 oxidation of a mixture containing 1-*n*-nonyl-7-cyclohexyltetralin.

The theoretical products from the ruthenium tetroxide oxidation of the mixture containing 1-*n*-nonyl-7-cyclohexyltetralin (56%), 6-cyclohexyltetralin (31%) and 1-methyl-7-cyclohexyltetralin (13%) are shown in Figure 112.

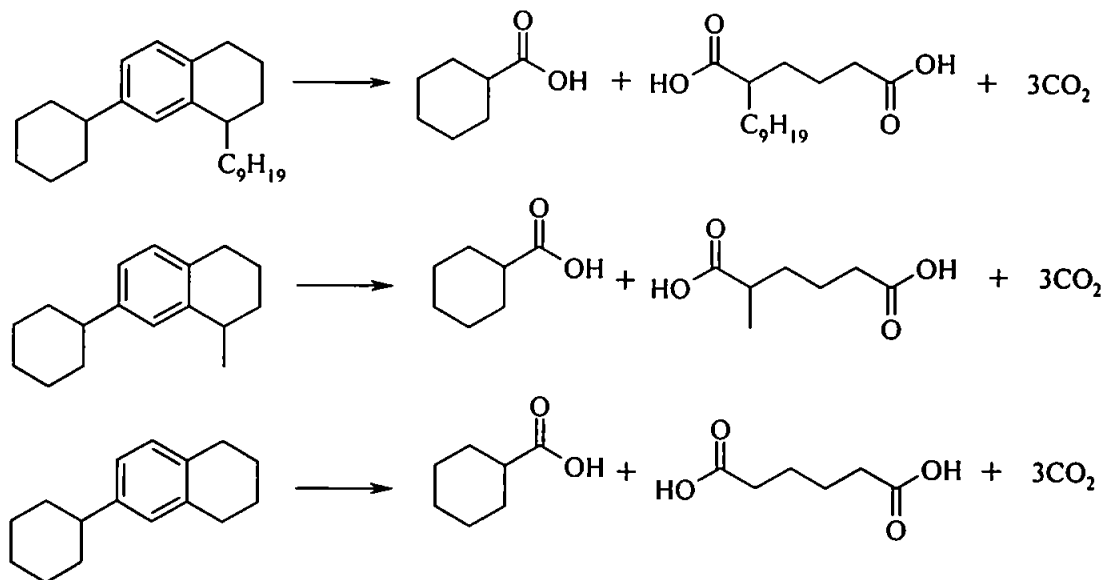


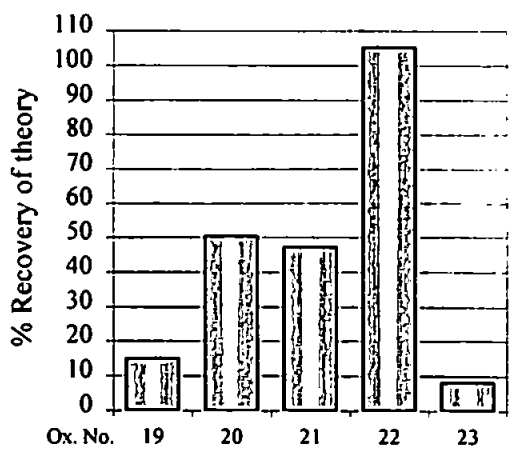
Figure 112. Theoretical products from the ruthenium tetroxide oxidation of a mixture containing 1-*n*-nonyl-7-cyclohexyltetralin, 6-cyclohexyltetralin and 1-methyl-7-cyclohexyltetralin.

When calculating the proportions of expected products, contributions from each of the components were taken into account. The 2-alkyl-1,6-hexanedioic acid was 'unique' to the particular substrate compound, but all three compounds contribute amounts of carbon dioxide and cyclohexane carboxylic acid to the total oxidation products.

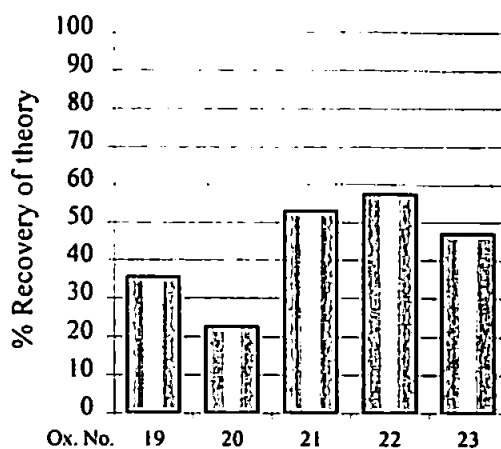
As was observed for tetralin and 6-cyclohexyltetralin, significant amounts of chain shortened acids were observed in the oxidation products of the mixture. These amounts were included with the figures for the relevant dicarboxylic acids.

| Ox. No. | Recovery (% of theory) | | | | | Un-accounted |
|----------------|-----------------------------|----------------------|-------------------------------|---|-----------------|--------------|
| | cyclohexane carboxylic acid | 1,6-hexanedioic acid | 2-methyl-1,6-hexanedioic acid | 2- <i>n</i> -nonyl-1,6-hexanedioic acid | CO ₂ | |
| 19 | 5.2 (15) | 4.1 (36) | 0.6 (11) | 10.6 (31) | 12.1 (82) | 67.4 |
| 20 | 17.4 (51) | 2.6 (23) | 0.2 (4) | 7.4 (22) | 10.0 (68) | 62.4 |
| 21 | 16.3 (47) | 6.1 (53) | 0.5 (9) | 2.6 (8) | 14.5 (98) | 60.0 |
| 22 | 36.3 (105) | 6.6 (57) | 0.5 (9) | 10.4 (30.8) | 11.6 (78) | 34.5 |
| 23 | 2.8 (8) | 5.4 (47) | 0.4 (8) | 20.6 (61) | 10.6 (72) | 60.1 |
| Mean | 15.6 (45) | 5.0 (43) | 0.5 (8) | 10.3 (31) | 11.8 (80) | 56.9 |
| σ_{n-1} | 13.3 (39) | 1.6 (14) | 0.2 (3) | 6.6 (20) | 1.7 (12) | 12.9 |
| Theory | 34.5 | 11.5 | 5.3 | 33.8 | 14.8 | - |

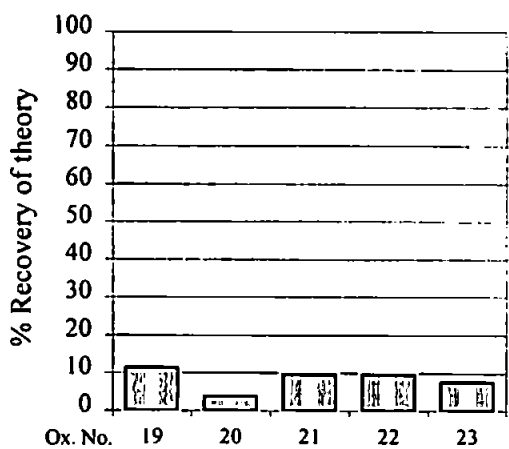
Table 25. Recovery (%) of products from the ruthenium tetroxide oxidation of a mixture containing 1-*n*-nonyl-7-cyclohexyltetralin, 6-cyclohexyltetralin and 1-methyl-7-cyclohexyltetralin.



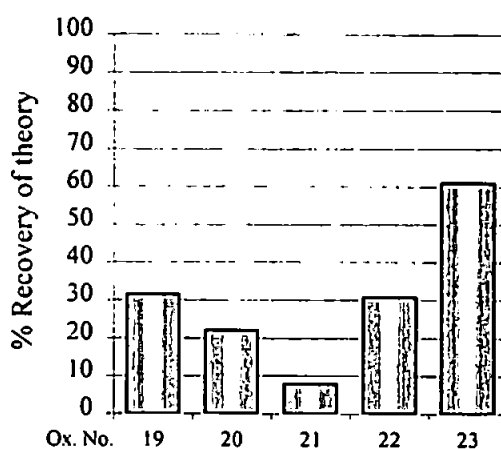
□ cyclohexane carboxylic acid



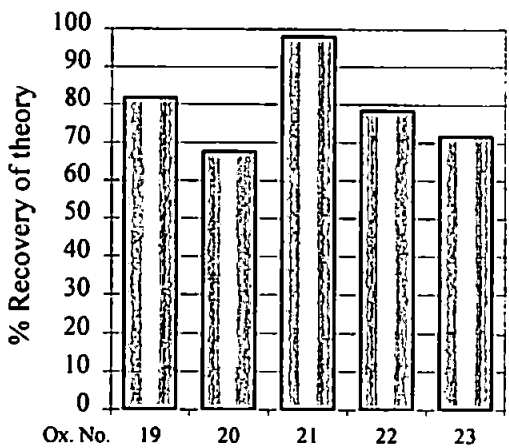
□ 1,6-hexanedioic acid



□ 2-methyl-1,6-hexanedioic acid



□ 2-n-nonyl-1,6-hexanedioic acid



□ carbon dioxide

Figure 113. Recovery of products from the ruthenium tetroxide oxidation of a mixture containing 1-n-nonyl-7-cyclohexyltetralin, 6-cyclohexyltetralin and 1-methyl-7-cyclohexyltetralin.

GCMS of the DCM-soluble oxidation products (as methyl esters, Figure 114) showed a range of carboxylic acid products. Hexanoic acid was present from the internal standards used and octadecane is presumably a small residual amount of the impurity in the crude synthetic product, although most of this was removed by column chromatography (Chapters 2 and 5). Several other monocarboxylic acids are observed; *i.e.* nonanoic acid and decanoic acid as well as trace amounts of octanoic acid. It is believed these monocarboxylic acids originate from the further oxidation of the primary oxidation product 2-*n*-nonyl-1,6-hexanedioic acid at the 2- position (chain shortening).

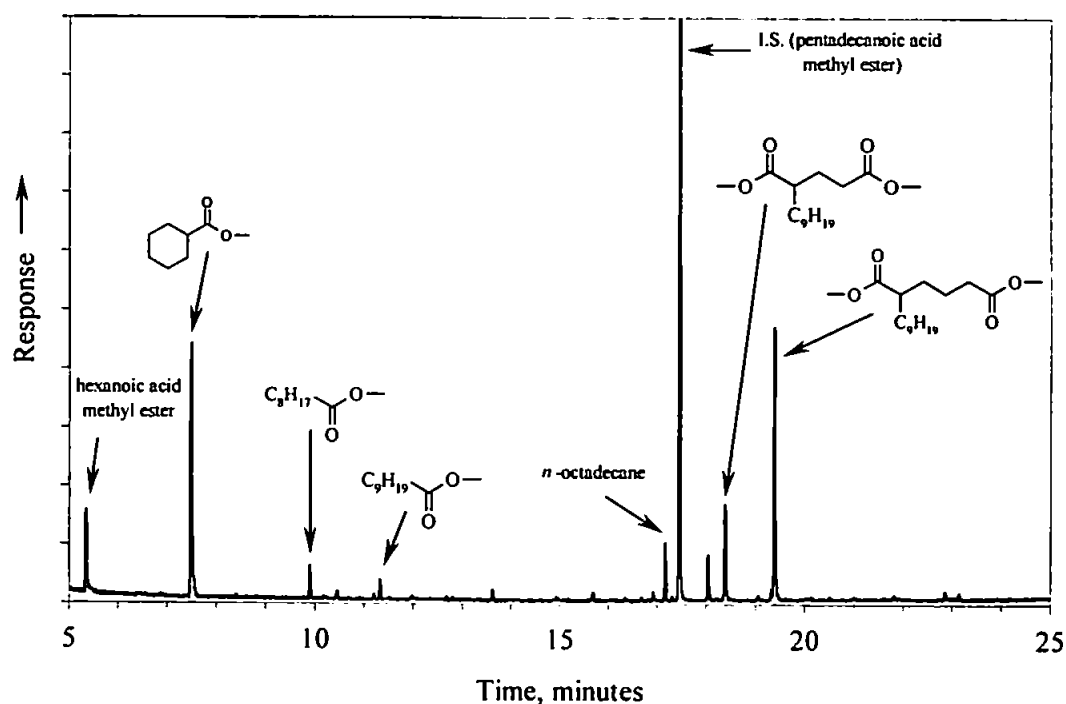


Figure 114. Partial TIC chromatogram of DCM-soluble products from the RuO_4 oxidation of a mixture containing 1-*n*-nonyl-7-cyclohexyltetralin, 6-cyclohexyltetralin and 1-methyl-7-cyclohexyltetralin (as methyl esters, oxidation No. 22). GC = 25m DB5, 40-300°C @ 10°C min⁻¹, held 10 min.

Oxidation products were identified on the basis of their mass spectra. The mass spectrum of 2-*n*-nonyl-1,6-hexanedioic acid (Figure 115) showed no molecular ion at m/z 300 while ions at m/z 169 and 241 show cleavage around a carboxyl group, typical of ester functionalities (*e.g.* Smith and Busch, 1999).

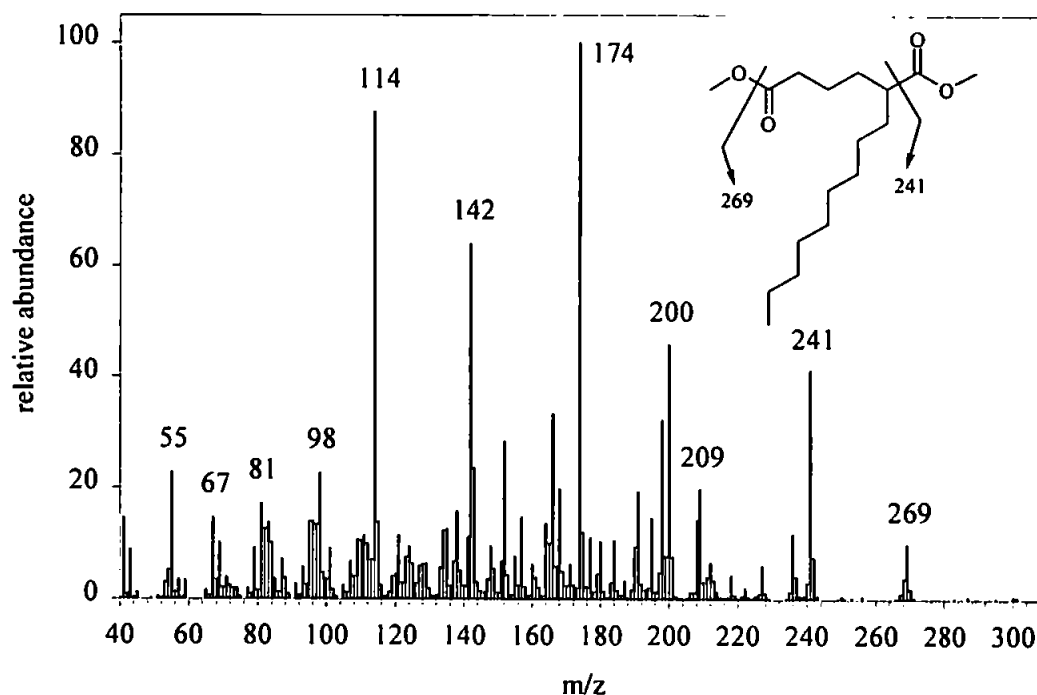


Figure 115. Mass spectrum of 2-*n*-nonyl-1,6-hexanedioic acid methyl ester.

GCMS of the water-soluble fraction (as *n*-butyl esters, Figure 117) showed 1,6-hexanedioic and 2-methyl-1,6-hexanedioic acid were produced on oxidation of 6-cyclohexyltetralin and 1-methyl-7-cyclohexyltetralin respectively. 1,6-Hexanoic acid (from the original internal standard) and cyclohexane carboxylic acid were observed at a retention time of 5.5 and 7.5 minutes. Other peaks in the chromatogram remained unidentified.

The peak area of 1,5-pentanedioic acid was increased compared to 1,6-hexanedioic acid (relative to that observed for tetralin, Figure 107). The mean ratio of 1,5-pentanedioic acid to 1,6-hexanedioic acid is 0.7 for 1-*n*-nonyl-7-cyclohexyltetralin ($n = 3$) and 0.2 for

both tetralin ($n = 8$) and 6-cyclohexyltetralin ($n = 10$). This relative increase in 1,5-pentanedioic acid over 1,6-hexanedioic acid together with the presence of nonanoic and decanoic acids in the DCM-soluble oxidation products confirms the chain shortening of 2-alkyl-1,6-hexanedioic acids (Figure 116).

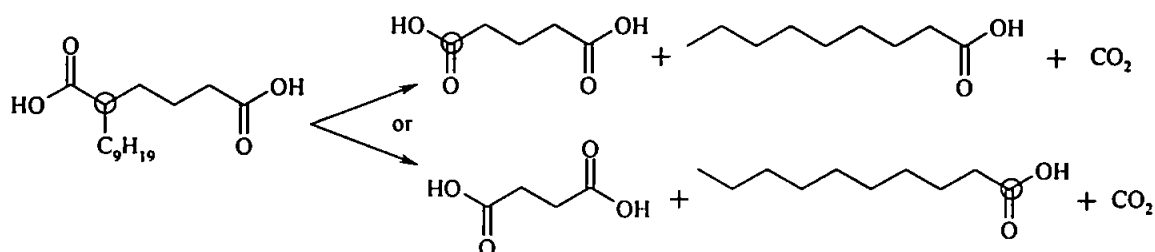


Figure 116. Products observed from the further oxidation of 2-*n*-nonyl-1,6-hexanedioic acid ('chain shortening').

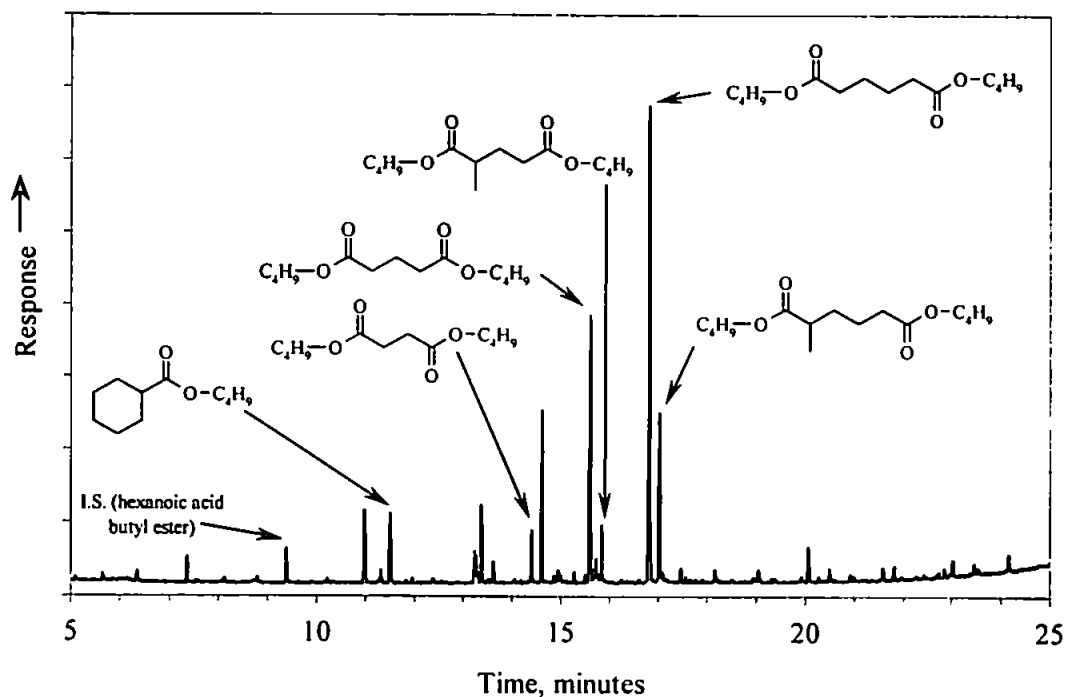


Figure 117. Partial TIC chromatogram of the water-soluble products from the RuO_4 oxidation of a mixture containing 1-*n*-nonyl-7-cyclohexyltetralin, 6-cyclohexyltetralin and 1-methyl-7-cyclohexyltetralin (as *n*-butyl esters, oxidation No. 23). GC = 25m DB5, 40-300°C @ 10°C min⁻¹, held 10 min.

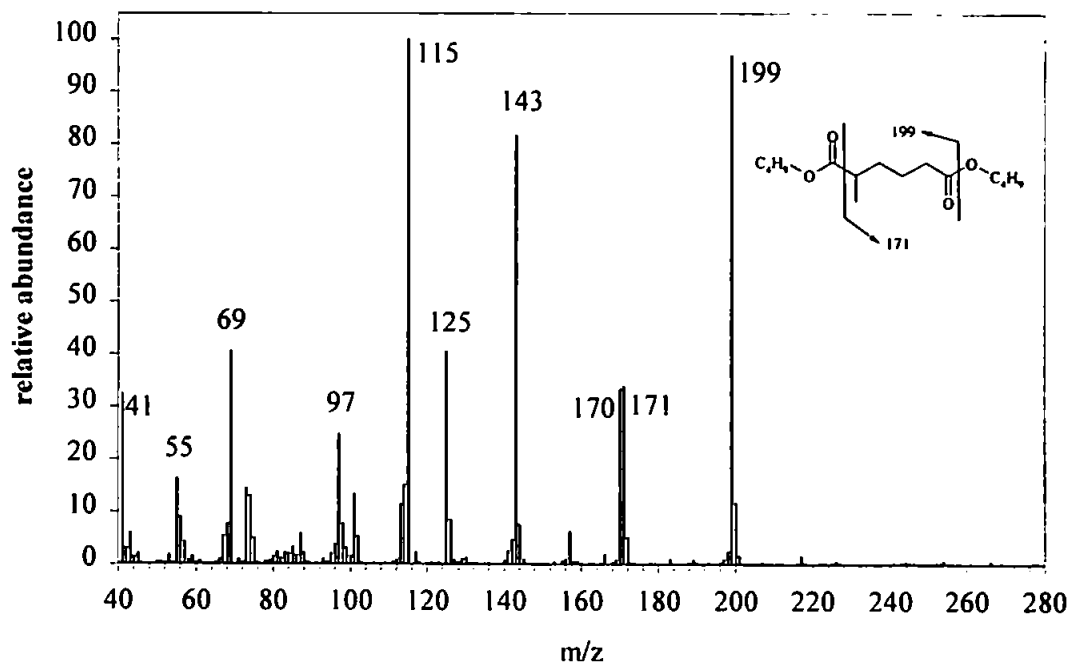


Figure 118. Mass spectrum of 2-methyl-1,6-hexanedioic acid *n*-butyl ester.

The mass spectrum of 2-methyl-1,6-hexanedioic acid (*n*-butyl ester) showed cleavage of the ester groups to give ions m/z 199 and 171. Consecutive losses of butyl- and butoxy-groups give rise to ion m/z 143, while loss of a butoxy-carbonyl (C_4H_9O-CO-) and a butyl group gives the ion at m/z 115.

The mass spectrum of 2-methyl-1,5-pentanedioic acid (*n*-butyl ester, Figure 119) showed cleavage around the carbonyl groups to give characteristic ions at m/z 185, 156 and 129.

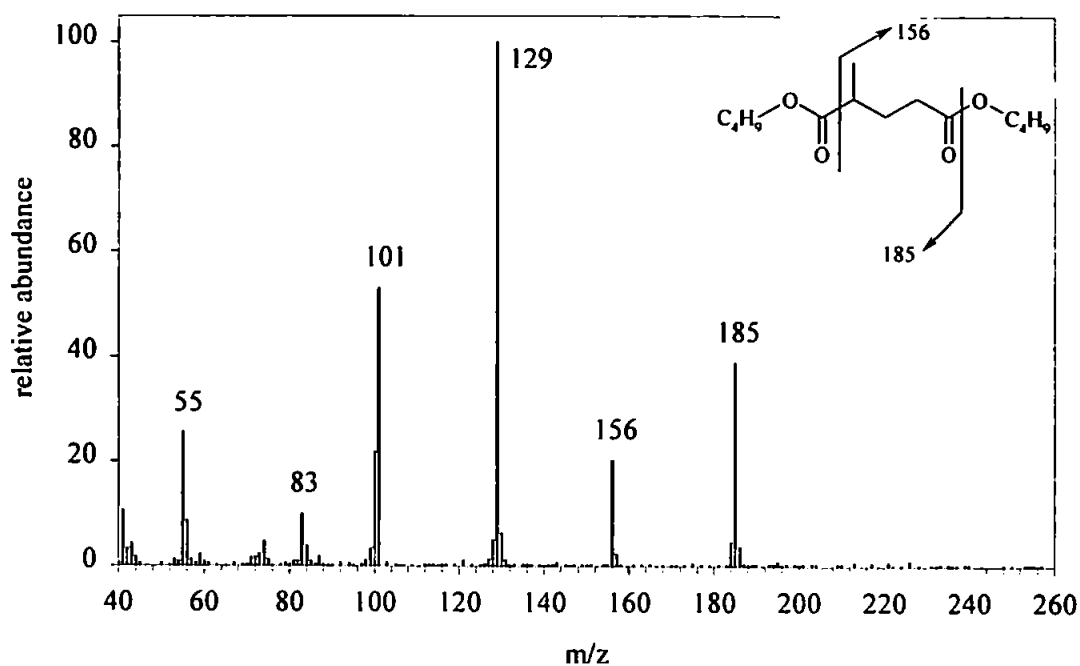


Figure 119. Mass spectrum of 2-methyl-1,5-pentanedioic acid n-butyl ester.

6.2.4 RuO_4 oxidation of 1-(3'-methylbutyl)-7-cyclohexyltetralin.

1-(3'-Methylbutyl)-7-cyclohexyltetralin was synthesised to examine the effect of branched alkyl substituents on the RuO_4 oxidation of an alkyltetralin.

Three replicate oxidations of 1-(3'-methylbutyl)-7-cyclohexyltetralin were carried out. The expected products from the oxidation of 1-(3'-methylbutyl)-7-cyclohexyltetralin were 3 mol carbon dioxide, cyclohexane carboxylic acid and 2-(3'-methylbutyl)-1,6-hexanedioic acid (Figure 120).

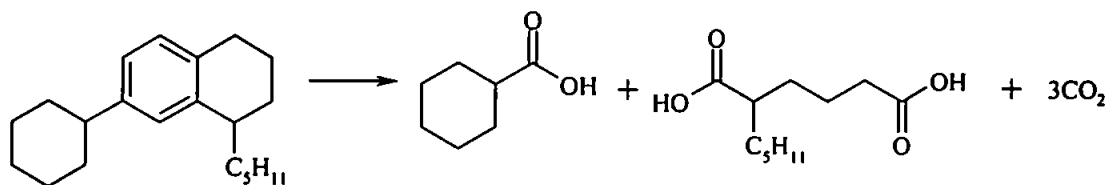


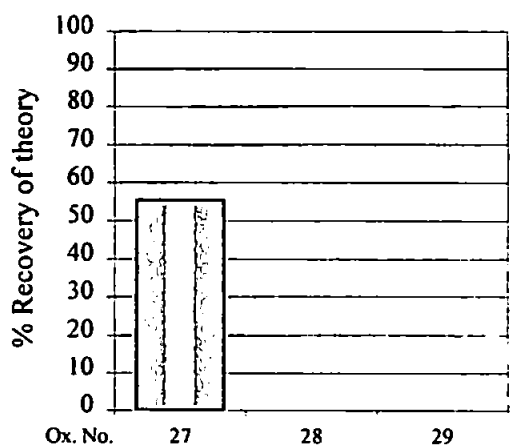
Figure 120. Theoretical products from the oxidation of 1-(3'-methylbutyl)-7-cyclohexyltetralin.

GCMS analysis of the synthetic 1-(3'-methylbutyl)-7-cyclohexyltetralin showed it to be 85% pure, with 4% 6-cyclohexyltetralin and 5% of 1-(3'-methylbutyl)-7-(4'-cyclohexyl)cyclohexyltetralin. These other components were taken into account when calculating product recoveries. Other minor impurities (total <6%) were unidentified and so were not included in the calculations.

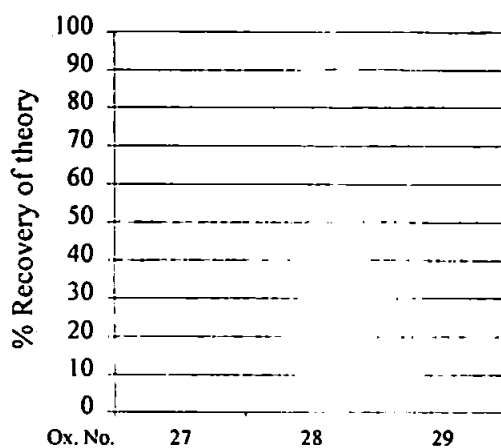
The acid, 2-(3'-Methylbutyl)-1,5-pentanedioic acid was observed as a significant oxidation product and was included in calculations for 2-(3'-methylbutyl)-1,6-hexanedioic acid.

| Ox no. | Recovery (% of theory) | | | | | Un-accounted |
|----------------|-----------------------------|---|----------------------|-------------------------------|-----------------|--------------|
| | Cyclohexane carboxylic acid | 4-Cyclohexane-cyclohexane carboxylic acid | 1,6-Hexanedioic acid | 2-Pentyl-1,6-hexanedioic acid | CO ₂ | |
| 27 | 16.7 (55) | 0.0 (0) | 1.0 (59) | 17.0 (37) | 13.0 (96) | 46.7 |
| 28 | 0.0 (0) | 0.0 (0) | 1.3 (77) | 20.9 (45) | 21.4 (159) | 50.7 |
| 29 | 0.0 (0) | 0.0 (0) | 1.9 (112) | 18.3 (39) | 18.7 (139) | 55.4 |
| Mean | 5.6 (19) | 0.0 (0) | 1.4 (82) | 18.8 (40) | 17.7 (131) | 50.9 |
| σ_{n-1} | 9.6 (32) | 0.0 (0) | 0.5 (27) | 2.0 (4) | 4.3 (32) | 4.4 |
| Theory | 30.1 | 2.5 | 1.7 | 46.5 | 13.5 | - |

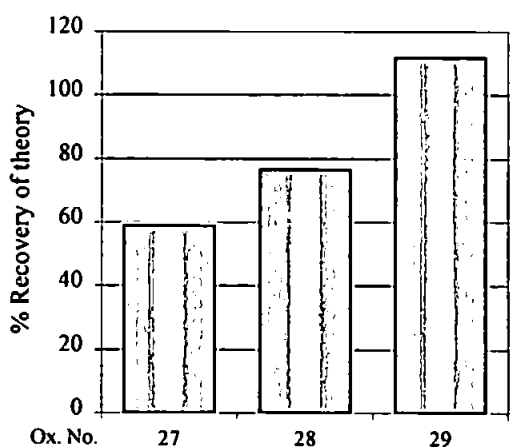
Table 26. Recovery of identified products from the RuO₄ oxidation of 1-(3'-methylbutyl)-7-cyclohexyltetralin.



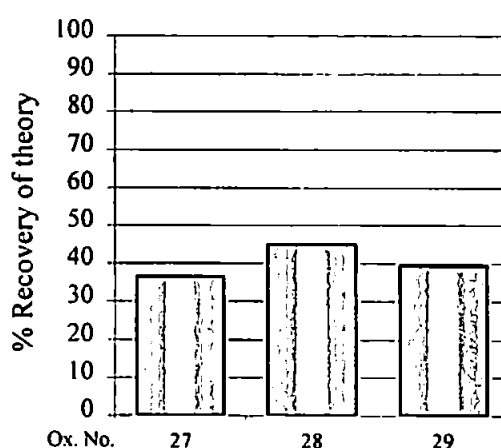
□ cyclohexane carboxylic acid



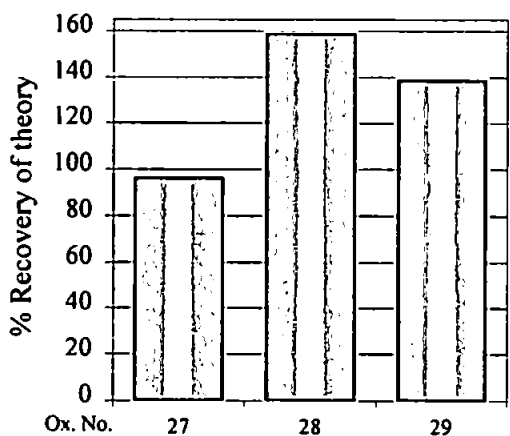
□ 4-cyclohexanecyclohexane carboxylic acid



□ 1,6-hexanedioic acid



□ 2-pentyl-1,6-hexanedioic acid



□ carbon dioxide

Figure 121. Recovery of products from the RuO_4 oxidation of 1-(3'-methylbutyl)-7-cyclohexyltetralin.

As with the other synthetic alkyltetralins, the recovery of carbon dioxide was close to that expected, but recovery of the expected alkylhexanedioic acid was poor (Table 26).

GCMS examination of the DCM-soluble products (Figure 122) from the oxidation of 1-(3'-methylbutyl)-7-cyclohexyltetralin revealed the presence of 2-(3'-methylbutyl)-1,6-hexanedioic acid, along with the pentanedioic acid homologue and cyclohexane carboxylic acid.

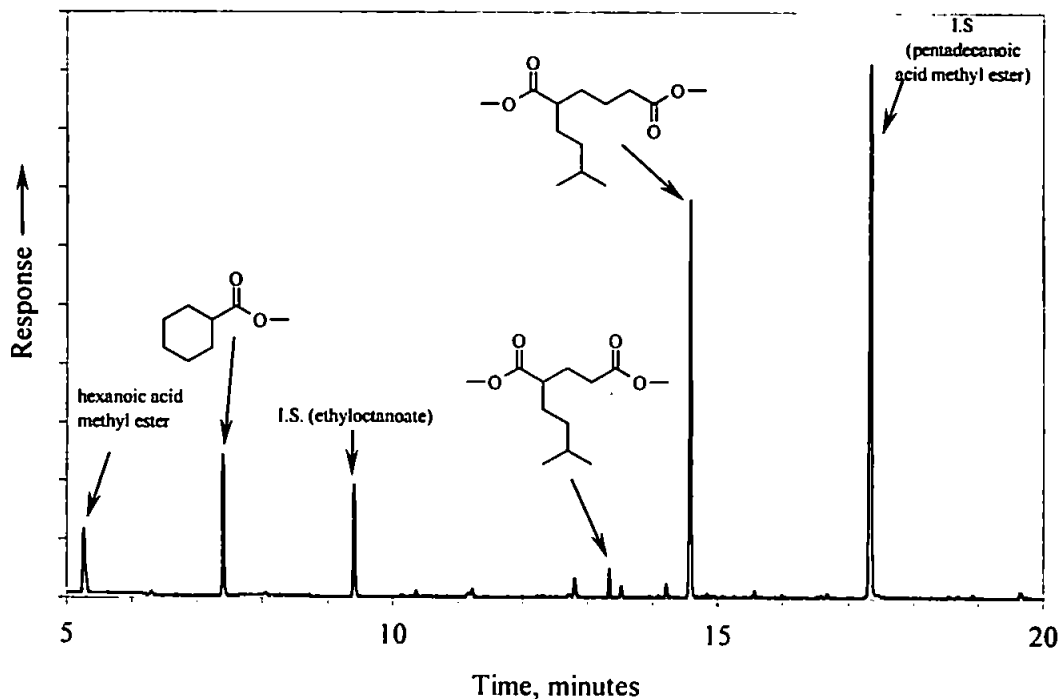


Figure 122. Partial TIC chromatogram of DCM-soluble products from the RuO_4 oxidation of 1-(3'-methyl)butyl-7-cyclohexyltetralin (as methyl esters, oxidation no. 27). GC = 25m DB5, 40 – 300°C @ 10°C min⁻¹, held 10 min.

2-(3'-Methylbutyl)-1,6-hexanedioic acid and 2-(3'-methylbutyl)-1,5-pentanedioic acid were identified from their mass spectra (Figure 123 and Figure 124). Both spectra showed ions due to cleavage around the carboxyl group, with ions at M-31 (loss of OCH₃) and M-59 (loss of COOCH₃).

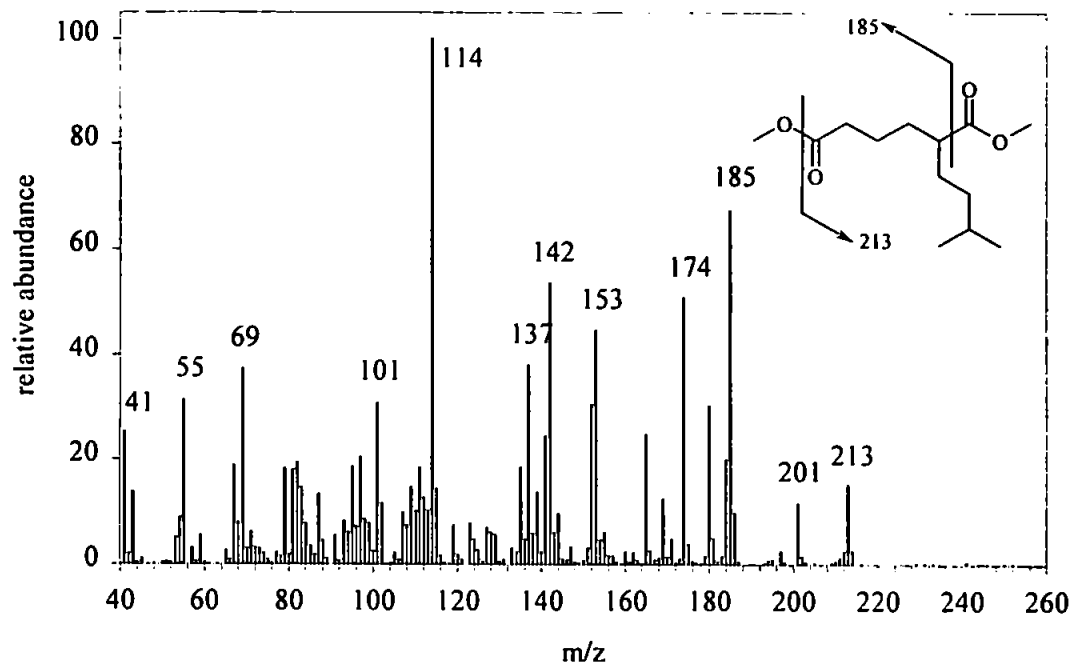


Figure 123. Mass spectrum of 2-(3'-methylbutyl)-1,6-hexanedioic acid methyl ester.

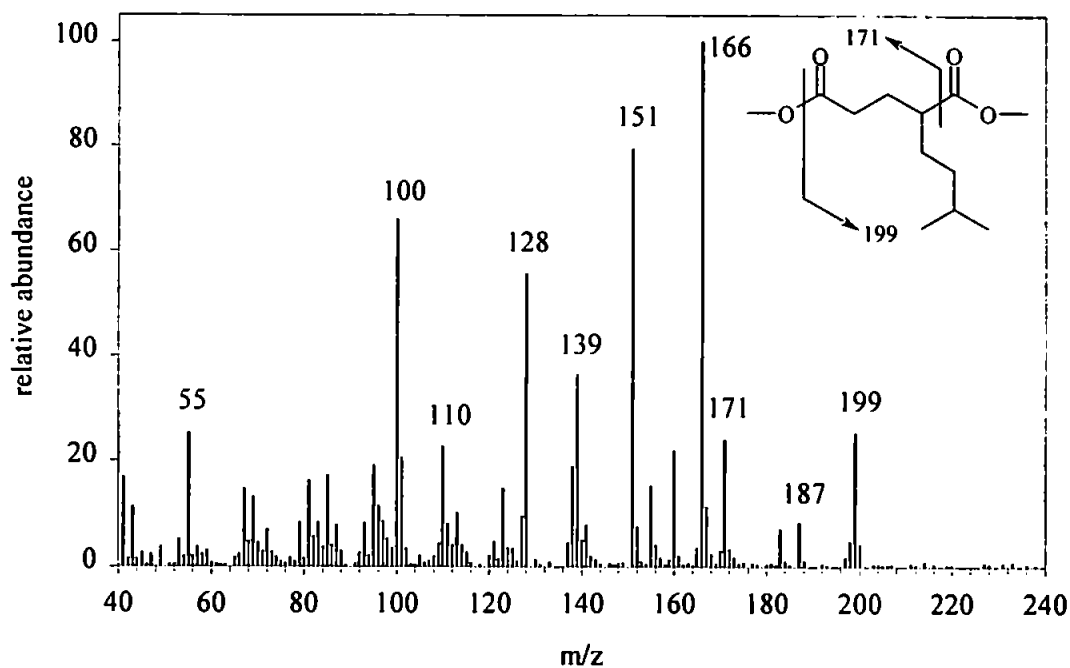
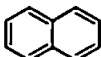
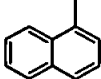
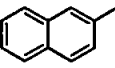
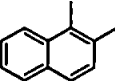
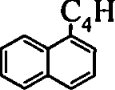
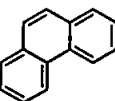
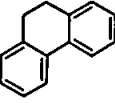
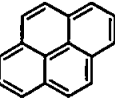


Figure 124. Mass spectrum of 2-(3'-methylbutyl)-1,5-pentanedioic acid methyl ester.

6.2.5 RuO₄ oxidation of 1-*n*-nonyl-7-cyclohexylnaphthalene.

Previous oxidations of polyaromatic hydrocarbons (Spitzer and Lee, 1974; Stock and Tse, 1983; Oberender and Dixon, 1959 cited by Lee and van den Engh, 1973) have shown that complete oxidation of naphthalene and phenanthrene is not usually observed (Table 27) However, those studies did not quantify all the products (*e.g.* carbon dioxide) or carry out replicate oxidations.

| Compound | conversion (%) | Products (yield %) | Reference |
|---|----------------|---|----------------------------|
|  Naphthalene | - | Phthalic acid (70) | Spitzer and Lee, 1974 |
|  1-Methylnaphthalene | - | Phthalic acid (24) 3-Methylphthalic acid (6) | Spitzer and Lee, 1974 |
|  2-Methylnaphthalene | - | Phthalic acid (50) 3-Methylphthalic acid (5) | Spitzer and Lee, 1974 |
|  2,3-Dimethylnaphthalene | - | Phthalic acid (25) | Spitzer and Lee, 1974 |
|  1-Butylnaphthalene | 90 | Butanoic acid (trace) Pentanoic acid (48) Phthalic acid (49) 3-Butylphthalic acid (43) | Stock and Tse, 1983 |
|  Phenanthrene | 100 | Phthalic acid (5) 2,2'-Biphenyldicarboxylic acid (91) Phenanthroquinone (4) | Stock and Tse, 1983 |
| | ? | 9,10-Phenanthraquinone (28) | Oberender and Dixon, 1959* |
|  9,10-Dihydrophenanthrene | 81 | Butanedioic acid (2) Phthalic acid (7) 3-(2-carboxyphenyl)-propionic acid (32) 2,2'-Biphenyldicarboxylic acid (91) | Stock and Tse, 1983 |
|  Pyrene | ? | Pyrene-4,5-quinone (11) Pyrene-1,6-quinone (2) 4-Formyl phenanthrene carboxylic acid lactol (1) | Oberender and Dixon, 1959* |

* cited by Lee and van den Engh (1973).

Table 27. Previous RuO₄ oxidations of polycyclic aromatic hydrocarbons.

Major products of the oxidation of such PAHs are shown to be aromatic carboxylic acids with small amounts of alkyl carboxylic acids. It would seem that mono and diaromatic carboxylic acids are resistant to further oxidation by RuO_4 (Lee and van den Engh, 1973). Therefore products to be expected from the oxidation of 1-*n*-nonyl-7-cyclohexylnaphthalene would include alkylphthalic acids (Figure 125) with correspondingly low recoveries of cyclohexane carboxylic acid and decanoic acid. Thomas (1995) observed keto acids in the products from the oxidation of 1-ethylnaphthalene and 9-ethylfluorene. Keto acids may also be expected in the products from the oxidation of 1-*n*-nonyl-7-cyclohexylnaphthalene (Figure 126).

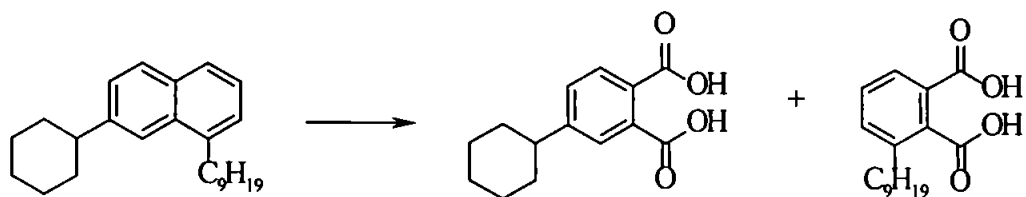


Figure 125. Phthalic acids expected from the oxidation of 1-*n*-nonyl-7-cyclohexylnaphthalene.

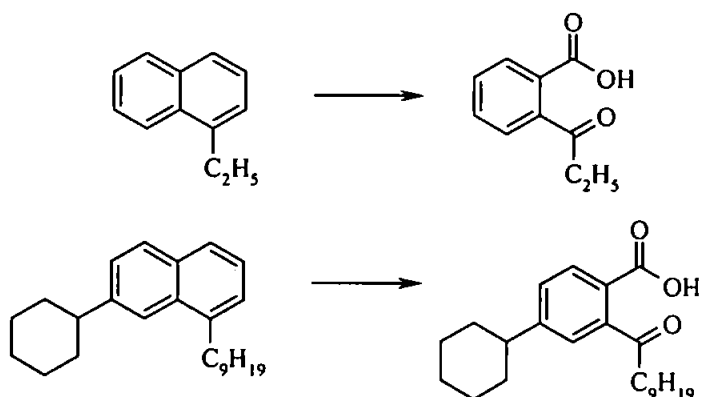


Figure 126. Formation of keto-acid from the RuO_4 oxidation of 1-ethylnaphthalene (Thomas, 1995) and possible keto acid formed from the RuO_4 oxidation of 1-*n*-nonyl-7-cyclohexylnaphthalene.

It is difficult to predict the relative proportions of phthalic acids and other partially oxidised products that may be produced, so the 'theoretical' values were calculated herein on the assumption of complete oxidation of the aromatic rings.

GCMS analysis of 1-*n*-nonyl-7-cyclohexylnaphthalene showed a purity of 97% with 2-cyclohexylnaphthalene (1%) and 1-*n*-nonyl-7-(4'-cyclohexylcyclohexyl)naphthalene (2%). Oxidation products from these compounds were taken into account when calculating the theoretical proportion of products from the oxidation of 1-*n*-nonyl-7-cyclohexylnaphthalene (Figure 127).

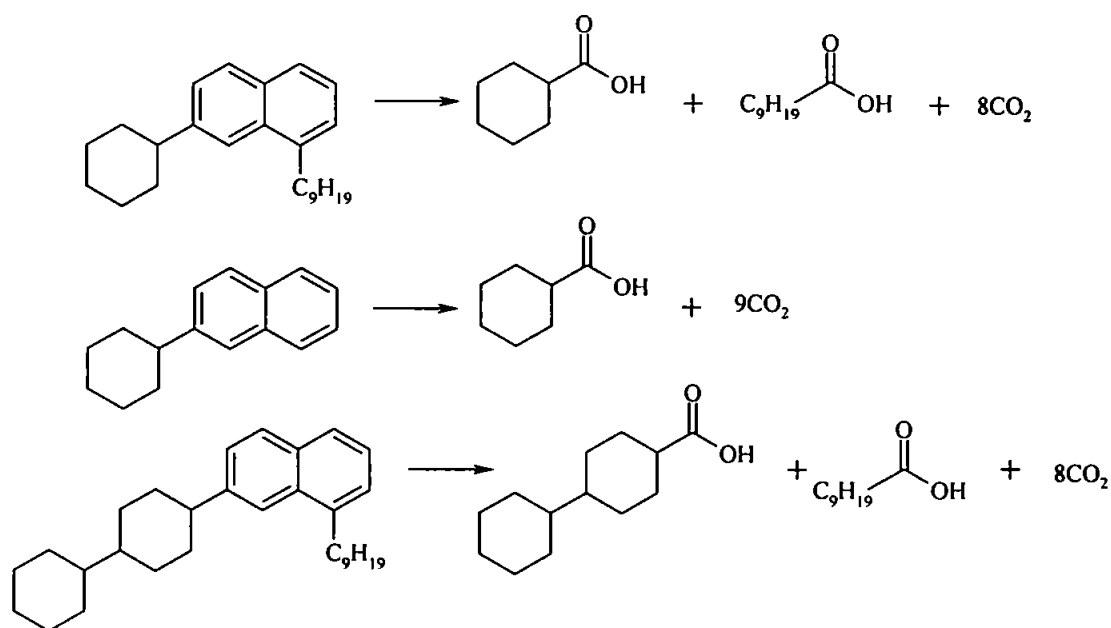


Figure 127. Theoretical products from the ruthenium tetroxide oxidation of 1-*n*-nonyl-7-cyclohexylnaphthalene, 2-cyclohexylnaphthalene and 1-*n*-nonyl-7-(4'-cyclohexyl)cyclohexylnaphthalene assuming complete oxidation of aromatic carbon.

| Oxidation No. | Recovery (% of theory) | | | | Un-accounted |
|----------------|-----------------------------|---|---------------|----------------|--------------|
| | Cyclohexane carboxylic acid | 4-cyclohexane-cyclohexane carboxylic acid | Decanoic acid | Carbon Dioxide | |
| 24 | 6.7 (24) | 0.0 (0) | 5.6 (14) | 11.7 (36) | 76.0 |
| 25 | 7.0 (25) | 0.0 (0) | 11.0 (28) | 14.7 (46) | 67.4 |
| 26 | 7.2 (26) | 0.0 (0) | 6.1 (16) | 13.4 (46) | 73.4 |
| Mean | 7.0 (25) | 0.0 (0) | 7.6 (19) | 13.2 (41) | 72.3 |
| σ_{n-1} | 0.3 (1) | 0.0 (0) | 3.0 (8) | 1.5 (5) | 4.4 |
| Theory* | 27.8 | 0.6 | 39.4 | 32.3 | - |

* Assuming complete oxidation of aromatic carbons.

Table 28. Recovery of identified products from the oxidation of 1-*n*-nonyl-7-cyclohexylnaphthalene.

Figure 128 and Table 28 show the recovery of identified products from the oxidation of 1-*n*-nonyl-7-cyclohexylnaphthalene. As discussed, the recoveries of cyclohexane carboxylic acid and decanoic acid were low. Along with low recovery of carbon dioxide, these results tend to confirm indirectly the formation of other partially oxidised products such as phthalic acids.

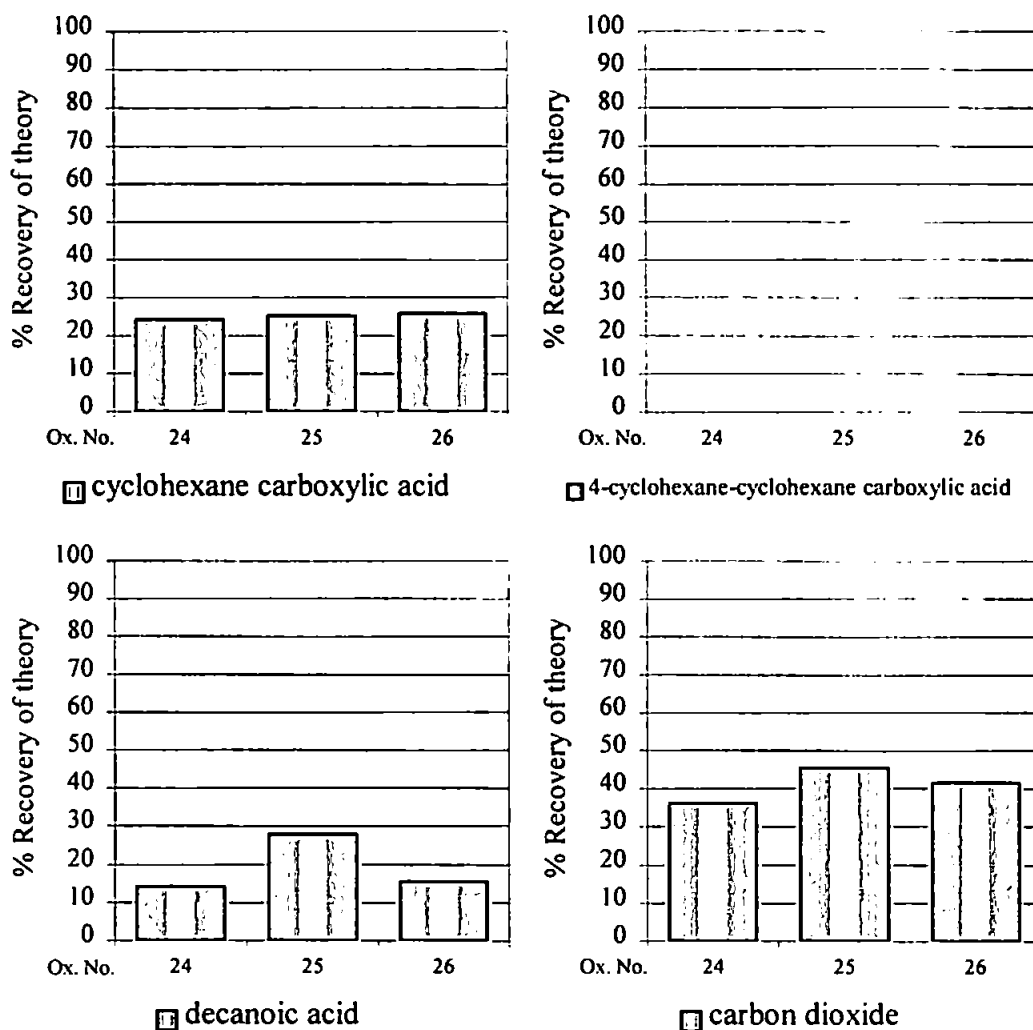


Figure 128. recovery of identified products from the ruthenium tetroxide oxidation of 1-n-nonyl-7-cyclohexylnaphthalene.

GCMS analysis of the water-soluble fraction showed only a trace of phthalic acid (di-n-butyl ester), presumably from the oxidation of the small amount of 2-cyclohexylnaphthalene present as an impurity.

GCMS analysis of the DCM-soluble products (Figure 129) from each of the oxidations ($n = 3$) show three high molecular weight (RMM $\sim 300+$) compounds as major products (mass spectra Figure 130, Figure 131 and Figure 134). None of these compounds were observed in the control (blank) oxidations or as products from the oxidation of any other hydroaromatic compound oxidised in this study.

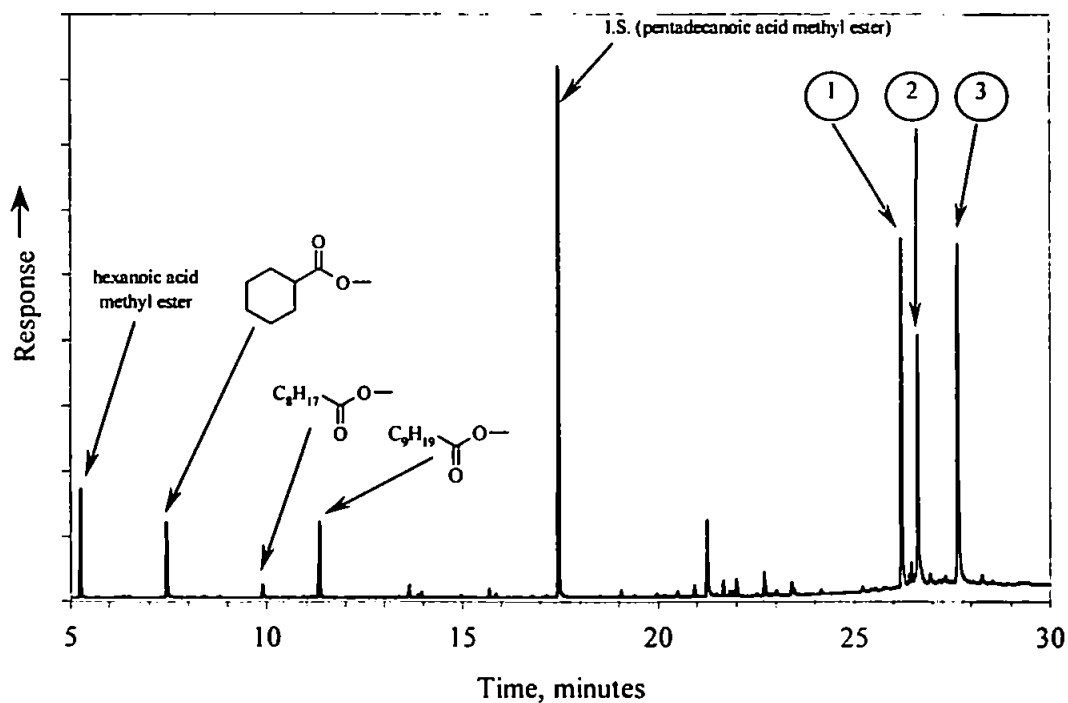


Figure 129. Partial TIC chromatogram of the DCM-soluble products from the oxidation of 1-n-nonyl-7-cyclohexylnaphthalene (as methyl esters, oxidation No. 25). GC = 25m DB5, 40 – 300°C @ 10°C min⁻¹, held 10 min.

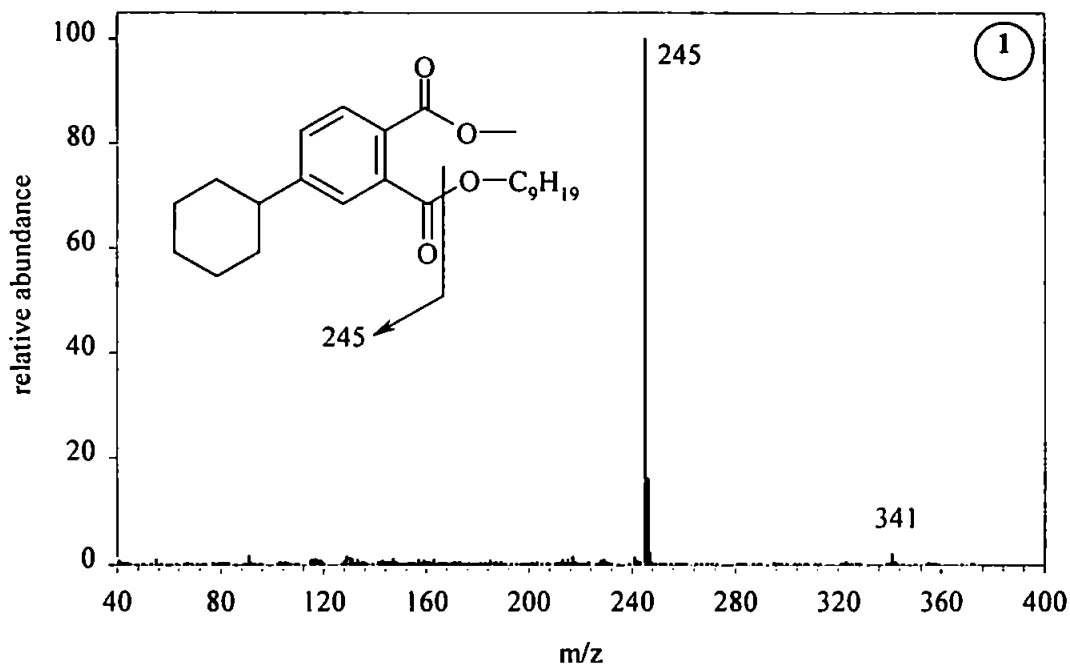


Figure 130. Mass spectrum of unknown product (1) from the DCM-soluble fraction of products from the RuO₄ oxidation of 1-n-nonyl-7-cyclohexylnaphthalene.

The mass spectrum of product 1 from the oxidation of 1-*n*-nonyl-7-cyclohexylnaphthalene (Figure 130) was tentatively identified as the mono *n*-nonyl ester of 4-cyclohexyl-*o*-phthalic acid, the other carboxylic acid group being methylated prior to analysis. This compound may have formed during oxidation by the migration of the *n*-nonyl to give the *o*-phthalic acid mono *n*-nonyl ester.

The mass spectrum shows an intense ion at m/z 245 and a weak ion at m/z 341 (2% relative intensity). The ion m/z 245 most probably corresponds to the fragment shown in Figure 133 although the lack of a molecular ion made it difficult to fully elucidate the compound.

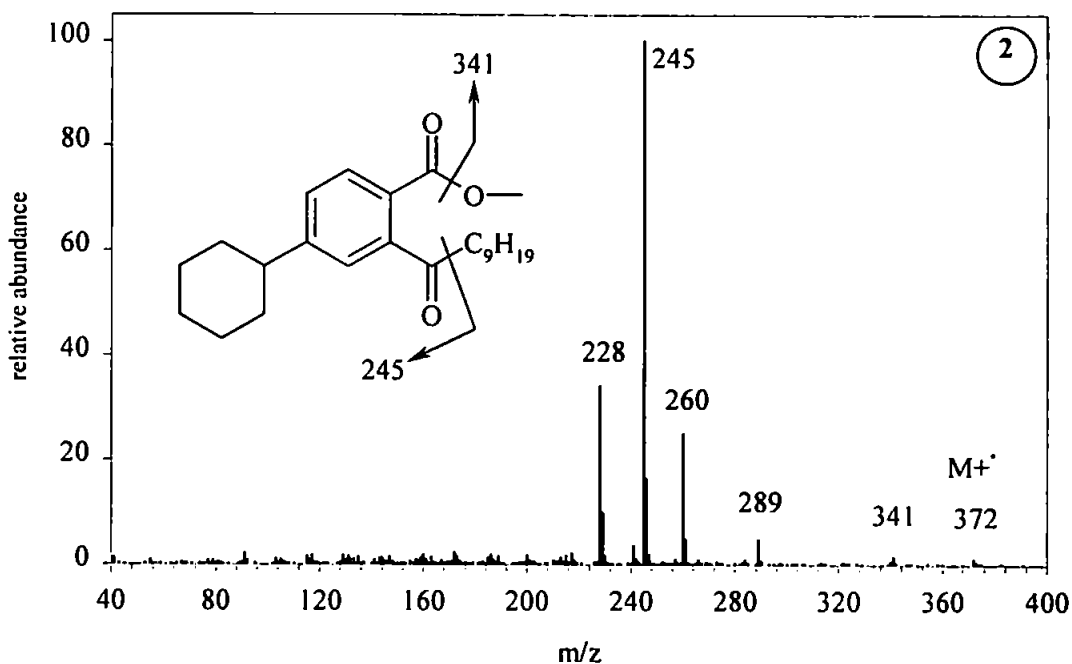


Figure 131. Mass spectrum of product (2) from the DCM-soluble fraction of products from the RuO_4 oxidation of 1-*n*-nonyl-7-cyclohexyltetralin.

Product 2 was tentatively identified as the methyl ester of the keto acid shown in Figure 126, namely 2-(1-oxo-*n*-decyl)-4-cyclohexylbenzoic acid. The mass spectrum showed a possible molecular ion at m/z 372. Loss of 31 ($-OCH_3$) from the ester group gave ion

m/z 341 and loss of the nonyl group gave ion m/z 245. As discussed, the ion m/z 245 corresponds to the ion shown in Figure 133 and a similar fragment is characteristic of electron impact mass spectra of methylated phthalates (Thomas, 1995) and the methyl esters of keto acids (Figure 133).

Ion m/z 245 is observed in two of the three mass spectra of oxidation products of 1-*n*-nonyl-7-cyclohexylnaphthalene. The high stability of this ion is probably due to the formation of an anhydride-type ion (Thomas, 1995; McLafferty and Turecek, 1993) as shown in Figure 132.

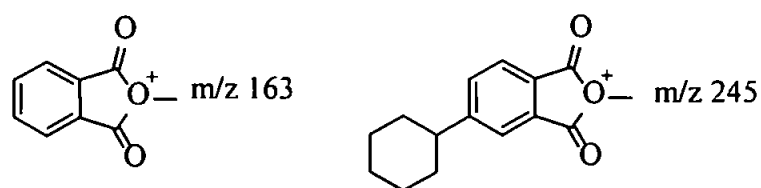


Figure 132. Postulated structure of fragment ions m/z 163 and 245 from *o*-methylphthalates (Thomas, 1995; McLafferty and Turecek, 1993) and the methyl esters of keto acids (Figure 133).

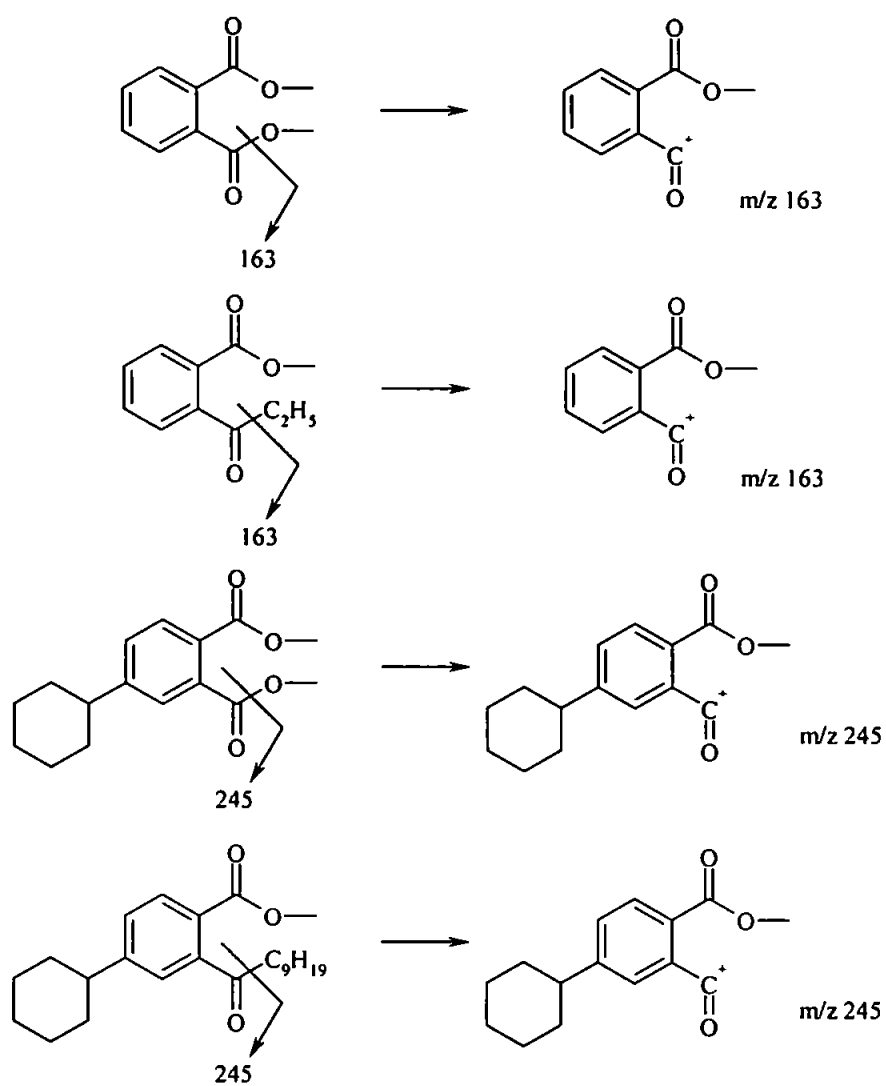
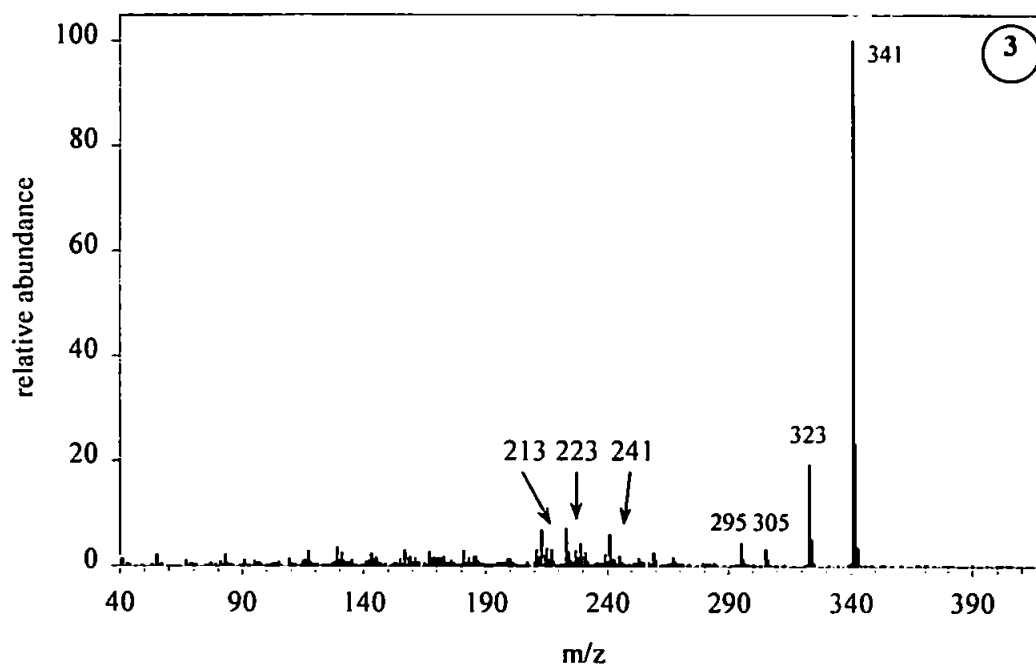


Figure 133. Fragment ions produced by dimethylphthalate and 2-(1-oxypropyl)benzoic acid methyl ester (Thomas, 1995) and extrapolation to possible RuO_4 oxidation products of 1-n-nonyl-7-cyclohexylnaphthalene.



*Figure 134. Mass spectrum of unidentified product (3) from the DCM-soluble fraction of products from the RuO₄ oxidation of 1-*n*-nonyl-7-cyclohexyltetralin.*

The mass spectrum of product 3 found in the DCM-soluble products from the RuO₄ oxidation of 1-*n*-nonyl-7-cyclohexylnaphthalene showed no apparent molecular ion. An intense ion at m/z 341 was observed that may correspond to an M-31 ion showing loss of a methoxy group from a methyl ester showing the original oxidation product to be a carboxylic acid. The compound remains unidentified.

| Compound | Oxidation no. | Mass substrate oxidised, mg | Mass compound observed, mg* | % of original substrate |
|----------|---------------|-----------------------------|-----------------------------|-------------------------|
| 1 | 24 | 24.9 | 5.6 | 22.5 ^a |
| | 25 | 20.3 | 2.9 | 14.4 ^a |
| | 26 | 24.5 | 6.2 | 25.3 ^a |
| 2 | 24 | 24.9 | 3.2 | 11.8 ^b |
| | 25 | 20.3 | 3.3 | 15.0 ^b |
| | 26 | 24.5 | 6.2 | 23.5 ^b |
| 3 | 24 | 24.9 | 5.2 | 21.0 ^a |
| | 25 | 20.3 | 4.1 | 20.0 ^a |
| | 26 | 24.5 | 9.4 | 38.3 ^a |

* - with respect to the internal standard (pentadecanoic acid).

^a - calculated by mass

^b - calculated by molar equivalent

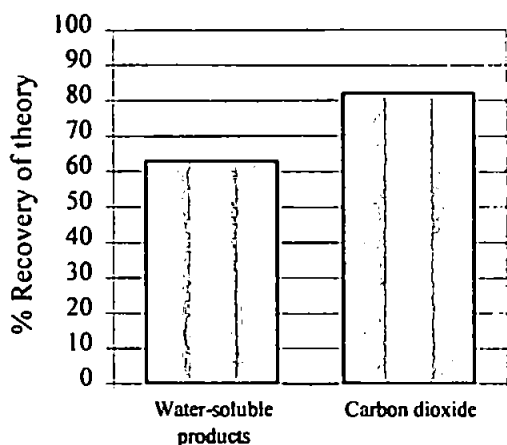
Table 29. Quantification of compounds (1, 2 and 3) in the DCM-soluble fraction of products from the RuO₄ oxidation 1-n-nonyl-7-cyclohexylnaphthalene.

Table 29 shows that the three oxidation products observed in the DCM-soluble fraction of the oxidation products accounted for a significant proportion of the original substrate. While the exact yields of the unknowns cannot be calculated, the calculated mass of each compound at least gives an estimate of the amount of products.

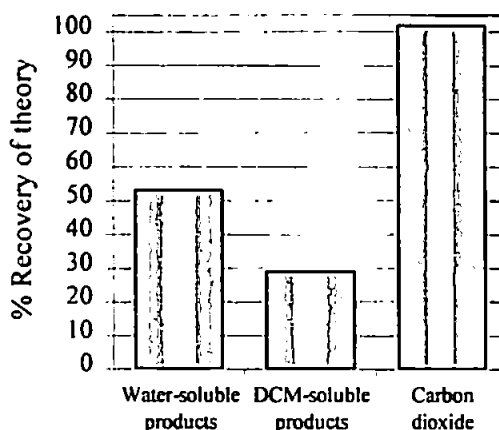
6.3 Conclusions.

Repeat oxidations of three synthetic hydroaromatic compounds, a diaromatic compound and commercial tetralin were successfully carried out.

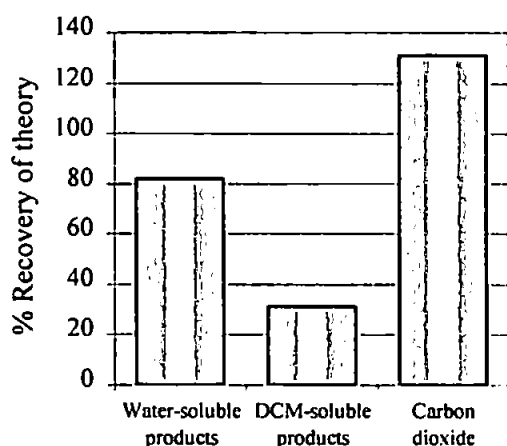
Figure 135 and Table 30 shows a summary of observed vs. theoretical RuO₄ oxidation products of the compounds synthesised herein. Cyclohexane carboxylic acid is included in the 'DCM' fraction though it is observed to partition between the aqueous and organic phases.



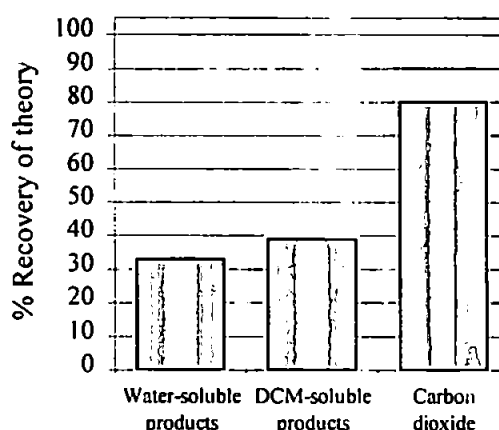
■ tetralin



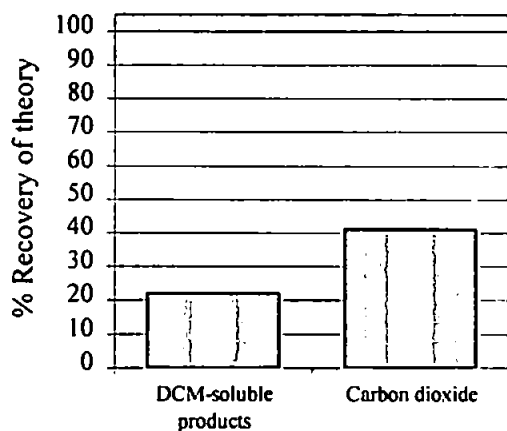
■ 6-cyclohexyltetralin



■ 1-(3'-methylbutyl)-7-cyclohexyltetralin



■ 1-n-nonyl-7-cyclohexyltetralin



■ 1-n-nonyl-7-cyclohexylnaphthalene

Figure 135. Summary of the recoveries of identified oxidation products from the RuO_4 oxidation of compounds synthesised by the author. Values for commercial tetralin are also included.

Recovery of carbon dioxide from the oxidation of hydroaromatic compounds appears to agree generally with the theoretical values, though in the cases of 6-cyclohexyltetralin and 1-(3'-methylbutyl)-7-cyclohexyltetralin the theoretical values were exceeded. Somewhat more importantly, recovery of water and DCM-soluble products consistently fell short of the theoretical values, and were about half of those expected.

No unoxidised starting material was observed in the oxidation products of any of the compounds.

Chain shortening of carboxylic acid primary oxidation products during prolonged oxidation may be partially responsible for the low figures observed for oxidation products. Complete oxidation of carboxylic acids would be expected to produce more carbon dioxide and indeed, this may account for higher than expected values for 1-(3'-methylbutyl)-7-cyclohexyltetralin and 6-cyclohexyltetralin.

Another factor that may account for the low recovery of oxidation products are losses of volatiles during work-up. Whilst every care was taken to reduce these, procedures such as rotary evaporation and nitrogen blow-down are inherently biased against the retention of volatile compounds (Ali, 1994).

Until the present study the only sources of monocarboxylic acids observed in the RuO_4 oxidation products of aromatic hydrocarbons were assumed to be alkyl substituents on aromatic rings (*e.g.* Thomas, 1995; Warton, 1999; Warton *et al.*, 2000). Thus the production of other monocarboxylic acids produced from chain shortening of 2-alkylhexanedioic acids would be misleading when the structure of the substrate is unknown, as would be the case of UCMs of hydrocarbons and other complex organic matter.

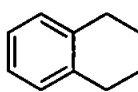
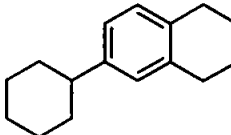
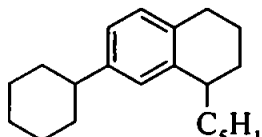
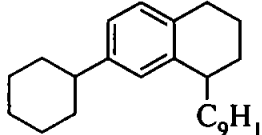
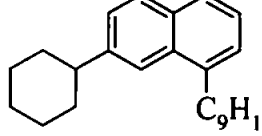
| Compound | | Recovery (% of theory) | | | Un- accounted |
|--|----------|------------------------------|----------------------------|-----------------|------------------|
| | | Water soluble products | DCM soluble products | CO ₂ | |
|  Tetralin | Theory | 60.0 | 0.0 | 40.0 | - |
| | Obs. | 37.9 (63) | 0.0 (n/a) | 32.9 (82) | 30.2 |
|  6-Cyclohexyltetralin | Theory | 37.5 | 43.8 | 18.8 | - |
| | Obs. | 19.7 (53) | 12.6 (29) | 19.2 (102) | 53.4 |
|  1-(3'-Methylbutyl)-7- cyclohexyltetralin | Theory | 1.7 | 79.1 | 13.5 | - |
| | Obs. | 1.4 (82) | 24.4 (31) | 17.7 (131) | 50.9 |
|  1-n-Nonyl-7- cyclohexyltetralin (mixture) | Theory | 16.8 | 68.3 | 14.8 | - |
| | Obs. | 5.5 (33) | 26.9 (39) | 11.8 (80) | 56.9 |
|  1-n-Nonyl-7- cyclohexylnaphthalene | 'Theory' | 0.0 | 67.8 | 32.3 | - |
| | Obs. | 0.0 (n/a) | 14.6 (22) | 13.2 (41) | 72.3 |

Table 30. Summary - recovery of identified oxidation products from the RuO₄ oxidation of compounds synthesised (except tetralin which was obtained from a commercial source) by the author.

Future work using RuO₄ of complex mixtures must take into account this new source of carboxylic acids, or else eliminate the problem of chain shortening. Thus it is possible that a proportion of the monocarboxylic acids observed in the products from the RuO₄ oxidation of UCMs and other complex organic matter could be derived from

hydroaromatic moieties. This is especially relevant to those UCMs likely to contain a significant proportion of hydroaromatic compounds, for example hydrotreated feedstocks.

Oxidation of 1-*n*-nonyl-7-cyclohexylnaphthalene showed relatively small amounts of both carbon dioxide and DCM-soluble oxidation products, although as previously discussed, it was not reasonable to assume complete oxidation of the naphthalene moiety. Three compounds making up the bulk of the reaction products were observed, product 1 was tentatively identified as the mono *n*-nonyl ester of 4-cyclohexyl-*o*-phthalic acid, product 2 was identified as 2-(1-oxo-*n*-decyl)-4-cyclohexylbenzoic acid and while product 3 remains unidentified it is not thought to be one of the predicted phthalic acids (Figure 125) since the retention time is probably too great and the characteristic ion m/z 245 expected was not observed (Figure 132).

The presence of relatively complex acids and keto acids in the oxidation products of 1-*n*-nonyl-7-cyclohexylnaphthalene means that the RuO_4 oxidation products of a UCM containing di-substituted naphthalene and similar structures would be as complex as the original mixture since the basic structure of the molecule is preserved. These findings are consistent with the study of Thomas (1995) where a diaromatic UCM was oxidised to give a UCM of oxidised products. The amount of CO_2 observed would also be misleading if used as a measure of the overall aromaticity of the sample, since aromatic rings are preserved in the oxidation products the amount of CO_2 produced would not reflect the number of unsubstituted aromatic carbons in the sample but the number of *oxidised* aromatic carbons in the sample.

7 Overall conclusions and future work.

7.1 Overall conclusion.

In conclusion, it has been shown by a series of computer modelling experiments that the composition of FCC feedstocks as revealed in the RuO_4 oxidation products (mainly carboxylic acids and carbon dioxide) can, in theory, significantly affect computer predictions of FCC product yields by the so-called Sunbury Riser Model (BP). Data for average economic values of refined fractions show that such differences in FCC operation would consequently make significant differences to both the economic value of the total FCC products and to the efficiency of refining heavy feedstocks to useful products.

Since such RuO_4 data oxidation was shown to be by these computer experiments a potentially useful tool in the analysis of FCC feedstocks, the problems experienced by Thomas (1995) and other workers (Djerassi and Engle, 1953; Stock and Tse, 1983) with losses of carbon dioxide water-soluble products from the oxidation of hydroaromatic compounds needed to be addressed. In order to achieve this the reproducibility of the RuO_4 oxidation procedure and work-up of the products was improved (Chapter 4). To calibrate the method on realistic substrates several novel hydroaromatic compounds thought to represent the unresolved hydrocarbons of FCC feedstocks were synthesised (Chapter 5) and oxidised (Chapter 6).

In Chapter 4 the RuO_4 oxidation procedure and subsequent work-up of the water and DCM-soluble oxidation products was examined and improved in an attempt to minimise losses of any oxidation products. The result was the introduction of a new carbon dioxide trap which utilises organic solvents to better absorb CO_2 and benzylamine to react with and chemically 'trap' CO_2 before titrimetric determination. Table 19 shows the improvement in recovery of carbon dioxide from replicate oxidations of tetralin.

Other improvements included removal of a step using Fuller's Earth as a filter aid which was shown to retain significant proportions of dicarboxylic acids, and the investigation of a liquid/liquid extraction procedure.

Three novel alkyltetralins and a di-substituted naphthalene were successfully synthesised and fully characterised (Chapter 3). The compounds synthesised were 6-cyclohexyltetralin, 1-(3'-methylbutyl)-7-cyclohexyltetralin, 1-*n*-nonyl-7-cyclohexyltetralin and 1-*n*-nonyl-7-cyclohexylnaphthalene.

Ruthenium tetroxide oxidation of the synthetic hydroaromatics (Chapter 6) showed that improvements made to the RuO₄ oxidation procedure were a significant advance on the procedure used by Thomas (1995, adapted from Standen, 1992; Standen and Eglinton, 1992). Carbon dioxide recoveries were generally good (>79%), while recoveries of water soluble carboxylic acids were generally ~50% of those expected and recoveries of DCM-soluble carboxylic acids were between 30 and 40% of those expected.

The apparent loss of carboxylic acid oxidation products can be partially accounted for by the over-oxidation of carboxylic acids to produce smaller carboxylic acids. For example, the RuO₄ oxidation of tetralin (Chapter 6, section 6.2.1) produced 1,6-hexanedioic acid as a major product but significant amounts of 1,5-pentanedioic acid were observed along with trace amounts of 1,4-butanedioic acid. Smaller acids produced by further oxidation of primary oxidation products were likely to be undetected because of elution with the solvent front or lost as butyl esters during the work-up prior to analysis. Where 2-*n*-nonyl-1,6-hexanedioic acid was produced from the oxidation of 1-*n*-nonyl-7-cyclohexyltetralin, decanoic and nonanoic acid as well as 1,5-pentanedioic acid and 1,4-butanedioic acid were observed corresponding to oxidation of the 2- position on the dicarboxylic acid (Chapter 6).

The three major products from RuO₄ oxidation of 1-*n*-nonyl-7-cyclohexylnaphthalene were partially oxidised compounds including 2-(1-oxo-*n*-decyl)-4-cyclohexylbenzoic acid. This was consistent with previous studies of the RuO₄ oxidation of diaromatic compounds (Chapter 6). This showed that the oxidation of diaromatic compounds in UCMs gives more complex oxidation products, consistent with previous studies (*e.g.* Thomas, 1995) where diaromatic UCMs were oxidised to give a more complex 'oxidised UCM' rather than simpler mixtures of carboxylic acids.

The observation of monocarboxylic acids in products from the RuO₄ oxidation of the alicyclic portion of a hydroaromatic compound has not previously been reported. This represents a new source of monocarboxylic acids in the RuO₄ oxidation products of UCMs and should be taken into account when oxidising UCMs likely to contain a significant proportion of hydroaromatic structures, such as hydro-treated FCC feedstocks. The synthesis and oxidation of di-substituted tetralins has increased the understanding of RuO₄ oxidation products from UCMs and consequently furthered the use of RuO₄ as a potentially useful tool in the elucidation of FCC feedstock compositions and aromatic UCMs from other natural and anthropogenic sources.

7.2 *Suggested further work.*

Results from the oxidation of synthetic hydroaromatics has shown that there is still room for improvement in the RuO₄ work-up procedure. It is suggested that the liquid/liquid extraction procedure be replaced by a solid phase extraction procedure. The extraction procedure could perhaps be replaced altogether if the water-soluble acids were analysed by a suitable normal phase high performance liquid chromatography (HPLC). Ion-exclusion chromatography seems ideal for the analysis of the water-soluble carboxylic acids, since separation is driven by the effective charge on the molecule giving

good separation of mono and multi-carboxylic acids. A review of the applications of ion-exclusion chromatography is presented by Fritz (1991).

Use of suitable HPLC methods would also help solve the problem of oxidation products undetected or lost during work-up since the amount of sample preparation required would be reduced. Applications of ion-exclusion chromatography to the separation of volatile and long-chain fatty acids are presented by *e.g.* Fischer *et al.* (1997) and Fuse *et al.* (1997). Johnson *et al.* (1997) present the determination of small carboxylic acids by ion-exclusion chromatography coupled to electrospray mass spectrometry. This technique, particularly where liquid chromatography is coupled to multistage ion trap electrospray mass spectrometry (*e.g.* McCormack *et al.*, 2000) would appear to be ideal for the identification and determination of a wide range of water and DCM-soluble acids.

An alternative oxidant for the oxidative degradation of polyaromatic compounds may be osmium tetroxide (OsO_4), which is a weaker oxidising agent than RuO_4 , and which is reported to show greater selectivity when used to oxidise PAHs (Lee and van den Engh, 1973).

The main thrust of future work should however concentrate on developing the RuO_4 oxidation technique so that it may be used a regular tool in the elucidation of FCC feedstocks and other sources of aromatic UCMs.

8 *References*

Al-Enezi G. and Elkamel A. (2000) Predicting the effect of feedstock on product yields and properties of the FCC process. *Petroleum Science and Technology* **18**, 407-428.

Al-Enezi, G., Fawzi, N. and Elkamel, A. (1999) Development of regression models to control product yields and properties of the fluid catalytic cracking process. *Petroleum Science and Technology* **17**, 535-552.

Ali, L.N. (1994) *The dissolution and photodegradation of Kuwait crude oil in seawater*. Ph.D. Thesis, University of Plymouth, Plymouth, U.K.

Altgelt K.H., and Boduszynski, M.M. (1994) *Composition and Analysis of Heavy Petroleum Fractions*. Marcel Dekker, New York, U.S.A.

Berliner, E. (1949) The Friedel and Crafts reaction with aliphatic and dibasic anhydrides. In: *Organic Reactions* **V**, 229-299.

Blom, L. and Edelhausen, L. (1955) Direct titration of carbon dioxide. *Analytica Chimica Acta* **13**, 120-128.

Blumer, M., Ehrhardt, M. and Jones, J.H. (1973) The environmental fate of stranded crude oil. *Deep Sea Research* **20**, 239-259.

Boucher R.J., Standen, G., Patience, R.L. and Eglinton, G. (1990) Molecular characterisation of kerogen from the Kimmeridge Clay Formation by mild selective chemical degradation and solid state ^{13}C NMR. *Organic Geochemistry* **16**, 951-958.

Boucher R.J., Standen, G., and Eglinton, G. (1991) Molecular characterisation of kerogens by mild selective chemical degradation – ruthenium tetroxide oxidation. *Fuel* **70**, 695-702.

Breitmaier, E. *Structure Elucidation by NMR in Organic Chemistry*. 1993, John Wiley and Sons Ltd., Chichester, U.K.

Christensen, G., Apelian, M. R., Hickey, K.J. and Jaffe, S.B. (1999) *Chemical Engineering Science* **54**, 2753-2764.

Courtney J.L., (1986) Ruthenium tetroxide oxidation. In; *Organic Synthesis by Oxidation with Metal Compounds*. Plenum New York. 445-465.

Djerassi, C. and Engle, R.R. (1953), Oxidations with ruthenium tetroxide. *Journal of the American Chemistry Society* **75**, 3838.

Eisenbraun, E.J., Hinman, C.W., Springer, J.M., Burnham, J.W., Chou, T.S., Flanagan, P.W. and Hamming, M.C. (1971) The synthesis of polyalkyl-1-tetralones and the corresponding naphthalenes. *Journal of Organic Chemistry* **36**, 2480-2485.

van der Eijk, H., den Otter, G.J., Blauhoff, P.M.M. and Maxwell, I.E. (1990) *Chemical Engineering Science* **45**, 2117-2124.

Fischer, K., Chodura, A., Kotalik, J., Bieniek, D. and Kettrup, A. (1997) Analysis of carboxylic acids and amino acids in effluents of landfills, composting plants and fermentation plants by ion-exclusion and ion-exchange chromatography. *Journal of Chromatography A* **770**, 229 – 241.

Fritz, J.S. (1991) Review: Principles and applications of ion-exclusion chromatography. *Journal of Chromatography* **546**, 111 – 118.

Fuse, T., Kusu, F. and Takamura, K. (1997) Determination of fatty acids in oils by high performance liquid chromatography with electrochemical detection. *Journal of Chromatography A*, **764**, 177 – 182.

Gandon, R., Boust, D. and Bedue, O. (1993) Ruthenium complexes originating from the Purex process: Coprecipitation with copper ferrocyanides *via* ruthenocyanide formation. *Radiochimica Acta* **61**, 41-45.

Gough, M.A. (1989) *Characterisation of unresolved complex mixtures of hydrocarbons*. Ph.D. Thesis Polytechnic South West, Plymouth, U.K.

Gray, M.R. (1994) *Upgrading Petroleum Residues and Heavy Oils*. Marcel Dekker, New York, U.S.A.

Huang-Minlon (1946) A simple modification of the Wolff-Kishner reduction. *Journal of the American Chemical Society* **68**, 2487-2488.

Johnson, S.K., Houk, L.L., Feng, J., Johnson, D.C. and Houk, R.S. (1997) Determination of small carboxylic acids by ion exclusion chromatography with electrospray mass spectrometry. *Analytica Chimica Acta* **341**, 205 – 216.

Killops, S.D. and Al-Juboori, M.A.H.A. (1990) Characterisation of the unresolved complex mixture (UCM) in the gas chromatograms of biodegraded petroleum. *Organic Geochemistry* **15**, 147-160.

Klopman, G., Li, J-Y., Wang, S. and Dimayuga, M. (1994) Computer automated log *P* calculations based on an extended group contribution approach. *J. Chem. Inf. Comput. Sci.* **34**, 752-781.

Lee D.G. and van den Engh, M. (1973) The Oxidation of Organic Compounds by Ruthenium Tetroxide. In *Oxidation in Organic Chemistry, Part B*. Ed. Trahanovsky, Academic Press, London, U.K.

Liguras, D.K., and Allen, D.T. (1989) Structural models for catalytic cracking. 1. Model compound reactions. *Industrial Engineering and Chemistry Research* **28**, 665-673.

March, J. (1992) *Advanced Organic Chemistry. Reactions, Mechanism and Structure*. John Wiley and Sons Ltd., Chichester, U.K.

McCormack, P., Jones, P. And Rowland, S.J. (2000) Analysis of oilfield produced waters and production chemicals by electrospray ionisation - multistage mass spectrometry (ES-MSⁿ). *Water Research* (submitted July 2000).

McLafferty, F.W. and Turecek, F. (1993) *Interpretation of Mass Spectra*, 4th Edition, University Science Books, Sausalito, California, U.S.

Mojelsky, T.W., Montgomery, D.S. and Strausz, O.P. (1985) Ruthenium (VIII) catalysed oxidation of high molecular weight components of Athabasca oil sand bitumen. *AOSTRA Journal of Research* **2**(2), 131-137.

Mojelsky, T.W., Ignasiak, T.M., Frakman, Z., McIntyre, D.D., Lown, E.M., Montgomery, D. S. and Strausz, O. P. (1992) Structural features of Alberta oil sand and heavy oil asphaltenes. *Energy & Fuels* **6**, 83-96.

Mosby, W.L. (1952) The Friedel-Crafts reaction with γ -valerolactone. I. The synthesis of various polymethylnaphthalenes. *Journal of the American Chemical Society* **74**, 2564-2569.

Muhammad, O.H.J. (1996) Development of micro-scale activity test strategy for FCC process economics enhancement. *Studies in Surface Science and Catalysis* **100**, 365-374.

van Nieuwenburg, C.J. and Hegge, L.A. (1951) On the absorption of carbon dioxide by baryta in an organic solvent. *Analytica Chimica Acta* **5**, 68-70.

- Oberender, F.G. and Dixon, J.A. (1959) *Journal of Organic Chemistry* **24**, 1226.
- Olson, E.S. and Diehl, J.W. (1984) Ruthenium tetroxide oxidation of lignite. *Fuel* **63**, 210-216.
- Olson, E.S., Diehl, J.W., Froehlich, M.L. and Miller, D.J. (1987) Elucidation of aliphatic structures in low rank coals with ruthenium tetroxide oxidations. *Fuel* **66**, 968-972.
- OPIS (Oil Price Information Service) weekly bulletin (2000). **20**, July 17.
- Patchornik, A. and Shalitin, Y. (1961) Titrimetric method for continuous determination of carbon dioxide and its application in amino acid chemistry. *Analytical Chemistry* **33**, 1887-1889.
- Peters, K.E. and Moldowan, J.M. (1993) *The Biomarker guide. Interpreting Molecular Fossils In Petroleum And Ancient Sediments*. Prentice-Hall Inc., New Jersey, U.S.A.
- Quann, R.J., and Jaffe, S.B. (1992) Structure-oriented lumping: describing the chemistry of complex hydrocarbon mixtures. *Industrial Engineering and Chemistry Research* **31**, 2484-2497.
- Revill A.T. (1992) *Characterisation of unresolved complex mixtures of hydrocarbons by degradative methods*. Ph.D. Thesis Polytechnic South West, Plymouth, U.K.

Revoll A.T., Carr, M. and Rowland, S.J. (1992) Use of oxidative degradation followed by capillary gas chromatography-mass spectrometry and multidimensional scaling analysis to finger-print unresolved complex mixtures of hydrocarbons. *Journal of Chromatography* **589**, 281-286.

Smith, R.M. and Busch, K.L. (1999) *Understanding Mass Spectra – A Basic Approach*. John Wiley and Sons Inc., Chichester, U.K.

Snyder H.R. and Weber, F.X. (1955) *Organic Syntheses* Collective Volume **III**, 78.

Spitzer, U.A., and Lee, D.G. (1974) Oxidation of hydrocarbons. V. Oxidation of Naphthalenes by ruthenium tetroxide. *Journal of Organic Chemistry* **39**, 2468-2469.

Spitzer, U.A., and Lee, D.G. (1975) Oxidation of hydrocarbons. VII. Kinetics of the oxidation of naphthalenes by ruthenium tetroxide. *Canadian Journal of Chemistry* **53**, 2865-2868.

Standen, G. (1992) *Carbon Skeletal Typing of Sedimentary Organic Matter*. Ph.D. Thesis, University of Bristol, Bristol, U.K.

Standen, G., Boucher, R.J., Rafalska-Bloch, J. and Eglinton, G. (1991) Ruthenium tetroxide oxidation of natural organic macromolecules: Messel kerogen. *Chemical Geology* **91**, 297-313.

Standen, G. and Eglinton G. (1992) A much modified and miniaturised chemical degradation procedure for the analysis of both organic compounds *and* biologically derived macromolecules: Ruthenium tetroxide oxidation. *Chemical Geology* **97**, 307 - 320.

Stuart, B. (1996) *Modern Infrared Spectroscopy*. John Wiley and Sons Ltd., Chichester, U.K.

Stock, L.M. and Tse, K. (1983) Ruthenium tetroxide catalysed oxidation of Illinois No. 6 coal and some representative hydrocarbons. *Fuel* **62**, 974-976.

Stock, L.M., Tse, K. and Wang, S. (1985) The Ruthenium (VIII) catalysed oxidation of Texas lignite and Illinois No. 6 bituminous coal. The aliphatic and aromatic carboxylic acids. *American Chemical Society Division of Fuel Chemistry* **30**, 493-502.

Stock, L.M. and Wang, S. (1986) Ruthenium tetroxide catalysed oxidation of Illinois No. 6 coal. The formation of volatile monocarboxylic acids. *Fuel* **64**, 1713-1717.

Strausz, O.P. and Lown, E.M. (1991) Structural features of Athabasca bitumen related to upgrading performance. *Fuel Science and Technology International*. **9**, 269-281.

Thomas, K.V. (1995) *Characterisation and environmental fate of unresolved complex mixtures of hydrocarbons*. Ph.D. Thesis, University of Plymouth, Plymouth, U.K.

Trefilieff, S. (1987) *Etude de la structure des fractions polaires de pétroles (résins et asphaltènes) par dégradations chimiques sélectives*. Ph.D. thesis, Louis Pasteur University, Strasbourg, France.

Truce, W.E. and Olsen, C.E. (1952) The aluminium chloride – catalysed condensation of γ -butyrolactone with benzene. *Journal of the American Chemical Society* **74**, 4721.

Vogel, A.I. (1989) *Vogel's Textbook of Practical Organic Chemistry*, 5th Edition. Ed; Furniss, B.S., Hannaford, A.J., Smith, P.W.G. and Tatchell, A.R., Longman Scientific and Technical.

Warton, B. (1999) *Studies of the saturate and aromatic hydrocarbon unresolved complex mixtures in petroleum*. Ph.D. Thesis, Curtin University of Technology, Perth, Australia.

Warton, B., Alexander, R. and Kagi, R.I. (2000) Characterisation of the ruthenium tetroxide oxidation products from the aromatic unresolved complex mixture of a biodegraded crude oil. *Organic Geochemistry* **30**, 1255-1272.

Wraige, E.J. (1997), *Studies of the Synthesis, Environmental Occurrence and Toxicity of Unresolved Complex Mixtures (UCMs) of Hydrocarbons*. Ph.D. Thesis Plymouth University, Plymouth, U.K.